DEUTSCHE GEODÄTISCHE KOMMISSION

bei der Bayerischen Akademie der Wissenschaften

Reihe B | Angewandte Geodäsie | Heft Nr. 313

Detlef Angermann, Hermann Drewes, Manuela Krügel,
Barbara Meisel, Michael Gerstl, Rainer Kelm, Horst Müller,
Wolfgang Seemüller, Volker Tesmer

ITRS Combination Center at DGFI:
A Terrestrial Reference Frame Realization 2003

München 2004

Verlag der Bayerischen Akademie der Wissenschaften
in Kommission beim Verlag C. H. Beck

ISSN 0065-5317 ISBN 3 7696 8593 8

DEUTSCHE GEODÄTISCHE KOMMISSION

bei der Bayerischen Akademie der Wissenschaften

Reihe B | Angewandte Geodäsie | Heft Nr. 313

Detlef Angermann, Hermann Drewes, Manuela Krügel,
Barbara Meisel, Michael Gerstl, Rainer Kelm, Horst Müller,
Wolfgang Seemüller, Volker Tesmer

ITRS Combination Center at DGFI:
A Terrestrial Reference Frame Realization 2003

München 2004

Verlag der Bayerischen Akademie der Wissenschaften
in Kommission beim Verlag C. H. Beck

ISSN 0065-5317 ISBN 3 7696 8593 8

Adresse des Herausgebers /
Address of the publisher

Deutsche Geodätische Kommission
Marstallplatz 8
D – 80 539 München
Telefon +49 - (0)89 - 23 031 -0 / -1113
Telefax +49 - (0)89 - 23 031 -1283 / -1100
E-mail hornik@dgfi.badw.de
Internet http://dgk.badw.de

Adresse der Autoren /
Address of the authors

Deutsches Geodätisches Forschungsinstitut
Marstallplatz 8
D – 80 539 München
Telefon +49 - (0)89 - 23 031 -0 / -1107
Telefax +49 - (0)89 - 23 031 -1240
E-mail angermann@dgfi.badw.de
Internet http://www.dgfi.badw.de

Diese Publikation ist als pdf-Dokument im Internet veröffentlicht unter der Adresse /
This volume is published as pdf-document in the internet under the address
http://dgk.badw.de/index.php?id=10

ISSN 0065-5317 ISBN 3 7696 8593 8

Preface

In 1999, the International Earth Rotation Service (IERS) re-organized its structure and published a Call for Participation (CfP) in the new components of the Service. The German Geodetic Research Institute (Deutsches Geodätisches Forschungsinstitut, DGFI) responded to the CfP in the frame of a joint proposal of the Forschungsgruppe Satellitengeodäsie (FGS), Munich, Germany, proposing to act as a Product Centre for the International Terrestrial Reference System (ITRS PC). In September 2000 the IERS Directing Board approved the DGFI proposal as an ITRS Analysis Centre (AC), changing slightly the new IERS structure by introducing the ACs in addition to the ITRS PC. Since then, there were a few minor changes by adopting the new Service name "International Earth Rotation and Reference Systems Service (IERS)" and "ITRS Combination Centre (CC)" instead of AC. Today there are three ITRS CCs at Institut Géographique National (IGN), Paris, France, Natural Resources Canada (NRCan), Ottawa, Canada, and DGFI.

The DGFI Proposal of 1999 culminates in six major topics to be accomplished in the ITRS combination procedure:

- Intra-techniques comparisons,
- Inter-techniques comparisons,
- Weighting of individual data sets,
- Final adjustments,
- Generation of final combined results,
- Documentation, publication and distribution of ITRF products.

With the present publication the taken tasks shall be fulfilled for the first 4-years period.

Besides the function as an ITRF CC, DGFI proposed to act as an IERS Combination Research Centre (IERS CRC) within the FGS proposal and together with the GeoForschungsZentrum Potsdam (GFZ). To perform both activities ITRS CC and IERS CRC, DGFI applied for a grant within the joint programme "Geotechnologien" of the German Bundesministerium für Bildung und Forschung (BMBF) and Deutsche Forschungsgemeinschaft (DFG). It was approved and sponsored by BMBF for three years (2002-2004) under grant no. 03F0336C. This financial support is gratefully appreciated.

The very close connection of the two DGFI activities as ITRS CC and IERS CRC allowed a thorough-going research of the fundamentals of modelling the methods for space geodetic positioning (VLBI, SLR, GPS, DORIS), terrestrial reference frames and Earth orientation parameters. This includes in particular the study on the strengths and weaknesses of the individual observation techniques, the mathematical and physical models, as well as the combination procedures. As a result, the present publication includes detailed descriptions of the mathematical foundation and the methodology of combination. The outcome of the processing is given in terms of comparisons, internally among the individual techniques and externally with other existing solutions. The complete results (e.g., station coordinates and velocities) are available at DGFI upon request. They are not published here in order not to produce confusions with the official IERS products.

DGFI will continue in its function as ITRF CC, in particular in the processing for the official IERS product ITRF2004. The experience gained during the mentioned activities as well as the methods and results presented here will serve as the basis for the future work.

Contents

List of Figures

List of Tables

1 Introduction and motivation

Consistent, accurate and reliable reference frames are required for measuring and mapping the Earth's surface and its variations in time. They are the basis for many practical applications, such as national and regional networks, engineering, precise navigation, geo-information systems, etc., as well as for scientific investigations in the Earth's system (e.g., plate tectonics, sea level change, seasonal and secular loading signals, atmosphere dynamics, Earth orientation excitation). Today, space geodetic observation techniques allow to determine geodetic parameters (e.g., station positions, Earth rotation) with a precision of a few millimeters (or even better). However, this is not reflected in the accuracy of current realizations of the terrestrial reference system. The reasons are manyfold, and reach from remaining biases between different observation techniques to deficiencies in the combination methodology. To fully exploit the potential of the space geodetic observations for investigations of various global and regional, short-term, seasonal and secular phenomena in the Earth's system, the reference frame must be realized with the highest accuracy, spatial and temporal consistency and stability over decades.

Future progress in Earth sciences will fundamentally depend on understanding the Earth as a system, into which the geodetic research in geometry, Earth rotation and gravity are to be integrated. This is the major goal of the Global Geodetic Observing System (GGOS) of the International Association of Geodesy (IAG), which was installed as the first project within the new structure of IAG during the XXIII General Assembly of the International Union of Geodesy and Geophysics (IUGG) in Sapporo, Japan, July 2003 (e.g., Rothacher, 2000; Rummel et al., 2002; Drewes, 2004). The vision of GGOS is to integrate the different space geodetic techniques, such as Global Navigation Satellite Systems (GNSS), Satellite and Lunar Laser Ranging (SLR/LLR), Very Long Baseline Interferometry (VLBI), Doppler Orbitography and Radio Positioning Integrated by Satellite (DORIS), satellite altimetry, and the new and upcoming satellite missions (e.g., GRACE, Jason1, ENVISAT, GOCE, Galileo) in order to achieve a better consistency, long-term reliability and understanding of geodynamic and global change processes.

Since 1988, the International Earth Rotation and Reference Systems Service (IERS) is responsible for the establishment and maintenance of the International Terrestrial Reference Frame (ITRF), a realization of the International Terrestrial Reference System (ITRS). The ITRF is realized by the positions at a reference epoch and constant velocities for the IERS network stations derived from a combination of individual space geodetic solutions. The contributing space techniques are Very Long Baseline Interferometry (VLBI), Satellite and Lunar Laser Ranging (SLR/LLR), Global Positioning System (GPS), and Doppler Orbitography and Radio Positioning Integrated by Satellite (DORIS).

A series of ten ITRF's was compiled by the responsible ITRS Product Center (the former IERS ITRF section) hosted at the Institute Géographique National (IGN), Paris, from ITRF88 to ITRF2000. The most recent IERS realization, the ITRF2000, consists of the positions and velocities of about 800 stations located at approximately 500 sites (Altamimi et al., 2002; Boucher et al., 2004). The input data for the ITRF2000 computation were multi-year solutions of different space geodetic techniques containing station positions and velocities with their full variance-covariance matrices. The ITRF2000 computation is based on altogether 3 VLBI, 7 SLR, 1 LLR, 6 global GPS, 2 DORIS, 2 multi-technique, and 9 GPS densification solutions, provided by various analysis centers. The current methodology is based on combining simultaneously station positions and velocities using the full variance-covarinace information provided by the individual Analysis Centers in the Solution INdependent EXchange format (SINEX) for space geodesy. A SINEX format description is available at, e.g., ftp://alpha.fesg.tu-muenchen.de/iers/sinex/format. The combi-

nation strategy is based on minimally constrained solutions by simultaneously estimating transformation parameters of each individual solution w.r.t. the combined frame together with the station positions and velocities. Details regarding the ITRF2000 data analysis and results are reported in Altamini et al. (2002) and Boucher et al. (2004); see also the webpage of the ITRS Product Center at http://lareg.ensg.ign.fr/ITRF/ITRF2000.

Within the re-organized IERS structure, the ITRS Product Center is supplemented by ITRS Combination Centers, which were included as new IERS components (see http://www.iers.org, IERS Annual Report, 2002) to ensure redundancy for the ITRF computations. Currently, three ITRS Combination Centers are established at Deutsches Geodätisches Forschungsinstitut (DGFI), Institute Géographique National (IGN), and National Resources Canada (NRCan). They are responsible for performing the combination of space geodetic solutions to derive the ITRS products, primarily the positions and velocities of the IERS network stations. According to the IERS Terms of Reference (http://www.iers.org/about/tor) the input data shall be provided by the services, i.e.,

the International GPS Service (IGS),
the International Laser Ranging Service (ILRS),
the International VLBI Service for Geodesy and Astrometry (IVS),
the International DORIS Service (IDS).

Each of the three ITRS Combination Centers uses its own combination software and applies its preferred methodology for the combination of the space geodetic data. This allows a decisive validation of the combination results and ensures an independent quality control. Further impact can be expected from the activities of the newly created IERS Combination Research Centers, and the IERS Analysis Coordinator who is taking care of the long-term stability and consistency of the IERS products, i.e., the ITRF, the International Celestial Reference Frame (ICRF), and the Earth orientation parameters (EOP).

In its function as an ITRS Combination Center and IERS Combination Research Center, DGFI is involved in the combination of space geodetic observations. Based on the most recent multi-years space techniques solutions (and normal equations) provided by individual analysis centers and/or services, DGFI has computed a combined terrestrial reference frame (TRF) solution for station positions and velocities. Major goals of this TRF computation were:
(1) the validation of the various components of the ITRS Combination Center; (2) the verification and enhancement of the combination strategy; (3) the quality assessment of the combined solution and an external comparison with ITRF2000; (4) the identification and analysis of remaining deficiencies regarding TRF combination; and (5) recommendations for the computation of future ITRF realizations.

This documentation consists of two main parts: Firstly, it presents the major components and the combination methodology of the ITRS Combination Center at DGFI (chapter 2) as well as the mathematical background for the combination, which is based on the level of unconstrained normal equations (chapter 3). The second part focusses on the computation of the terrestrial reference frame realization 2003. Chapter 4 describes the input data used for this TRF computation. The processing strategies and results for the intra- and inter-technique combination are presented in chapters 5 and 6, respectively. Chapter 7 concentrates on the TRF accuracy evaluation and presents the results of a comparison with ITRF2000. The current status regarding TRF computations, remaining deficiencies and recommendations for the future are addressed in chapter 8. Finally, chapter 9 presents conclusions and future plans.

Figures and short tables are included in the respective chapters, whereas long tables of more than one page are provided in the appendix.

2 ITRS Combination Center at DGFI

2.1 Overview

The ITRS Combination Center (ITRS CC) at DGFI is closely related to the joint IERS Combination Research Center at DGFI, the "Forschungseinrichtung Satellitengeodäsie, TU München" (FESG), and the "Geodätisches Institut, Universität Bonn" (GIUB), all embedded in the "Forschungsgruppe Satellitengeodäsie" (FGS). A significant part of the work is funded by the programme GEOTECHNOLOGIEN of the "Bundesministerium für Bildung und Forschung" (BMBF) and the "Deutsche Forschungsgemeinschaft" (DFG). In addition to the components mentioned above this IERS project also includes the IERS Analysis Coordination (FESG), the IERS Central Bureau at the "Bundesamt für Kartographie und Geodäsie" (BKG), and the IERS Combination Research Center at the "GeoForschungsZentrum Potsdam" (GFZ).

The data flow and combination procedure of the ITRS CC is shown in figure 2.1. The main components of the ITRS CC are:

1. **ITRF database**: A database and information system for the IERS is under development at BKG (Schwegmann and Richter, 2003). In cooperation with BKG, the work at DGFI concentrates on ITRS relevant data and products, such as station information, local ties, SINEX files of the different space techniques, and TRF results.

2. **Data analysis and TRF combination**: This represents the major tasks of an ITRS CC. Specifically they are:

- Validation and analysis of submitted input data (SINEX files);
- Generation of unconstrained normal equations;
- Combination and solution of normal equations with the DGFI software DOGS-CS.

3. **Visualization and quality control**: The DGFI software DOGS-OV comprises various tools for the visualization of the individual solutions and combination results, as well as for the quality assessment and external comparisons (e.g., with ITRF2000).

2.2 Methodology for TRF combination

The combination methodology of the ITRS CC at DGFI is based on several major steps, described in the following sections:

- Validation and preprocessing (2.2.1),
- Datum realization (2.2.2),
- Intra-technique combination (2.2.3),
- Inter-technique combination (2.2.4).

2.2.1 Validation and preprocessing

Analysis of TRF input data: From the experiences of previous TRF computations it is well-known that the characteristics of the individual solutions are quite heterogeneous. Therefore it is essential to analyse them concerning various aspects, especially the suitability for the combination. The major tasks include (1) to check SINEX format compatibility; (2) to check solutions con-

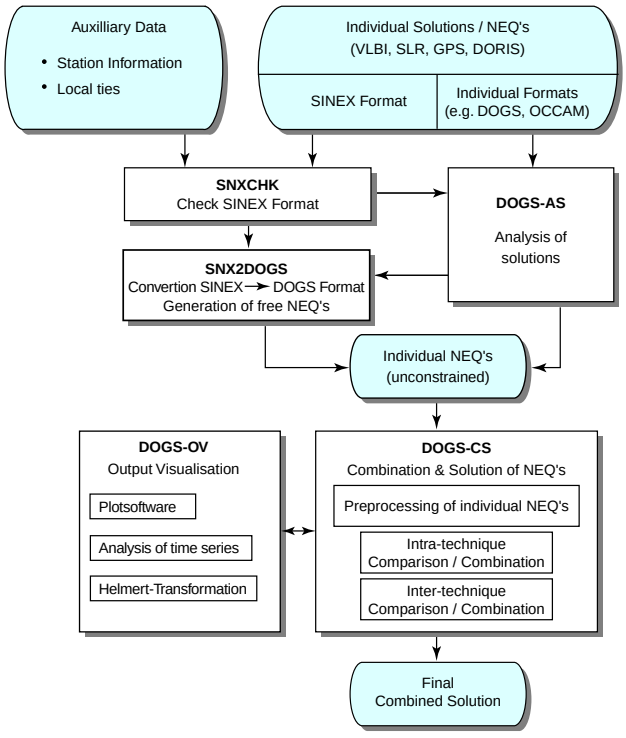

Fig. 2.1: *TRF combination procedure.*

cerning parameterization, constraints, datum realization; (3) to ensure that all constraints can be removed and to perform a rank defect analysis.

Datum characteristics of solutions: The geodetic datum of the contributing solutions is realized differently by the individual analysis centers. The datum characteristics of ITRF2000 submissions are: (1) loosely constrained solutions, which should result in very large standard deviations for the adjusted parameters; (2) minimum constrained solutions, for which constraints are introduced exclusively for the "non-observable" datum components; (3) over-constrained solutions with more constraints than necessary, so that the constraints have to be removed completely before the combination procedure in order to avoid network deformations.

In addition to these constraints (which are supposed to be documented in the SINEX files), the solutions might also be influenced by so-called "hidden" constraints. This can happen, if a-priori information is introduced for some "auxilliary" parameters which are correlated with station positions (e.g., troposphere parameters, clocks), or if velocities for different occupations on a site are set identical. Furthermore individual solutions may be implicitely constrained by the applied models, e.g. by the used gravity field that fixes the origin by means of the lower spherical harmonic coefficients (C_{10}, C_{11}, S_{11}).

A proof of such constraints is essential before performing the combination. This can preferably be done by removing the constraints from the individual solutions, accompanied by a rank defect analysis of the resulting normal equations.

Removing constraints: This is of major importance, since unremoved constraints may produce significant biases, systematic errors, and deformations in the combination results. The procedure and formulas are given in chapter 3.

Preprocessing: For some of the input data it may be necessary to perform various preprocessing steps, e.g., transformation of station positions to the reference epoch of the combined solution, renaming of stations with a wrong station information, a-priori reduction of poorly observed stations (e.g., less than one year of data, mobile stations with only few occupations).

2.2.2 Datum realization

The TRF realization consists of three-dimensional position coordinates for a specified reference epoch and station velocities derived from sufficiently long time series of space geodetic observations. The TRF datum is defined by the Earth's center of mass (geocenter) as the origin, a mean Earth rotation vector for the orientation, and a scale given by the velocity of light, as well as the rates of these seven parameters.

The individual space geodetic observations do not contain the complete information to realize the TRF datum. Satellite methods, such as SLR, GPS and DORIS, are (more or less) sensitive to geocenter motions relative to the TRF, because they use the geocenter as dynamical origin for computing the satellite orbits. VLBI is quasi-independent of the gravity field and does not contribute at all to the realization of the geocenter. Thus, it is necessary to introduce no-net-translation (NNT) conditions for VLBI. All the space geodetic techniques contain, in principle, information to realize the TRF scale by fixing the speed of light.

Since (1) the orientation of the frame is attached to a mean rotation vector which can only be defined with respect to an external frame, and (2) the computation of the satellite orbits needs an external inertial frame, and (3) both external frames are supposed to coincide in the ICRF, we have to solve for the EOP parameters connecting the TRF with the adopted external quasi inertial frame. The separation of station position and velocity coordinates from the EOP parameters is achieved by appropriate condition equations, the (NNR) conditions, minimizing the common rotation of the TRF solution w.r.t. its approximate values for the orientation at the reference epoch, and minimizing the horizontal velocity field over the whole Earth for the time evolution of orientation (e.g., Drewes, 1998; Drewes and Meisel, 2003; Altamimi et al., 2003).

For each of the different techniques' solutions we realize the datum in a consistent way by applying minimum constraints in the form of NNR and NNT conditions depending on the rank defect of the particular space technique. For each technique we use a subset of stations, the core stations, to realize the datum w.r.t. ITRF2000. These core stations were selected with regard to

data quality and a good spatial distribution over the Earth's surface. As described in chapter 3, the datum conditions were applied as pseudo observations with appropriate weights.

2.2.3 Intra-technique combination

The idea within the IERS and the participating groups is, that the combination of data and/or solutions of each observation technique shall be done by the responsible technique centres (services), i.e. IGS, ILRS, IVS and IDS. At present, combined multi-year TRF solutions with station positions and velocities are produced only by the IGS; in future also the other services will provide such products. Thus, the ITRS Combination Centers have to perform the intra-technique combination of the VLBI, SLR and DORIS data.

At DGFI, these combinations are performed on the basis of unconstrained normal equations. Before combining the individual normal equations of a particular space technique, the corresponding solutions have to be compared to identify possible problems, which can cause systematic effects (biases) in the combination results. These comparisons require a consistent datum realization for the contributing solutions, as described in the previous section. Other important tasks include the computation of weighting factors, the handling of different velocity estimations for a station, as well as the detection and rejection of outliers. The data and processing flow is shown in figure 2.2.

Weighting: In principle, individual solutions of a particular space technique should have the same accuracy level for the estimated station positions and velocities, since the analysis centers use (almost) identical observations and the software systems should be consistent with the IERS Conventions. However, the standard deviations for the estimated parameters might differ between solutions, because of (small) differences regarding the implemented models, the parameterization, the a-priori weighting, the observations rejected in the processing, etc. Thus the solutions have to be balanced against each other by estimating weighting factors. This is done by computing mean standard deviations (formal errors) for station positions for a subset of core stations, which are then used to estimate scaling factors for the corresponding normal equations. This procedure provides relative weights for the solutions of a single technique, whereas the "absolute" variance level needs to be estimated within the inter-technique combination.

Equating station velocities: For each of the techniques, there are stations with two or more occupations (e.g., mobile VLBI and SLR systems, stations with equipment changes). This raises the question how to handle different velocity estimations for these occupations. Typically, the velocities of different occupations are equated to stabilize the solutions. But on the other hand, "real" velocity differences may exist, because of local site dependent effects (e.g., subsidences) or changes in motion due to geodynamic effects (e.g., earthquakes). Then, the equating of velocities may produce systematic errors in the combination results. Thus we used the different (not equated) velocity estimations for a particular station together with their standard deviations to decide whether the velocities should be equated or not. In principle, statistical tests can be applied, but it has to be considered that probably the data do

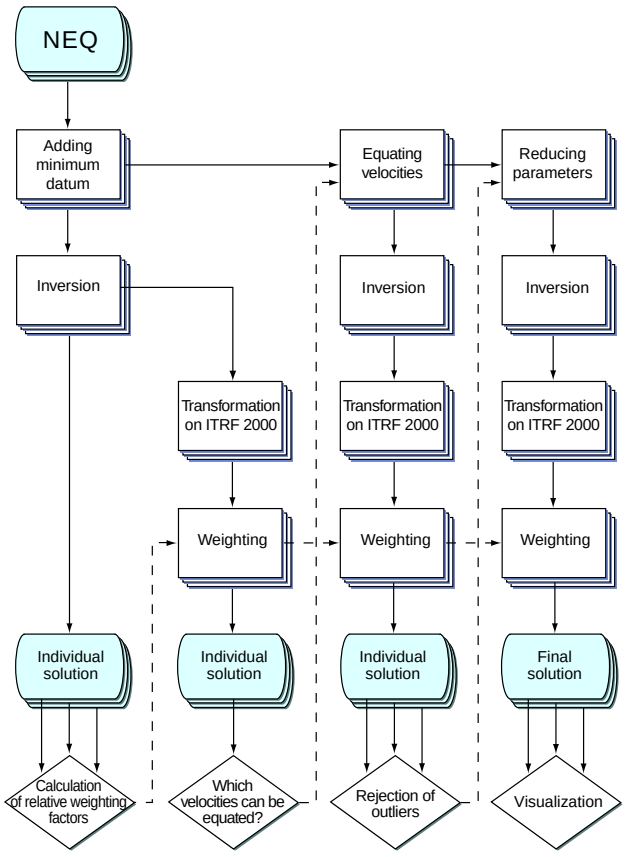

Fig. 2.2: *Intra-technique comparison.*

not follow a normal distribution (e.g., due to systematic errors in the solutions). Equating station velocities is dchieved by pseudo observations with appropriate weights. The results obtained for the different techniques are presented in chapter 5. These pseudo observations are not included in the combined intra-technique normal equations, they are primarily used to stabilize the solutions (e.g., for outlier detection). The final equating of station velocities is done within the inter-technique combination (see chapter 6).

Outlier detection: Outliers, such as erroneous station position and/or velocity estimations in a particular solution can lead to "biased" results and to deformations in the combined intra-technique network. We have implemented an iterative procedure to identify and reduce outliers in the contributing solutions. We estimate station position and velocity differences of a single solution compared to the mean of the other solutions, along with their standard deviations. Based on this information we decide whether an adjusted parameter in a particular solution can be considered as an outlier or not.

Combined intra-technique solution: The individual normal equations of each of the space techniques are added by applying the estimated weighting factors. Then minimum datum conditions (as described in section 2.2.2) are introduced. The resulting normal equation system is inverted to generate the combined intra-technique solution. Figure 2.3 shows the methodology of the intra-technique combination.

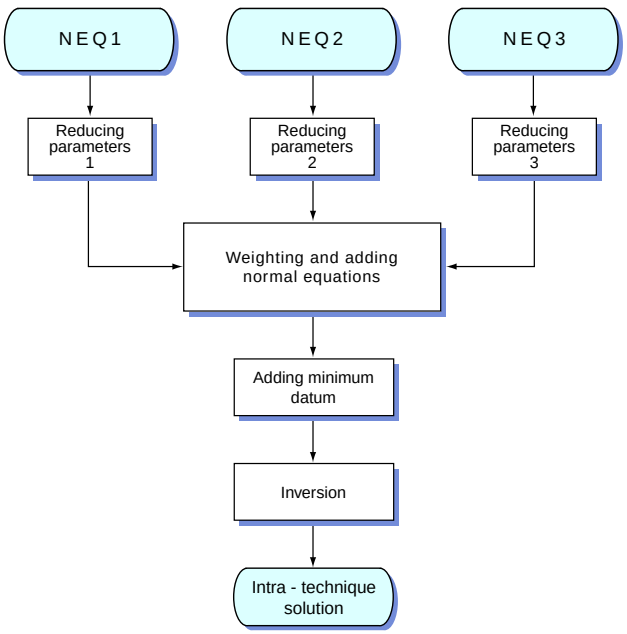

Fig. 2.3: *Intra-technique combination.*

2.2.4 Inter-technique combination

Input for the inter-technique combination are the combined intra-technique normal equations of VLBI, SLR, GPS and DORIS. The data flow and procedure for the inter-technique combination is shown in figure 2.4. We compare the solutions of the different techniques (especially at co-location sites) to identify systematic effects and outliers. Other important steps are the estimation of weighting factors, the handling of local ties, the equating of station velocities, and the datum realization for the combined solution.

Weighting: The weighting of the heterogeneous input from the different space geodetic observation methods may be performed by variance component estimation as described, e.g., in (Koch, 1999). This method has been

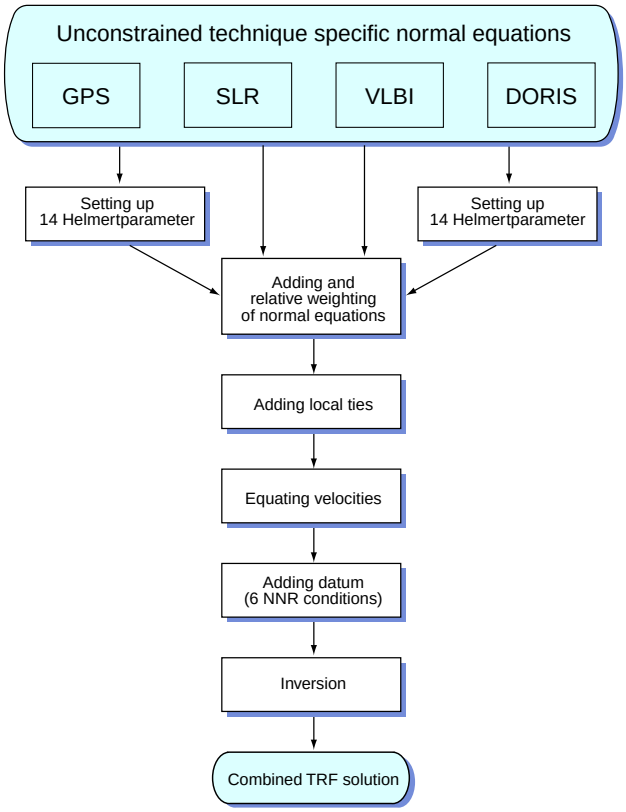

Fig. 2.4: *Inter-technique combination.*

implemented at DGFI (Kelm, 2003), and detailed studies for the feasibility of this method are carried out under the specific conditions of the inter-technique combination. Problematic issues are a proper implementation of local tie information and the handling of remaining biases between techniques. The weighting procedure applied for the computation of the TRF realization 2003 is described in chapter 6.

Local tie implementation: The local tie information (i.e. intra-site vectors) at co-location sites is a key element for the inter-technique combination. From various TRF computations (e.g., ITRF2000) it is well-known that the available local ties (see ftp://lareg.ensg.ign.fr/pub/itrf/itrf2000/tiesnx/) are quite heterogeneous regarding accuracy and the completeness of information (e.g., missing standard deviations and/or variance-covariance matrices for many ties), and that some intra-site vectors are not well determined or even dubious. Considering this situation, it is essential, a) to validate the local ties, b) to select suitable local ties for the combination, and c) to ensure that poorly observed ties do not degrade the internal accuracy of the individual space techniques within the combination. The procedure for this validation and the selection of suitable local ties is described in section 6.2. Finally, the local ties are added as pseudo observations with appropriate weights to the combined inter-technique normal equations.

Equating station velocities: Are velocity estimates for different occupations at co-location sites identical? In principle, they should be identical within certain error limits, if no biases between different techniques' solutions exist and if the site conditions are stable for the co-located instruments. In reality, these assumptions are probably not always fulfilled, i.e., different motions between techniques may occur. Especially, if the observation periods for co-located instruments are disjunctive, changes in site motion (e.g., caused by geodynamic effects) can lead to "real" differences in the velocity estimates. Thus, equating the co-located velocity estimations (as it was done in previous ITRF computations) may lead to biases in the combined solution. Therefore we do not in advance force velocity estimates at co-location sites to be identical. Instead we use the velocity differences between techniques together with their standard deviations to decide whether velocities at a co-location site can be equated or not. Additional information, like the time series of station positions is helpful to validate the decision. The equating of velocities is performed by adding pseudo observations with appropriate weights. However, it has to be considered that this procedure may yield different technique-specific velocities at co-location sites, which is not the case with ITRF2000, in which one common velocity estimate is computed for co-located stations.

Combined inter-technique solution: The combined VLBI, SLR, GPS and DORIS normal equations are added by applying the weighting factors between the different space techniques. The resulting normal equations are completed by pseudo observations for the selected local ties and for equating velocities at co-location sites. To generate the combined TRF solution, we add datum conditions and invert the resulting normal equation system. The geodetic datum is realized with NNR conditions for the orientation offsets and their rates w.r.t. ITRF2000 station positions and velocities by using a subset of reliable and globally distributed stations of each technique. Currently, the origin (translation parameters and their rates) is realized by SLR, and the scale and its rate by SLR and VLBI. In the future, also GPS and DORIS may contribute to realize the datum of the combined TRF solution.

2.3 Description of relevant software

Various software programs of the DGFI Orbit and Geodetic Parameter Estimation System (DOGS) are used by the ITRS CC at DGFI. The relevant software may be classified as follows:

Validating, unconstraining and reformatting software: For checking the SINEX format of the contributing solutions, generating unconstrained normal equations, and reformatting SINEX into DOGS-CS format (and vice versa) the following programs were developed:

SNXCHK: This program validates the contributing SINEX solution files regarding

various aspects, such as format errors, missing information or inconsistencies of the contents. The official SINEX format description (see ftp://alpha.fesg.tu-muenchen.de/iers/sinex/format), the station information of the ITRF data base (e.g., DOMES number, 4-char ID, site names, CDP number) serve as a reference. Furthermore, the IGS log files are used to verify the GPS information about antennas, receivers, observation time spans, etc.

SNX2DOGS: The program SNX2DOGS transforms the normal equation systems and/or solutions from SINEX into DOGS-CS format. If free normal equation systems are provided in SINEX format, the reformatting into DOGS-CS format can be performed directly. If (loosely) constrained SINEX solutions are provided, the constraints have to be removed to generate the unconstrained normal equations.

DOGS2SNX: This program allows the reformatting of the combined solution from DOGS-CS into SINEX format. The SINEX blocks containing the major adjustment results are directly obtained from DOGS-CS. Additional scripts and programs are necessary to generate the complete SINEX file, including solution comments, header information as well as the complete set of station information.

DOGS-AS (Analysis of Solutions): This program package provides tools for the analysis of space geodetic solutions and combination results. For numerical algorithms OCTAVE software and DOGS-CS program tools are included. The following tasks may be performed with DOGS-AS:

- conversion of various formats;
- rank defect analysis of space geodetic solutions (eigenvalue and rank defect type analysis);
- reduction of constraints and generation of free normal equation matrices;
- comparison of solutions;
- combination of normal equation systems and application of minimal constraints;
- variance component estimation.

DOGS-CS (Combination and Solution): This software package consists of various programs to combine and solve systems of equations obtained from the same and/or different observation types. It enables various features for the combination of space geodetic data and/or solutions (e.g., elimination and reduction of auxilliary parameters, equating parameters, performing parameter transformations, as well as a flexible handling of local tie information and datum conditions). Some relevant programs of the DOGS-CS software package are:

CS_ADD: Adding normal equations and/or observation equations;

CS_COND: Generating condition equations, e.g. for the datum definition, the handling of local ties, and equating station velocities;

CS_ELIM: Eliminating parameters by various relations to other parameters or approximate values, e.g. by equating two parameters;

CS_INPAR: Introducing additional parameters to a given system of equations, e.g. setting up Helmert-transformation parameters, parameter velocities or periodic motions;

CS_INVERT: Inversion and solution of normal equation systems;

CS_REDUC: Reducing parameters from a system of equations;

CS_RENAM: Renaming parameters;

CS_RESOL: Back-substitution and solution of reduced parameters;

CS_TRAFO: Parameter transformations as a similarity mapping, a change of approximate values, and a epoch transformation of a mathematical model of, e.g., station coordinates.

DOGS-OV (Output Visualization): This software package comprises various tools for the analysis and visualization of the combination results. All programs are designed to read different input formats, e.g., SINEX, DOGS format. Some relevant routines are:

OV_TIMESERIES: Analyses and visualization of parameter time series using software such as GNUPLOT, MATLAB or OCTAVE.

OV_HELMERT: Helmert transformation program. It comprises an epoch conversion, an estimation of transformation parameters, and a calculation of residuals in cartesian and spherical coordinates.

OV_MAP: Create maps to visualize station velocities (including error ellipses) using the GMT software package.

3 Mathematical foundation

In the following the most important formulae of the several steps of combination are given and explained. The used combination strategy bases on the combination of normal equations. The resulting adjustment problem is solved in a least squares adjustment according to the Gauß-Markov model.

3.1 Preliminaries

Given a vector $q \in \mathbb{R}^m$ of observations, a set of $n \leq m$ parameters, arranged in a vector $p \in \mathbb{R}^n$, has to be adjusted such that the model $f(p)$ is the "best" approximation to the measurements q. The problem is linearized in a neighborhood of given a-priori values p^o for p.

1. The **functional model** is the linearized observation equations

$$Ax \;=\; b + v \;=\; b - e \qquad (3.1)$$

with the design matrix $A = \dfrac{\partial f}{\partial p}(p^o) \in \mathbb{R}^{m \times n}$

vector of variables $x = p - p^o \in \mathbb{R}^n$

observation vector $b = q - f(p^o) \in \mathbb{R}^m$

vector of residuals $v = Ax - b \in \mathbb{R}^m$

vector of errors $e = -v \in \mathbb{R}^m$.

2. The **linear least squares problem** is to find the unique solution $\hat{x}$ of (3.1) which minimizes the weighted square sum of residuals or error norm

$$e^T P e \;=\; v^T P v \;=\; \|v\|_P^2 \;=\; \|Ax - b\|_P^2$$

with a positive definite weight matrix $P \in \mathbb{R}^{m \times m}$. The set of all solutions to the linear least squares problem,

$$\mathcal{S}(A,b) \;:=\; \left\{ x \in \mathbb{R}^n \;\middle|\; \|Ax - b\|_P = \min \right\},$$

is characterized by the condition

$$x \in \mathcal{S}(A,b) \quad \Longleftrightarrow \quad A^T P(b - Ax) \;=\; 0 \qquad (3.2)$$

If in the observation space orthogonality is defined by the norm-generating scalar product $\langle u, v \rangle_P = u^T P v$, then (3.2) is an orthogonality condition saying that the residuals $v = Ax - b$ are orthogonal to the range of A, $\mathcal{R}(A)$, which is spanned by the columns of A. With respect to the norm-generating scalar product the adjoint of the linear mapping A is defined by $A^* = A^T P$. Hence, $\mathcal{S}(A,b) = A^- b + \mathcal{N}(A)$, where A^- is a generalized inverse of A.

From (3.2) it follows that a least squares solution $\hat{x} \in \mathcal{S}(A,b)$ satisfies the **normal equations**

$$Nx \;=\; y \quad \text{with} \quad N = A^T P A\,, \quad y = A^T P b\,.$$

The solution $\hat{x}$ is unique if and only if $\operatorname{rank}(A) = \operatorname{rank}(A^T P A) = n$. In that case, it holds

$$\hat{x} \;=\; N^{-1} y \;=\; (A^T P A)^{-1} A^T P b.$$

3. The **Gauß-Markov model** is the statistical equivalent to the above-mentioned least squares problem. Here, the vector v in (3.1) is assumed to be a random vector with expectation and variance given by

$$\mathcal{E}(v) \;=\; 0\,, \qquad \mathcal{V}(v) \;=\; C(v,v) \;=\; \sigma_0^2 P^{-1}.$$

The variance-covariance matrix splits into a variance factor σ_0^2 and a positive definite cofactor matrix P^{-1}. Secondly, it is assumed that v is the only stochastic quantity in the model (3.1), then the variance of v equals the variance of the observations. Let A have full rank n. Then the best (minimum variance) unbiased linear estimate for x is the solution of the least squares problem

$$\min_x \|Ax - b\|_P^2\,.$$

If $\hat{x}$ denotes the estimated vector of corrections to the parameters p, the further elements of the solution get the following statistical interpretation

residuals of observations $v \;=\; A\hat{x} - b$

cofactor matrix of estimates $N^{-1} \;=\; (A^T P A)^{-1}$

a-posteriori variance factor $\hat{\sigma}_0^2 \;=\; \dfrac{v^T P v}{m - n}$

variance of corrections $C(\hat{x}, \hat{x}) \;=\; \hat{\sigma}_0^2 N^{-1}$

where m is the number of observation equations and n is the number of solved unknowns.

4. A linear system of equations according to the Gauß-Markov model is defined by the quantities

$$\begin{aligned} \text{observation equations:} \quad & \{A,\ b,\ P,\ \sigma_0^2,\ p^o\} \\ \text{normal equations:} \quad & \{N,\ y,\ b^TPb,\ \sigma_0^2,\ p^o\} \\ \text{solution system:} \quad & \{N^{-1},\ \hat{x},\ v^TPv,\ \hat{\sigma}_0^2,\ p^o\} \end{aligned}$$

The relation between the square sum of observations and residuals is the numerically sensitive difference

$$b^TPb \ - \ v^TPv \ = \ y^T\hat{x}\,.$$

5. A **change of variance factor** may become necessary, for instance, when combining systems of equations. In addition, the variance level is rarely known exactely.

For the moment, let us regard P, N, y, b^TPb, and v^TPv as functions of σ_0. In the definition of the Gauß-Markov model, the variance was arbitrarily decomposed into a variance factor σ_0^2 and a cofactor matrix $Q = P^{-1}$,

$$C(b,b) \ = \ \sigma_0^2\, Q \ = \ \sigma_0^2\, P^{-1}.$$

Inversion of this equation yields

$$P(\sigma_0) \ = \ \sigma_0^2\, C(b,b)^{-1} \ = \ \sigma_0^2\, P(1)\,.$$

Therefrom, identical results are derived for $N = A^TPA$, $y = A^TPb$, b^TPb, and v^TPv. Finally, we have the σ_0-transformation rules

$$\begin{aligned} P(\tilde{\sigma}_0) \ &= \ \Big(\frac{\tilde{\sigma}_0}{\sigma_0}\Big)^2 \cdot \ P(\sigma_0) \\ N(\tilde{\sigma}_0) \ &= \ \Big(\frac{\tilde{\sigma}_0}{\sigma_0}\Big)^2 \cdot \ N(\sigma_0) \\ y(\tilde{\sigma}_0) \ &= \ \Big(\frac{\tilde{\sigma}_0}{\sigma_0}\Big)^2 \cdot \ y(\sigma_0) \\ b^TP(\tilde{\sigma}_0)b \ &= \ \Big(\frac{\tilde{\sigma}_0}{\sigma_0}\Big)^2 \cdot \ b^TP(\sigma_0)b \\ v^TP(\tilde{\sigma}_0)v \ &= \ \Big(\frac{\tilde{\sigma}_0}{\sigma_0}\Big)^2 \cdot \ v^TP(\sigma_0)v \end{aligned} \qquad (3.3)$$

3.2 Combining uncorrelated linear systems

Consider two linear Gauß-Markov models with uncorrelated observation vectors, denoted at the observation level by

$$\{A_i,\ b_i,\ P_i,\ \sigma_{0i}^2,\ p_i^o\}\,, \quad i = 1,2\,.$$

Adapting the parameter vectors: If the systems have different sets of parameters to be corrected, then the parameter vectors are conformed to each other by inserting zeros between the columns of A_i (columns and rows of N_i respectively). Thus, we can assume without restriction that the parameter vectors coincide: $p_1 = p_2 =: p$.

Adapting the a-priori values: If two systems with $p_1{=}p_2{=}p$ differ in their a-priori values p_i^o, then the second system has to be transformed to the a-priori values of the first system. This is obtained by expressing the correction x_2 through x_1

$$x_2 \ = \ p - p_1^o + p_1^o - p_2^o \ = \ x_1 + (p_1^o{-}p_2^o).$$

Inserting that expression into the corresponding equations yields

$$\begin{aligned} \tilde{A}_2x_1 \ &= \ \tilde{b}_2 \quad \text{with} \begin{cases} \tilde{A}_2 \ = \ A_2\,, \\ \tilde{b}_2 \ = \ b_2 \ - \ A_2(p_1^o{-}p_2^o)\,, \end{cases} \\ \tilde{N}_2x_1 \ &= \ \tilde{y}_2 \quad \text{with} \begin{cases} \tilde{N}_2 \ = \ N_2\,, \\ \tilde{y}_2 \ = \ y_2 \ - \ N_2(p_1^o{-}p_2^o)\,, \end{cases} \\ \tilde{b}_2^TP_2\tilde{b}_2 \ &= \ b_2^TP_2b_2 \ - \ 2(p_1^o{-}p_2^o)^Ty_2 \\ &\quad + \ (p_1^o{-}p_2^o)^TN_2(p_1^o{-}p_2^o)\,. \end{aligned} \qquad (3.4)$$

Combining the equations: Assume now that both systems coincide in the parameter vector p and its a priori values p^o. Hence, the corrections are equal: $x_1 = x_2 =: x$. Then, combining the observation equations simply means to stack the equations to a system $Ax = b + v$ with

$$A \ := \ \begin{bmatrix} A_1 \\ A_2 \end{bmatrix}, \quad b \ := \ \begin{bmatrix} b_1 \\ b_2 \end{bmatrix}, \quad v \ := \ \begin{bmatrix} v_1 \\ v_2 \end{bmatrix}.$$

The assumption that the observations b_1 and b_2 are uncorrelated determines the combined variance matrix as

$$\mathcal{V}(b) \ = \ \begin{bmatrix} \mathcal{V}(b_1) & 0 \\ 0 & \mathcal{V}(b_2) \end{bmatrix} \ = \ \begin{bmatrix} \sigma_{01}^2\, P_1^{-1} & 0 \\ 0 & \sigma_{02}^2\, P_2^{-1} \end{bmatrix}.$$

There is the freedom to prescribe the variance factor of the combined system, σ_0^2. With it the weight matrix of the combined system becomes

$$P \ = \ \sigma_0^2\, \mathcal{V}(b)^{-1} = \ \begin{bmatrix} \dfrac{\sigma_0^2}{\sigma_{01}^2}P_1 & 0 \\ 0 & \dfrac{\sigma_0^2}{\sigma_{02}^2}P_2 \end{bmatrix}.$$

A simple calculation leads to

$$\begin{aligned} N &= \frac{\sigma_0^2}{\sigma_{01}^2}\cdot N_1 + \frac{\sigma_0^2}{\sigma_{02}^2}\cdot N_2 \\ y &= \frac{\sigma_0^2}{\sigma_{01}^2}\cdot y_1 + \frac{\sigma_0^2}{\sigma_{02}^2}\cdot y_2 \\ b^TPb &= \frac{\sigma_0^2}{\sigma_{01}^2}\cdot b_1^TP_1b_1 + \frac{\sigma_0^2}{\sigma_{02}^2}\cdot b_2^TP_2b_2 \end{aligned} \qquad (3.5)$$

In practice, two systems of normal equations are added using

$$N = \lambda_1\frac{\sigma_0^2}{\sigma_{01}^2}\cdot N_1 + \lambda_2\frac{\sigma_0^2}{\sigma_{02}^2}\cdot N_2.$$

The factors λ_1 and λ_2 are weighting factors. They are introduced to account for different variance levels of the normal equations.

Shrinkage and embedding: As long as two systems of equations are combined, we could assume that $p_1 = p_2$. When K systems of equations are summed up, it may become necessary (in variance component estimation e.g.) to distinguish the parameters of the k-th system, p_k, and the parameters of the combined system, p, which are the union of all the elements of the p_k. The relation between p_k and p is uniquely defined as a linear mapping $E_k : p \longmapsto p_k$ the matrix of which contains in every row precisely one 1 and 0 elsewhere. Since the rows of the matrix E_k are linearly independent, it follows

$$E_kE_k^T = \mathrm{I}, \qquad E_k^+ = E_k^T(E_kE_k^T)^{-1} = E_k^T.$$

Thus we have got well matched mappings

$$\begin{aligned} &\text{shrinkage:} && p_k = E_k\,p, \\ &\text{embedding:} && \bar{p} = E_k^T p_k. \end{aligned} \qquad (3.6)$$

Conformality of approximate values means $p_k^o = E_kp^o$. Then, by subtracting this, we get for the corrections as well

$$x_k = E_k\,x \quad \text{and} \quad \bar{x} = E_k^T x_k.$$

In a computer program there is no need of E_k. Its functionality is substituted by a vector index.

3.3 Constraining singular systems

A linear least squares problem of non-full rank $r < \min\{n,m\}$ has an infinite solution space $\mathcal{S}(A,b) = x_0 + \mathcal{N}(A)$. In order to find a unique "best" solution, the solution or the model is **constrained** with additional information $Bx - c = 0$ where $B \in \mathbb{R}^{p\times n}$ and $m + p \geq n$. Constraining the solution or **sequential** minimization means:

Minimize $\|Bx - c\|^2$ for $x \in \mathcal{S}(A,b)$.

Constraining the model or **hybrid** minimization:

Minimize $\|Ax - b\|_P^2 + \|Bx - c\|^2$ for $x \in \mathbb{R}^n$.

Geodesy uses the second method, usually speaking of "fixing the datum" or "regularization".

The normal equations for the second method are

$$\left(A^TPA + B^TB\right)x = A^TPb + B^Tc \qquad (3.7)$$

which equally are the normal equations of the extended linear model

$$\begin{bmatrix} A \\ B \end{bmatrix} x = \begin{bmatrix} b \\ c \end{bmatrix} + \begin{bmatrix} v \\ w \end{bmatrix}.$$

These normal equations have always a solution. Remember that generally holds

$$\begin{aligned} \mathcal{N}\left(\begin{bmatrix} A \\ B \end{bmatrix}\right) &= \mathcal{N}(A) \cap \mathcal{N}(B) && \subset \mathbb{R}^n \\ \mathcal{R}\left(\begin{bmatrix} A \\ B \end{bmatrix}\right) &= \mathcal{R}\left(\begin{bmatrix} A \\ 0 \end{bmatrix}\right) \oplus \mathcal{R}\left(\begin{bmatrix} 0 \\ B \end{bmatrix}\right) && \subset \mathbb{R}^{m+p} \\ \mathcal{R}\left(\begin{bmatrix} A \\ B \end{bmatrix}^*\right) &= \mathcal{R}(A^TP) + \mathcal{R}(B^T) && \subset \mathbb{R}^n. \end{aligned} \qquad (3.8)$$

Sufficient constraints: $Bx - c = 0$ will be called **sufficient constraints**, if the constrained least squares problem has a unique solution $\hat{x}_c$. That is the case if and only if any of the following three equivalent conditions holds:

$$\begin{aligned} &\text{(a)} \quad \operatorname{rank}\begin{bmatrix} A \\ B \end{bmatrix} = n \\ &\text{(b)} \quad \mathcal{N}(A) \cap \mathcal{N}(B) = \{0\} \\ &\text{(c)} \quad \mathcal{R}(A^TP) + \mathcal{R}(B^T) = \mathbb{R}^n. \end{aligned} \qquad (3.9)$$

This follows from (3.8) and from

$$\begin{aligned} \mathcal{R}(A^TP) + \mathcal{R}(B^T) &= \mathcal{R}\left(\begin{bmatrix} A \\ B \end{bmatrix}^*\right) = \\ &= \mathcal{N}\left(\begin{bmatrix} A \\ B \end{bmatrix}\right)^\perp = \left(\mathcal{N}(A) \cap \mathcal{N}(B)\right)^\perp. \end{aligned}$$

Since $\mathbb{R}^n$ is spanned by $\mathcal{R}(A^TP)$ and $\mathcal{R}(B^T)$, it must hold: $\operatorname{rank} B \geq n - \operatorname{rank} A = n - r$ or

$$\begin{aligned} \dim\mathcal{R}(B) &\geq n - \dim\mathcal{R}(A) \\ \dim\mathcal{N}(B) &\leq n - \dim\mathcal{N}(A) \end{aligned}$$

Minimum constraints: We define minimum constraints to be sufficient constraints with minimal rank: $\operatorname{rank} B = n - \operatorname{rank} A$. From (3.9(c)) and

$$n = \operatorname{rank} A + \operatorname{rank} B = \operatorname{rank}(A^T P) + \operatorname{rank}(B^T)$$

follows that $Bx = c$ are minimum constraints if and only if any of the following equivalent conditions holds:

$$\begin{aligned} &\text{(a)} \quad \mathcal{R}(A^T P) \oplus \mathcal{R}(B^T) = \mathbb{R}^n \\ &\text{(b)} \quad \mathcal{N}(A) \oplus \mathcal{N}(B) = \mathbb{R}^n . \end{aligned} \tag{3.10}$$

Thus we have

$$\mathcal{R}(A^T P) \cap \mathcal{R}(B^T) = \{0\} .$$

Note that for minimum constraints, the matrix $B^T B$ must be singular, $\operatorname{rank}(B^T B) = \operatorname{rank}(B) = n - \operatorname{rank}(A) < n$.

Non-distorting constraints: If for instance the model equations (3.1) determine the inner geometry of a network but not its position in space, and the unknowns of the problem are the absolute positions of the nodes, the design matrix A must be singular. In such a case, optimal constraints should remove the singularity without distorting the inner geometry of the network as far as determined by the model $Ax = b$. The solution of the constrained equations, $\hat{x}_c$, must satisfy the model equations (3.1) as good as any solution of the unconstrained problem, $\hat{x}_u \in \mathcal{S}(A, b)$, which means that

$$\|A\hat{x}_c - b\|_P = \|A\hat{x}_u - b\|_P = \min$$

or $\hat{x}_c \in \mathcal{S}(A, b)$, or with (3.2)

$$\begin{aligned} 0 = A^T P v(\hat{x}_c) &= A^T P b - A^T P A \hat{x}_c \overset{(3.7)}{=} \\ &= B^T B \hat{x}_c - B^T c = B^T\big(B\hat{x}_c - c\big). \end{aligned}$$

Therefore we define **non-distorting constraints** to be sufficient constraints such that the unique solution $\hat{x}_c$ also solves the unconstrained problem. The relationship to minimum constraints is thus:

> Minimum constraints always are non-distorting constraints.

Proof. Let $Bx = c$ be minimum constraints and $\hat{x}_c$ the solution to the constrained problem. Applying the orthogonality relation (3.2) to the constrained problem gives

$$\begin{aligned} &\hat{x}_c \in \mathcal{S}\Big(\begin{bmatrix} A \\ B \end{bmatrix}, \begin{bmatrix} b \\ c \end{bmatrix}\Big) \\ \overset{(3.2)}{\iff} \quad &0 = \begin{bmatrix} A \\ B \end{bmatrix}^* \left(\begin{bmatrix} A \\ B \end{bmatrix} \hat{x}_c - \begin{bmatrix} b \\ c \end{bmatrix} \right) = \\ &= \begin{bmatrix} A^T P, B^T \end{bmatrix} \begin{bmatrix} A\hat{x}_c - b \\ B\hat{x}_c - c \end{bmatrix} = \\ &= A^T P\big(A\hat{x}_c - b\big) + B^T\big(B\hat{x}_c - c\big) \\ \iff \quad &\xi := \underbrace{A^T P\big(A\hat{x}_c - b\big)}_{\in \mathcal{R}(A^T P)} = \underbrace{-B^T\big(B\hat{x}_c - c\big)}_{\in \mathcal{R}(B^T)} \\ \implies \quad &\xi \in \mathcal{R}(A^T P) \cap \mathcal{R}(B^T) = \{0\} \\ \implies \quad &\xi = 0 \overset{(3.2)}{\iff} \hat{x}_c \in \mathcal{S}(A, b) \qquad \text{qed.} \end{aligned}$$

The conversion is not true. As seen above, sufficient constraints are then non-distorting, if $\xi \in \mathcal{R}(A^T P) \cap \mathcal{R}(B^T)$ is the zero vector. Even if the constraints are non-minimal, i.e. $\mathcal{R}(A^T P) \cap \mathcal{R}(B^T) \neq \{0\}$, the zero vector is contained in the intersection of the two subspaces $\mathcal{R}(A^T P)$ and $\mathcal{R}(B^T)$. To it we will always find the appropriate constraints

Choose a solution $\hat{x} \in \mathcal{S}(A, b)$ and a constraint matrix $B \in \mathbb{R}^{p \times n}$ with $\mathcal{R}(A^T P) + \mathcal{R}(B^T) = \mathbb{R}^n$ and $\mathcal{R}(A^T P) \cap \mathcal{R}(B^T) \neq \{0\}$. Then by (3.9) it holds that $(A^T P A + B^T B)$ is invertible and $Bx = c$ are sufficient but non-minimal constraints for all $c \in \mathbb{R}^p$. For $B^T B\hat{x} \in \mathcal{R}(B^T B) = \mathcal{R}(B^T)$ exists a $c \in \mathbb{R}^p$ with

$$\text{(a)} \quad B^T B\hat{x} = B^T c,$$

hence $\xi = B^T(c - B\hat{x}) = 0$. Since $\hat{x} \in \mathcal{S}(A, b)$,

$$\text{(b)} \quad A^T P A\hat{x} = A^T P b.$$

Adding (a) and (b) yields

$$(A^T P A + B^T B)\hat{x} = A^T P b + B^T c.$$

Hence $\hat{x}$ is the unique solution to the constrained problem with constraints $Bx = c$ and $\hat{x} \in \mathcal{S}(A, b)$.

Loose constraints: This notion still lacks a mathematical definition. It is used for **non-minimum constraints**, and the term "loose" should suggest that the weight of the constraints is such small that we may neglect their distorting effect on the equations or on the solution. By

(3.7) every solution of a suffciently constrained problem satisfies

$$\begin{aligned} b - A\hat{x}_c &= b - AN_c^{-1}(A^TPb + B^Tc) \\ c - B\hat{x}_c &= c - BN_c^{-1}(A^TPb + B^Tc) \\ y - N\hat{x}_c &= B^T\big(B\hat{x}_c - c\big)\,, \end{aligned}$$

where N_c denotes the constrained normal equation matrix $N + B^TB$. In case of non-distorting constraints if holds

$$0 = y - N\hat{x}_c = B^T\big(B\hat{x}_c - c\big)\,,$$

and for distorting constraints

$$0 \neq y - N\hat{x}_c = B^T\big(B\hat{x}_c - c\big)\,.$$

Thus a possible definition could be

$$0 \leq \big\| y - N\hat{x}_c \big\| = \big\| B^T\big(B\hat{x}_c - c\big) \big\| \leq \delta$$

whereby the term "loose" has to be complemented by a bound δ.

To look at another way, the weight $\lambda = 1/\sigma_c$ is separated from the constraining equations $Bx = c$ when summing them onto the given normal equations:

$$\big(N + \lambda^2\, B^TB\big)\, x = y + \lambda^2\, B^Tc\,. \qquad (3.11)$$

Hence there is a formal accordance with the **regularization** where λ^2 plays the role of the regularization or ridge parameter. To find an optimal λ or σ_c we have to minimize the bias or the error norm or the condition of the normal matrix N_c. Usually B^TB is singular (that is always the case if the constraining equations do not include all of the parameters of the given system). The behaviour of the condition number $\kappa(N_c)$ of a loosely constrained normal matrix as function of the weight λ is illustrated by the graph:

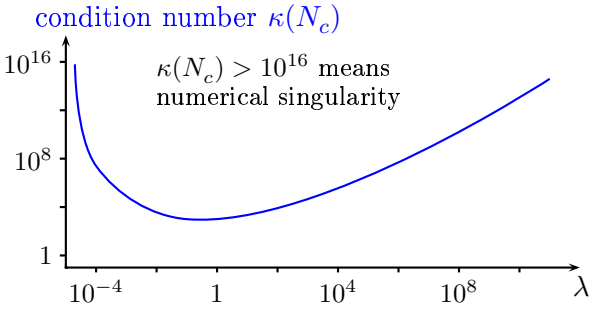

When applying loose constraints to singular systems, there arises a conflict: The regularization parameter should be large (i.e. at the level of the observation weights) to remove the singularities and it should be small to keep down bias and distortion.

Thus we recommend: Distinguish and handle apart (i) minimum constraints weighted at observation level to remove (known) rank deficiencies, and (ii) loose constraints with small weight for the purpose of regularization.

3.4 Reconstruction of free normal equations

Equation systems provided in the SINEX format contain either the normal equations itself or the solution of a constrained normal equation system (3.7). In the second case, the file must deliver the weighted square sum of residuals, v^TPv, the a-posteriori variance factor, $\hat{\sigma}_0^2$, the variance of the estimated parameters, $C(\hat{x},\hat{x})$, and the invertible a-priori variance, $C(x,x)$, which was applied as constraint. This information is used to reconstruct the free normal equation system

$$\begin{aligned} N &= \hat{\sigma}_0^2\, C(\hat{x},\hat{x})^{-1} - \sigma_0^2\, C(x,x)^{-1} \\ y &= \hat{\sigma}_0^2\, C(\hat{x},\hat{x})^{-1}\hat{x} \\ b^TPb &= v^TPv + y^T\hat{x} \\ &\text{(if not given explicitely).} \end{aligned} \qquad (3.12)$$

A critical point is the lack of the a-priori variance factor σ_0^2 in the SINEX format.

The a-priori variance factor of the reconstructed normal equations is now equal to $\hat{\sigma}_0^2$. If it should have the value 1.0, the system has to be rescaled according to (3.3). For equations (3.12), this leads to

$$\begin{aligned} \tilde{N} &= C(\hat{x},\hat{x})^{-1} - \frac{\sigma_0^2}{\hat{\sigma}_0^2}\, C(x,x)^{-1} \\ \tilde{y} &= C(\hat{x},\hat{x})^{-1}\hat{x} \\ b^T\tilde{P}b &= \frac{1}{\hat{\sigma}_0^2} v^TPv + \tilde{y}^T\hat{x} \\ \sigma_0^2 &= 1 \end{aligned} \qquad (3.13)$$

3.5 Regular transformations of the parameter space

Such transformations of parameters $p \in \mathbb{R}^n$ with approximate values p^o and corrections $x = p - p^o$ shall be composed of firstly a translation of the

approximate values, $p^o \mapsto p^o + t$, $x \mapsto x - t$, and secondly an affine mapping $p \mapsto Rp + d$,

$$\tilde{p} \;=\; Rp + d\,, \qquad \tilde{x} \;=\; R(x - t)\,.$$

For the application to normal and observation equations we have to use the inverse mapping with $T := R^{-1}$,

$$p \;=\; T\,(\tilde{p} - d)\,, \qquad x \;=\; T\,\tilde{x} + t\,.$$

It is important to distinguish the two translation vectors d and t. We speak of **conformal transformation of approximate values** or **conformal approximate values** if the approximate values p^o are transformed by the same rule as the parameters p. In this case it follows $t = 0$. Otherwise, the new approximate values $\tilde{p}^o$ have to be prescribed. In the latter case, t results from p^o and $\tilde{p}^o$. Thus, the general model reads

$$\begin{aligned} p \;&=\; T\,(\tilde{p} - d)\,, \qquad x \;=\; T\,\tilde{x} + t\,, \\ \tilde{p} \;&=\; T^{-1}p + d\,, \qquad \tilde{x} \;=\; T^{-1}(x - t)\,, \end{aligned}$$

with **conformal** approximate values

$$\tilde{p}^o \;=\; T^{-1}p^o + d\,, \qquad t \;=\; 0\,,$$

or with prescribed approximate values

$$\tilde{p}^o \;=\; \text{prescribed}, \qquad t \;=\; T(\tilde{p}^o - d) \;-\; p^o \qquad (3.14)$$

Applying (3.14) to observation equations gives

$$\begin{aligned} &\tilde{A} \;=\; AT\,, \quad \tilde{b} \;=\; b - At\,, \quad \tilde{P} \;=\; P\,, \\ &\tilde{b}^T P \tilde{b} \;=\; b^T P b \;-\; t^T A^T P\big(2b - At\big)\,, \qquad (3.15) \\ &\tilde{e} \;=\; e\,. \end{aligned}$$

Applying (3.14) to normal equations yields

$$\begin{aligned} &\tilde{N} \;=\; T^T N\,T\,, \quad \tilde{y} \;=\; T^T(y - Nt)\,, \\ &\tilde{b}^T P\,\tilde{b} \;=\; b^T P\,b \;-\; t^T\big(2y - Nt\big)\,, \qquad (3.16) \\ &\tilde{e}^T P\,\tilde{e} \;=\; e^T P\,e\,. \end{aligned}$$

Applying (3.14) to solutions yields

$$\begin{aligned} &\tilde{N}^{-1} \;=\; RN^{-1}R^T, \quad \tilde{x} \;=\; R(x - t)\,, \\ &\tilde{b}^T P\,\tilde{b} \;=\; b^T P\,b \;-\; t^T N\big(2x - t\big)\,, \qquad (3.17) \\ &\tilde{e}^T P\,\tilde{e} \;=\; e^T P\,e\,, \qquad R \;=\; T^{-1}\,. \end{aligned}$$

Besides station coordinates there may be additional types of parameters in a system of equations determining a TRF. Thus, the parameter vector will be partitioned into subvectors $\{\,\vec{p}_i,\, i = 0, \ldots, N\,\}$ such that each subvector has it's own transformation rule (3.14) represented by $(T_i,\, d_i,\, t_i)$. Thereby the unchanged parameters should be collected in $\vec{p}_0$ and transformed by means of $(T_0 = \mathrm{I},\, d_0 = 0,\, t_0 = 0)$. If the parameter vector p is arranged as

$$p \;=\; \big(\vec{p}_0^{\,T},\, \vec{p}_1^{\,T},\, \ldots\,,\, \vec{p}_N^{\,T}\big)^T,$$

then the system as a whole is transformed through

$$\begin{aligned} T \;&=\; \mathrm{diag}\big(T_0 = \mathrm{I},\, T_1,\, \ldots\,,\, T_N\big), \\ d \;&=\; \big(d_0^T = 0,\, d_1^T,\, \ldots\,,\, d_N^T\big)^T, \\ t \;&=\; \big(t_0^T = 0,\, t_1^T,\, \ldots\,,\, t_N^T\big)^T. \end{aligned}$$

In this way the parameter transformation of subvectors is extended to the whole system of equations.

We shall now give some applications of the parameter transformation (3.14). Thereby we may be restricted to appropriate subvectors of the parameters.

(a) Transformation of a-priori values

The change of approximate values $p^o \mapsto \tilde{p}^o$ is the most simple case of (3.14) with prescribed approximate values

$$T \;=\; R \;=\; \mathrm{I}\,, \quad d \;=\; 0\,, \quad t \;=\; \tilde{p}^o - p^o\,.$$

(b) Scaling parameters

When a unit is changed or equations are equilibrated, parameters have to be scaled. Scaling is the simple case of (3.14) with conformal approximate values,

$$T \;=\; \mathrm{diag}(s_1,\, s_2,\, \ldots,\, s_n)\,, \quad d \;=\; 0\,, \quad t \;=\; 0\,,$$

where $\tilde{p}_i = p_i / s_i$ for $i = 1, \ldots, n$. From (3.15) to (3.17) it follows in particular

$\tilde{A}_{jk} = A_{jk}\, s_k$	for observation equations,
$\tilde{N}_{jk} = s_j N_{jk} s_k$	for normal equations, and
$\tilde{N}_{jk}^{-1} = s_j^{-1} N_{jk}^{-1} s_k^{-1}$	for solutions.

(c) Transformation of parameters to a new model epoch

Let a physical parameter $p_i(t)$ be represented by a linear-trigonometric model relativ to epoch t_k,

$$p_i(t) = a_i(t_k) + (t-t_k)\,b_i(t_k) + \\ + c_i(t_k)\cos\big(\omega(t-t_k)\big) + s_i(t_k)\sin\big(\omega(t-t_k)\big),$$

and let the vector of the four model parameters

$$\vec{p}_i = \vec{p}_i(t_k) = \big(a_i(t_k),\, b_i(t_k),\, c_i(t_k),\, s_i(t_k)\big)^T$$

be a subvector of the parameter vector solved for. A transformation of the model epoch from t_0 to t_1 yields an equation of the form (3.14),

$$\vec{p}_i(t_1) = T_i^{-1}\vec{p}_i(t_0)\,, \quad T_i^{-1} = T_{\rm E}(t_1-t_0)\,,$$
$$\vec{p}_i(t_0) = T_i\;\vec{p}_i(t_1)\,, \quad T_i = T_{\rm E}(t_0-t_1)\,,$$

where

$$T_{\rm E}(\triangle t) = \begin{bmatrix} 1 & \triangle t & 0 & 0 \\ 0 & 1 & 0 & 0 \\ 0 & 0 & \cos(\omega\triangle t) & \sin(\omega\triangle t) \\ 0 & 0 & -\sin(\omega\triangle t) & \cos(\omega\triangle t) \end{bmatrix}.$$

Let us also note that $T_{\rm E}(0) = {\rm I}$ and

$$T_{\rm E}(\triangle t_2)\cdot T_{\rm E}(\triangle t_1) = T_{\rm E}(\triangle t_2 + \triangle t_1)\,.$$

(d) Datum transformation of position and velocity parameters

If a system of equations is given in a different geodetic datum, equations and approximate values have to be transformed to the datum of the other systems, using a 7-parameter similarity (1 scale factor, 3 rotation angles, 3 translation parameters) or a 14-parameter similarity (the 7 parameters from above and their rates in time). The similarity parameters themselves can be estimated using a Helmert transformation as described in section 3.6.

The seven similarity parameters shall be noted as

$\mu = \mu(t) \in \mathbb{R}$: the scale parameter,
$\alpha = \alpha(t) \in \mathbb{R}^3$: the Cardan angles of rotation,
$d = d(t) \in \mathbb{R}^3$: the translation vector of origin.

Then the transformation equations as applied to the cartesian coordinates of position $\vec{x}$ and velocity $\dot{\vec{x}}$ read

$$\begin{aligned} \tilde{\vec{x}} &= (1+\mu)R(\alpha)\,\vec{x} + d \\ \dot{\tilde{\vec{x}}} &= (1+\mu)R(\alpha)\,\dot{\vec{x}} + \dot{d} + \\ &\quad + \big((1+\mu)\dot{R}(\alpha) + \dot{\mu}R(\alpha)\big)\,\vec{x} \end{aligned} \qquad (3.18)$$

with $R = R_1(\alpha_1)R_2(\alpha_2)R_3(\alpha_3)$. Here we define the elementary rotations about the unit axes by

$$R_1(\varphi) = \begin{bmatrix} 1 & 0 & 0 \\ 0 & \cos\varphi & \sin\varphi \\ 0 & -\sin\varphi & \cos\varphi \end{bmatrix},$$

$$R_2(\varphi) = \begin{bmatrix} \cos\varphi & 0 & -\sin\varphi \\ 0 & 1 & 0 \\ \sin\varphi & 0 & \cos\varphi \end{bmatrix},$$

$$R_3(\varphi) = \begin{bmatrix} \cos\varphi & \sin\varphi & 0 \\ -\sin\varphi & \cos\varphi & 0 \\ 0 & 0 & 1 \end{bmatrix}.$$

Contrary to that convention, (Altamimi et al., 2002) use elementary rotations with opposite sign of the angle φ.

How can we obtain the form of (3.14) for the similarity transformation? For the 7-parameter transformation, the first equation of (3.18) is sufficient. And for the 14-parameter similarity, we have to rewrite (3.18) into

$$\begin{bmatrix} \tilde{\vec{x}} \\ \dot{\tilde{\vec{x}}} \end{bmatrix} = \begin{bmatrix} (1+\mu)R & 0 \\ (1+\mu)\dot{R}+\dot{\mu}R & (1+\mu)R \end{bmatrix}\begin{bmatrix} \vec{x} \\ \dot{\vec{x}} \end{bmatrix} + \begin{bmatrix} d \\ \dot{d} \end{bmatrix}.$$

The submatrix $(1+\mu)\dot{R}+\dot{\mu}R$ was neglected in the geodetic literature.

(e) Infinitesimal similarity transformation

We inspect the latter 7-parameter similarity transformation as a function of two variables,

$$H(\vec{x},\eta) = (1+\mu)R(\alpha)\,\vec{x} + d\,, \quad \eta = \begin{bmatrix} \mu \\ \alpha \\ d \end{bmatrix} \in \mathbb{R}^7.$$

Firstly, a Taylor series expansion of the function $\eta \longmapsto H(\vec{x},\eta)$ about $\eta^o = 0$ gives

$$H(\vec{x},\eta^o+\delta\eta) = \\ = H(\vec{x},0) + H_\eta(\vec{x},0)\cdot\delta\eta + \mathcal{O}(\|\delta\eta\|^2)$$

for $\delta\eta = \big[\,\delta\mu\;\delta\alpha^T\;\delta d^T\big]^T \to 0$, where

$$H(\vec{x},0) = \vec{x},$$
$$H_\eta(\vec{x},0) = \big[\,H_\mu(\vec{x},0)\;\; H_\alpha(\vec{x},0)\;\; H_d(\vec{x},0)\,\big]$$

and

$$H_\mu(\vec{x},0) = \vec{x} = \big[\,x_1\;\; x_2\;\; x_3\,\big]^T,$$

$$H_\alpha(\vec{x},0) = \begin{bmatrix} 0 & -x_3 & x_2 \\ x_3 & 0 & -x_1 \\ -x_2 & x_1 & 0 \end{bmatrix} = S(\vec{x})\,,$$

$$H_d(\vec{x},0) = {\rm I}_{3\times 3}$$

The derivative $H_\alpha(\vec{x},0)$ is the antisymmetric matrix $S(\vec{x})$ which represents the vector product $S(\vec{x})\,\delta\alpha = \vec{x}\times\delta\alpha = -\delta\alpha\times\vec{x} = -S(\delta\alpha)\cdot\vec{x} = S(-\delta\alpha)\,\vec{x}$. This allows to define an **infinitesimal similarity transformation of the first kind** as

$$\begin{aligned} h_1(\vec{x},\delta\eta) &:= \vec{x} + H_\eta(\vec{x},0)\cdot\delta\eta = \\ &= \vec{x} + \delta\mu\,\vec{x} + \begin{bmatrix} 0 & \delta\alpha_3 & -\delta\alpha_2 \\ -\delta\alpha_3 & 0 & \delta\alpha_1 \\ \delta\alpha_2 & -\delta\alpha_1 & 0 \end{bmatrix}\vec{x} + \delta\vec{d} \\ &= \begin{bmatrix} (1+\delta\mu) & \delta\alpha_3 & -\delta\alpha_2 \\ -\delta\alpha_3 & (1+\delta\mu) & \delta\alpha_1 \\ \delta\alpha_2 & -\delta\alpha_1 & (1+\delta\mu) \end{bmatrix}\vec{x} + \delta\vec{d} \end{aligned} \tag{3.19}$$

This represents an affinity, because the matrix has eigenvalues $(1+\delta\mu)$ and $(1+\delta\mu)\pm i\|\delta\alpha\|$ near to 1 if $\delta\mu$ and $\delta\alpha$ are small. It should be pointed out that the corresponding formula (A1) in the description of ITRF 2000 (Altamimi et al., 2002) has the opposite sign of the rotation angles according to an opposite definition of the elementary rotations $R_i(\alpha_i)$. The choice of sign of ITRF 2000 also entered into the IERS Conventions.

Secondly, the function $(\vec{x},\eta) \longmapsto H(\vec{x},\eta)$ is expanded about $(\vec{x}^o,0)$, which yields

$$\begin{aligned} H(\,\vec{x}^o+\delta\vec{x},\,\eta^o+\delta\eta\,) &= \\ &= H(\vec{x}^o,0) + H_x(\vec{x}^o,0)\cdot\delta\vec{x} + \\ &\quad + H_\eta(\vec{x}^o,0)\cdot\delta\eta + \mathcal{O}(\|\delta\vec{x}\|^2+\|\delta\eta\|^2) = \\ &= (\vec{x}^o+\delta\vec{x}) + H_\eta(\vec{x}^o,0)\cdot\delta\eta + \\ &\quad + \mathcal{O}(\|\delta\vec{x}\|^2+\|\delta\eta\|^2) \end{aligned}$$

for $(\delta\vec{x}^T,\,\delta\eta^T)\to 0$. Hence we can define an **infinitesimal similarity transformation of the second kind** as

$$h_2(\vec{x}^o+\delta\vec{x},\delta\eta) := \vec{x}^o + \delta\vec{x} + H_\eta(\vec{x}^o,0)\,\delta\eta\,. \tag{3.20}$$

Since $\vec{x}^o+\delta\vec{x} = \vec{x}$ the difference between h_1 and h_2 is due to the first argument of H_η only. In comparison, the infinitesimal similarity of the second kind has a larger linearization error than h_1, but it can be inverted simply by reversing the sign of $\delta\eta$, i.e.

$$\begin{aligned} h_2(\,\cdot\,,\delta\eta_2)\circ h_2(\,\cdot\,,\delta\eta_1) &= h_2(\,\cdot\,,\delta\eta_2+\delta\eta_1)\,, \\ h_2(\,\cdot\,,\delta\eta)^{-1} &= h_2(\,\cdot\,,-\delta\eta)\,. \end{aligned}$$

Thirdly, we will extend h_1 and h_2 to velocity coordinates. For this purpose linear models with epoch t_0,

$$\begin{aligned} \vec{x}(t) &= \vec{x}(t_0) + (t-t_0)\,\dot{\vec{x}}(t_0)\,, \\ \delta\eta(t) &= \delta\eta(t_0) + (t-t_0)\,\dot{\delta\eta}(t_0)\,, \end{aligned}$$

are substituted into $\tilde{\vec{x}}(t) = h_i(\vec{x}(t),\delta\eta(t))$ (3.19 and 3.20 respectively). Differentiating with respect to t and setting $t=t_0$, we obtain

$$\begin{bmatrix} \tilde{\vec{x}}(t_0) \\ \dot{\tilde{\vec{x}}}(t_0) \end{bmatrix} = \begin{bmatrix} \vec{x}(t_0) \\ \dot{\vec{x}}(t_0) \end{bmatrix} + H\begin{bmatrix} \delta\eta(t_0) \\ \dot{\delta\eta}(t_0) \end{bmatrix} + \ldots$$

where

$$\text{for } h_1\text{:}\quad H = \begin{bmatrix} H_\eta(\vec{x}(t_0),0) & 0 \\ \dot{H}_\eta(\vec{x}(t_0),0) & H_\eta(\vec{x}(t_0),0) \end{bmatrix}$$

$$\text{for } h_2\text{:}\quad H = \begin{bmatrix} H_\eta(\vec{x}^o,0) & 0 \\ \dot{H}_\eta(\vec{x}^o,0) & H_\eta(\vec{x}^o,0) \end{bmatrix} \tag{3.21}$$

and

$$\begin{aligned} H_\eta(\vec{x},0) &= [\,\vec{x},\,S(\vec{x}),\,\mathrm{I}\,]\,, \\ \dot{H}_\eta(\vec{x},0) &= [\,\dot{\vec{x}},\,S(\dot{\vec{x}}),\,0\,]\,. \end{aligned}$$

3.6 Introduction of additional parameters

The aim of this section is the mathematical formulation of extending a given system of equations by additional parameters q which stand in an affine relation to the given parameters p. If there is no such relation, the equations for p and q can be added like independent systems. This relation will change the given parameters p into $\tilde{p}$, in a manner corresponding to the parameter transformation (3.14). Since the new parameter vector $[\,\tilde{p},q\,]$ is of greater dimension than p, the relation between them can be uniquely defined only in the direction

$$\begin{bmatrix} \tilde{p} \\ q \end{bmatrix} \longmapsto p\,.$$

A functional definition according to (3.14) is

$$p = f(\tilde{p},q) = T(\tilde{p}-d) + Sq$$

which is applicable to observation as well as normal equation systems. For solution systems

$$\begin{aligned} q &= \text{must be given, then} \\ \tilde{p} &= Rp + d - RSq\,. \end{aligned}$$

Thus, T must be invertible with $T^{-1} = R$.

The general model for normal and observation equations reads

$$p = T(\tilde{p}-d) + Sq = \begin{bmatrix} T\,S \end{bmatrix}\begin{bmatrix} \tilde{p} \\ q \end{bmatrix} - Td$$

$$x = T\tilde{x} + S\xi + t = \begin{bmatrix} T\,S \end{bmatrix}\begin{bmatrix} \tilde{x} \\ \xi \end{bmatrix} + t$$

with **conformal** approximate values

$$\tilde{p}^o = T^{-1}(p^o - Sq^o) + d\,, \qquad t = 0\,,$$

or with prescribed approximate values

$$\tilde{p}^o = \text{given}, \qquad t = T(\tilde{p}^o - d) + Sq^o - p^o \tag{3.22}$$

Applying (3.22) to observation equations gives

$$\tilde{A} = \begin{bmatrix} AT\;AS \end{bmatrix}, \quad \tilde{b} = b - At\,, \quad \tilde{P} = P\,,$$
$$\tilde{b}^T P \tilde{b} = b^T P b - t^T A^T P\big(2b - At\big)\,,$$
$$\tilde{e} = e\,. \tag{3.23}$$

Applying (3.22) to normal equations yields

$$\tilde{N} = \begin{bmatrix} T^T N T & T^T N S \\ S^T N T & S^T N S \end{bmatrix}, \quad \tilde{y} = \begin{bmatrix} T^T(y - Nt) \\ S^T(y - Nt) \end{bmatrix},$$
$$\tilde{b}^T P\,\tilde{b} = b^T P\,b - t^T\big(2y - Nt\big)\,,$$
$$\tilde{e}^T P\,\tilde{e} = e^T P\,e\,. \tag{3.24}$$

Applying (3.22) to solutions yields

$$\tilde{N}^{-1} = R N^{-1} R^T, \quad \tilde{x} = R(x - t)\,,$$
$$\tilde{b}^T P\,\tilde{b} = b^T P\,b - t^T N\big(2x - t\big)\,, \tag{3.25}$$
$$\tilde{e}^T P\,\tilde{e} = e^T P\,e\,, \qquad R = T^{-1}\,.$$

When transformations of type (3.22) apply to some subvectors of the parameters to be solved in a system of equations, these transformations should be extended to a transformation of the whole system. Thus, the parameter vector is supposed to contain subvectors $\{\vec{p}_i,\, i = 0, \ldots, N\}$, each of which beeing supplemented by new parameters $\vec{q}_i$ through a transformation (3.22) defined by $(T_i,\, S_i,\, d_i,\, t_i)$. If all non-transformed parameters are collected in a subvector $\vec{p}_0$, and if the $\vec{p}_i$, $\vec{q}_i$ are supposed to be elementwise disjunct, then

$$p^T = \big(\vec{p}_0^{\,T}, \vec{p}_1^{\,T}, \ldots, \vec{p}_N^{\,T}\big),$$
$$(\tilde{p}^T, q^T) = \big(\vec{p}_0^{\,T}, \tilde{\vec{p}}_1^{\,T}, \ldots, \tilde{\vec{p}}_N^{\,T}, \vec{q}_1^{\,T}, \ldots, \vec{q}_N^{\,T}\big)$$

are partitions of the old and the new parameter vector respectively. Then the system as a whole is transformed with the matrix

$$\left[\begin{array}{c|ccc|ccc} \mathrm{I} & & 0 & & & 0 & \\ \hline & T_1 & & & S_1 & & \\ 0 & & \ddots & & & \ddots & \\ & & & T_N & & & S_N \end{array}\right]$$

$$\underbrace{\qquad\qquad}_{T} \qquad \underbrace{\qquad\qquad}_{S}$$

and the translation vectors

$$d = \big(d_0^T = 0,\, d_1^T, \ldots, d_N^T\big)^T,$$
$$t = \big(t_0^T = 0,\, t_1^T, \ldots, t_N^T\big)^T.$$

T has always the form of a block-diagonal matrix

$$T = \mathrm{diag}\big(T_0 = \mathrm{I},\, T_1, \ldots, T_N\big)\,,$$

but the arrangement of S may vary. Other forms are obtained if for instance $\vec{q}_i = \vec{q}_k$ for some $i \neq k$. The case $\vec{q}_1 = \vec{q}_2 = \ldots = \vec{q}_N$ is shown in application (c).

We shall now go onto applications of the parameter transformation (3.22), thereby restricting ourselves to appropriate subvectors of the parameters.

(a) Introduction of velocities

Let a single physical parameter p_i be represented by different mathematical models: a constant model at mean observation epoch t_0

$$p_i(t) = p_i(t_0)\,,$$

a linear model relative to epoch t_0

$$p_i(t) = p_i(t_0) + (t - t_0)\,\dot{p}_i(t_0)\,,$$

a linear-trigonometric model at epoch t_0

$$p_i(t) = a_i(t_0) + (t - t_0)\,b_i(t_0) + \\ + c_i(t_0)\cos\big(\omega(t - t_0)\big) + s_i(t_0)\sin\big(\omega(t - t_0)\big)\,.$$

How transforms a system of equations containing the parameter p_i, if the mathematical model for p_i is enlarged?

First the trivial case that the parameter p_i is expressed through a constant model at mean observation epoch t_i in the given system, and a linear

model at epoch t_0 in the new system. The corresponding parameter subvectors are

$$\begin{aligned} &\text{old model:} && \vec{p}_i \;= [\,p_i(t_i)\,], \\ &\text{new model:} && \tilde{\vec{p}}_i \;= [\,p_i(t_0)\,], \quad \vec{q}_i \;= [\,\dot{p}_i(t_0)\,]. \end{aligned}$$

Evaluating the linear representation at $t = t_i$,

$$p_i(t_i) \;=\; p_i(t_0) \;+\; (t_i - t_0)\,\dot{p}_i(t_0)\,,$$

gives the required transformation equation

$$\vec{p}_i \;=\; T_i\,(\tilde{\vec{p}}_i - d_i) \;+\; S_i\,\vec{q}_i$$

with

$$T_i \;=\; [\,1\,], \quad d_i \;=\; 0\,, \quad S_i \;=\; [\,t_i - t_0\,]\,.$$

Secondly, suppose that the parameter p_i is expressed through a linear model at epoch t_i in the given system, and a linear-trigonometric model with epoch t_0 and frequency ω in the new system. Then the parameter vectors of both systems contain as subvectors

old model:

$$\vec{p}_i(t_i) \;=\; \begin{bmatrix} p_i(t_i) \\ \dot{p}_i(t_i) \end{bmatrix},$$

new modell:

$$\vec{p}_i(t_0) \;=\; \begin{bmatrix} a_i(t_0) \\ b_i(t_0) \end{bmatrix}, \quad \vec{q}_i(t_0) \;=\; \begin{bmatrix} c_i(t_0) \\ s_i(t_0) \end{bmatrix}.$$

Equating both models at time t_i yields the transformation equations as a function of epoch difference $\triangle t_i = t_i - t_0$ and frequency

$$\begin{aligned} p_i(t_i) \;&=\; a_i(t_0) \;+\; \triangle t_i \cdot b_i(t_0) \;+ \\ &\quad +\; \cos(\omega \triangle t_i) \cdot c_i(t_0) \;+\; \sin(\omega \triangle t_i) \cdot s_i(t_0) \\ \dot{p}_i(t_i) \;&=\; 0 \;+\; 1 \cdot b_i(t_0) \;- \\ &\quad -\; \omega \sin(\omega \triangle t_i) \cdot c_i(t_0) \;+\; \omega \cos(\omega \triangle t_i) \cdot s_i(t_0) \end{aligned}$$

or in matrix form

$$\vec{p}_i(t_i) \;=\; T_i\,(\vec{p}_i(t_0) - d_i) \;+\; S_i\,\vec{q}_i(t_0)$$

with

$$T_i \;=\; \begin{bmatrix} 1 & \triangle t_i \\ 0 & 1 \end{bmatrix}, \qquad d_i \;=\; 0\,,$$

$$S_i \;=\; \begin{bmatrix} \cos(\omega \triangle t_i) & \sin(\omega \triangle t_i) \\ -\omega \sin(\omega \triangle t_i) & \omega \cos(\omega \triangle t_i) \end{bmatrix}$$

(b) Estimation of the coordinate epoch

In a given system of equations, a physical parameter $p_i(t)$ such as a station coordinate for example should be mathematically represented by a linear model the epoch of which is not exactly known. If we are able to determine the unknown epoch t_i in combination with other equations, the epoch must be introduced as an additional parameter into the given system which is thereby transformed to a new system with a given model epoch t_0. Then the parameters are

old system:

$$p \;=\; \begin{bmatrix} p_i(t_i) \\ \dot{p}_i(t_i) \end{bmatrix} \quad \text{with unknown } t_i,$$

new system:

$$\tilde{p} \;=\; \begin{bmatrix} p_i(t_0) \\ \dot{p}_i(t_0) \end{bmatrix}, \quad q \;=\; \begin{bmatrix} t_i - t_0 \end{bmatrix}$$

The possible forms of epoch transformation are

$$\begin{aligned} p_i(t_i) \;&=\; p_i(t_0) \;+\; (t_i - t_0)\,\dot{p}_i(t_0) \\ \dot{p}_i(t_i) \;&=\; \dot{p}_i(t_0) \end{aligned}$$

or

$$\begin{aligned} p_i(t_0) \;&=\; p_i(t_i) \;-\; (t_i - t_0)\,\dot{p}_i(t_i) \\ \dot{p}_i(t_0) \;&=\; \dot{p}_i(t_i)\,. \end{aligned}$$

Both of them are linear in $p_i(t)$ and nonlinear in $\dot{p}_i(t)$ and $(t_i - t_0)$. To get an equation of type (3.22), any of the epoch transformations has to be linearized. Since the velocity is constant, it makes no difference if linearized about an approximation of $(\dot{p}_i(t_i), \triangle t_i)$ or of $(\dot{p}_i(t_0), \triangle t_i)$. Good approximate values can be taken from a solution of the old system. Given

$$\begin{aligned} \widehat{\dot{p}}_i \;&\approx\; \dot{p}_i(t_i) \;=\; \dot{p}_i(t_0) && \text{solution of old system,} \\ \widehat{\triangle t}_i \;&\approx\; t_i - t_0 && \text{by guess,} \end{aligned}$$

we get a linearized transformation of type (3.22)

$$\underbrace{\begin{bmatrix} p_i(t_i) \\ \dot{p}_i(t_i) \end{bmatrix}}_{p} \;=\; \underbrace{\begin{bmatrix} 1 & \widehat{\triangle t}_i \\ 0 & 1 \end{bmatrix}}_{T} \Bigg(\underbrace{\begin{bmatrix} p_i(t_0) \\ \dot{p}_i(t_0) \end{bmatrix}}_{\tilde{p}} - \underbrace{\begin{bmatrix} \widehat{\triangle t}_i \widehat{\dot{p}}_i \\ 0 \end{bmatrix}}_{d} \Bigg) + \underbrace{\begin{bmatrix} \widehat{\dot{p}}_i \\ 0 \end{bmatrix}}_{S} \underbrace{\begin{bmatrix} \triangle t_i \end{bmatrix}}_{q}.$$

Here we have assumed that the given system of equations already contained the parameter veloc-

ity. The reasoning is that the simulaneous introduction of a constant velocity and its model epoch as estimable parameters leads to an instable problem.

(c) Estimation of Helmert transformation parameters to partial solutions

If several normal equations or solutions are combined, it may happen that the k-th system contains unremovable datum information (constraints), which should not influence the combined solution. To remove these constraints we set up an infinitesimal similarity transformation (Helmert transformation) between the k-th partial solution and the combined solution, the transformation parameters of which have to be estimated together with the combined solution.

Regard the i-th station which shall be represented by the six cartesian coordinates of position and velocity. Its given coordinates in the k-th partial solution (index ik) are mapped onto the unknown coordinates in the combined solution (index i) by means of the infinitesimal similarity transformation of the first kind (3.21) with Helmert parameters h_k

$$\underbrace{\begin{bmatrix}\vec{x}_i\\ \dot{\vec{x}}_i\end{bmatrix}}_{p_i} = \underbrace{\begin{bmatrix}\vec{x}_{ik}\\ \dot{\vec{x}}_{ik}\end{bmatrix}}_{p_{ik}} + \begin{bmatrix}H_\eta(\vec{x}_{ik},0) & 0\\ \dot{H}_\eta(\vec{x}_{ik},0) & H_\eta(\vec{x}_{ik},0)\end{bmatrix}\underbrace{\begin{bmatrix}\delta\eta_k\\ \dot{\delta\eta}_k\end{bmatrix}}_{h_k}$$

If solved for p_{ik}, we get

$$p_{ik} \;=\; T_{ik}p_i \;+\; S_{ik}h_k$$

with

$$T_{ik} = \mathrm{I}\,, \quad S_{ik} = -\begin{bmatrix}H_\eta(\vec{x}_{ik},0) & 0\\ \dot{H}_\eta(\vec{x}_{ik},0) & H_\eta(\vec{x}_{ik},0)\end{bmatrix}.$$

If a partial solution for the k-th system of equations is not available, a similar equation can be set up through an infinitesimal similarity of the second kind. Thereby $\vec{x}_{ik}$ in S_{ik} is replaced by the common approximate values $\vec{x}_i^{\,o}$.

Combining the station vectors p_{ik} $(i{=}1,\ldots,M_k)$ from the k-th partial system to the parameter vector p_k, and embedding the corresponding station vectors p_i into the parameter vector p of the combined system yields

$$\underbrace{\begin{bmatrix}p_{1k}\\ p_{2k}\\ \vdots\end{bmatrix}}_{p_k} = \underbrace{\begin{bmatrix}T_{1k} & & \\ & T_{2k} & \\ & & \ddots\end{bmatrix}}_{T_k} \cdot \underbrace{\begin{bmatrix}p_1\\ p_2\\ \vdots\end{bmatrix}}_{E_k p} + \underbrace{\begin{bmatrix}S_{1k}\\ S_{2k}\\ \vdots\end{bmatrix}}_{S_k} \cdot h_k$$

If the approximate values for the Helmert parameters are taken to be $h_k = 0$, the latter equation extends to the corrections,

$$\begin{aligned} p_k &= T_k E_k\, p \;+\; S_k\, h_k \\ x_k &= T_k E_k\, x \;+\; S_k\, h_k \;+\; t \end{aligned}$$

Since $T_k = \mathrm{I}$, conformal approximate values of p and p_k mean $p_k = E_k\, p$, in other words, identical values.

A similar equation can be set up for every subset of the 14 Helmert parameters.

3.7 Estimation of similarity parameters between solutions

If two solutions share a set of common reference stations, the small datum difference between them is evaluated through an infinitesimal similarity transformation with 7 parameters, or 14 parameters if both solutions contain station velocities too.

Let the common stations have in solution $k = 1$ or 2 the coordinate vectors $\vec{x}_{ik}$, $i = 1,\ldots,M$. In case of 7 similarity parameters $\delta\eta \in \mathbb{R}^7$, the $3M$ observation equations for $\delta\eta$ derived from (3.19) read

$$\vec{x}_{i2} - \vec{x}_{i1} \;=\; H_\eta(\vec{x}_{i1},0)\,\delta\eta \quad (i = 1,\ldots,M),$$

and as derived from (3.20)

$$\vec{x}_{i2} - \vec{x}_{i1} \;=\; H_\eta(\vec{x}_i^{\,o},0)\,\delta\eta \quad (i = 1,\ldots,M).$$

If the solution $\{\vec{x}_{i1},\ i{=}1,\ldots,M\}$ is regarded as fixed, both observation equations can be weighted with

$$P \;=\; \mathcal{V}(\vec{x}_{i2})^{-1}\,.$$

The second equation should be weighted with

$$P \;=\; \big(\,\mathcal{V}(\vec{x}_{i2}) + \mathcal{V}(\vec{x}_{i1}) - 2\,\mathcal{C}(\vec{x}_{i1},\vec{x}_{i2})\,\big)^{-1},$$

but the covariance is never known.

In case of 14 parameters, the observation equations to be solved for $(\delta\eta, \dot{\delta\eta})$ are given in (3.21).

3.8 Special condition equations

Let a space of points be furnished with a "space-fixed" orthonormal reference system $\{\mathrm{O}_{\mathrm{sf}}, \vec{E}_1, \vec{E}_2, \vec{E}_3\}$ and a "body-fixed" orthonormal basis $\{\mathrm{O}_{\mathrm{bf}}{=}\mathrm{P}_o(t), \vec{e}_1(t), \vec{e}_2(t), \vec{e}_3(t)\}$. The naming is arbitrary while physics is disregarded. It is only supposed to signify that the one triad moves relative to the other. Allowing for a change of scale being independent of direction, means that the associated vector spaces only differ in their inner product,

$$\langle \vec{e}_i(t), \vec{e}_k(t) \rangle_{\mathrm{sf}} \;=\; m^2(t)\, \langle \vec{e}_i(t), \vec{e}_k(t) \rangle_{\mathrm{bf}}\,.$$

If the time-derivative (velocity) in the space-fixed system is denoted by a dot, we can decompose the movement $\dot{\vec{e}}_i(t)$ of the triad into a tangential part (perpendicular to $\vec{e}_i$) and a radial part (parallel to $\vec{e}_i$)

$$\dot{\vec{e}}_i(t)^{\perp} \;=\; \vec{\omega}(t) \times \vec{e}_i(t)\,, \quad \dot{\vec{e}}_i(t)^{\parallel} \;=\; \frac{\dot{m}(t)}{m(t)}\, \vec{e}_i(t)$$

with $\vec{\omega}(t)$ being the angular velocity vector. This extends to any point $\mathrm{P}(t)$ with position and velocity $\vec{R}(t)$, $\vec{V}(t)$ in the space-fixed basis and $\vec{r}(t)$, $\vec{v}(t)$ in the body-fixed system.

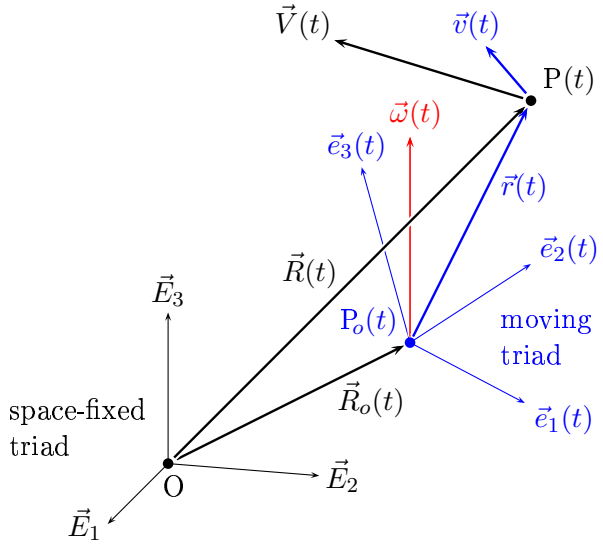

Thus $\vec{R}(t) - \vec{R}_o(t) \;=\; \vec{r}(t)$ and

$$\vec{V}(t) - \vec{V}_o(t) \;=\; \vec{\omega}(t){\times}\vec{r}(t) + \frac{\dot{m}(t)}{m(t)}\,\vec{r}(t) + \vec{v}(t)\,.$$

For point coordinates, this results in a similarity transformation (3.18) with $(1+\mu) = 1/m(t)$.

Consider a network of at least three non-collinear points $\{\mathrm{P}_1(t),\ldots,\mathrm{P}_n(t)\}$ in the three-dimensional space. By the declaration of a continuously differentiable body-fixed (net-fixed) triad every movement of a knot P_i in space decomposes in a translation $\vec{V}_o(t)$, a rotation $\vec{\omega}(t) \times \vec{r}_i(t)$, a change of scale $\dot{m}(t)/m(t){\cdot}\vec{r}_i(t)$, and a deformation $\vec{v}_i(t)$. Since such a body-fixed triad is not unique, we need for its declaration some condition equations, for instant, to minimize the local deformation.

Associate with each knot P_i a normed weight μ_i which shall be piecewise constant in time,

$$\mu_i \;>\; 0 \quad \text{and} \quad \sum_{i=1}^{n} \mu_i \;=\; 1\,.$$

Therewith we establish a mean position and mean velocity, expressed in both systems as

$$\vec{R}_{\mathrm{M}}(t) \;=\; \sum_{i=1}^{n} \mu_i \vec{R}_i(t)\,, \quad \vec{r}_{\mathrm{M}}(t) \;=\; \sum_{i=1}^{n} \mu_i \vec{r}_i(t)\,,$$

$$\vec{V}_{\mathrm{M}}(t) \;=\; \sum_{i=1}^{n} \mu_i \vec{V}_i(t)\,, \quad \vec{v}_{\mathrm{M}}(t) \;=\; \sum_{i=1}^{n} \mu_i \vec{v}_i(t)\,.$$

With $\vec{r}_{\mathrm{M}}(t)$ we defined a weightet **center** of the network which is generally different from the body-fixed origin P_o and different from the geocenter. But the weights can be choosen such that this difference vanishes for a single instant of time. As all the knots, the network center satisfies

$$\vec{R}_{\mathrm{M}} \;=\; \vec{R}_o + \vec{r}_{\mathrm{M}}\,, \qquad \vec{V}_{\mathrm{M}} \;=\; \vec{V}_o + \vec{\omega}{\times}\vec{r}_{\mathrm{M}} + \vec{v}_{\mathrm{M}}\,.$$

If the weights μ_i are regarded as relative masses of the knots, then $\mu_i\vec{v}_i(t)$ can be interpreted as linear momentum, and $\mu_i(\vec{r}_i(t){\times}\vec{v}_i(t))$ corresponds to angular momentum.
In the actual combination no weighting of velocities is implemented. Thus, $\mu_i = 1$ for $i = 1,..,n$.

(a) No-net-translation condition

A network with at least 3 non-collinear knots $\{\mathrm{P}_1(t),\ldots,\mathrm{P}_n(t)\}$ is in its body fixed reference system **free from translation**, if any of the following three equivalent conditions holds:

(a) $\vec{r}_{\mathrm{M}} = \sum_{i=1}^{n} \mu_i\, \vec{r}_i(t)$ is constant in the body fixed system.

(b) $\vec{v}_{\mathrm{M}} = \sum_{i=1}^{n} \mu_i\, \vec{v}_i(t) \;=\; 0.$

(c) $\sum_{i=1}^{n} \mu_i\, |\, \vec{v}_i(t)\, |^2$ is minimal as function of $\vec{V}_o(t)$ for every t.

Thus, the translation of a network coincides with the movement of its center.

Let now the station coordinates be parameters of an adjustment problem with approximate values $(\vec{r}_i^{\,o}, \vec{v}_i^{\,o})$ and corrections $(\triangle\vec{r}_i, \triangle\vec{v}_i)$. Then the solution reads

$$\vec{r}_i \;=\; \vec{r}_i^{\,o} + \triangle\vec{r}_i\,, \qquad \vec{v}_i \;=\; \vec{v}_i^{\,o} + \triangle\vec{v}_i\,.$$

The concept of no-net-translation can be applied fourfold, to the correction of a rigid network, and for a nonrigid network, to the approximate values, to the correction, and to the solution.

1. The correction of a **rigid network** ($\vec{v}_i \equiv 0$) can be interpreted as two shnapshots of a network with a linear movement $\vec{r}_i(t) \;=\; \vec{r}_i(t_0) + (t - t_0)\vec{v}_i$. Thereby we suppose to get

for $t_0 = 0$ the approximate values $\vec{r}_i(t_0) = \vec{r}_i^{\,o}$,
for $t_1 = 1$ the seeked solution $\vec{r}_i(t_1) = \vec{r}_i$.

Then $\triangle\vec{r}_i$ coincides with the constant velocity

$$\vec{v}_i \;=\; \vec{r}_i(t_1) - \vec{r}_i(t_0) \;=\; \triangle\vec{r}_i\,.$$

Thus, condition (b) yields

$$\triangle\vec{r}_{\rm M} \;=\; \sum_{i=1}^{n} \mu_i \triangle\vec{r}_i \;=\; 0\,. \qquad (3.26)$$

2. The nonrigid network of **approximate values** is free from translation, if it holds for every t

$$\vec{v}_{\rm M}^{\,o}(t) \;=\; \sum_{i=1}^{n} \mu_i \vec{v}_i^{\,o} \;=\; 0\,.$$

3. The network of the **solution** is free from translation, if

$$\vec{v}_{\rm M}(t) \;=\; \sum_{i=1}^{n} \mu_i \vec{v}_i \;=\; 0$$

is fulfilled for every t. Expressed by the variables of the equation system, this equation becomes

$$\sum_{i=1}^{n} \mu_i \triangle\vec{v}_i \;=\; -\sum_{i=1}^{n} \mu_i \vec{v}_i^{\,o} \;=\; -\,\vec{v}_{\rm M}^{\,o}\,. \qquad (3.27)$$

4. The **correction** by itself is free from translation, if it satifies for every t

$$\begin{aligned} \vec{v}_{\rm M} - \vec{v}_{\rm M}^{\,o} \;&=\; \sum_{i=1}^{n} \mu_i \triangle\vec{v}_i^{\,o} \;=\; 0 \quad \text{and} \\ \triangle\vec{r}_{\rm M}(t_0) \;&=\; \sum_{i=1}^{n} \mu_i \triangle\vec{r}_i(t_0) \;=\; 0\,. \end{aligned} \qquad (3.28)$$

It was necessary to take the additional second equation from the rigid network (3.26), because any movement is detemined from the initial state $\vec{r}_i(t_0)$ and the velocity $\vec{v}_i(t)$ in course of time. The second equation also guaranties that the relation between the network and the geocenter doesn't change at the reference epoch t_0.
The two condition equations in (3.28) correspond to keeping fixed the center position and velocity. Since in this case the correction should not move the network relative to the approximate values, the condition (3.28) is also called "**no residual net translation**".

If the weights μ_i are taken as relative masses, the physical analogue of the first equation of (3.28) is the conservation of (linear) momentum (Gerstl and Richter, 1998; Gerstl, 1999).

Each of the equations (3.26) to (3.28) can be used as a **no-net-translation condition** to define the datum of an estimated network. If the approximate values and the corrections are free from translation, then is the solution too.

(b) No-net-rotation condition

The angular momentum relative to any center of the net is conserved under translations of the origin. Using $\vec{r}_{\rm M}$ as the center we get

$$\begin{aligned} \vec{h}_{\rm M}(t) \;&=\; \sum_{i=1}^{n} \mu_i\, (\vec{r}_i - \vec{r}_{\rm M}) \times (\vec{v}_i - \vec{v}_{\rm M}) \;= \\ &=\; \sum_{i=1}^{n} \mu_i\, \vec{r}_i \times \vec{v}_i \;-\; \vec{r}_{\rm M} \times \vec{v}_{\rm M}\,. \end{aligned}$$

A network with at least 3 non-collinear knots $\{\mathrm{P}_1(t), \ldots, \mathrm{P}_n(t)\}$ is in its body fixed reference system **free from rotation around its center**, if any of the following equivalent conditions holds:

(b) $\vec{h}_{\rm M}(t) \;=\; \sum_{i=1}^{n} \mu_i\, (\vec{r}_i - \vec{r}_{\rm M}) \times (\vec{v}_i - \vec{v}_{\rm M}) \;=$
$= \sum_{i=1}^{n} \mu_i\, \vec{r}_i \times \vec{v}_i \;-\; \vec{r}_{\rm M} \times \vec{v}_{\rm M} \;=\; 0$ for every t.

(c) $\sum_{i=1}^{n} \mu_i\, |\, \vec{v}_i - \vec{v}_{\rm M}\, |^2$ is minimal as function of $\vec{\omega}_o$ for every t.

Net rotation in an adjustment: Denote by $(\vec{r}_i^{\,o}, \vec{v}_i^{\,o})$ the approximate values and by $(\triangle\vec{r}_i, \triangle\vec{v}_i)$ the correction of the three-dimensional cartesian coordinates of the i-th knot. Then is the solution of the adjustment

$$\vec{r}_i = \vec{r}_i^{\,o} + \triangle\vec{r}_i\,, \qquad \vec{v}_i = \vec{v}_i^{\,o} + \triangle\vec{v}_i$$

1. The correction of a **rigid network** ($\vec{v}_i \equiv 0$) shall be handled as before by a linear model with

$$\vec{r}_i(t_0{=}0) \;=\; \vec{r}_i^{\,o}, \quad \vec{r}_i(t_1{=}1) \;=\; \vec{r}_i\,, \quad \vec{v}_i = \triangle\vec{r}_i\,.$$

The vector product $\vec{r}_i(t_1){\times}\vec{v}_i \;=\; (\vec{r}_i^{\,o}{+}\triangle\vec{r}_i){\times}\triangle\vec{r}_i$ $= \vec{r}_i^{\,o}{\times}\triangle\vec{r}_i \;=\; \vec{r}_i(t_0){\times}\vec{v}_i$ is independent of time. Then we have from (b)

$$\triangle\vec{p} \;=\; \sum_{i=1}^{n} \mu_i\, \vec{r}_i^{\,o}{\times}\triangle\vec{r}_i \;=\; 0\,. \qquad (3.29)$$

2. The network of the **approximate values** is free from rotation around the origin, if it holds for every t

$$\vec{h}^{\,o}(t) \;=\; \sum_{i=1}^{n} \mu_i\big(\vec{r}_i^{\,o}{\times}\vec{v}_i^{\,o}\big) \;=\; 0\,.$$

3. The network of the **solution** is free from rotation around the origin, if for every t

$$\vec{h}(t) \;=\; \sum_{i=1}^{n} \mu_i\big(\vec{r}_i{\times}\vec{v}_i\big) \;=\; 0$$

is fullfilled. That is a non-linear equation with respect to the unknowns $\triangle\vec{r}_i$ and $\triangle\vec{v}_i$, because

$$\begin{aligned}\vec{h}(t) \;=\; &\sum_{i=1}^{n} \mu_i \left(\vec{r}_i^{\,o}{\times}\vec{v}_i^{\,o}\right) + \\ &+ \sum_{i=1}^{n} \mu_i\Big(\vec{r}_i^{\,o}{\times}\triangle\vec{v}_i \;+\; \triangle\vec{r}_i{\times}\vec{v}_i^{\,o}\Big) + \\ &+ \sum_{i=1}^{n} \mu_i\Big(\triangle\vec{r}_i{\times}\triangle\vec{v}_i\Big)\,.\end{aligned}$$

Neglecting the quadratic term $\triangle\vec{r}_i{\times}\triangle\vec{v}_i$ reduces $\vec{h}(t) = 0$ to a linear equation

$$\begin{aligned}&\sum_{i=1}^{n} \mu_i\Big(\vec{r}_i^{\,o}{\times}\triangle\vec{v}_i \;+\; \triangle\vec{r}_i{\times}\vec{v}_i^{\,o}\Big) \;\approx \\ &\qquad \approx\; -\sum_{i=1}^{n} \mu_i\, \vec{r}_i^{\,o}{\times}\vec{v}_i^{\,o} \;=\; -\vec{h}^{\,o}(t)\,.\end{aligned} \qquad (3.30)$$

4. The **correction** by itself is free from rotation, if it satisfies $\vec{h}(t) = \vec{h}^{\,o}(t)$ for every t. This equation is linearized as function of $\triangle\vec{r}_i$ and $\triangle\vec{v}_i$ by omission of quadratic terms and supplemented by a condition for the initial values at epoch t_0, which are regarded like a rigid network in (3.29). Thus, we get

$$\begin{aligned}\vec{h} - \vec{h}^{\,o} \;&\approx\; \sum_{i=1}^{n} \mu_i\Big(\vec{r}_i^{\,o}{\times}\triangle\vec{v}_i \;+\; \triangle\vec{r}_i{\times}\vec{v}_i^{\,o}\Big) \;=\; 0 \\ \triangle\vec{p}(t_0) \;&=\; \sum_{i=1}^{n} \mu_i\Big(\vec{r}_i^{\,o}(t_0){\times}\triangle\vec{r}_i(t_0)\Big) \;=\; 0\,.\end{aligned} \qquad (3.31)$$

The equations (3.31) fix the initial orientation and the change in the orientation (= rotation) to their approximate values. That is why they are called "**residual no-net-rotation conditions**".

If the weights μ_i are interpreted as relative masses, the physical analogue of the first equation of (3.31) is the conservation of angular momentum (Gerstl and Richter; 1998; Gerstl, 1999).

Each of the equations (3.29) to (3.31) can be used as a **no-net-rotation condition** to define the datum of an estimated network.

(c) Conservation of scale

A network with at least 3 non-collinear knots $\{\mathrm{P}_1(t),\ldots,\mathrm{P}_n(t)\}$ is in its body fixed reference system **true to scale**, if any of the following equivalent conditions holds:

(a) $f_{\mathrm{M}}(t) \;=\; \sum_{i=1}^{n} \frac{\mu_i}{2}\,|\,\vec{r}_i - \vec{r}_{\mathrm{M}}|^2$ is constant in the body-fixed system.

(b) $s_{\mathrm{M}}(t) \;=\; \sum_{i=1}^{n} \mu_i\,(\vec{r}_i - \vec{r}_{\mathrm{M}}){\cdot}(\vec{v}_i - \vec{v}_{\mathrm{M}}) \;=$
$= \sum_{i=1}^{n} \mu_i\, \vec{r}_i \cdot \vec{v}_i \;-\; \vec{r}_{\mathrm{M}}{\cdot}\,\vec{v}_{\mathrm{M}} \;=\; 0$ for every t.

(c) $\sum_{i=1}^{n} \mu_i\,|\,\vec{v}_i - \vec{v}_{\mathrm{M}}|^2$ is minimal as function of $(1{+}\mu(t))$ for every t.

Net scaling in an adjustment: Denote by $(\vec{r}_i^{\,o}, \vec{v}_i^{\,o})$ the approximate values and by $(\triangle\vec{r}_i, \triangle\vec{v}_i)$ the correction of the three-dimensional cartesian coordinates of the i-th knot. Then is the solution of the adjustment

$$\vec{r}_i = \vec{r}_i^{\,o} + \triangle\vec{r}_i\,, \qquad \vec{v}_i = \vec{v}_i^{\,o} + \triangle\vec{v}_i$$

1. The correction of a **rigid network** ($\vec{v}_i \equiv 0$) shall be handled as before by a linear model with

$$\vec{r}_i(t_0{=}0) \;=\; \vec{r}_i^{\,o}, \quad \vec{r}_i(t_1{=}1) \;=\; \vec{r}_i\,, \quad \vec{v}_i = \triangle\vec{r}_i\,.$$

The scalar product $\vec{r}_i(t_1)\cdot\vec{v}_i \;=\; (\vec{r}_i^{\,o}{+}\triangle\vec{r}_i)\cdot\triangle\vec{r}_i$ $= \vec{r}_i^{\,o}\cdot\triangle\vec{r}_i \;=\; \vec{r}_i(t_0)\cdot\vec{v}_i$ is independent of time. Then we have from (b)

$$\triangle f \;=\; \sum_{i=1}^{n} \mu_i\, \vec{r}_i^{\,o}\cdot\triangle\vec{r}_i \;=\; 0\,. \qquad (3.32)$$

2. The network of the **approximate values** is true to scale, if it holds for every t

$$s^o(t) \;=\; \sum_{i=1}^{n} \mu_i \big(\vec{r}_i^{\,o} \cdot \vec{v}_i^{\,o}\big) \;=\; 0\,.$$

3. The network of the **solution** is true to scale, if for every t

$$s(t) \;=\; \sum_{i=1}^{n} \mu_i \big(\vec{r}_i \cdot \vec{v}_i\big) \;=\; 0$$

is fullfilled. That is a non-linear equation with respect to the unknowns $\triangle\vec{r}_i$ and $\triangle\vec{v}_i$, because

$$\begin{aligned} s(t) \;=\; & \sum_{i=1}^{n} \mu_i \left(\vec{r}_i^{\,o} \cdot \vec{v}_i^{\,o}\right) + \\ & + \sum_{i=1}^{n} \mu_i \Big(\vec{r}_i^{\,o} \cdot \triangle\vec{v}_i \;+\; \triangle\vec{r}_i \cdot \vec{v}_i^{\,o}\Big) + \\ & + \sum_{i=1}^{n} \mu_i \Big(\triangle\vec{r}_i \cdot \triangle\vec{v}_i\Big)\,. \end{aligned}$$

Neglecting the quadratic term $\triangle\vec{r}_i \cdot \triangle\vec{v}_i$ reduces $s(t) = 0$ to a linear equation

$$\begin{aligned} & \sum_{i=1}^{n} \mu_i \Big(\vec{r}_i^{\,o} \cdot \triangle\vec{v}_i \;+\; \triangle\vec{r}_i \cdot \vec{v}_i^{\,o}\Big) \;\approx \\ & \qquad \approx\; -\sum_{i=1}^{n} \mu_i\, \vec{r}_i^{\,o} \cdot \vec{v}_i^{\,o} \;=\; -s^o(t)\,. \end{aligned} \tag{3.33}$$

4. The **correction** by itself is true to scale, if it satisfies $s(t) = s^o(t)$ for every t. This equation is linearized as function of $\triangle\vec{r}_i$ and $\triangle\vec{v}_i$ by omission of quadratic terms and supplemented by a condition for the initial values at epoch t_0, which are regarded like a rigid network in (3.32). Thus, we get

$$\begin{aligned} s - s^o \;&\approx\; \sum_{i=1}^{n} \mu_i \Big(\vec{r}_i^{\,o} \cdot \triangle\vec{v}_i \;+\; \triangle\vec{r}_i \cdot \vec{v}_i^{\,o}\Big) \;=\; 0 \\ \triangle f(t_0) \;&=\; \sum_{i=1}^{n} \mu_i \Big(\vec{r}_i^{\,o}(t_0) \cdot \triangle\vec{r}_i(t_0)\Big) \;=\; 0\,. \end{aligned} \tag{3.34}$$

The equations (3.34) fix the initial extent and the change in extent to their approximate values. That is why they are called "**residual no-net-scaling conditions**".

The physical analogue of the first equation of (3.34) is the conservation of volume (Gerstl and Richter, 1998; Gerstl, 1999).

Each of the equations (3.32) to (3.34) can be used as a **no-net-scaling condition** to define the datum of an estimated network.

(d) Adding condition equations

Conditions, that are set up as described above, have to be added as additional observations to the given adjustment problem, in form of either observation equations or normal equations. To make sure, that these conditions have an impact on the given system of equations, the condition equations must be given a relative weight that is greater than the product of the anticipated relative precision and the spectral norm of the given Jacobi matrix.

We implemented the choice of an automated weigthing procedure where the spectral norm of the given design matrix A is approximated by the so called Frobeniusnorm $\|A\|_F$,

$$\| A \|_F \;=\; \sqrt{\sum_{i=1}^{m}\sum_{j=1}^{n} |\, a_{ij}|^2} \;=\; \sqrt{\mathrm{trace}(A^T P A)}\,.$$

The weight of a condition equation is computed as

$$w \;=\; \frac{1}{\sigma_{i_0}^2 \|\bar{A}\|_F}$$

where σ_{i_0} is a choosen a-priori standard deviation of the condition equation.

3.9 Modifications of the normal equations

3.9.1 Reduction of parameters

For notational convenience the normal equations are partitioned such that the parameters to be reduced are collected in the subvector $x_1 \in \mathbb{R}^{n_1}$ and the parameters remaining in subvector $x_2 \in \mathbb{R}^{n_2}$.

$$\begin{bmatrix} N_{11} & N_{12} \\ N_{12}^T & N_{22} \end{bmatrix} \begin{bmatrix} x_1 \\ x_2 \end{bmatrix} \;=\; \begin{bmatrix} y_1 \\ y_2 \end{bmatrix}\,. \tag{3.35}$$

In order to reduce the block N_{12}^T in the second row by Gaussian elimination, the invertibility of the quadratic submatrix N_{11} is necessary. Premultiplying the first row by N_{11}^{-1} yields

$$x_1 + N_{11}^{-1} N_{12} x_2 \;=\; N_{11}^{-1} y_1 \tag{3.36}$$

which can be used to retrieve the reduced parameters from a solution x_2. If again the first row of

(3.35) is premultiplied by $N_{12}^T N_{11}^{-1}$ and then subtracted from the second row of (3.35), we obtain the reduced normal equations

$$\underbrace{\left(N_{22} - N_{12}^T N_{11}^{-1} N_{12}\right)}_{\tilde{N}} x_2 \;=\; \underbrace{y_2 \;-\; N_{12}^T N_{11}^{-1} y_1}_{\tilde{y}} . \tag{3.37}$$

It remains to supplement the reduction of the norm of the observation vector

$$\tilde{b}^T P \tilde{b} \;=\; b^T P b \;-\; y_1^T N_{11}^{-1} y_1 .$$

3.9.2 Elimination of parameters

There are several applications of parameter elimination: to fix a parameter p_k to the value z_k and to take the parameters p_k and p_l to be equal. In the second case two parameters are set equal using the restriction equation $x_k - x_l = p_l^o - p_k^o$.

Both cases can be generalized by the restriction equation

$$B_1 x_1 \;+\; B_2 x_2 \;=\; z$$

where $x_1 \in \mathbb{R}^{n_1}$ contains the parameters to be eliminated, $x_2 \in \mathbb{R}^{n_2}$ the remaining parameters, and B_1 is a (quadratic) invertible matrix. After the inversion of B_1 the elimination equation becomes

$$x_1 \;=\; B_1^{-1} z \;-\; B_1^{-1} B_2 x_2 . \tag{3.38}$$

We have to establish a transformation to a new parameter space,

$$\mathbb{R}^{n_1+n_2} \ni x = \begin{bmatrix} x_1 \\ x_2 \end{bmatrix} \longmapsto \tilde{x} = x_2 \in \mathbb{R}^{n_2},$$

the reversal of which is defined by the elimination equation (3.38) as

$$x \;=\; \underbrace{\begin{bmatrix} -B_1^{-1} B_2 \\ \mathrm{I} \end{bmatrix}}_{=:\,T} \tilde{x} \;+\; \underbrace{\begin{bmatrix} B_1^{-1} z \\ 0 \end{bmatrix}}_{=:\,t} \tag{3.39}$$

The given observation and normal equations are partitioned in correspondence to the splitting of the variable vector,

$$\begin{aligned} \begin{bmatrix} A_1 & A_2 \end{bmatrix} \begin{bmatrix} x_1 \\ x_2 \end{bmatrix} \;&=\; b + v \\ \begin{bmatrix} N_{11} & N_{12} \\ N_{12}^T & N_{22} \end{bmatrix} \begin{bmatrix} x_1 \\ x_2 \end{bmatrix} \;&=\; \begin{bmatrix} y_1 \\ y_2 \end{bmatrix} , \end{aligned} \tag{3.40}$$

where $N_{ik} = A_i^T P A_k$ and $y_i = A_i^T P b$. When we substitute (3.39) for x, we obtain the decreased equations

$$\begin{aligned} \tilde{A}\tilde{x} \;&=\; \tilde{b} - e \quad \text{with} \\ \tilde{A} \;&=\; AT \;=\; A_2 - A_1 B_1^{-1} B_2 \\ \tilde{x} \;&=\; x_2 \\ \tilde{b} \;&=\; b - At \;=\; b - A_1 B_1^{-1} z \\ \tilde{N}\tilde{x} \;&=\; \tilde{y} \quad \text{with} \\ \tilde{N} \;&=\; T^T N T \;= \\ &=\; \left(N_{22} - N_{12}^T B_1^{-1} B_2\right) - \\ &\quad -\; (B_1^{-1} B_2)^T \left(N_{12} - N_{11} B_1^{-1} B_2\right) \\ \tilde{y} \;&=\; T^T (y - Nt) \;= \\ &=\; \left(y_2 - (B_1^{-1} B_2)^T y_1\right) - \\ &\quad -\; \left(N_{12}^T - (B_1^{-1} B_2)^T N_{11}\right) B_1^{-1} z \end{aligned} \tag{3.41}$$

3.10 Variance component estimation

Solving the equations of a Gauß-Markov model, the variance of the solution is provided except for a scaling factor. If several systems of solutions or normal equations are combined, it is then the level of variance relative to each other which is hardly known. The variance component estimation was implemented to estimate realistic relative scaling factors for the intra- or inter-technique combination on base of observation equations, normal equations, or solution systems.

1. Combination of observation equations

Suppose we have to combine K systems of observation equations $A_k x_k \;=\; b_k - e_k$ with

$$\mathcal{E}(b_k) = A_k x_k , \quad \mathcal{V}(b_k) = \sigma_k^2 P_k^{-1} \quad (k{=}1, \ldots, K).$$

Embedding the parameters p_k in the joined parameter vector p with the formularization of (3.6), we obtain the combined system $Ax \;=\; b - e$ with

$$A = \begin{bmatrix} A_1 E_1 \\ \vdots \\ A_K E_K \end{bmatrix}, \quad b = \begin{bmatrix} b_1 \\ \vdots \\ b_K \end{bmatrix}, \quad e = \begin{bmatrix} e_1 \\ \vdots \\ e_K \end{bmatrix}.$$

In case of **uncorrelated** observations $b_k \in \mathbb{R}^{m_k}$, the weight matrix P of the combined system is of block diagonal form,

$$P = \mathrm{diag}\left(P_1, \ldots, P_K\right) \quad \text{with} \quad P_k = \sigma_k \mathcal{V}(b_k)^{-1}.$$

With it goes the system of normal equations

$$N = A^T P A = \sum_{k=1}^{K} E_k^T \underbrace{A_k^T P_k A_k}_{N_k} E_k ,$$
$$y = A^T P\, b = \sum_{k=1}^{K} E_k^T \underbrace{A_k^T P_k\, b_k}_{y_k} .$$

In case of **correlated** observations b_k we will get

$$N = A^T P A = \sum_{i=1}^{K}\sum_{k=1}^{K} E_i^T \underbrace{A_i^T P_{ik} A_k}_{N_{ik}} E_k ,$$
$$y = A^T P\, b = \sum_{i=1}^{K}\sum_{k=1}^{K} E_i^T \underbrace{A_i^T P_{ik}\, b_k}_{y_{ik}} .$$

Usually A is not of full column rank and N is then singular. For that case constraints $Bx = d$ are added to the observation equations such that $(N + D) = (A^T P A + B^T B)$ becomes invertible. With a non-distorting datum, e.g. minimum constraints, $N^- := (N + D)^{-1}$ becomes a generalized inverse of the unconstrained normal matrix N, and $A^- := N^- A^T P = (A^T P A)^- A^T P$ is then a reflexive generalized inverse of the designmatrix A. The least squares problem is solved by

$$\begin{aligned} \hat{x} &= A^- b \quad \text{with} \quad A^- = (A^T P A)^- A^T P , \\ \hat{e} &= e(\hat{x}) = b - A\,\hat{x} = \big(\mathrm{I} - AA^-\big) b . \end{aligned} \tag{3.42}$$

2. Properties of the projector $(\mathrm{I} - AA^-)$

If A^- is a reflexive generalized inverse of A then $(\mathrm{I}–AA^-)$ is a P-orthogonal projector onto $\mathcal{R}(A)^\perp$ which satisfies the symmetry relation

$$\big(P(\mathrm{I}–AA^-)\big)^T = (\mathrm{I}–AA^-)^T P = P(\mathrm{I}–AA^-) . \tag{3.43}$$

Since $(\mathrm{I} - AA^-)$ projects onto $\mathcal{R}(A)^\perp$, we have

$$(\mathrm{I} - AA^-)\,\mathcal{E}(b) = (\mathrm{I} - AA^-) A\hat{x} = 0 .$$

Applying the symmetry and the idempotency of that projector to the error norm we get

$$\begin{aligned} \|e(\hat{x})\|_P^2 &= \hat{e}^T P \hat{e} = \\ &= b^T (\mathrm{I} - AA^-)^T P\, (\mathrm{I} - AA^-) b = \\ &= b^T P (\mathrm{I} - AA^-)(\mathrm{I} - AA^-) b = \\ &= b^T P (\mathrm{I} - AA^-) b \end{aligned}$$

Thus, the error norm has two expressions as a quadratic form of b, which will be referred to as

long form:

$$\| e(\hat{x})\|_P^2 = b^T (\mathrm{I} - AA^-)^T P\, (\mathrm{I} - AA^-)\, b ,$$

short form:

$$\| e(\hat{x})\|_P^2 = b^T P (\mathrm{I} - AA^-)\, b .$$

Mathematically the two forms agree, but they give rise to different iterative methods.

Recall that a quadratic form of a random vector b with a symmetric matrix S satisfies

$$\mathcal{E}(b^T S b) = \mathcal{E}(b)^T S\, \mathcal{E}(b) + \mathrm{trace}(S\, \mathcal{V}(b)) .$$

Applied to the error norm, we obtain with $D := (\mathrm{I} - AA^-)$ and $D\,\mathcal{E}(b) = 0$

for the long form:

$$\begin{aligned} \mathcal{E}(\hat{e}^T P \hat{e}) &= \mathcal{E}\big(b^T D^T P D\, b\big) = \\ &= \mathrm{trace}\big(D^T P D\, \mathcal{V}(b)\big), \end{aligned} \tag{3.44}$$

and for the short form:

$$\begin{aligned} \mathcal{E}(\hat{e}^T P \hat{e}) &= \mathcal{E}\big(b^T P D\, b\big) = \\ &= \mathrm{trace}\big(P D\, \mathcal{V}(b)\big). \end{aligned} \tag{3.45}$$

3. Uncorrelated observation groups

The variance to be computed is written

$$\mathcal{V}(b) = \begin{bmatrix} \mathcal{V}(b_1) & & \\ & \ddots & \\ & & \mathcal{V}(b_K) \end{bmatrix} = \begin{bmatrix} \sigma_1^2 P_1^{-1} & & \\ & \ddots & \\ & & \sigma_K^2 P_K^{-1} \end{bmatrix} .$$

To isolate the factor σ_k, $\mathcal{V}(b)$ is decomposed into

$$\mathcal{V}(b) = \sum_{k=1}^{K} \sigma_k^2\, C^k \quad \text{with} \tag{3.46}$$
$$C^k = \mathrm{diag}\big(\underbrace{0, \ldots, 0}_{k-1}, P_k^{-1}, \underbrace{0, \ldots, 0}_{K-k}\big) .$$

Conformally the weight matrix P splits up in

$$P = \sum_{k=1}^{K} P^k \quad \text{with} \tag{3.47}$$
$$P^k = \mathrm{diag}\big(\underbrace{0, \ldots, 0}_{k-1}, P_k , \underbrace{0, \ldots, 0}_{K-k}\big) ,$$

and then is the product

$$PC^k = \mathrm{I}^k = C^k P \quad \text{with}$$
$$\mathrm{I}^k = \mathrm{diag}\big(\underbrace{0, \ldots, 0}_{k-1}, \mathrm{I}_{m_k} , \underbrace{0, \ldots, 0}_{K-k}\big) .$$

To evaluate the long form of the error norm, recall the notation $D := (\mathrm{I} - AA^-)$. Inserting (3.46) into (3.44) gives

$$\mathcal{E}(\hat{e}^T P \hat{e}) \;=\; \sum_{k=1}^{K} \sigma_k^2 \,\mathrm{trace}\big(D^T P D\, C^k\big)\,.$$

Replacing P on both sides by (3.47) results in

$$\sum_{l=1}^{K} \mathcal{E}(\hat{e}^T P^l \hat{e}) \;=\; \sum_{l=1}^{K}\sum_{k=1}^{K} \mathrm{trace}\big(D^T P^l D\, C^k\big)\,\sigma_k^2\,.$$

This equation is satisfied by every solution $\xi = (\sigma_1^2, \ldots, \sigma_K^2)^T$ to the system of equations

$$S\,\xi \;=\; q \quad \text{with} \begin{cases} S_{lk} = \mathrm{trace}\big(D^T P^l D\, C^k\big), \\ q_l \;=\; \hat{e}^T P^l \hat{e} \;=\; \hat{e}_l^T P_l \hat{e}_l\,. \end{cases} \tag{3.48}$$

We shall now compute S_{lk}. With $PC^lP = P^l$ and the symmetry relation (3.43) applied to D^TP we can write

$$S_{lk} \;=\; \mathrm{trace}(D^T P^l D C^k) \;=\; \mathrm{trace}(PDC^l \cdot PDC^k)\,.$$

Within the argument of the trace-function, factors may be cyclically permuted. Thus we obtain

$$\begin{aligned} S_{lk} \;&=\; \mathrm{trace}\big((\mathrm{I}^l - AA^-\mathrm{I}^l)(\mathrm{I}^k - AA^-\mathrm{I}^k)\big) \;= \\ &=\; \mathrm{trace}\big(\mathrm{I}^l\mathrm{I}^k\big) - 2\,\mathrm{trace}\big(AA^-\mathrm{I}^l\mathrm{I}^k\big) + \\ &\qquad + \;\mathrm{trace}\big(AA^-\mathrm{I}^l\, AA^-\mathrm{I}^k\big) \;= \\ &=\; \delta_{lk}\Big[\, m_k - 2\,\mathrm{trace}\big(AA^-\mathrm{I}^k\big)\Big] + \\ &\qquad + \;\mathrm{trace}\big(AA^-\mathrm{I}^l\, AA^-\mathrm{I}^k\big)\,. \end{aligned}$$

Divide A^- into blocks according to A^T,

$$A^- = \Big[\, A_1^-, \ldots, A_K^- \Big] \quad \text{with } A_k^- \in \mathbb{R}^{n \times m_k}. \tag{3.49}$$

Then with $AA^- = \big[A_i E_i A_j^-\big]_{ij}$, $\mathrm{I}^k = \big[\delta_{ik}\mathrm{I}^k\delta_{kj}\big]_{ij}$,

$$\begin{aligned} S_{lk} \;&=\; \delta_{lk}\big[\, m_k - 2\,\mathrm{trace}\big(A_k^- A_k E_k\big)\big] \\ &\qquad + \;\mathrm{trace}\big(A_l^- A_l E_l \cdot A_k^- A_k E_k\big). \end{aligned} \tag{3.50}$$

If A^- is computed from the normal matrix, then

$$A^- = N^- A^T P = \Big[\, N^- E_1^T A_1^T P_1, \ldots, N^- E_K^T A_K^T P_K \Big]$$

Compared with (3.49) we obtain

$$A_k^- \;=\; N^- E_k^T A_k^T P_k\,, \quad A_k^- A_k E_k \;=\; N^- E_k^T N_k E_k\,.$$

Thus, (3.50) can be expressed by normal matrices

$$\begin{aligned} S_{lk} \;&=\; \delta_{lk}\big[\, m_k - 2\,\mathrm{trace}\big((E_k N^- E_k^T) N_k\big)\big] \\ &\qquad + \;\mathrm{trace}\big((E_k N^- E_l^T) N_l \cdot (E_l N^- E_k^T) N_k\big) \end{aligned} \tag{3.51}$$

Turning to the short form of the error norm, we insert (3.46) into (3.45) to obtain

$$\mathcal{E}(\hat{e}^T P \hat{e}) \;=\; \sum_{k=1}^{K} \sigma_k^2 \,\mathrm{trace}\big(P D\, C^k\big)\,.$$

Substituting (3.47) for P on both sides results in

$$\sum_{l=1}^{K} \mathcal{E}(\hat{e}^T P^l \hat{e}) \;=\; \sum_{l=1}^{K}\sum_{k=1}^{K} \mathrm{trace}\big(P^l D\, C^k\big)\,\sigma_k^2\,.$$

This equation is satisfied by every solution $\xi = (\sigma_1^2, \ldots, \sigma_K^2)^T$ to the system of equations

$$S\,\xi \;=\; q \quad \text{with} \begin{cases} S_{lk} = \mathrm{trace}\big(P^l D\, C^k\big), \\ q_l \;=\; \hat{e}^T P^l \hat{e} \;=\; \hat{e}_l^T P_l \hat{e}_l\,. \end{cases} \tag{3.52}$$

With a similar argumentation as in the case of the long form we get a diagonal matrix

$$\begin{aligned} S_{lk} \;&=\; \delta_{lk}\big[\, m_k - \mathrm{trace}\big(A_k^- A_k E_k\big)\big], \\ S_{lk} \;&=\; \delta_{lk}\big[\, m_k - \mathrm{trace}\big((E_k N^- E_k^T) N_k\big)\big]. \end{aligned} \tag{3.53}$$

4. Correlated observation groups

To isolate the unknown variance factors write

$$\mathcal{V}(b) \;=\; \sum_{n=1}^{K} \sigma_{nn} C^{nn} \;+\; \sum_{n=1}^{K}\sum_{k=n+1}^{K} \sigma_{nk} C^{nk}$$

with

$$C^{nn} \;=\; \begin{bmatrix} 0 & \ldots & 0 \\ & Q_{nn} & \\ \vdots & 0 & \vdots \\ & & \ddots \\ 0 & \ldots & 0 \end{bmatrix} \begin{matrix} \\ \\ n\text{-th row} \\ \\ \\ \end{matrix},$$

$$C^{nk} \;=\; \begin{bmatrix} 0 & \ldots & 0 \\ & \ddots \quad Q_{nk} & \\ \vdots & \ddots & \vdots \\ & Q_{kn} \quad \ddots & \\ 0 & \ldots & 0 \end{bmatrix} \begin{matrix} \\ \\ n\text{-th row} \\ \\ k\text{-th row} \\ \\ \end{matrix},$$

and $Q_{nk} = \mathcal{C}(b_n, b_k)$. This can also be written as

$$\mathcal{V}(b) \;=\; \sum_{l=1}^{K(K+1)/2} \sigma_l C^l \quad \text{with} \begin{cases} \sigma_l \;=\; \sigma_{nk}\,, \\ C^l \;=\; C^{nk} \end{cases} \tag{3.54}$$

where $l \;=\; (K{+}1)(n{-}1) + \frac{1}{2}n(n{-}1) + k$. Now, there is no blockwise correspondence between Q_{nk} and P_{nk}. All we have is that P is a (reflexive generalized) inverse of the variance, in other words

$$P \;=\; PQP \;=\; \sum_{l=1}^{K(K+1)/2} PC^l P\,. \tag{3.55}$$

Considering the long form of the error norm, we insert (3.54) into (3.44) to obtain

$$\mathcal{E}(\hat{e}^T P \hat{e}) \;=\; \sum_{k=1}^{K(K+1)/2} \sigma_k \,\mathrm{trace}\big(D^T P D\, C^k\big)\,.$$

Replacing P on both sides by (3.55) results in

$$\sum_{l=1}^{K(K+1)/2} \mathcal{E}(\hat{e}^T P C^l P \hat{e}) \;= \;= \sum_{l=1}^{K(K+1)/2}\sum_{k=1}^{K(K+1)/2} \mathrm{trace}\big(D^T P C^l P D\, C^k\big)\cdot\sigma_k\,.$$

This equation is satisfied by every solution $\xi = (\sigma_1,\ldots,\sigma_K)^T$ to the system of equations

$$S\,\xi \;=\; q \quad \text{with} \begin{cases} S_{lk} = \mathrm{trace}\big(D^T P C^l P D\, C^k\big)\,, \\ q_l \;=\; \hat{e}^T P C^l P \hat{e}\,. \end{cases} \tag{3.56}$$

The use of (3.43) gives the notion of Koch:

$$D^T P C^l P D\, C^k \;=\; P D C^l P D C^k \;=:\; W C^l W C^k\,.$$

Turning to the short form of the error norm, we insert (3.54) into (3.45) to obtain

$$\mathcal{E}(\hat{e}^T P \hat{e}) \;=\; \sum_{k=1}^{K(K+1)/2} \sigma_k \,\mathrm{trace}\big(P D\, C^k\big)\,.$$

Substituting (3.55) for P on both sides results in

$$\sum_{l=1}^{K(K+1)/2} \mathcal{E}(\hat{e}^T P C^l P \hat{e}) \;= \;= \sum_{l=1}^{K(K+1)/2}\sum_{k=1}^{K(K+1)/2} \mathrm{trace}\big(P C^l P D\, C^k\big)\,\sigma_k\,.$$

This equation is satisfied by every solution $\xi = (\sigma_1,\ldots,\sigma_K)^T$ to the system of equations

$$S\,\xi \;=\; q \quad \text{with} \begin{cases} S_{lk} = \mathrm{trace}\big(P C^l P D\, C^k\big) \\ \qquad = \mathrm{trace}\big(P C^l D^T P C^k\big)\,, \\ q_l \;=\; \hat{e}^T P C^l P \hat{e}\,. \end{cases} \tag{3.57}$$

5. Iterative solution

An approximate solution for the variance factors is obtaind from (3.48), (3.52), (3.56), or (3.57). Once we have solved for σ_k and $\sigma_k > 0$, the process is iterated with

$$\sigma_k\,\mathcal{V}(b_k) \;\longmapsto\; \mathcal{V}(b_k)$$

until $\sigma_k \approx 1$ for $k = 1,\ldots,K$.

6. Application

a) Combination of observation equations:

$$\begin{bmatrix} A_1 E_1 \\ \vdots \\ A_K E_K \end{bmatrix} x \;=\; \begin{bmatrix} b_1 \\ \vdots \\ b_K \end{bmatrix} - \begin{bmatrix} e_1 \\ \vdots \\ e_K \end{bmatrix} \tag{3.58}$$

with $\quad P \;=\; \mathrm{diag}\big(P_1,\ldots,P_K\big)\,.$

b) Combination of normal equations:

$$\begin{bmatrix} N_1 E_1 \\ \vdots \\ N_K E_K \end{bmatrix} x \;=\; \begin{bmatrix} y_1 \\ \vdots \\ y_K \end{bmatrix} - \begin{bmatrix} e_1 \\ \vdots \\ e_K \end{bmatrix} \tag{3.59}$$

with $\quad P \;=\; \mathrm{diag}\big(N_1^-,\ldots,N_K^-\big)\,,$

because, by the law of error propagation, it holds

$$\mathcal{V}(y_k) = A_k^T P_k\,\mathcal{V}(b_k) P A \;=\; \sigma_0^2\, A_k^T P_k A_k \;=\; \sigma_0^2\, N_k\,.$$

c) Combination of solutions: The given parameters are the partial solutions $\hat{x}_k$ $(k = 1,\ldots,K)$ which make up the "observation vector", and their variance matrices going into the weight matrix.

$$\begin{bmatrix} E_1 \\ \vdots \\ E_K \end{bmatrix} x \;=\; \begin{bmatrix} \hat{x}_1 \\ \vdots \\ \hat{x}_K \end{bmatrix} - \begin{bmatrix} e_1 \\ \vdots \\ e_K \end{bmatrix} \tag{3.60}$$

with $\quad P \;=\; \mathrm{diag}\big((N_1{+}D_1)^{-1},\ldots,(N_K{+}D_K)^{-1}\big)\,.$

4 Input data for the TRF realization 2003

4.1 Space geodetic solutions

In response to the ITRF2000 Call for Participation released by the ITRS Product Center (the former IERS Terrestrial Reference Frame Section) at IGN, various analysis centers submitted multi-year solutions of station positions and velocities. A summary of all submissions is available at the IGN website (http://lareg.ensg.ign.fr/ITRF/ITRF2000/).
Most of the submitted solutions were used for the ITRF2000 computation, i.e., 3 VLBI, 7 SLR, 1 LLR, 6 global GPS, 2 DORIS, 2 multi-technique and 9 GPS densification solutions (e.g., Altamimi et al., 2002; Boucher et al., 2004). The solutions were provided in the SINEX format. The observations used in these solutions span about 20 years for VLBI, SLR and LLR, and less than 10 years in the case of GPS and DORIS.

According to the initial constraints applied to all or a subset of stations the solutions included in the ITRF2000 combination are of three types:
(1) removable constraints: solutions for which the estimated station positions/velocities are constrained to a-priori values with an uncertainty of e.g., $\sigma \approx 10^{-5}$ m and 10^{-5} m/yr, respectively;
(2) loose constraints: solutions where the uncertainty of the constraints is, e.g., $\sigma \geq 1$ m for positions and ≥ 10 cm/yr for velocities; and
(3) minimum constraints, that are used to realize the TRF by a minimum of required information.

In addition to parts of the ITRF2000 input data we used for our realization also some later multi-year solutions with station positions and velocities containing more recent observations, i.e., VLBI and SLR solutions computed at DGFI, a DORIS solution provided by IGN/JPL, and a cumulative combined IGS solution (IGS03P01) provided by National Resources Canada (NRCan), Ferland (2002).

The available solutions were analysed concerning their SINEX format compatibility and the suitability for combination of unconstrained normal equations. For this approach it is necessary to remove the a-priori datum constraints which normally are included in the solutions. For some of the solutions submitted for the ITRF2000 realization, the a-priori constraints were not (or not clearly) reported in the SINEX files, for a few other solutions the generation of unconstrained normal equations failed (e.g., due to numerical reasons). Solutions with unremovable constraints may cause biases and deformations in the combined network. Furthermore it has to be considered, that the number of submitted ITRF2000 input solutions differs considerably between techniques, i.e. 15 GPS (6 global and 9 densification), 7 SLR, 3 VLBI, 2 DORIS solutions. This complicates the weighting within the inter-technique combination.

We used the following solutions to compute the TRF realization 2003 (see table 4.1):

VLBI: Three VLBI solutions from the ITRF2000 data pool, provided by the Geodetic Institute of the University Bonn (GIUB), the Goddard Space Flight Center (GSFC), NASA, USA, the Shanghai Astronomical Observatory (SHA), China as well as the DGFI solution (DGFI02R02, the processing strategy being similar to that described in Tesmer, 2002).

SLR/LLR: Three of the SLR solutions submitted for ITRF2000, provided by the Communications Research Laboratory (CRL), Japan, the Center of Space Research (CSR), USA, the Joint Center for Earth System Technology (JCET), NASA/GSFC, USA. The DGFI solution DGFI00L01 from the ITRF2000 data pool was replaced by a more recent SLR computation (DGFI01L01, the processing strategy being similar to that described in Angermann et al., 2002).

GPS: At present, IGS is the only service that provides combined multi-year solutions with

station positions and velocities. For this TRF computation we used the cumulative combined IGS solution (IGS03P01.snx) provided by National Resources Canada (NRCan, see Ferland 2002). This combined IGS solution contains about 3 more years of data than the GPS solutions contributing to ITRF2000, and includes the individual GPS solutions computed by various IGS analysis centers.

DORIS: We used the latest DORIS solution from IGN/JPL (IGN02D04, available at ftp://cddisa.gsfc.nasa.gov/pub/doris/products/sinex_global/ign) and a solution of the ITRF2000 data pool provided by the Groupe de Researche de Géodésie Spatiale (GRGS), France.

4.2 Preprocessing of solutions

Before combining the contributing solutions on the level of unconstrained normal equations various preprocessing steps were performed:

Reduction of constraints: The a-priori (datum) constraints, which normally were applied by the analysis centers, were removed to generate unconstrained normal equations as input for the TRF combination. Below, the situation regarding datum constraints is summarized for the different techniques and solutions:

VLBI: Loose a-priori constraints were applied for the solutions provided by GIUB, GSFC (in both cases 10 m on positions and 1 m/yr on velocities), and SHA (10 m and 0.1 m/yr). For the GIUB solutions the unconstrained normal equations could be reconstructed without problems, whereas in case of the GSFC and SHA solutions the constraints could not be removed because of numerical problems. As indicated by the very large standard deviations for positions and velocities of the GSFC and SHA solutions, the unremoved loose constraints should not affect the combination results. The unconstrained normal equations of the DGFI solution could be directly used for the combination.

SLR: The DGFI solution was submitted in form of unconstrained normal equations, whereas different a-priori constraints were applied to the SLR solutions provided by CRL, CSR and JCET. The constraints could be removed from the CRL solution. For the JCET solution the reported constraints of 1.28 m on positions and 1.28 m/yr on velocities could not be removed, but the large r.m.s. errors confirm that this solution is loosely constrained. The CSR solution contains a rotation datum (different from ITRF2000), which could not be removed. Thus, this solution was rotated to the ITRF2000 datum.

GPS: The cumulative IGS solution was aligned to ITRF2000 by a 14 parameter Helmert-transformation. We reduced this datum information by setting up respective Helmert-transformation parameters. The statistical information (e.g., number of observations, number of unknowns, variance factor), necessary for combining at the normal equation level, was kindly provided by NRCan (Ferland, 2003).

DORIS: The constraints of the GRGS solution were not reported in the SINEX file and could consequently not be removed. Since origin and scale differ significantly between both DORIS solutions and ITRF2000, we transformed both of them onto ITRF2000 in order to realize a consistent datum.

As mentioned above, the reduction of constraints was not possible for some of the selected solutions, and consequently these solutions are not fully compatible with the combination strategy on the level of unconstrained normal equations. Nevertheless, we decided to include them because it is important to have redundancy, especially for the DORIS intra-technique combination. Furthermore, the selected loosely constrained solution may not bias the combination results. The problems of reducing contraints can be avoided, if the analysis centers provide SINEX files with unconstrained normal equations.

Parameter transformations: The DGFI combination software DOGS-CS provides various options to perform parameter transformations (see chapter 3). In order to generate consistent normal equations for the TRF computation, we primarily used the two following features:
(1) The transformation of station positions to the TRF reference epoch 1997.0 was necessary

Tab. 4.1: *Summary of solutions used for the TRF realization 2003.*

Technique	AC/Solution	Data Span	# Stations [a] original	# Stations [b] used	Constraints [c]	Source
VLBI	(DGFI)02R02	1984–2002	49	49	free NEQ	DGFI
	(GIUB)00R01	1984–1999	53	53	loose	ITRF2000
	(GSFC)00R01	1979–1999	138	88	loose	ITRF2000
	(SHA)00R01	1979–1999	129	88	loose	ITRF2000
SLR	(CRL)00L02	1990–2000	62	62	loose	ITRF2000
	(CSR)00L04	1976–2000	141	106	loose	ITRF2000
	(DGFI)01L01	1981–2001	113	96	free NEQ	DGFI
	(JCET)00L05	1993–2000	63	55	loose	ITRF2000
GPS	(IGS)03P01	1996–2002	216	207	minimum	NRCan
DORIS	(GRGS)00D01	1993–1998	70	69	minimum	ITRF2000
	(IGN)02D04	1993–2002	111	109	loose	IGN/CDDIS

[a] Number of stations that were originally included in the contributing solutions.
[b] Note that stations with observation time span less than 1 year were excluded.
[c] TRF input data are loosely or minimum constrained solutions, or free normal equations.

for the combined IGS solution, which is referred to epoch 1998.0, for the SLR solution provided by JCET (epoch 2000.0), and for the DORIS solution provided by GRGS (epoch 1993.0).
(2) The transformation of normal equations to identical a-priori values, i.e., ITRF2000 station positions and velocities.

Reduction of stations: The contributing solutions include position and velocity estimates of "poorly" observed stations (e.g., mobile VLBI and SLR stations with few occupations, GPS and DORIS stations with too short observation time spans). For these stations, the estimated positions and velocities get very large standard deviations. As the quality and reliability of the results should be emphasized rather than the quantity of stations (see section 8.1), we excluded stations with an observation period less than one year from this TRF computation (see Appendix C). These "poorly" observed stations were reduced from the respective normal equations.

Renaming of stations: The IERS network stations are identified by uniform station information, such as a DOMES number, 4-character ID (e.g. for GPS and DORIS), CDP number (e.g. for SLR and VLBI). The station information provided in the SINEX solution files must be consistent with the IERS reference, to ensure that the estimated station positions and velocities refer to a unique reference point. In a few cases, it was necessary to rename stations to achieve a consistent station information.

5 Intra-technique combination

5.1 VLBI

Input data are normal equations obtained from four individual VLBI solutions, provided by GIUB (Geodetic Institute of University Bonn, Germany), GSFC (Goddard Space Flight Center, USA), SHA (Shanghai Astronomical Observatory, China), and DGFI (see table 4.1). The intra-technique combination consists of the following major steps:

Datum realization: The unit of length is defined by the speed of light as a fundamental constant. Since VLBI most precisely measures the delay of light, VLBI observations contains information about the scale of a terrestrial reference frame. The origin and orientation of a VLBI network have to be realized by external constraints. This was done by applying NNT and NNR conditions to minimize the common translation and rotation components of station positions and velocities w.r.t. ITRF2000 by using the selected VLBI reference frame stations (see figure 5.1, table C.1).

Weighting: Mean variances for station positions were computed for each solution, which were then used to compute scaling factors for the individual VLBI normal equations (see table 5.1). As these scaling factors are referred to a mean variance level of the four contributing solutions, the standard deviations of the combined VLBI solution reflect the "internal" VLBI accuracy, which is probably too optimistic (see table 6.1).

Equating VLBI station velocities: There are various stations with two or more occupations (see table C.1). For each single VLBI solution and for all stations with two or more velocity estimations, we computed the respective velocity differences, their standard deviations, and the ratios between them (see table 5.2). These ratios, which served as a test quantity to decide whether different velocity estimations can be equated or not, are in many cases quite large (up to 15). This may result to a certain extent from too optimistic standard deviations for the station velocity differences, on the other hand the observed velocity differences may also reflect physically different motions (e.g., station Goldstone). Furthermore, for some VLBI stations the results of individual analysis centers disagree considerably. Thus various effects have to be considered, which are difficult to separate (e.g., solution related problems, biases, changes of site motion with time). This complicates the application of statistical tests. However, the VLBI solutions mostly provide stable velocity estimations without equating. In order to avoid possibly deforming constraints on the solutions, we performed the outlier detection (see next paragraph), without equating velocities.

Identification and rejection of outliers: We applied an iterative procedure to identify outliers in the contributing VLBI solutions. For each station and for each solution we computed position and velocity differences w.r.t. the mean of the other solutions, along with the corresponding standard deviations for these differences. The resulting numbers served as test quantity to identify outliers. The spherical position differences should not exceed a certain limit (we used 3 cm)

Tab. 5.1: *VLBI weighting.*

Solution	Variances[a] for positions	Scaling[b] factors
(DGFI)02R02	0.35 mm^2	0.64
(GIUB)00R01	0.54 mm^2	0.98
(GSFC)00R01	0.62 mm^2	1.12
(SHA)00R01	0.72 mm^2	1.30

[a] For each of the contributing VLBI solutions mean variances for station positions were computed by using the VLBI reference frame stations.

[b] This column represents the scaling factors for the VLBI normal equations.

Tab. 5.2: *Spherical velocity differences between different VLBI occupations of the same station, along with their standard deviations [mm/yr]. The ratios $\triangle/\sigma$ represent the normalized velocity differences.*

Occupations	Station	DGFI			GIUB			GSFC			SHA		
		$\triangle_{vel}$	$\sigma_{\triangle vel}$	$\triangle/\sigma$	$\triangle_{vel}$	$\sigma_{\triangle vel}$	$\triangle/\sigma$	$\triangle_{vel}$	$\sigma_{\triangle vel}$	$\triangle/\sigma$	$\triangle_{vel}$	$\sigma_{\triangle vel}$	$\triangle/\sigma$
14201S004/S100	Wettzell	—	—	—	—	—	—	2.1	1.3	1.6	7.5	4.2	1.8
21701S001/S004	Kashima	3.9	0.7	5.5	4.8	0.5	9.6	2.5	0.3	8.4	4.2	0.5	9.3
21730S001/S007	Tsukuba	—	—	—	—	—	—	2.2	2.8	0.8	45.7	33.7	1.4
40405S009/S014	Goldstone	—	—	—	11.3	2.1	5.5	2.8	1.0	2.9	3.2	0.9	3.5
40405S009/S019	Goldstone	5.7	0.5	12.4	3.5	0.5	6.7	3.3	0.4	7.4	2.5	0.4	7.2
40424S001/S007	Kokee Park	1.5	0.3	4.8	1.1	0.4	2.7	2.2	0.2	9.0	1.6	0.3	5.4
40427M001/M002	Ford Ord	—	—	—	—	—	—	5.7	7.5	0.8	7.4	6.9	1.1
40439S002/S006	Owens Vall	6.1	1.8	3.4	4.5	2.1	2.2	1.4	0.6	2.5	3.8	0.6	6.1
40440S002/S003	Westford	2.5	0.8	3.1	1.5	0.6	2.4	1.4	0.3	5.3	1.3	0.2	5.6
40441S007/S001	Greenbank	2.7	1.4	1.9	20.3	8.0	2.5	3.9	0.4	11.1	2.1	0.4	5.4
40441S007/S004	Greenbank	3.6	0.4	9.1	4.5	0.4	11.1	4.8	0.3	15.4	3.0	0.3	9.5
40442S003/S017	Fort Davis	1.9	0.6	3.5	2.0	0.6	3.4	4.2	0.4	11.4	5.7	0.4	13.1
40451M102/M125	Washington	—	—	—	—	—	—	3.5	3.5	1.0	5.8	3.2	1.8
40499S001/S019	Richmond	—	—	—	20.6	8.4	2.4	18.1	9.1	2.0	16.9	8.3	2.0

to exclude dubious or poorly estimated stations in a single solution. The corresponding normalized values (the spherical position differences divided by their standard deviations) served as a second test quantity. Remaining systematic errors complicate the definition of a reasonable limit factor to identify outliers. Therefore it is not possible to perform the outlier detection "fully automated" based on statistical tests. Table D.1 in the appendix represents all stations that were reduced from the contributing VLBI normal equations before the intra-technique combination.

Combination and final comparisons: The unconstrained normal equations of the four contributing VLBI solutions were scaled by the previously estimated weighting factors and summed up. Then we added minimum datum conditions to the combined normal equations and inverted the resulting normal equation system. Finally, we compared the individiual solutions with the combined solution by means of 14 parameter Helmert-transformations. The results proves the high quality of VLBI to realize the scale of the terrestrial reference frame and to estimate precise station positions and velocities (see table 5.3). The scale agrees within 0.3 parts per billion (ppb) and 0.08 ppb/yr for the rate. The RMS residuals of the individual solutions w.r.t. the combined intra-technique solution are a few mm for station positions and below 1 mm/yr for velocities. Figures 5.2 and 5.3 confirm the good agreement for the VLBI station velocities between different solutions. The residuals of station positions and velocities of the individual VLBI solutions w.r.t. the combined solution are provided in Appendix D (see table D.2).

Tab. 5.3: *Helmert-transformation results of individual VLBI solutions w.r.t. the combined intra-technique solution, using the VLBI reference frame stations.*

Parameter	DGFI	GIUB	GSFC	SHA
Scale [ppb]	0.17	-0.15	-0.34	-0.06
Scale rate [ppb/yr]	0.03	-0.08	-0.01	-0.02
Pos RMS [mm]	±3.4	±2.7	±2.2	±3.1
Vel RMS [mm/yr]	±0.43	±0.72	±0.22	±0.81

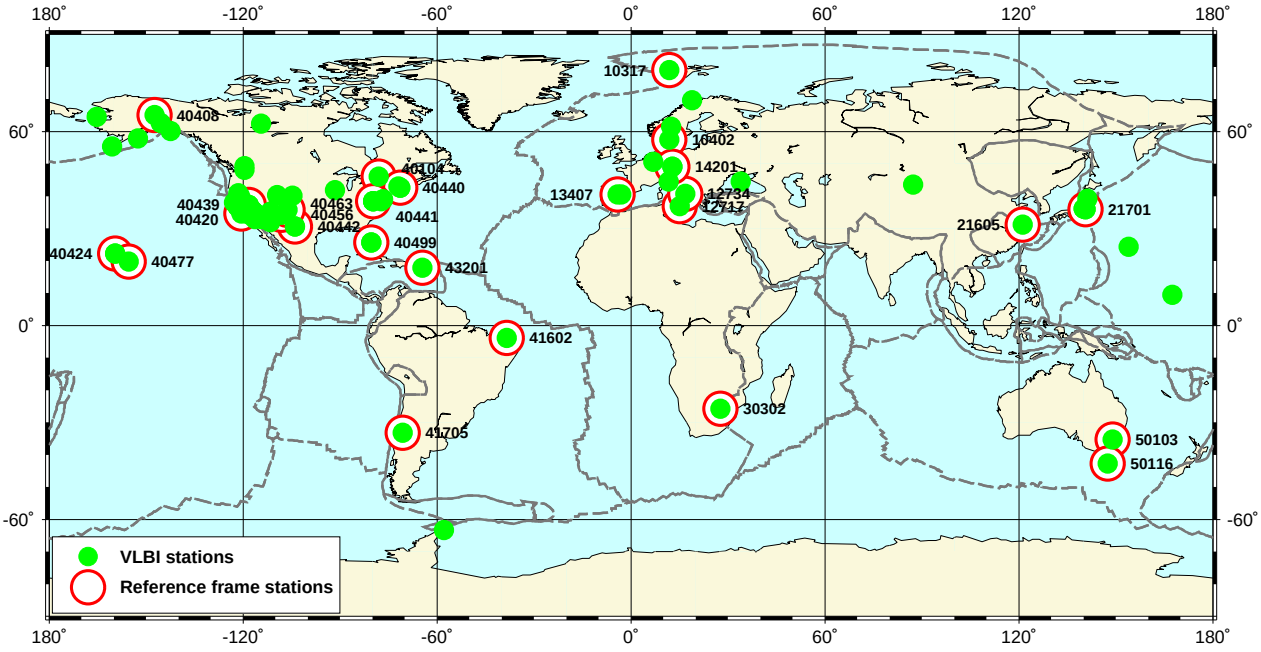

Fig. 5.1: *VLBI stations used for intra-technique combination. The reference frame stations are highlighted.*

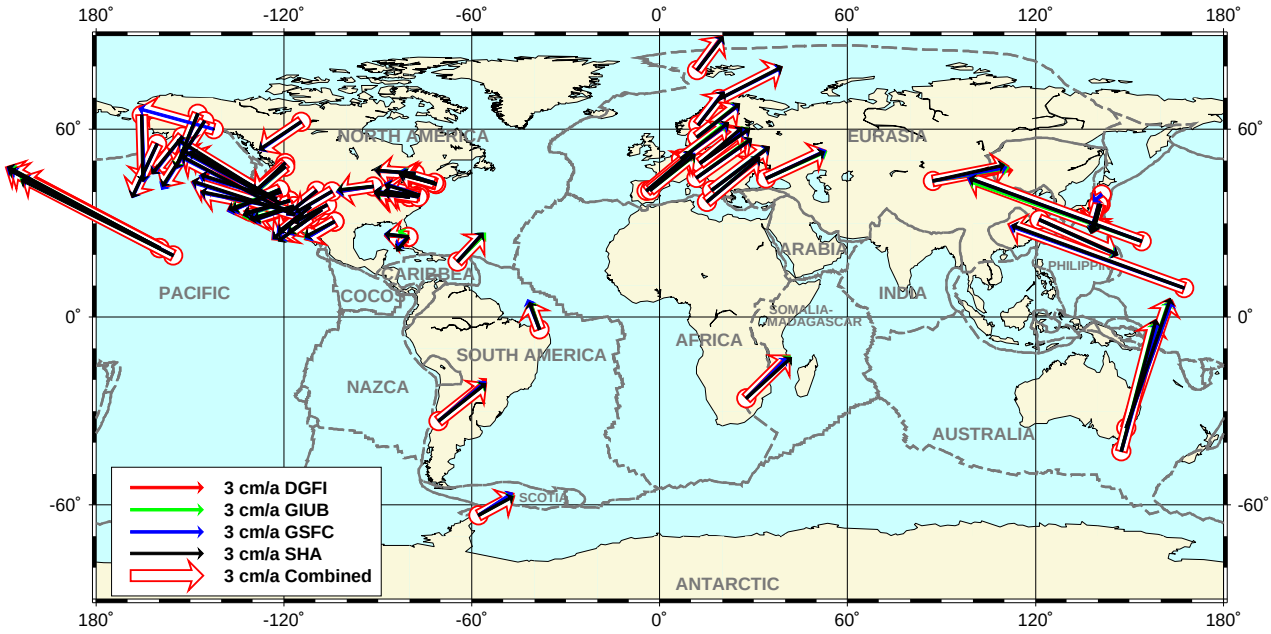

Fig. 5.2: *Horizontal VLBI station velocities for the intra-technique and individual solutions.*

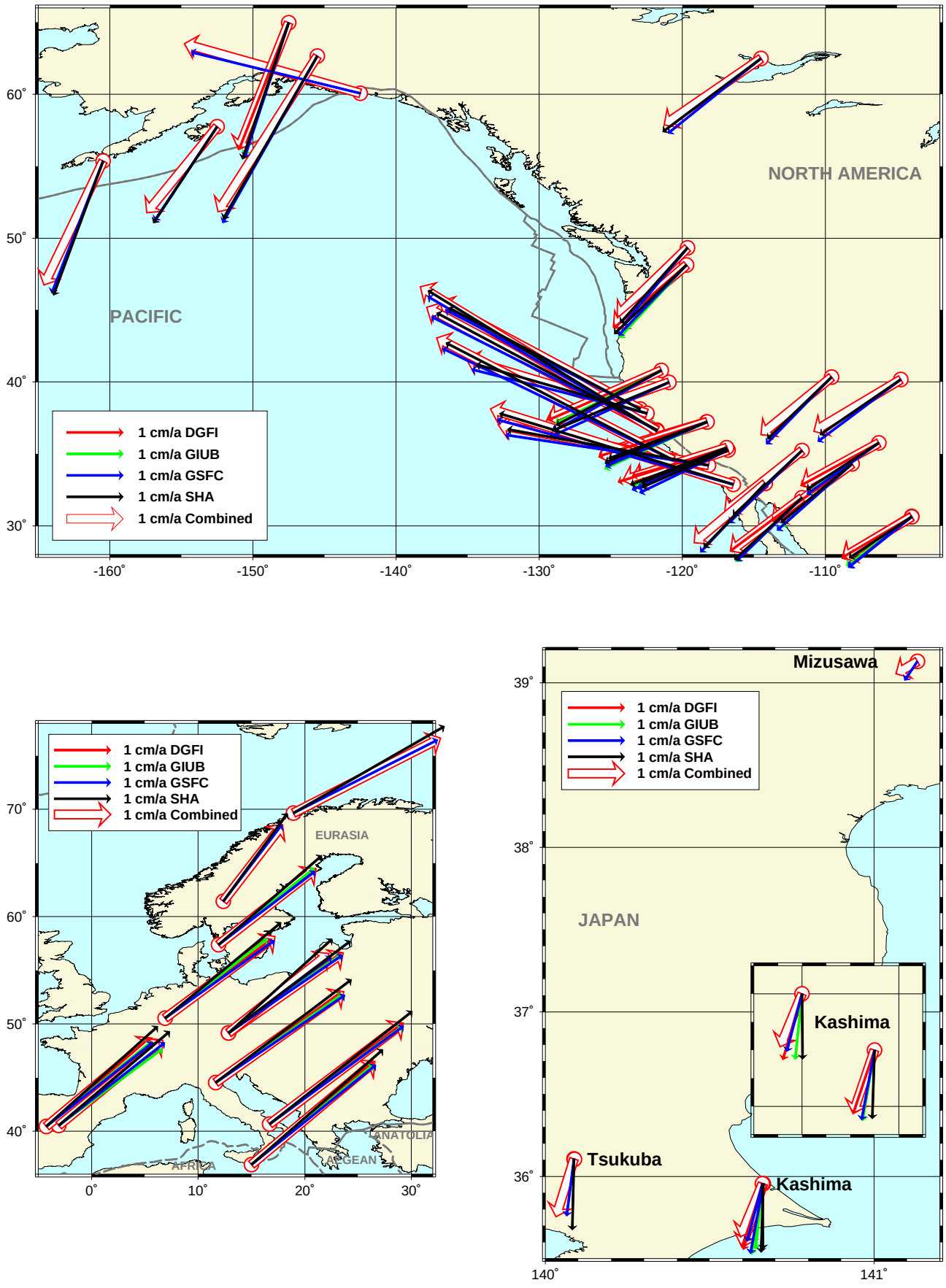

Fig. 5.3: *Horizontal VLBI station velocities (up: North America, down left: Europe, down right: Japan) from the intra-technique and individual solutions.*

5.2 SLR

Input data are normal equations obtained from four individual SLR solutions, provided by CRL (Communications Research Laboratory, Japan), CSR (Center of Space Research, USA), JCET (Joint Center for Earth System Technology, USA), and DGFI (see table 4.1). The intra-technique combination procedure consists of the following major steps:

Datum realization: SLR observations contain information to realize the origin (center of mass) and the scale of the terrestrial reference system. The orientation of the SLR network needs to be defined by external information. This was done by applying NNR condition equations (pseudo observations) to minimize the common rotation components and their rates of station positions and velocities w.r.t. ITRF2000 by using the selected SLR reference frame stations (see figure 5.4, table C.2).

Weighting: Like for VLBI, we computed mean variances for station coordinates of each individual SLR solution by using the SLR reference frame stations, which were then used to compute scaling factors for the SLR normal equations. The results indicate that the a-priori variance levels of the SLR solutions differ considerably (table 5.4). The reason for these discrepancies is not fully clear yet, however they may result from differences regarding, e.g., the number of observations included in the processing, the implemented models, the a-priori weighting, the parameterization, etc.

Tab. 5.4: *SLR weighting.*

Solution	Variances[a] for positions	Scaling[b] factors
(CRL)00L02	2.88 mm^2	2.2
(CSR)00L04	2.28 mm^2	1.7
(DGFI)01L01	0.051 mm^2	0.039
(JCET)00L05	0.111 mm^2	0.085

[a] For each of the contributing SLR solutions mean variances for station positions were computed by using the SLR reference frame stations.

[b] This column represents the scaling factors for the SLR normal equations.

Equating SLR station velocities: For various stations (e.g., Wettzell, Washington, Fort Davis) two or more occupations do exist (table 5.5). To decide whether different velocity estimates for a particular station can be equated or not, we computed for each contributing SLR solution the velocity differences between the occupations, their standard deviations, and the normalized velocity differences. The respective results are presented in table 5.5. The standard deviations differ considerably, because the observation time spans for the different occupations range from a few month to more than ten years (table C.2). Furthermore large discrepancies exist between the contributing SLR solutions, indicating that the estimated velocity differences probably do not reflect "real" changes in motion, but may result from biases in the individual solutions. For the SLR station in Arequipa (Peru), which is located in the Andean deformation zone, we assume that the observed velocity difference of about 1 cm/yr between the two occupations probably reflects a physically different motion. Furthermore, it has to be considered that the estimated standard deviations are too optimistic due to remaining systematic errors. We equated all station velocities, if the normalized differences between occupations are below a factor of 4.0. Then, about 80% of the velocities presented in table 5.5 were equated, which stabilizes the SLR solutions considerably.

Identification and rejection of outliers: We applied the same procedure and similar criteria as for VLBI. However, the discrepancies in station positions and velocities between the individual SLR solutions are larger than for VLBI, which leads to a higher limit factor for the outlier detection (i.e., 5 cm for station positions). Table E.1 represents all stations that were reduced from the contributing SLR solutions before the intra-technique combination.

Combination and final comparisons: The (reduced) normal equations of the four contributing SLR solutions were added by applying the previously estimated scaling factors. Then we added minimum datum conditions as pseudo observations, and inverted the resulting normal equation system. Finally, we compared the individual SLR solutions with the combined solution by

Tab. 5.5: *Spherical velocity differences between different SLR occupations of the same station, along with their standard deviations [mm/yr]. The ratios $\triangle/\sigma$ represent the normalized velocity differences. Remark: The large uncertainties observed in some cases, are probably caused by too short observation periods (e.g. a few months only) for an occupation (table A.2).*

Occupations	Site	CRL			CSR			DGFI			JCET		
		$\triangle_{vel}$	$\sigma_{\triangle vel}$	$\triangle/\sigma$	$\triangle_{vel}$	$\sigma_{\triangle vel}$	$\triangle/\sigma$	$\triangle_{vel}$	$\sigma_{\triangle vel}$	$\triangle/\sigma$	$\triangle_{vel}$	$\sigma_{\triangle vel}$	$\triangle/\sigma$
10002S001/S002	Grasse	7.1	8.1	0.9	2.5	1.7	1.4	4.7	1.8	2.6	—	—	—
10503S001/S014	Metsahovi	353.9	67.8	5.3	70.3	14.5	4.8	11.6	9.0	1.3	—	—	—
12337S003/S006	Simeiz	27.2	7.2	3.8	5.4	27.4	0.2	10.5	3.3	3.2	27.3	57.4	0.5
12725M002/S013	Cagliari	37.0	9.7	3.8	30.9	30.9	1.0	7.0	4.3	1.6	—	—	—
12734S001/M004	Matera	—	—	—	6.3	4.6	1.4	2.8	2.4	1.2	—	—	—
13402S004/S007	San Fernando	97.4	29.8	3.3	—	—	—	23.3	17.6	1.3	53.5	23.0	2.3
13504M002/S001	Kootwijk	—	—	—	49.9	11.5	4.3	87.3	50.8	1.7	—	—	—
14001S001/S007	Zimmerwald	10.5	3.1	3.4	—	—	—	5.3	1.7	3.1	15.5	4.5	3.4
14106S001/S009	Potsdam	207.0	101.6	2.1	43.0	16.0	2.7	5.7	7.4	0.8	—	—	—
14201M005/S018	Wettzell	40.2	7.4	5.4	18.7	10.0	1.9	21.0	12.5	1.0	138.3	23.6	5.9
14201S002/S018	Wettzell	75.5	20.5	3.7	2.4	2.1	1.1	1.2	1.2	1.0	—	—	—
21602S003/S006	Wuhan	—	—	—	—	—	—	98.9	40.5	2.5	93.4	211.6	0.5
21704M001/S002	Tokyo	47.4	7.0	6.8	18.0	6.0	3.0	14.1	16.3	0.9	29.4	21.5	1.4
40433M002/M005	Quincy	—	—	—	36.7	20.1	1.8	84.9	26.0	3.3	—	—	—
40438M001/M002	Bear Lake	—	—	—	110.6	13.9	7.9	69.1	22.7	3.0	—	—	—
40439M001/M004	Owens Valley	—	—	—	7.5	10.0	0.8	85.7	27.7	3.1	—	—	—
40442M001/M006	Fort Davis	—	—	—	3.8	1.1	3.5	5.7	2.2	2.6	—	—	—
40451M102/M105	Washington	—	—	—	51.2	8.9	5.7	48.5	17.0	2.9	—	—	—
40451M117/M105	Washington	—	—	—	5.0	11.0	0.5	8.7	14.1	0.6	53.7	32.6	1.6
40451M120/M105	Washington	2.4	0.9	2.6	7.1	2.4	3.0	0.9	1.3	0.7	1.6	6.2	0.3
42202M003/S001	Arequipa	8.8	4.9	1.8	12.5	1.4	8.7	8.8	0.9	9.2	—	—	—
92202M002/M004	Huahine	—	—	—	31.4	5.8	5.4	31.3	9.5	3.3	—	—	—

means of 14 parameter Helmert-transformations. The results demonstrate the high stability of the SLR solutions to realize the TRF origin and scale (table 5.6). The positions and velocities of the individual solutions agree within 5 mm and 1–2 mm/yr, respectively. These numbers reflect the accuracy of the SLR reference frame stations. Figure 5.5 shows the station velocities for the complete SLR network and figure 5.6 displays enlargements for Europe, North America and Asia. For the SLR reference frame stations there is a reasonable agreement between different solutions, whereas for some other stations larger discrepancies exist. The residuals of station positions and velocities of the individual SLR solutions w.r.t. the combined solution are provided in table E.2.

Tab. 5.6: *Helmert-transformation results of individual SLR solutions w.r.t. the combined intra-technique solution, using the reference frame stations.*

Parameter	CRL	CSR	DGFI	JCET
Tx [mm]	-0.1	1.4	0.9	2.4
Ty [mm]	1.5	-0.6	-1.3	-5.0
Tz [mm]	0.3	1.0	0.2	0.8
Scale [ppb]	0.03	0.09	-0.26	-0.10
Tx rate [mm/yr]	0.8	0.1	-0.2	-0.4
Ty rate [mm/yr]	-1.4	-0.1	0.1	1.1
Tz rate [mm/yr]	-1.6	-0.3	1.1	-0.1
Scale rate [ppb/yr]	-0.09	0.04	-0.08	0.18
Pos RMS [mm]	±4.1	± 4.9	±2.3	±3.7
Vel RMS [mm/yr]	±1.6	± 1.4	±0.7	±1.2

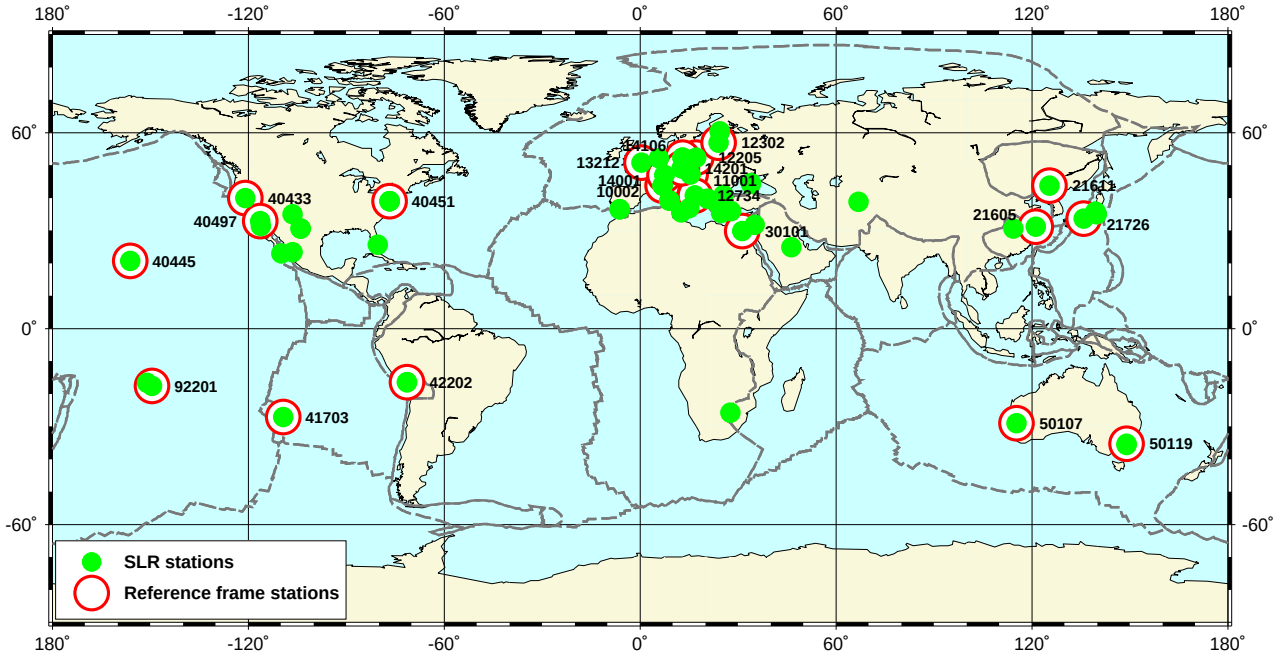

Fig. 5.4 : *SLR stations used for the intra-technique combination. The reference frame stations are highlighted.*

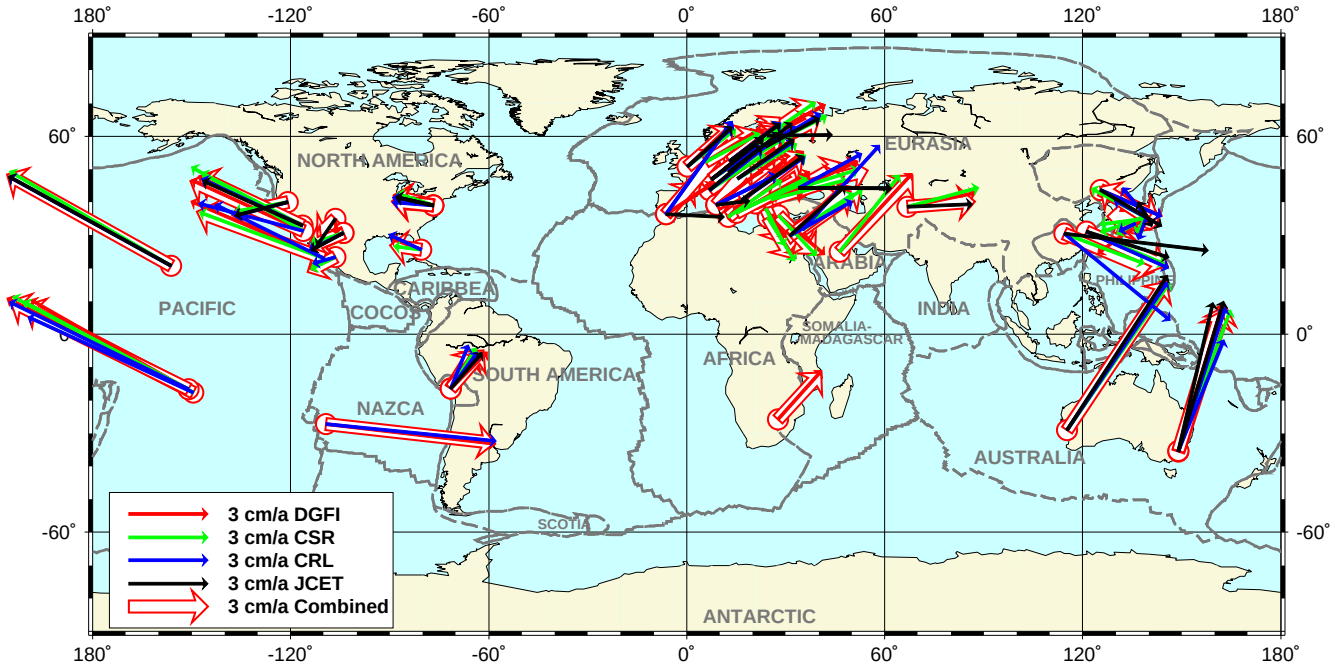

Fig. 5.5 : *Horizontal SLR station velocities for the intra-technique and individual solutions.*

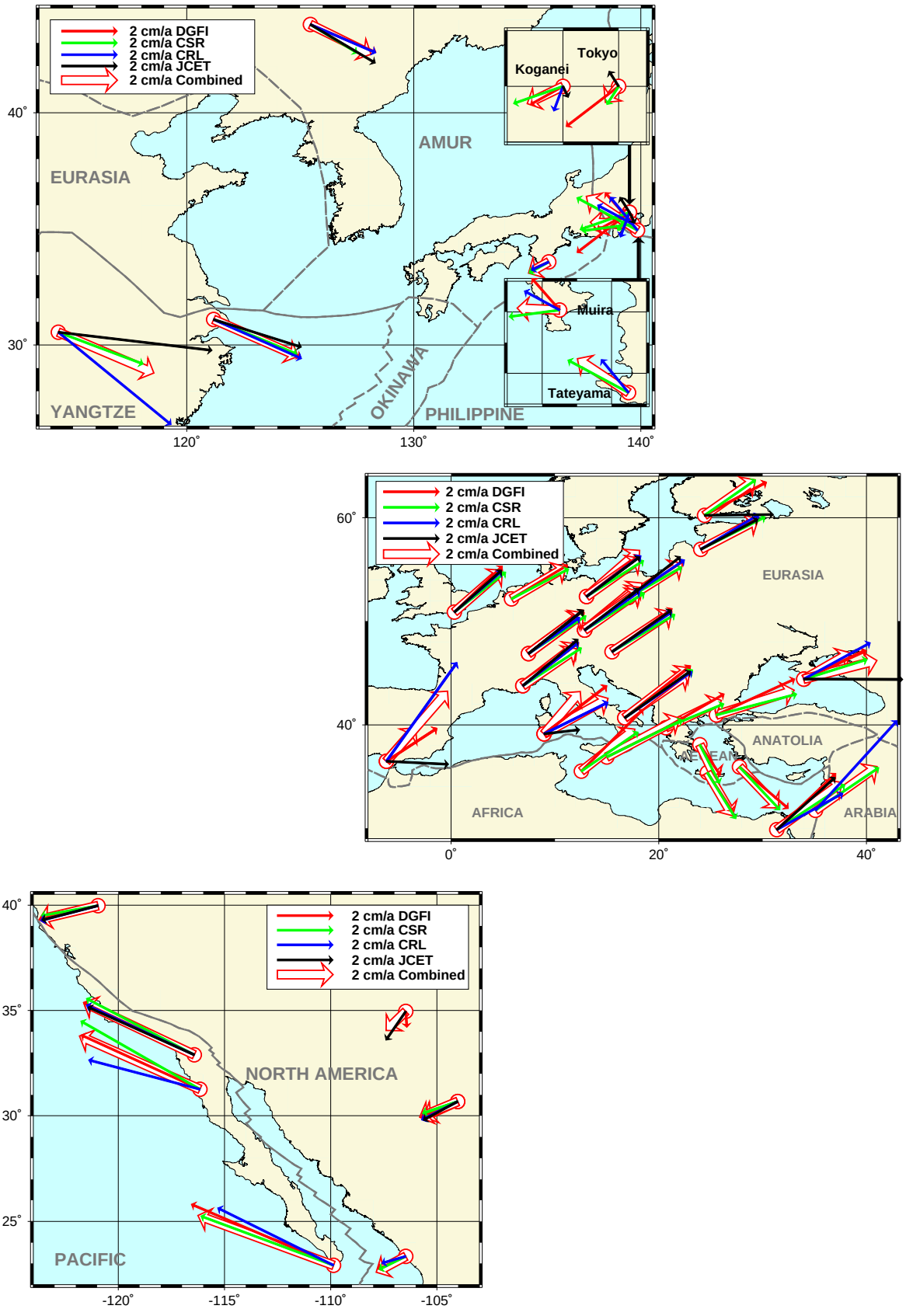

Fig. 5.6 : *Horizontal SLR station velocities (up left: Asia, middle: Europe, down left: North America) for the intra-technique and individual solutions.*

5.3 GPS

In the case of GPS, the situation concerning intra-technique combination is completely different from the other techniques, since the IGS provides combined multi-year solutions with station positions and velocities. Natural Resources Canada (NRCan), Geodetic Survey Division, on behalf of the IGS and its Reference Frame Working Group, combines a consistent set of station coordinates, velocities, Earth Rotation Parameters (ERP) and apparent geocenter positions to produce the official IGS station position/ERP solutions in SINEX format (Ferland, 2002).

This weekly combination includes solutions from the IGS Analysis Centers containing estimates of weekly station coordinates, apparent geocenter positions and daily ERPs. Each weekly solution generally includes estimates of coordinates of 120 to 140 globally distributed stations. The weekly combined station coordinates are accumulated in a multi-year solution containing station coordinates and velocities. Details of the processing strategy and combination results are presented in (Ferland, 2000; Ferland, 2002).

The cumulative IGS solution (IGS03P01), which we used for this TRF computation, originally includes 216 stations. We reduced 10 "poorly" estimated GPS stations with an observation time span less than one year (see table C.3 in the appendix).

The intra-technique combination consists of the following steps:

Datum realization: In principle, GPS observations contain information to realize the origin and scale of the terrestrial reference system, whereas the orientation of the network has to be defined by external information. However, at present the determination of TRF scale and origin with GPS is problematic (e.g. because of uncertainties of the GPS antenna and satellite phase center definition). The cumulative IGS solution was transformed by NRCan to ITRF2000 (reference epoch 1998.0) by means of a 14 parameter Helmert-transformation (3 translations, 3 rotations, 1 scale and their respective rates). The transformation parameters were determined from a subset of 51 high quality, globally distributed and generally with other techniques co-located stations, known as reference frame stations (see ftp://igscb.jpl.nasa.gov/igscb/station/coord/-IGS01P37_RS54.snx.Z, figure 5.7).

Weighting: Within the GPS intra-technique combination procedure at NRCan, all weekly analysis center solutions are re-scaled by variance factors determined during a comparison with the cumulative solution. The applied variance factors are reported for each weekly combination (see ftp://cddisa.gsfc.nasa.gov/gps/products/wwww).

Equating GPS station velocities: There are several GPS stations with more than one occupation, for which different velocities were estimated in the cumulative IGS solution. Table 5.7 shows the spherical velocity differences, their standard deviations, and the ratio between both values. If these ratios (normalized velocity differences) are below a certain limit (i.e., 3.0) the respective station velocities were equated. For this purpose we applied pseudo observations with appropriate weights like for the other intra-technique combinations.

Identification and rejection of outliers: As described in (Ferland et al. 2000), several comparisons were made by NRCan to detect and reject outliers, in order to produce reliable weekly and updated cumulative solutions. Any detected (rejected) outlier is reported (see ftp://cddisa.gsfc.nasa.gov/gps/products/wwww). In addition we compared the cumulative IGS solution (IGS03P01) used for this TRF computation with the cumulative solution (IGS02P32) based on about a half year less observation data and with ITRF2000 to identify "problematic" GPS stations.

A Helmert-transformation between both IGS solutions led to the rejection of two stations: AMCT (40472S003) and AOA1 (40483S001), because their station position residuals exceed the boundary value of 3 cm (see table C.3).

In comparison with ITRF2000 about 10 stations were identified with station position residuals exceeding 3 cm. But it has to be considered that the observed discrepancies are probably caused by "weakly" estimated ITRF2000 station positions and velocities, due to about 3 years less GPS data

Tab. 5.7: *Spherical velocity differences between different occupations on the same station, along with their standard deviations [mm/yr]. The ratios $\triangle/\sigma$ represent the normalized velocity differences.*

Occupations	Site	IGS		
		$\triangle_{vel}$	$\sigma_{\triangle vel}$	$\triangle/\sigma$
10003M004/M009	Toulouse, France	2.6	2.1	1.3
10302M003/M006	Tromsoe, Norway	2.1	0.6	3.6
10317M001/M003	Ny Alesund, Norway	1.4	0.6	2.4
12353M001/M002	Yakutsk, Russia	24.4	8.6	2.8
12353M001/M002	Yakutsk, Russia	25.4	8.3	3.0
12355M001/M002	Petropavlosk, Russia	42.5	6.0	7.1
12717M003/M004	Noto, Italy	6.1	1.2	5.1
14201M009/M010	Wettzell, Germany	29.2	2.7	10.8
23902M001/M002	Taejon, Korea	16.1	0.8	21.4
30302M007/M004	Pretoria, South Africa	5.9	0.8	7.4
30302M009/M004	Pretoria, South Africa	1.6	1.0	1.6
35001M001/M002	Rabat, Morocco	20.5	41.9	0.5
40133M001/M002	Schefferville, Canada	21.6	8.0	2.7
40400M007/ S201	Pasadena, USA	11.7	22.1	0.5
40451M123/ S003	Washington, USA	1.2	0.6	2.0
40472S003 / S004	Colorado Springs, USA	26.0	9.3	2.8
40499S018 / S020	Richmond, USA	10.9	1.4	8.1
40508M001/M002	Ensenada, Mexico	4.4	2.7	1.7
92201M003/M009	Pamatai, Tahiti	9.9	2.9	3.4
92201M006/M009	Pamatai, Tahiti	16.5	3.3	5.0

compared to the cumulative IGS solution. Therefore we did not reject those stations before the inter-technique combination.

Combined GPS normal equation: In the VLBI and SLR intra-technique combination we have generated unconstrained normal equations as input for the TRF computation. This was not possible for the cumulative IGS solution, since we were not able to reduce the datum information completely.

A rank defect analysis of the resulting GPS normal equations indicates that this matrix is not singular. This conflicts with our preferred combination strategy on the level of unconstrained normal equations. To overcome this problem, we reduced the GPS datum information within the inter-technique combination by setting up respecitive Helmert-transformation parameters (see chapter 6). As a consequence, we suggest for future TRF computations, that SINEX files with unconstrained normal equations should be provided by the services (see section 8.4).

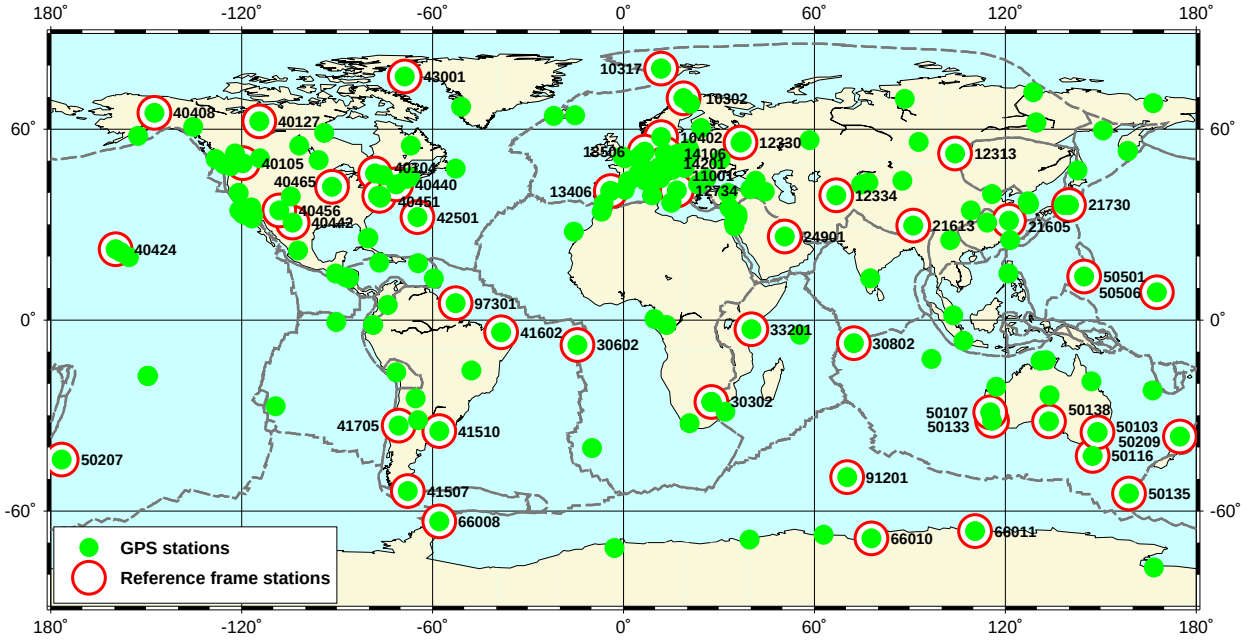

Fig. 5.7: *GPS stations used for TRF computation. The reference frame stations are highlighted.*

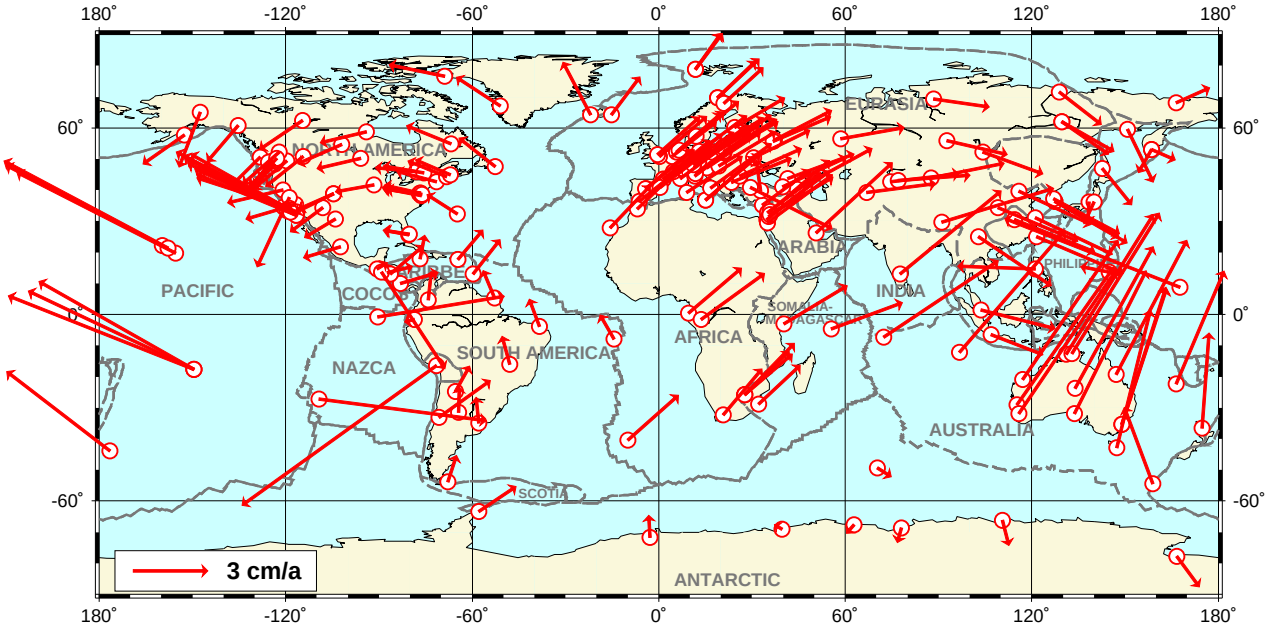

Fig. 5.8: *Horizontal GPS station velocities (obtained from the IGS solution provided by NRCan).*

5.4 DORIS

For the DORIS intra-technique combination we used two solutions provided by IGN/JPL and GRGS (Groupe de Reserches de Géodésie Spatiale, France), see table 4.1. The procedure consists of the following major steps:

Datum realization: DORIS observations contain information to realize the origin and scale of the terrestrial reference system like SLR. The two contributing solutions differ considerably from ITRF2000 regarding scale and origin. In the GRGS solution, no constraints were reported in the SINEX file, and consequently the a-priori datum could not be removed. To realize a consistent datum for both DORIS solutions, we transformed them to ITRF2000 by means of a 14 parameter Helmert-transformation. In addition we applied NNR conditions for the loosely constrained IGN/JPL solution by using the DORIS reference frame stations (see figure 5.9).

Weighting: The scaling factors were computed on the basis of mean position variances for the DORIS reference stations. It has to be considered, that for the GRGS solution all station velocities for different occupations on a site were equated a-priori. Thus, we applied the same procedure for the IGN/JPL solution to achieve comparable solutions for computing scaling factors. The results (table 5.8) indicate that the position variances of both DORIS solutions differ considerably, which requires further studies.

Tab. 5.8: *DORIS weighting.*

Solution	Variances [a] for positions	Scaling [b] factors
(GRGS)00D01	121.4 mm^2	1.96
(IGN)00D04	2.5 mm^2	0.041

[a] For each of the contributing DORIS solutions mean variances for station positions were computed by using the DORIS reference frame stations.

[b] This column represents the scaling factors for the DORIS normal equations.

Equating DORIS station velocities: This procedure was applied for the IGN/JPL solution only, as the equating of station velocites was already done by GRGS analysis center. Like for the other techniques we computed for different occupations on a station the respective velocity differences, their standard deviations, and the ratio between both values. The results shown in table 5.9 indicate for some stations significant velocity differences between occupations (e.g., Ny Alesund, Santiago, Syowa). Finally, we equated the station velocities if the normalized differences were below a limit of 4.0.

Identification and rejection of outliers: We applied the same procedure as for VLBI and SLR, but we have to consider that the identification of outliers is problematic as only two DORIS solutions were contributing. To exclude poorly estimated stations from the DORIS intra-technique combination we used a limit factor (i.e., 7 cm for station positions). Again, the normalized station and velocity differences served as a second test quantity. Table F.1 summarizes all stations that were reduced from the contributing DORIS solutions.

Combination and final comparisons: The (reduced) DORIS normal equations were added by applying the previously estimated relative scaling factors. Then we computed the combined DORIS solution by adding minimum datum constraints and inverting the normal equation system. Finally, we compared the individiual solutions with the combined solution by means of 14 parameter Helmert-transformations (table 5.10). Since both solutions were transformed to ITRF2000 before combining them, the Helmert-transformation parameters are close to zero. The station positions and velocities between the IGN/JPL and the GRGS solution agree in the order of 7–8 mm and 2 mm/yr, respectively. The station velocities of both individual solutions and the combined intra-technique solution are displayed in figure 5.10. The residuals of station positions and velocities of the individual DORIS solutions w.r.t. the combined solution are presented in table F.2.

Tab. 5.9: *Equating DORIS station velocities. Spherical velocity differences between different occupations, along with their standard deviations [mm/yr]. The ratios $\triangle/\sigma$ represent the normalized velocity differences.*

Occupations	Site	IGN $\triangle_{vel}$	IGN $\sigma_{\triangle vel}$	IGN $\triangle/\sigma$
10003S001/S003	Toulouse, France	3.8	2.0	1.9
10202S001/S002	Reykjawik, Island	11.3	1.3	8.4
10317S002/S004	Ny Alesund, Norway	15.5	1.3	11.8
10503S013/S015	Metsahovi, Finland	27.7	4.9	5.6
12334S004/S005	Kitab, Uzbekistan	6.3	2.2	2.9
12334S004/S006	Kitab, Uzbekistan	27.2	5.9	4.6
23101S001/S002	Cibinong, Indonesia	22.4	4.5	5.0
30302S005/S006	Hartebeesthoek, S. Africa	13.7	3.7	3.7
30302S005/S002	Hartebeesthoek, S. Africa	14.3	3.5	4.1
30313S001/S002	Marion Island, S. Africa	13.8	2.9	4.7
30604S001/S002	Tristan da Cunha, UK	28.9	15.2	1.9
30606S002/S003	Sainte Helene, UK	15.6	2.8	5.6
31906S001/S002	Ponta Delgada, Portugal	36.2	9.7	3.7
32809S002/S003	Libreville, Gabun	10.7	2.2	5.0
39901S002/S003	Djibouti, Djibouti	14.9	3.1	4.7
40102S009/S011	Ontarion, Canada	10.1	2.9	3.5
40127S007/S008	Yellowknife, Canada	22.6	5.8	3.9
40405S005/S035	Goldstone, USA	29.2	7.4	3.9
40405S005/S037	Goldstone, USA	5.7	3.5	1.6
40408S004/S005	Fairbanks, USA	8.9	1.7	5.4
40503S003/S004	Socorro Island, Mexico	69.1	158.6	0.4
41507S003/S004	Rio Grande, Argentina	8.8	3.2	2.7
41507S003/S005	Rio Grande, Argentina	21.1	4.5	4.7
41703S008/S009	Easter Island, Chile	17.9	11.0	1.6
41705S007/S008	Santiago, Chile	31.7	3.1	10.2
41705S007/S009	Santiago, Chile	73.7	7.5	9.8
42202S005/S006	Arequipa, Peru	219.4	39.8	5.5
50103S201/S202	Canberra, Australia	47.2	9.2	5.1
50107S006/S010	Canberra, Australia	9.3	2.0	4.5
51101S001/S002	Port Moresby, Papua N.	56.4	25.6	2.2
66006S001/S003	Syowa, Antartica	17.9	1.3	13.9
91201S002/S003	Kerguelen, Kerguelen Isl.	7.1	3.8	1.9
91201S002/S004	Kerguelen, Kerguelen Isl.	25.3	5.3	4.7
91401S002/S003	Amsterdam, Amsterdam Isl.	33.1	4.8	6.8
91501S002/S002	Ile de Petrels, Terre Adelie	273.9	130.9	2.1
92201S007/S008	Pamatai, Tahiti	15.6	3.8	4.1
92701S001/S002	Noumea, New Caledonia	94.6	25.2	3.8
97401S001/S002	La Reunion, Reunion	10.1	1.7	5.9

Tab. 5.10: *Helmert-transformation results of individual DORIS solutions w.r.t. the combined intra-technique solution, using the DORIS reference frame stations. The transformation parameters are close to zero, since both DORIS solutions were transformed to ITRF2000 before combining them.*

Parameter	GRGS	IGN
Tx [mm]	−0.6	−0.2
Ty [mm]	−1.1	−0.2
Tz [mm]	1.4	1.5
Scale [ppb]	0.11	−0.05
Tx rate [mm/yr]	0.0	0.0
Ty rate [mm/yr]	−0.6	−0.6
Tz rate [mm/yr]	−0.2	0.2
Scale rate [ppb/yr]	0.05	0.03
Pos RMS [mm]	±6.4	±7.4
Vel RMS [mm/yr]	±1.8	±1.8

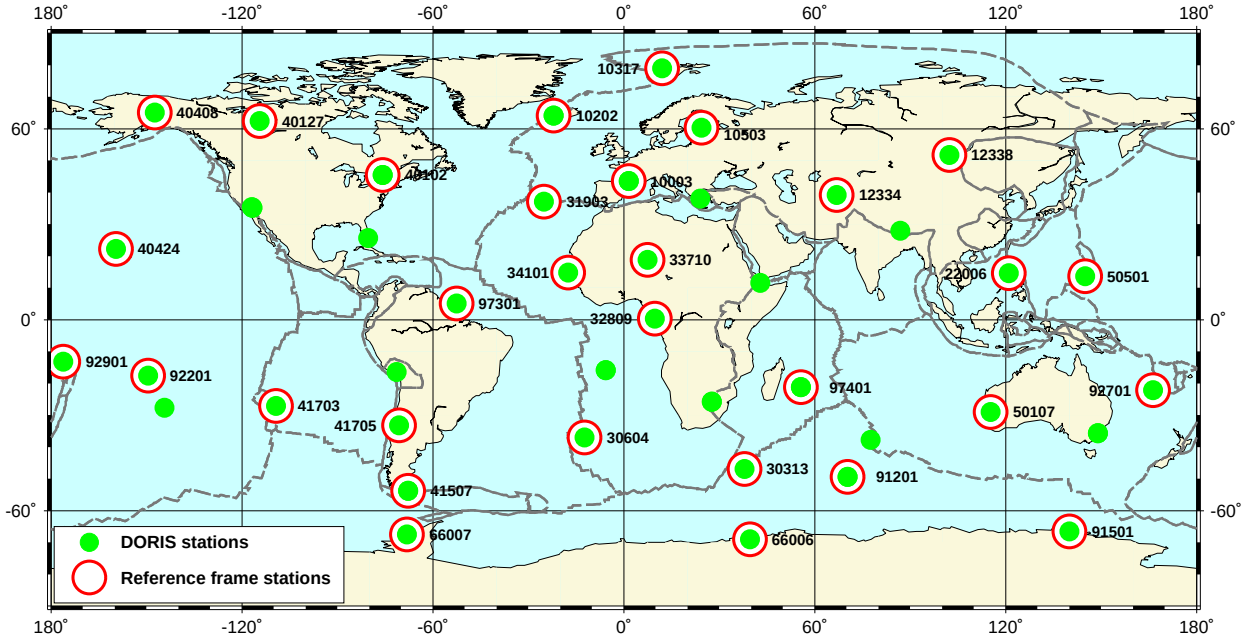

Fig. 5.9 : *DORIS stations used for intra-technique combinations. The reference frame stations are highlighted.*

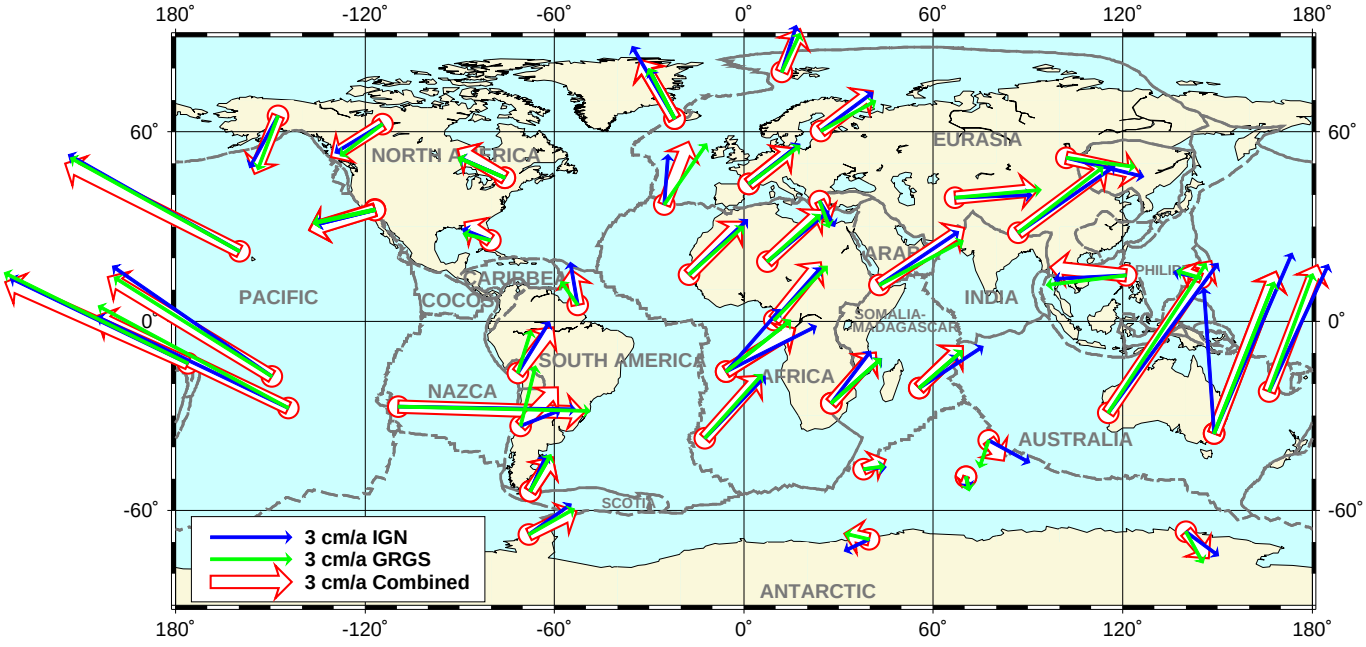

Fig. 5.10 : *Horizontal DORIS station velocities for the intra-technique and individual solutions.*

6 Inter-technique combination

6.1 Characteristics of intra-technique solutions and weighting

Input for the inter-technique combination are the unconstrained normal equations of VLBI, SLR, GPS and DORIS resulting from the intra-technique combination. The characteristics of these input data are summarized in table 6.1.

For the TRF combination we applied a weighting procedure described in the next paragraph to estimate scaling factors for the normal equations of the different techniques. As for the intra-technique combination, we estimated for each technique's combined solution mean standard deviations for positions and velocities, using the reference frame stations. Within the intra-technique combination, we assumed a comparable accuracy level for the estimated parameters for each of the contributing solutions. However, in the case of the inter-technique combination the situation is different, as VLBI, SLR, GPS and DORIS solutions do not provide the same accuracy level for station position and velocity estimations (see table 6.1).

It is essential to estimate a "realistic" accuracy level for the different techniques. This was done by applying two different approaches: (i) A comparison of the individual solutions w.r.t. the combined intra-technique solutions (see chapter 5), and (ii) by comparing the combined intra-technique solutions with ITRF2000 station positions and velocities (see table 7.5). As both approaches provided similar results (see table 6.1), we considered the average as a realistic accuracy level for station positions and velocities. On this basis we computed for each technique scaling factors for station positions and velocities (see table 6.1). The resulting scaling factors are quite large for SLR and VLBI, indicating that the standard deviations (formal errors) obtained from the intra-technique combinations are probably too optimistic. In the case of GPS and DORIS the intra-technique standard deviations seem to be more realistic. The last row of table 6.1 shows the scaling factors, that finally were applied to the combined intra-technique normal equations.

6.2 Co-location sites and local ties

In the inter-technique combination co-location sites and local ties play a dominant role. These intra-site vectors are a key element to integrate and combine the technique-specific reference frames into a common TRF frame and to identify biases between different space techniques. Figure 6.1 shows the stations that were used in this TRF computation, furthermore the co-location sites are highlighted in this figure.

Are the local ties sufficiently well determined to introduce them as a constraint, and are different velocity estimations at the same site identical? To find the answers it is essential to validate the local tie information and the velocity estimations at co-location sites, before combining different techniques. This validation was done by comparing the local ties with the station coordinate differences obtained from the intra-technique solutions, and by analysing the velocity differences of co-located instruments. The results of these comparisons are summarized in table 6.2; a detailed documentation is provided in appendix G.

The comparisons between local ties and space geodetic results indicate that the current situation is not satisfying. An excellent agreement was found for six co-locations, for which the spherical differences between local ties and the intra-technique solutions are below 5 mm (see table 6.2). On the other hand, there are many other co-locations, where the differences exceed 2 cm. Regarding station velocity estimations there are eight co-locations with spherical velocity differences below 1 mm/yr, but in many other cases the differences exceed 5 mm/yr. An interpretation of these discrepancies is difficult, since various factors have to be considered. So, uncertainties of the space geodetic solutions and systematic differences between them, local site effects, such as different motions of the co-located instru-

Tab. 6.1 : *Characteristics of intra-technique solutions used for TRF computation.*

Solution characteristics	VLBI	SLR	GPS	DORIS
# stations	81	65	202	53
# observations [a]	11841870	5094864	525313	26051465
# unknowns (pos+vel)	489	390	1212	318
# reduced parameters [b]	3908468	119155	156	444
variance factors	1.477	0.931	1.0	1.956
square sum of residuals (v^TPv)	11717571.9	4634613.0	524105.2	50962616.9
mean standard deviations [c]				
– σ_{pos} [mm]	0.30	0.36	1.60	7.43
– σ_{vel} [mm/yr]	0.10	0.11	0.45	3.47
Intra-technique RMS residuals [d]				
– positions [mm]	2.9	3.8	—	6.9
– velocities [mm/yr]	0.56	0.89	—	1.8
RMS residuals (w.r.t. ITRF2000) [e]				
– positions [mm]	3.9	4.7	1.6	14.6
– velocities [mm/yr]	0.54	1.2	0.89	2.7
scaling factors for standard deviations [f]				
– station positions	11.3	11.7	1.0	1.4
– station velocities	5.5	9.5	2.0	0.6
– average of σ_{pos} and σ_{vel}	8.4	10.6	1.5	1.0
scaling factors for normal equations	0.0142	0.0089	0.444	1.0

[a] For VLBI, SLR and DORIS the number of the original observations is displayed, whereas in case of GPS the number of observations is the total number of station coordinates provided by the IGS analysis centers in their weekly solutions (over 7 years).

[b] The reduced parameters for VLBI and SLR include also auxilliary parameters, such as VLBI clock corrections and SLR orbit parameters.

[c] We used the intra-technique solutions defined by minimum datum conditions to estimate mean standard deviations, using the reference frame stations for each technique.

[d] RMS residuals for station positions and velocities were obtained from a comparison of individual solutions w.r.t. combined intra-technique solutions. As in the case of GPS the intra-technique combination was done by the IGS in a different way, the respective values are not available.

[e] RMS residuals for station positions and velocities are obtained from a comparison of combined intra-technique solutions with ITRF2000.

[f] To compute the scaling factors the RMS residuals (average of [d] and [e]) are divided by the standard deviations (see [c]).

ments, small remaining datum inconsistencies between different techniques and errors in local tie measurements could be the reasons for these discrepancies.

Furthermore, most of the co-locations exist between GPS and the other techniques, i.e., there are less direct connections between the other techniques. Thus, the GPS network plays a dominant role for the integration of the different techniques, which is rather problematic for the identification of remaining technique-specific biases. This underlines that there is an urgent need to improve the current situation regarding co-locations and local tie accuracy and reliability.

6.3 Selection of local ties and equating station velocities

Taking into account the present situation regarding co-location sites and local tie accuracy, the

selection of suitable local ties is an important aspect to ensure that "poorly" observed local ties do not degrade the high internal accuracy of the individual space techniques within the combination. Furthermore, the station velocity estimations of co-located instruments differ significantly for various co-location sites (table G.2 in the appendix). Thus, we did not automatically force different velocities on co-location sites to be identical, as it was done, e.g., for ITRF2000 computation.

We applied an iterative procedure for the selection of suitable local ties and for equating station velocities. Table 6.3 summarizes the criteria for the various processing steps. Detailed results are provided in table G.2. In principle, the procedure is based on the following steps:

1. In the first step, we used the combined intra-technique solutions to compare the coordinate differences between co-located instruments with the official local ties obtained from the ITRF data base (ftp://lareg.ensg.ign/fr/pub/itrf/itrf2000). In addition, we compared the velocity estimations of different techniques at co-location sites. The results of these comparisons are summarized in table 6.2. Note that in this first iteration, each of the intra-technique solutions was solved separately (without introducing any local tie information) by applying NNR and NNT datum conditions w.r.t. ITRF2000. As a result of this processing step we identified six high quality co-locations, three between GPS and VLBI and another three between GPS and SLR. For these stations the spherical coordinate differences between the space geodetic solutions and the local ties are below 5 mm. The station velocites agree within 2.5 mm/yr between these co-located instruments (table 6.4).

2. Then, the six previously selected high-quality co-locations were used for the inter-technique combination. The information was applied as pseudo observations with a-priori standard deviations of 1.0 mm and 1.0 mm/yr for local ties and velocities, respectively. Again, we compared the space geodetic coordinates with the local ties, and the velocities of co-located instruments. In this second processing step, we selected 13 additional co-locations between GPS, SLR, and VLBI, the corresponding boundary values being 10 mm for the discrepancies in local ties and 4.5 mm/yr for the spherical velocity differences of co-located instruments. Re-iterations were performed by applying less strong criteria (table 6.3). Altogether 50 local ties were selected and introduced in the TRF combination, these are 37 ties between different techniques and 13 intra-technique ties (table 6.5). For all these co-locations the station velocites were equated.

3. Finally, we performed the equating of station velocities for all remaining co-locations, which were not considered in the previous steps. These were about 50% of the co-located sites, having too large discrepancies or missing local tie information. For all these co-locations that were not considered so far, we used the corresponding station velocity differences together with their standard deviations to decide whether the velocities can be equated or not. Altogether, about 75% of the station velocities of co-located instruments were equated (table 6.5), detailed results are provided in table G.2.

6.4 Combined solution: TRF realization 2003

Input for the TRF computation are the unconstrained normal equations resulting from the intra-technique combination of the different space techniques. These normal equations were added by applying the previously estimated scaling factors (see table 6.1). The resulting combined normal equations were completed by pseudo-observations for local ties and for equating station velocities at co-location sites (see previous section). For the GPS and DORIS normal equations, Helmert-transformation parameters were set up, to reduce the datum information already included for these techniques. Finally, the combined TRF solution was computed by adding datum conditions as pseudo-observations and inverting the resulting normal equation system. The geodetic datum was realized by NNR conditions for the orientation and its rate w.r.t. ITRF2000 station positions and velocities using about 100 globally distributed sites. The origin (translation components and their rates) was realized by SLR, and the scale and its rate by VLBI and SLR.

The TRF realization 2003 includes 401 stations located at 259 sites. Figure 6.2 shows the horizontal station velocities of the combined solution in comparison with the intra-technique solutions.

Tab. 6.2: *Comparison of space techniques at co-location sites. Shown are differences between local ties and the space geodetic derived intra-site vectors (upper part), as well as the spherical velocity differences of co-located instruments (lower part).*

	GPS-VLBI	GPS-SLR	SLR-VLBI	GPS-DORIS	SLR-DORIS	VLBI-DORIS
# co-locations	33	28	11	19	3	2
# local surveys	28	22	9	18	3	2
Δ local ties						
< 5 mm	3	3	–	–	–	–
5 - 10 mm	5	3	1	–	–	–
10 - 20 mm	10	8	2	2	–	–
> 20 mm	10	8	8	16	3	2
Δ velocities						
< 1 mm/yr	5	2	1	–	–	–
1 - 2.5 mm/yr	10	8	2	1	–	–
2.5 - 5 mm/yr	7	11	1	8	–	1
> 5 mm/yr	11	7	7	10	3	1

Tab. 6.3: *Summary of the criteria applied for the selection of suitable co-locations. For each iteration the number of selected local ties is provided along with the respective boundary values (limits) and the a-priori standard deviations applied for local ties and equating station velocities at co-location sites.*

Iter. No.	# ties selected	Local ties [mm]		Velocities [mm/yr]	
		limit	σ_{tie}	limit	σ_{vel}
1	6	5.0	1.0	2.5	1.0
2	13	10.0	3.0	4.5	3.0
3	18	20.0	3.0	4.5	3.0
4	13	34.0	5.0	4.5	5.0

Tab. 6.4: *Differences between space geodetic solutions and local ties as well as station velocity differences at the selected "high-quality" co-location sites.*

Co-location sites	Techniques	Difference in position [mm]			Difference in velocity [mm/yr]		
		$\Delta\phi$	$\Delta\lambda$	Δh	$\Delta\phi$	$\Delta\lambda$	Δh
Wettzell, Germany	GPS-VLBI	-0.01	-0.76	3.71	0.17	0.03	0.77
Mauna Kea, Hawaii	GPS-VLBI	-1.46	-4.75	1.32	-0.07	-0.74	1.89
North Liberty, USA	GPS-VLBI	-1.68	-2.89	-2.01	-0.79	-0.53	2.23
Potsdam, Germany	GPS-SLR	2.85	1.75	-2.81	0.15	-0.03	0.29
Graz, Austria	GPS-SLR	3.61	-0.19	1.84	-0.02	-0.37	0.85
Yarragadee, Australia	GPS-SLR	-1.18	0.61	-3.14	0.84	-0.92	0.46

Tab. 6.5: *Statistic of selected local ties and equated station velocities used for the TRF computation. This information is provided for ties and velocities of co-locations between different techniques.*

	GPS-VLBI	GPS-SLR	SLR-VLBI	GPS-DORIS	SLR-DORIS	VLBI-DORIS
local ties						
# available ties	28	22	9	18	3	2
# selected ties	16	12	3	5	0	1
station velocities						
# co-locations	33	28	11	19	3	2
# equated velocities	26	26	9	7	2	1

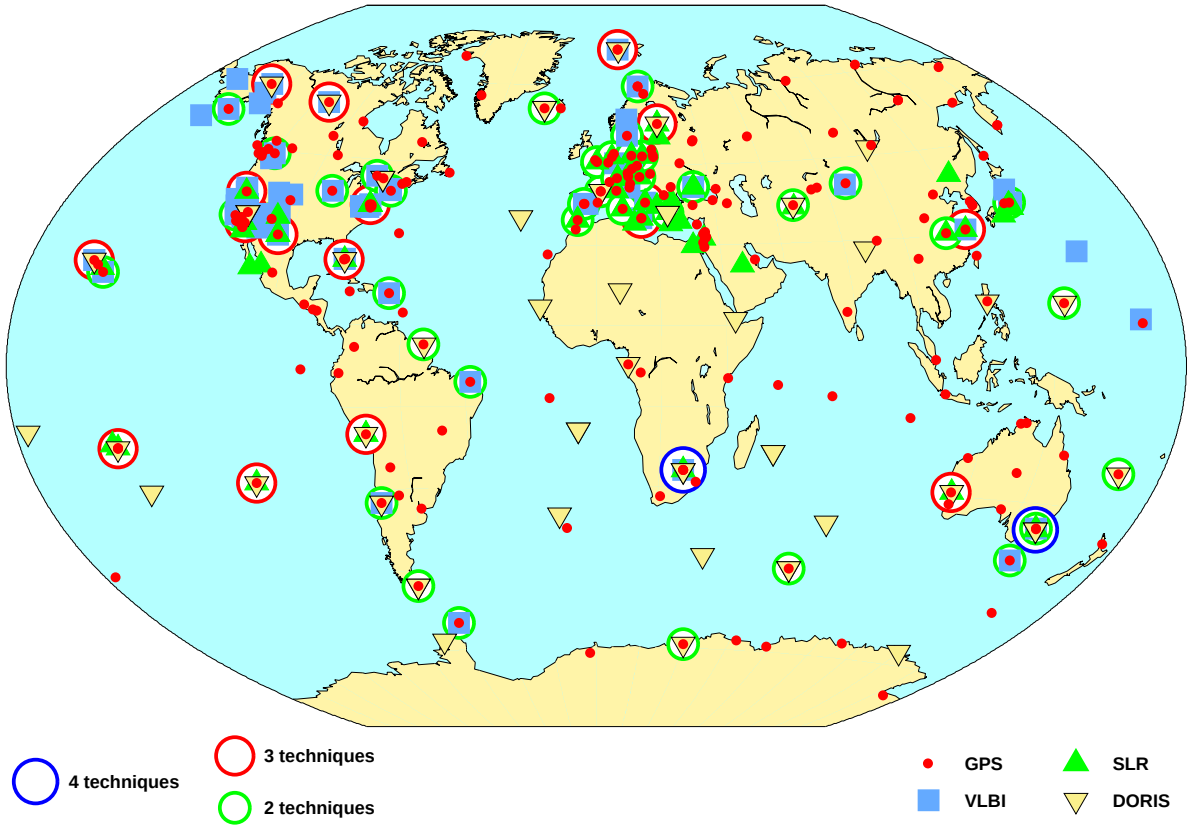

Fig. 6.1: *VLBI, SLR, GPS and DORIS stations used for the TRF computation at DGFI. Furthermore co-location sites with two, three and four techniques are shown. Stations with only few observations (e.g., less than one year of data) were excluded.*

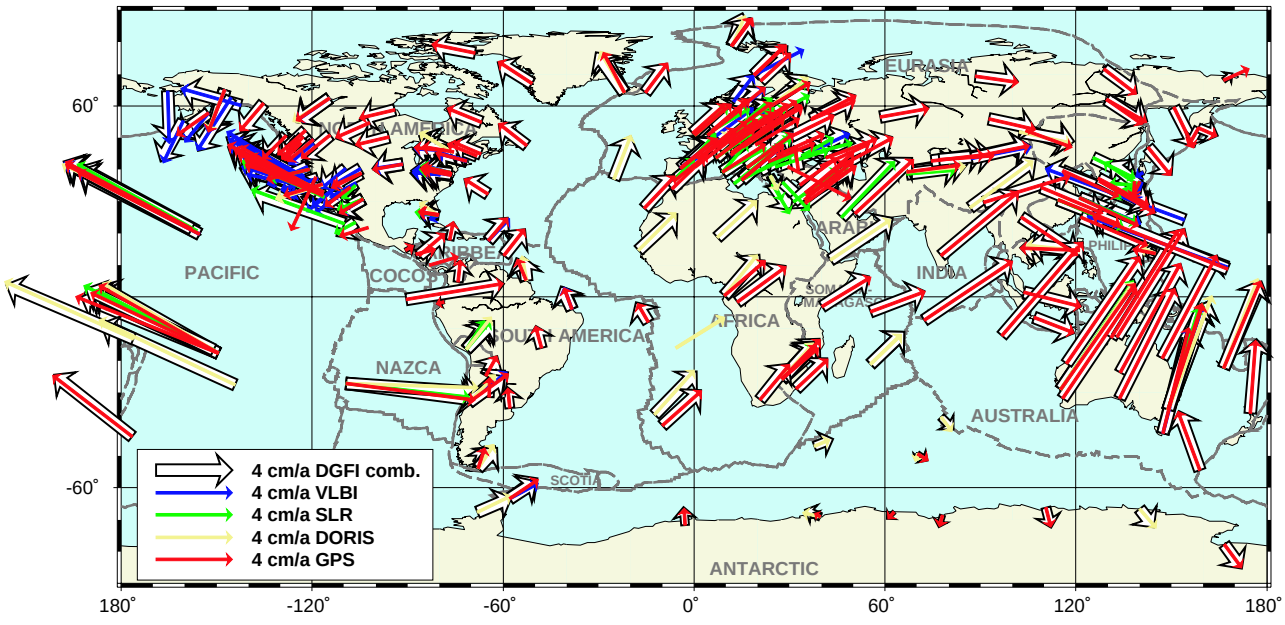

Fig. 6.2: *Horizontal station velocities of the TRF realization 2003 compared to the intra-technique solutions.*

7 Current TRF accuracy

7.1 Overview

The accuracy of space geodetic observations, as well as the software systems, models and processing strategies have been improved steadily. As a consequence also a remarkable progress has been achieved for the realization and the scope of the terrestrial reference frame since the first ITRS realization, the ITRF88. The most recent is the ITRF2000 comprising station velocities of about 800 stations located at about 500 sites (Altamimi et al., 2002; Boucher et al., 2004).

Altamimi et al. (2002) evaluated the accuracy of the ITRF2000 as follows: The accuracy and the long-term stability of the ITRF2000 scale and origin definition was estimated based on the contributing SLR and VLBI solutions. The WRMS values (propagated over 10 years) suggest a frame stability better than 4 mm in origin and better than 0.5 ppb in scale (equivalent to a shift of approximately 3 mm in station height). The accuracy of ITRF2000 station positions and velocities is not homogeneous, as the data quality and quantity for the ITRF2000 sites differ considerably (see section 8.1). About 40% of station positions have an error less than 1 cm, and the velocities of about 100 sites have been determined at the 1 mm/yr error level (or better). However, for about 25% of the ITRF sites the standard deviations for velocities are larger than 1 cm/yr, and for 5% the uncertainties exceed 10 cm/yr. Furthermore, the ITRF2000 results reveal that some of the contributing individual solutions differ considerably from the combined solution. The discrepancies reach up to 5 cm for the origin and a few ppb for the scale (Altamimi et al., 2002, see also: http://lareg.ensg.ign.fr/ITRF/ITRF2000/T.gif and D.gif). Technique- and/or solution-related systematic effects have to be considered as a major limiting factor for the accuracy of the space geodetic observations and the combination results.

The series of past ITRS realizations, from ITRF88 to ITRF2000, was compiled by one combination center, the responsible ITRS Product Center (the former IERS ITRF section) hosted at the Institute Géographique National (IGN, Paris). Consequently, there was no redundancy for the computation of the ITRS products. The recently computed TRF solution at DGFI provides a basis for a validation and external quality assessment of the results. The respective combination centers IGN and DGFI use different processing software (IGN: CATREF software, see Altamimi et al., 2002, DGFI: DOGS software, see this volume). Furthermore different methodologies are applied, as IGN performs the combination on the solution level and DGFI on the level of unconstrained normal equations. However, it has to be considered that ITRF2000 and the combined DGFI solution are based on partly identical input data, namely multi-year solutions of the different space techniques and (almost) identical local tie information.

There are two major consequences: Firstly, the comparison of both TRF realizations is not fully independent, as possible errors in the more or less identical input data (i.e. SINEX solution files, local ties) may not be detected. Secondly, nonlinear effects in site positions and datum parameters (see sections 8.2 and 8.3) may affect the accuracy of the terrestrial reference frame. The influence of those effects on the TRF results cannot be assessed by combining multi-year solutions with positions and constant station velocities. This would require the analysis of time series of station positions and datum parameters, and in a final step the combination of epoch (e.g., daily/weekly) input data of the different space techniques (see section 8.4).

7.2 Accuracy of TRF realization 2003

The accuracy evaluation of the TRF realization 2003 was performed on the basis of the intra- and inter-technique combination results (see chapters 5 and 6).

Firstly, the combined intra-technique solutions were used to evaluate the accuracy of the different space geodetic techniques. Mean standard deviations for station positions and velocities were estimated by using the reference frame stations for each technique. In addition, we have estimated also RMS residuals for station positions and velocities by applying two different approaches: i) by comparing individual solutions of a specific technique w.r.t. the combined intra-technique solution (see chapter 5), and ii) by comparing the combined intra-technique solutions with ITRF2000 (see section 7.3). The results are summarized in figure 7.1. The mean standard deviations, which represent the formal errors of the combined intra-technique solutions are for DORIS and GPS in reasonable agreement with the respective RMS residuals, whereas in the case of VLBI and SLR the standard deviations are probably too optimistic (see also table 6.1). The RMS residuals obtained from both approaches agree quite well, they suggest an accuracy for the station positions of about 10 mm for DORIS, 2 mm for GPS, 4 mm for SLR, and 3 mm for VLBI. The respective values for station velocities are 2 mm/yr for DORIS, 1 mm/yr for GPS and SLR, and 0.5 mm/yr for VLBI.

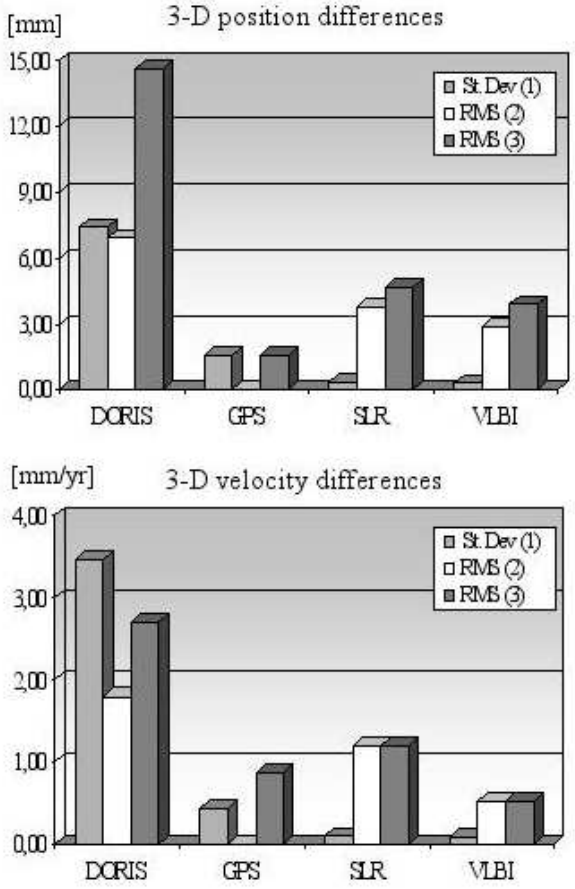

Fig. 7.1: *Accuracy of combined intra-technique solutions. (1) mean standard deviations (formal errors) for station positions and velocities, (2) RMS residuals obtained from a comparison of the individual solutions of a specific technique with the combined intra-technique solution, and (3) RMS residuals obtained from a comparison of the combined intra-technique solution with ITRF2000.*

Within the inter-technique combination co-location sites and local ties are a key element to integrate the technique-specific solutions into a common TRF frame and to identify systematic biases between different techniques. Besides this, co-location sites and local ties between co-located instruments are essential to validate the station position and velocity estimations of the different space geodetic techniques. For this purpose we used the combined intra-technique solutions to assess the TRF accuracy by two methods: (1) by comparing the space geodetic estimated station coordinates differenences with the local ties, and (2) by comparing velocity estimations of co-located instruments. The results of these inter-technique comparisons are summarized below (see also chapter 6, appendix G).

(1): A comparison of the local ties and the computed station coordinate differences obtained from the intra-technique solutions reveals for six co-locations (3 GPS–VLBI, 3 GPS–SLR) an excellent agreement; the spherical differences are below 5 mm, see table 6.4. But on the other hand, there are many other co-locations (especially those with DORIS), where the differences exceed 2 cm. Again, any interpretation of these discrepancies is difficult since various factors need to be considered (e.g. systematic biases of space geodetic solutions, local site-dependent effects, small inconsistencies related to the datum definition, and finally errors in local tie measurements). Regarding a better separation of these effects and to identify technique-specific biases, both the distribution of co-location sites and the accuracy of local ties need to be improved (see section 8.1).

(2): The comparison of station velocity estimates of co-located instruments is not directly connected to possible local tie errors, which is a great

Tab. 7.1: *Helmert-transformation results of the DORIS, SLR and VLBI network w.r.t. the GPS network.*

Parameter	DORIS	SLR	VLBI
Tx [mm]	-9.6 ± 3.4	2.7 ± 1.4	-0.4 ± 1.7
Ty [mm]	8.4 ± 3.3	0.0 ± 1.3	-2.8 ± 1.7
Tz [mm]	2.9 ± 3.3	-2.2 ± 1.3	3.1 ± 1.7
Rx [mm]	3.2 ± 4.1	-3.3 ± 1.6	-4.6 ± 2.2
Ry [mm]	2.1 ± 4.0	-1.2 ± 1.6	1.8 ± 2.2
Rz [mm]	-18.9 ± 5.2	-2.2 ± 1.6	1.8 ± 2.2
Scale [mm]	-3.0 ± 3.2	1.9 ± 1.2	-4.7 ± 1.6
Tx rate [mm/yr]	-0.3 ± 3.4	-0.6 ± 1.4	-1.1 ± 1.7
Ty rate [mm/yr]	0.2 ± 3.3	0.0 ± 1.3	-0.4 ± 1.7
Tz rate [mm/yr]	-1.6 ± 3.3	0.5 ± 1.3	-0.1 ± 1.7
Rx rate [mm/yr]	-1.2 ± 4.1	0.5 ± 1.6	-0.1 ± 2.2
Ry rate [mm/yr]	0.8 ± 4.0	-0.5 ± 1.6	0.8 ± 2.2
Rz rate [mm/yr]	2.6 ± 5.2	1.8 ± 1.6	-0.0 ± 2.2
Scale rate [mm/yr]	2.1 ± 3.2	0.6 ± 1.2	0.7 ± 1.6
Pos RMS [mm]	± 8.2	± 4.1	± 5.4
Vel RMS [mm/yr]	± 1.5	± 0.9	± 0.9

advantage compared to the previous method. As shown in table 6.2 there are eight co-locations with an excellent agreement regarding station velocities of co-located instruments. But there are also many co-locations with significant velocity differences larger than 5 mm/yr. As possible local tie errors should not influence this comparison so much, the major error source for the observed discrepancies are probably technique-specific biases that need to be identified (e.g, by analysing time series of position estimates, see section 8.3).

To investigate the stability of the TRF datum realization and the consistency of the selected local ties with the space geodetic solutions we applied the following approach: Since GPS is the dominant technique regarding the number and spatial distribution of co-locations with the other techniques we consider the GPS solution as reference for this specific TRF accuracy evaluation. We used the co-location sites and local ties selected within the inter-technique combination (see section 6.3, appendix G) to refer the DORIS, SLR and VLBI solutions to the GPS reference frame. This was done by adding the local tie measurements to the DORIS, SLR and VLBI station coordinates; thus these "transformed" station coordinates refer to the GPS markers for the respective co-location sites. Then, we performed a 14 parameter Helmert-transformation between the GPS solution and the "transformed" solutions of the other techniques.

A great advantage of this approach is, that the transformation results are independent of a specific TRF datum (e.g., ITRF2000), as the comparisons are performed in an (arbitrary) GPS reference frame. However, as also for any other accuracy evaluation method, it is not possible to separate local tie errors from position and velocity errors in the space technique solutions. This again underlines the importance of accurate local tie information.

The Helmert-transformation parameters of the DORIS, SLR and VLBI network w.r.t. to the GPS network are shown in table 7.1. The corresponding station position and velocity residuals for the transformation stations are provided in tables 7.2–7.4 for each of these techniques. It has to be considered that these results are sensitive to the selection of transformation stations, and thus the numbers themselves should not be overinterpreted. However, these transformations provide valuable information about the accuracy for the integration of different space techniques (via the local ties). In the case of VLBI and SLR the discrepancies w.r.t. the GPS network are in the order of a few millimeters for the transformation parameters, which is consistent with the corresponding standard deviations (see table 7.1). As shown in tables 7.2 and 7.3, about half of the GPS-VLBI and GPS–SLR co-locations agree quite well in station positions and velocities, but there are also stations with position differences larger than 1 cm. Larger discrepancies exist for co-locations between GPS and DORIS (see table 7.4).

Tab. 7.2: *Position and velocity residuals of GPS and VLBI co-locations in north, east and height.*

Co-location site	GPS Domes No.	VLBI Domes No.	$\triangle N$	$\triangle E$	$\triangle H$	$\triangle \dot{N}$	$\triangle \dot{E}$	$\triangle \dot{H}$
			[mm]			[mm/yr]		
Onsala, Sweden	10402M004	10402S002	3.8	−0.5	2.7	−0.5	0.0	2.9
Madrid, Spain	13407S012	13407S010	13.3	−6.3	−3.4	0.2	0.1	4.6
Wettzell, Germany	14201M010	14201S004	0.2	0.6	−0.1	−0.3	−0.2	−1.1
Tsukuba, Japan	21730S005	21730S001	2.2	−6.5	−11.5	−1.5	1.4	0.5
Hartebeesthoek, S. Afr.	30302M004	30302S001	−13.2	12.9	9.4	−0.9	0.3	−0.1
Algonquin, Canada	40104M002	40104S001	1.0	−1.8	13.9	−0.8	−0.6	−2.1
Yellowknife, Canada	40127M003	40127M004	−4.8	−3.5	−14.3	−0.4	−0.2	1.1
Kokee Park Hawaii, USA	40424M004	40424S001	1.2	−1.2	5.0	0.8	0.5	−0.9
Westford, USA	40440S020	40440S003	0.7	5.5	15.7	−0.3	0.1	−2.1
Fort Davis, USA	40442M012	40442M006	−3.4	−1.0	1.9	0.1	−0.3	1.2
Pie Town, USA	40456M001	40456S001	−2.8	−4.2	−17.7	−0.5	−1.7	−1.5
North Liberty, USA	40465M001	40465S001	2.3	−1.6	−3.6	0.3	−0.1	−1.6
Mauna Kea, USA	40477M001	40477S001	3.0	−3.0	−0.7	0.5	0.6	0.3
Fortaleza, Brazil	41602M001	41602S001	3.4	2.0	8.2	−0.2	−1.0	0.3
Tidbinbilla, Australia	50103M108	50103S010	6.2	5.5	−5.4	0.1	1.1	−1.4

Tab. 7.3: *Station position and velocity residuals of GPS and SLR co-locations in north, east and height.*

Co-location site	GPS Domes No.	SLR Domes No.	$\triangle N$	$\triangle E$	$\triangle H$	$\triangle \dot{N}$	$\triangle \dot{E}$	$\triangle \dot{H}$
			[mm]			[mm/yr]		
Grasse, France	10002M006	10002S001	−3.0	1.3	−5.7	0.6	0.7	−1.6
Graz, Austria	11001M002	11001S002	0.8	−0.5	4.2	0.6	1.1	−0.7
Borowiec, Poland	12205M002	12205S001	7.2	−1.4	6.5	−0.9	−0.4	0.7
Matera, Italy	12734M008	12734S001	−7.7	−8.5	8.4	−1.5	−0.3	0.6
Herstmonceux, UK	13212M007	13212S001	−0.5	5.0	−3.8	−0.4	−1.0	0.2
Potsdam, Germany	14106M003	14106S009	0.9	2.3	−0.3	0.1	1.1	−0.1
Wettzell, Germany	14201M010	14201S018	−3.6	−2.4	−11.5	0.2	0.6	1.8
Quincy, USA	40433M004	40433M002	0.5	0.0	5.9	−1.1	2.0	2.0
Fort Davis, USA	40442M012	40442M006	−8.4	1.2	−3.4	0.8	−0.3	0.6
Washington D.C., USA	40451M123	40451M105	2.6	−2.6	−4.3	−2.3	−0.8	−0.2
Monument Peak, USA	40497M004	40497M001	−0.1	−1.9	−12.9	0.2	−0.5	−1.3
Arequipa, Peru	42202M005	42202M003	4.5	8.1	−10.6	1.1	−1.8	−1.5
Yarragadee, Australia	50107M004	50107M001	−4.4	−4.7	4.1	1.3	0.6	1.3
Canberra, Australia	50119M002	50119S001	3.6	3.2	−2.5	−2.4	−0.4	−1.9

Tab. 7.4: *Position and velocity residuals of GPS and DORIS co-locations in north, east and height. Note: The transformation results are sensitive to the selected co-locations. As various sites show too large differences (> 3 cm) between the solutions, we used eight co-locations with the "best" agreement.*

Co-location site	GPS Domes No.	DORIS Domes No.	$\triangle N$	$\triangle E$	$\triangle H$	$\triangle \dot{N}$	$\triangle \dot{E}$	$\triangle \dot{H}$
			[mm]			[mm/yr]		
Toulouse, France	10003M009	10003M004	7.6	−10.1	6.4	−2.2	−0.1	−0.5
Reykjawik, Iceland	10202M001	10202S002	7.4	−17.2	3.1	−0.2	1.0	−0.1
Ny-Alesund, Norway	10317M003	10317S002	−14.8	20.7	−8.4	0.4	−1.6	−1.5
Metsahovi, Finland	10503S011	10503S013	−11.7	7.8	−0.7	0.8	1.2	2.3
Yellowknife, Canada	40127M003	40127S007	−16.6	15.3	10.9	0.6	−2.2	−1.9
Rio Grande, Argentina	41507M004	41507S003	−12.0	−2.3	−17.5	1.3	5.3	−0.6
Santiago, Chile	41705M003	41705S008	1.0	0.1	9.7	−1.3	−5.3	−0.2
Noumea, New Caledonia	92701M003	92701S001	−6.9	5.6	−1.9	0.2	1.1	0.0

Tab. 7.5: *Estimated Helmert-transformation parameters between DGFI combined TRF solution and ITRF2000 separately for each technique. The displayed RMS residuals for station positions and velocities are mean values for the reference frame stations.*

H.-T. Results	VLBI	SLR	GPS	DORIS
Tx [mm]	0.8 ± 0.5	-2.5 ± 1.3	-0.8 ± 0.3	1.9 ± 2.2
Ty [mm]	-1.3 ± 0.5	0.1 ± 1.3	-1.2 ± 0.3	0.1 ± 2.2
Tz [mm]	0.9 ± 0.5	-2.1 ± 1.2	2.8 ± 0.3	1.1 ± 2.2
Rx [mas]	-0.00 ± 0.02	0.05 ± 0.05	-0.05 ± 0.01	0.20 ± 0.08
Ry [mas]	-0.05 ± 0.02	0.09 ± 0.05	0.06 ± 0.01	0.19 ± 0.08
Rz [mas]	-0.08 ± 0.02	0.05 ± 0.04	0.01 ± 0.01	0.21 ± 0.08
Scale [ppb]	0.05 ± 0.07	-0.08 ± 0.19	-0.50 ± 0.04	0.60 ± 0.35
Tx rate [mm/yr]	1.0 ± 0.2	0.4 ± 0.4	0.0 ± 0.2	-0.4 ± 0.7
Ty rate [mm/yr]	0.3 ± 0.2	-0.8 ± 0.4	0.4 ± 0.2	-0.5 ± 0.7
Tz rate [mm/yr]	-0.6 ± 0.2	0.3 ± 0.4	-0.6 ± 0.2	-0.2 ± 0.7
Rx rate [mas/yr]	-0.00 ± 0.01	-0.03 ± 0.02	0.00 ± 0.01	-0.04 ± 0.03
Ry rate [mas/yr]	-0.03 ± 0.01	-0.01 ± 0.02	-0.01 ± 0.01	0.02 ± 0.03
Rz rate [mas/yr]	0.00 ± 0.01	-0.01 ± 0.01	-0.01 ± 0.01	-0.03 ± 0.03
Scale rate [ppb/yr]	0.02 ± 0.03	-0.14 ± 0.06	0.12 ± 0.02	0.01 ± 0.12
Pos RMS [mm]	± 2.2	± 4.4	± 1.6	± 12.8
Vel RMS [mm/yr]	± 0.51	± 0.90	± 0.89	± 2.07

7.3 Comparison of combined DGFI solution with ITRF2000

A comparison of the DGFI solution with ITRF2000 provides an optimal basis for a first "quasi" independent validation and quality assessment of the ITRS products. The computations of DGFI and IGN were done with different software packages and different combination strategies were applied. However, the TRF input data (solutions) used by both ITRS combination centers are to a certain extent identical (see table 4.1). Thus the outcome of the comparisons is not completely independent.

We compared the combined DGFI solution with ITRF2000 by means of a 14 parameter Helmert-transformation. The results are summarized in table 7.5. Both TRF solutions agree quite well in origin and scale, but it has to be considered that the datum of both TRF realizations was defined in a similar way, i.e., the origin is realized by SLR and the scale by SLR and VLBI. The origin of both TRF realizations agrees within 3 mm (related to the reference epoch 1997.0) and the rates differ by up to 1 mm/yr. The scale differences are very small for VLBI and SLR, which is not surprising since these techniques were used by IGN and DGFI to realize the TRF scale. In the case of GPS and DORIS the scale differences are 0.5 ppb and 0.6 ppb, respectively (this is equivalent to station height differences of 3–4 mm). The scale rate differences reach the level of 0.1 ppb/yr. To get comparable results to the ITRF2000 quality evaluation performed by Altamimi et al. (2002) we propagated the observed discrepancies in origin and scale between both TRF realizations (as shown in table 7.5) over 10 years. The resulting values of this external comparison reach the level of 1 cm for the origin and 1 ppb for the scale, which is slightly larger than those reported by Altamimi et al. (2002).

Table 7.5 also shows the RMS residuals for station positions and velocities for each technique separately. These RMS residuals reflect the (averaged) spherical differences between both TRF realizations for the common reference frame stations of a particular space technique. The agreement for VLBI and GPS station positions and velocities is better than for the other space techniques. The discrepancies are largest for DORIS.

Figure 7.2 shows the respective RMS residuals in north, east and height components for the different space techniques, indicating that the discrepancies between ITRF2000 and the DGFI solution are for all techniques (except DORIS) larger in station heights than in the horizontal components.

In figure 7.3 histograms with position and velocity differences between both TRF realizations are presented for all 369 common VLBI, SLR, GPS and DORIS stations, and for each technique separately. For about 60% of all common stations the differences in positions and velocities are below 1 cm and 2.5 mm/yr, respectively. On the other hand there are too many stations (10%) with position and velocity differences larger than 5 cm and 1 cm/yr, which is not tolerable for a precise reference frame. As expected, the discrepancies in the height components are generally larger than for the horizontal components. VLBI and GPS station positions and velocities are in better agreement than those of SLR and DORIS. In the case of DORIS about half of the station positions and velocities differ by more than 1 cm and 2.5 mm/yr, respectively. Also a few SLR stations disagree considerably between both TRF realizations (see below).

Figure 7.4 shows the horizonal station velocities of the DGFI solution compared to ITRF2000. There is in general a good agreement between both TRF realizations. However, for some stations significant discrepancies exist, which are shown in the enlargements for Europe and South America, as examples (see figures 7.5 and 7.6).

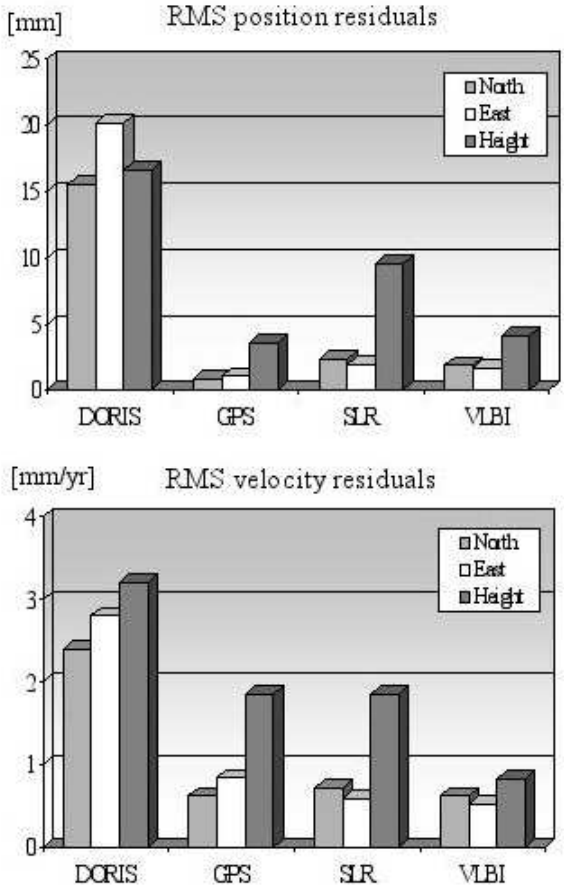

Fig. 7.2 : *RMS station position and velocity residuals obtained from a comparison of ITRF2000 with the combined DGFI solution.*

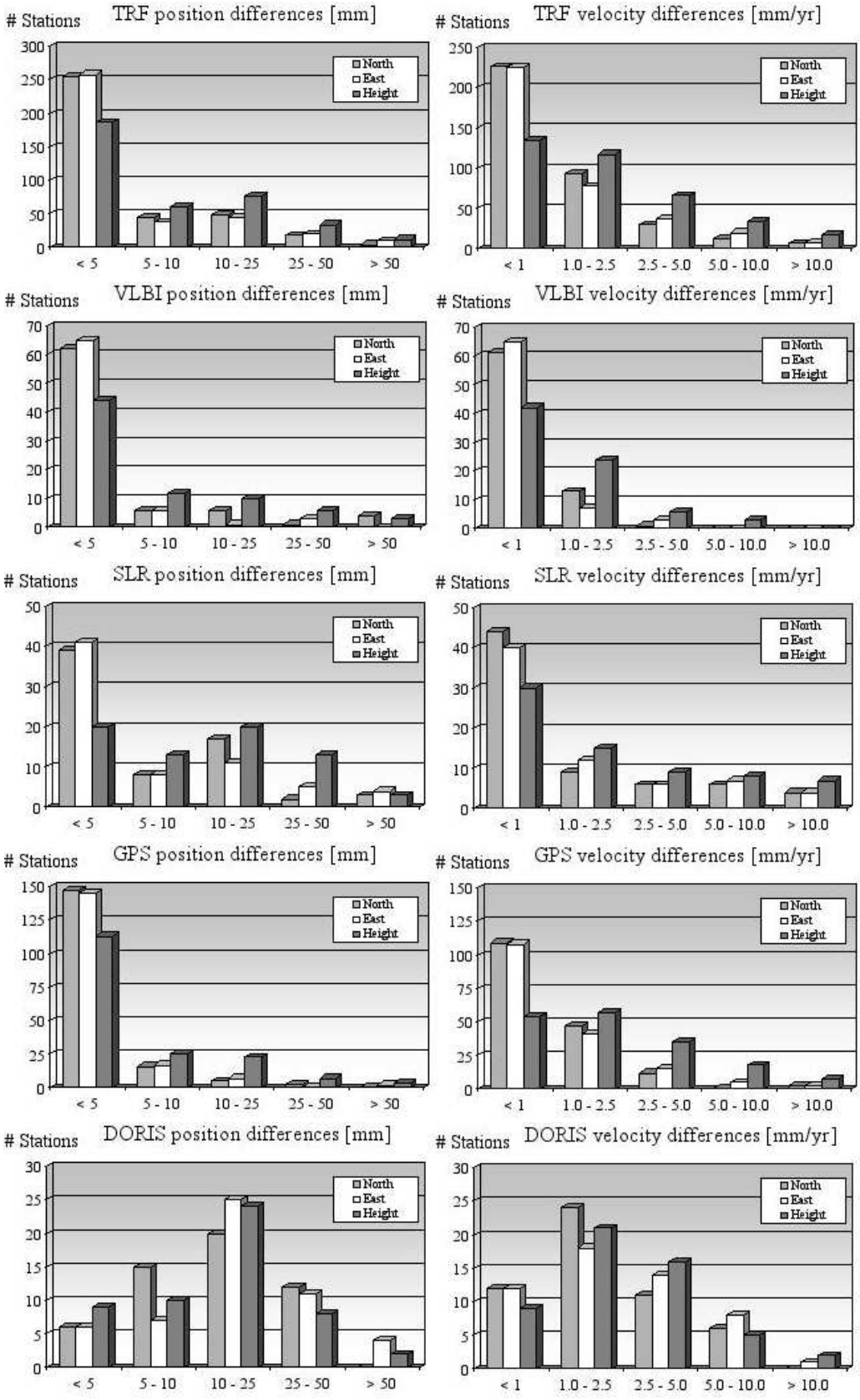

Fig. 7.3 : *Differences between the combined DGFI solution and ITRF2000 in station positions (left) and velocities (right) in north, east and height components for all 369 common TRF stations, and for each technique separately.*

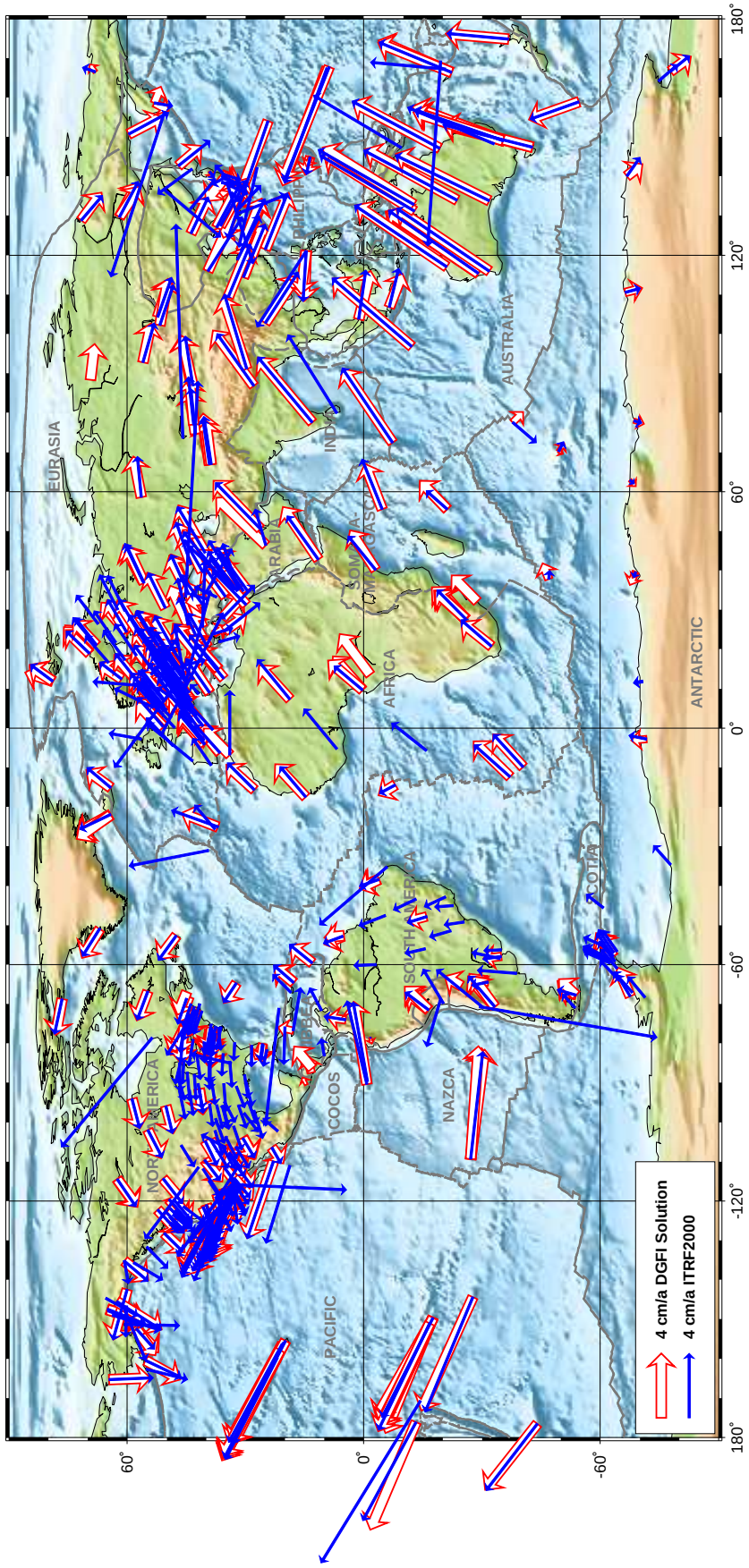

Fig. 7.4: *Horizontal station velocities of TRF realization 2003 compared to ITRF2000. The DGFI solution contains less sites than ITRF2000, since stations with short data time spans (e.g. < 1 yr) were excluded, which do not allow an accurate and reliable velocity estimation.*

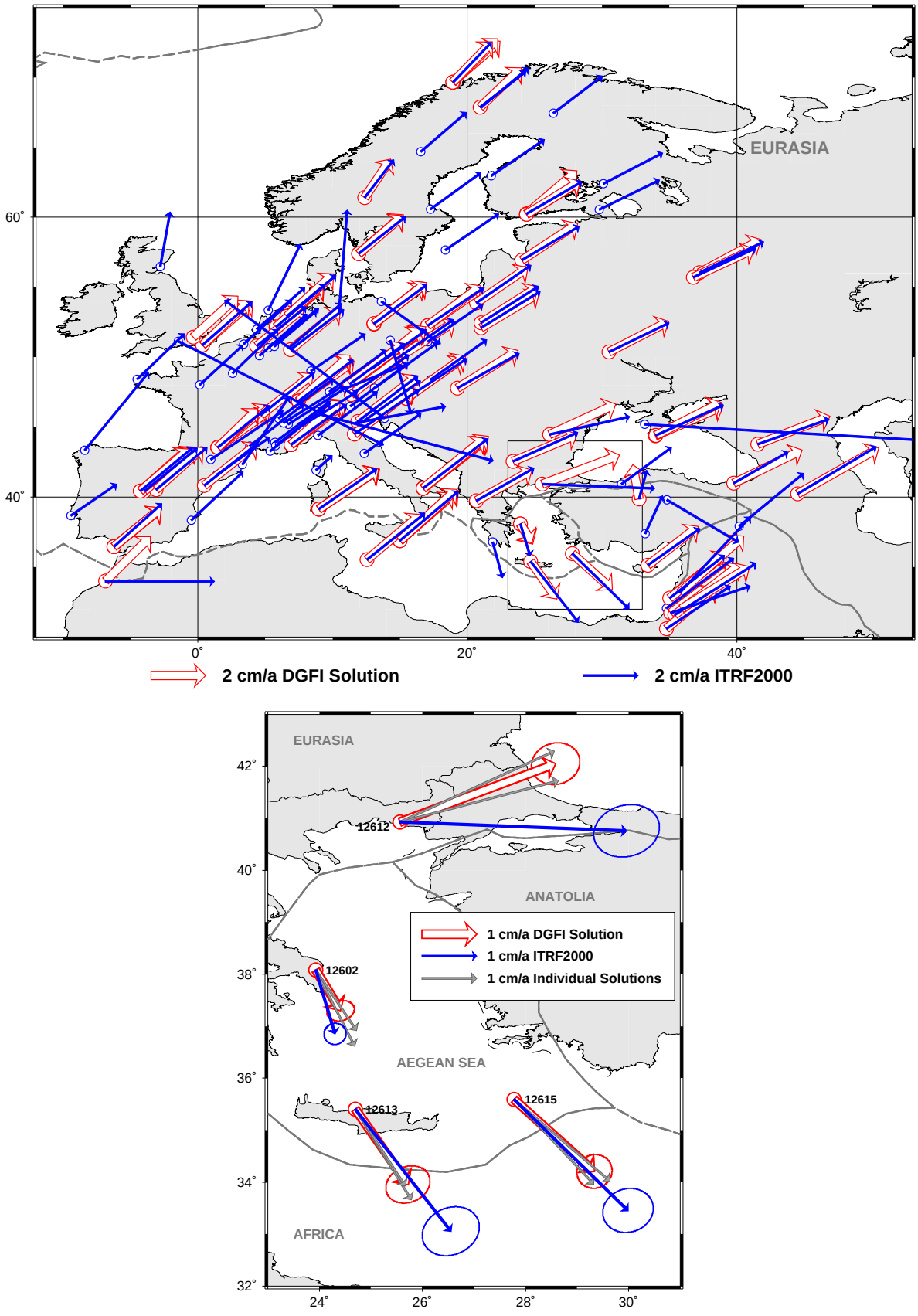

Fig. 7.5 : *Horizontal station velocities of DGFI solution compared to ITRF2000 for Europe. The enlargement for the Mediterranean region shows stations with significant discrepancies between both TRF realizations, which result probably from "old" mobile SLR occupations.*

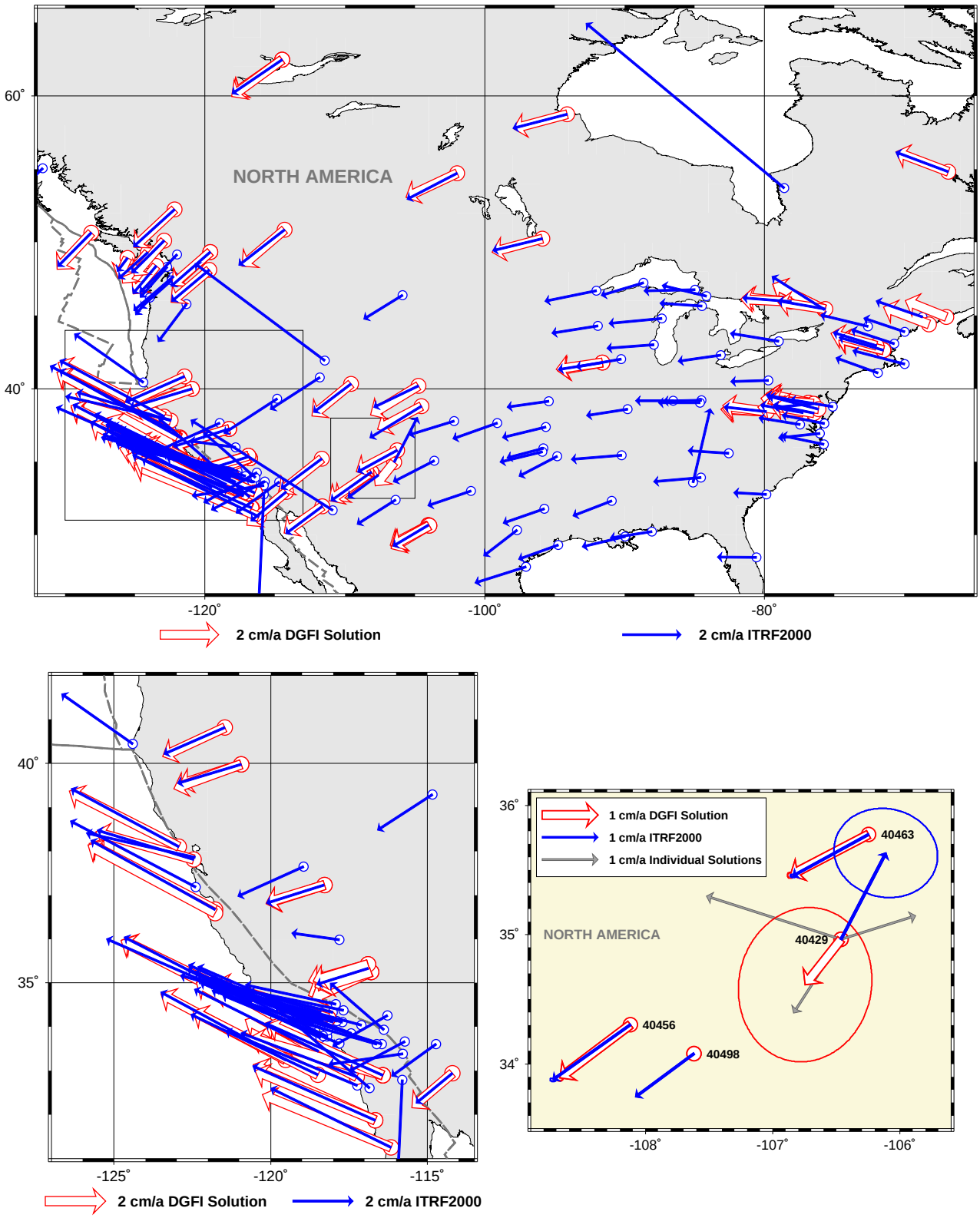

Fig. 7.6: *Horizontal station velocities of DGFI solution compared to ITRF2000 for North America. Enlargements show the western part of North America (down left), and an SLR station (Albuquerque, DOMES No. 40429) with significant differences between both TRF realizations (down right). This station was observed only for about 2 years (1995–1997) during mobile campaigns, which obviously not allows a precise velocity estimation.*

8 TRF computations: Status, deficiencies and recommendations

In the following sections, the current status regarding TRF computations is evaluated, still remaining deficiencies and shortcomings are identified, and finally recommendations for future TRF realizations are proposed at the end of each section.

8.1 IERS network, site co-locations, and local ties

The IERS network is defined through all tracking instruments used by the individual analysis centers contributing to the IERS. The first IERS network, the ITRF88, included SLR, LLR and VLBI systems with about 100 stations and 22 co-locations. The IERS network has improved continuously in terms of the number of sites and co-locations as well as their global distribution. Since 1991, GPS stations were added, and the DORIS tracking network is included since 1994. The ITRF2000 network comprises station positions and velocities of about 800 stations located at about 500 sites (Altamimi et al. 2002). The IERS network also included, from its beginning, a selection of ground markers, especially those used for mobile equipment and those currently included in local surveys performed to monitor local eccentricities between instruments at co-location sites. For details, see relevant publications or webpages, e.g., Altamimi et al., (2002); Boucher et al., (2004); IERS Conventions (2003), http://www.iers.org/iers/products/conv; IGN webpage, http:/lareg.ensg.ign.fr/ITRF.

The ITRF2000 stations are not homogeneous in terms of quality and quantity of observation data. The data time span ranges from, e.g., less than 1 month for some mobile SLR and VLBI stations up to more than 20 years for permanently operating systems. In the case of GPS, stations with observation times less than one year and also regional solutions for densification networks were included in the ITRF2000. The standard deviations for station positions and velocities range from 1 mm to 50 m, and $<$ 1 mm/yr to 3 m/yr, respectively. As an example, the spectrum of standard deviations for ITRF2000 site velocities is:

- $<$ 1 cm/yr for 360 sites (75%),
- 1 cm/yr – 10 cm/yr for 89 sites (19%),
- 10 cm/yr – 1 m/yr for 23 sites (5%),
- $>$ 1 m/yr for 5 sites (1%).

The current definition of the IERS network does not fully satisfy accuracy, reliability and homogeneity requirements of a precise reference frame. Consequently, we excluded in the TRF realization 2003 computed at DGFI poorly observed stations with too few observations (e.g., less than one year), which do not allow for a reliable estimation of station positions and velocites. Altogether, the DGFI solution consists of 401 stations (81 VLBI, 65 SLR, 202 GPS, 53 DORIS) with 92 co-locations (see figure 6.1).

In terms of the long-term stability of the reference frame, the current and future status of the operating stations is important. Currently, about 30 VLBI and 25 SLR stations are operational. A major problem for these techniques is that the spatial distribution of the sites is not optimal, and in the case of VLBI typically only 4–6 telescopes observe simultaneously within one daily session, and the station configuration often changes from one session to the other. The DORIS network consists of about 60 stations with a homogeneous global coverage, and the IGS network with more than 300 permanently observing GPS stations expands continuously. This is mainly due to the low cost and easy installation and operation of GPS equipment, compared to the other space geodetic systems. In addition more than thousand permanent GPS stations are operated in regional networks.

Co-location sites and local ties (intra-site vectors) are a key element to connect and combine the technique-specific reference frames into a unique TRF. Both, the current situation regarding geo-

graphical distribution of co-location sites and accuracy of local ties is not satisfying. Figure 6.1 shows, that there are two co-locations of all four techniques, 20 sites with co-locations of three techniques, and 39 with co-locations of two techniques. Most of the co-locations are between GPS and one of the other techniques.

The ITRF2000 results and the DGFI combination efforts indicate that there are several dubious or erroneous local ties. The results displayed in table 6.2 show that the discrepancies between local ties and coordinates determined with space geodetic techniques are unacceptably large in many cases. Spatially well-distributed co-location sites and accurate local ties are an essential requirement to fully exploit the unique capabilities and individual strengths of the different space geodetic techniques, and to identify remaining technique-specific systematic effects.

Recently, an IERS Working Group on site co-locations has been established (see http://www.iers.org) and an IERS Workshop on the same topic was held in Matera, Italy in October 2003. Thus, some progress regarding site co-locations and local tie issues can be expected.

These considerations can be summarized in three recommendations.

Recommendation 8.1.1 : IERS network: The quality and reliability of stations and their observations should be emphasized. There is an urgent need to define an ITRF core network with good global coverage and stable site locations to ensure high long-term stability of the frame. Especially in the case of VLBI and SLR, the networks should be improved in particular in terms of spatial distribution.

Recommendation 8.1.2 : Site co-locations: A well-coordinated effort is necessary to improve VLBI and SLR co-locations. This is critical to ensure long-term stability and maintenance of the frame. GPS receivers should be installed on all VLBI, SLR and DORIS sites.

Recommendation 8.1.3 : Local ties: All missing and questionable local ties should be resurveyed with highest priority, then followed by the other ties. The surveys should be performed according to the recommendations of the IERS Workshop on site co-location. The accuracy requirement for the local ties is 1 mm. The local ties should be provided with full variance/covariance information in SINEX format.

8.2 TRF datum

The current status of the realization of the TRF datum is characterized as follows :

In the ITRF2000 and the DGFI computations the origin is realized by SLR solutions, and the scale is realized by SLR and VLBI solutions.

The orientation of ITRF2000 is aligned to that of ITRF97 at 1997.0 with its rate conventionally being aligned to that of the geological model NNR-NUVEL-1A (DeMets et al., 1994). The ITRF2000 orientation and its rate were established using a selection of ITRF sites with high geodetic quality and locations far away from plate boundaries and deformation zones (Altamimi et al., 2003).

The orientation of the DGFI solution is aligned to that of ITRF2000 to achieve comparable results for a TRF validation. The NNR NUVEL-1A model currently used for the realization of the TRF kinematic datum has major disadvantages. Firstly, it contains only fourteen rigid plates. Deformation zones (e.g., Andes, California, East Asia, Mediterranean), which cover about 15% of the Earth's surface (e.g., Gordon 1995), are not included. Secondly, the model reflects plate motions averaged over millions of years. Significant deviations from present-day motions are observed (e.g., Drewes, 1998; Angermann et al., 1999; Altamimi et al., 2003).

The current accuracy of the TRF datum realization has been assessed by comparing the DGFI solution with ITRF2000 (see section 7.3). As already mentioned, this comparison is not fully independent since partly identical input data were used, and the datum of both TRF computations is based on VLBI and SLR solutions. To gain further insight into the characteristics and the contribution of the different space techniques to the realization of the terrestrial reference system, we have analysed the time series of scale and translation variations (e.g., Angermann et al., 2004; Meisel et al., 2004).

The time series of scale and translation (origin) variations w.r.t. ITRF2000 derived from various

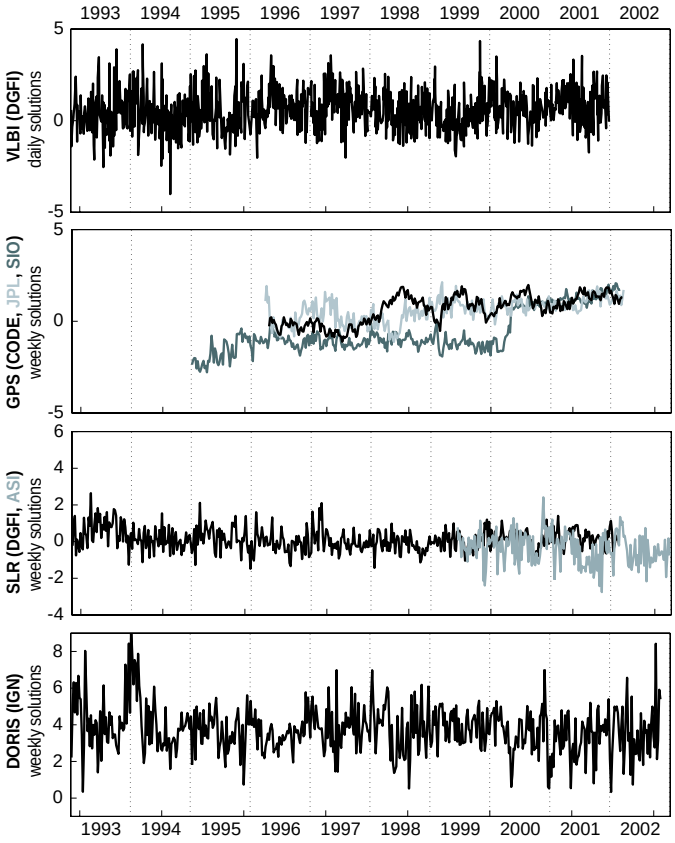

Fig. 8.1 : *Time series of scale variations in parts per billion [ppb].*

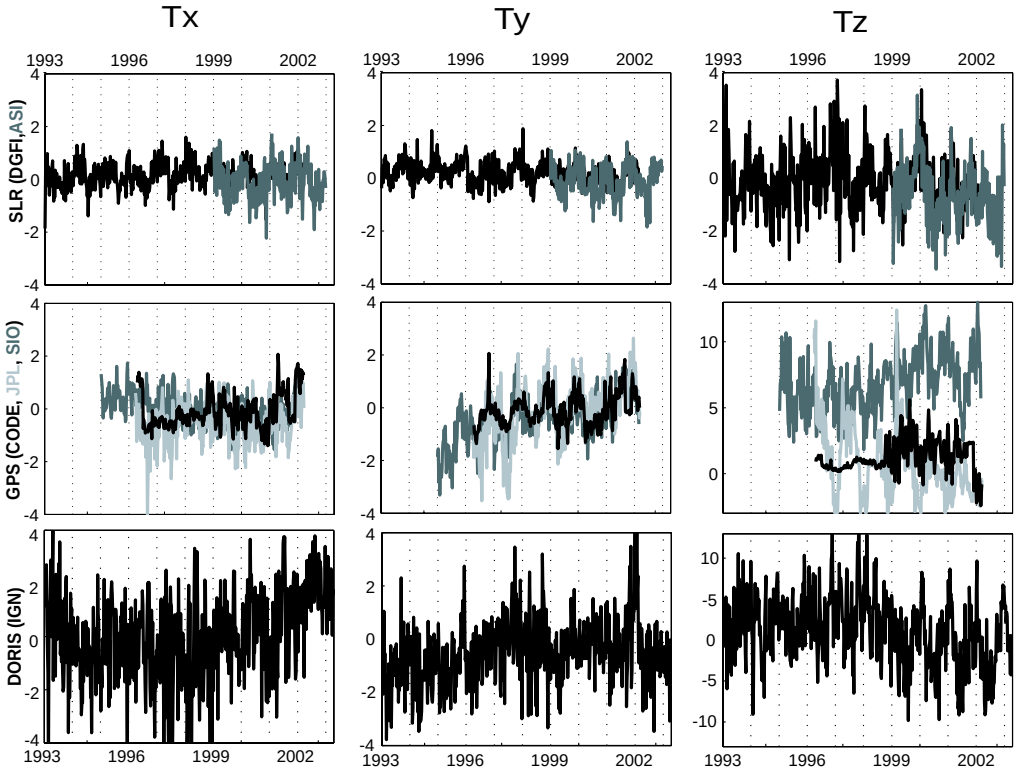

Fig. 8.2 : *Time series of weekly translation variations [cm].*

individual solutions are shown in figures 8.1 and 8.2. In principle, the VLBI and SLR scales are in good agreement with the ITRF2000 scale. The VLBI scale variations of the daily session solutions have a higher noise level than the weekly solutions of the other techniques, mainly due to the fact that the solutions span only one day, and due to the relatively poor network geometry of single VLBI sessions. The DORIS scale has an offset of about 4 ppb w.r.t. ITRF2000. The three GPS series (CODE, JPL and SIO) agree well (within 1 ppb) during the last two years, whereas before 2000 larger discrepancies and some irregularities exist. The significant jump of about 2 ppb in the SIO scale in early 2000 was probably caused by a change of the elevation cut-off angle (Herring, 2002). The most stable results for the origin were obtained from SLR. Both SLR solutions show annual signals with amplitudes of a few millimeter for the three translation components (see, e.g., Angermann et al., 2002, Dong et al., 2003). The time series for the translation parameters derived from the GPS and DORIS solutions show larger variations than SLR, in particular for the z-component.

Recommendation 8.2.1: Origin: Currently, only SLR has been used to realize the TRF origin. This is not optimal, as the SLR network has no homogeneous distribution (e.g., lack of stations in the southern hemisphere). Improvements in the GPS and DORIS solutions seem necessary to get redundancy from these techniques. The observed seasonal variations should be considered in future ITRS realizations.

Recommendation 8.2.2: Scale: The current scale realization is based on SLR and VLBI, both techniques have relatively sparse networks. As various effects may affect the scale (e.g., vertical station motions, troposphere modelling, VLBI, GPS and DORIS antenna-related effects, SLR station-dependent range biases), improvements to GPS and DORIS seem necessary to get better redundancy and better station network geometry.

Recommendation 8.2.3: Orientation and its rate: For future TRF realizations kinematic models based on space geodetic data, such as APKIM2000 (Drewes and Meisel, 2003) or the NNR model published by Kreemer and Holt (2001), should be used to ensure that the NNR condition for the orientation rates is more accurately fulfilled.

8.3 Parameterization of site motions

Conventionally, TRF realizations are based on station positions (referred to a specific reference epoch) and constant velocities for a set of global tracking sites. However, the assumption of constant site velocities is in conflict with non-linear effects caused by various geophysical phenomena (e.g., seismic or volcanic effects, deformations at plate boundary zones, unstable site conditions). Seasonal variations can be caused by mass redistributions within the Earth's system, from various internal processes and from surface mass changes associated with the atmosphere, oceans and the continental hydrological cycle.

These time variable effects have to be verified and studied. This was done by analysing time series of site positions obtained from epoch solutions (e.g., daily or weekly) of the different space geodetic techniques over several years (e.g., Angermann et al., 2004, Meisel et al., 2004). The site position time series show non-linear motions and discontinuities for a large number of sites. Reasons for that can be manifold, e.g., effects of deformation processes caused by large earthquakes, equipment changes on a site due to system upgrades, changes of software, models and processing strategies, as well as seasonal signals.

The effect of large earthquakes on the position time series is illustrated for three stations (figure 8.3). Earthquakes in Arequipa, Peru in June 2001 caused a jump of about 50 cm horizontally (Kaniuth et al., 2002), and the station motion after the earthquake differs significantly from the expected long-term motion. This change in motion is probably caused by post-seismic relaxation processes, which also have been observed after the 1995 Mw 8.0 Antofagasta earthquake in Northern Chile (Klotz et al., 1999, Klotz et al., 2001). For two other stations displayed in figure 8.3 (Ankara and Cocos Island) earthquakes caused significant jumps of some cm in the position time series, accompanied by site motions after the earthquakes that are different from their long-term behaviour. These changes in motion are not considered in ITRF2000 and preceeding TRF realizations, as the velocities before and after the event are forced

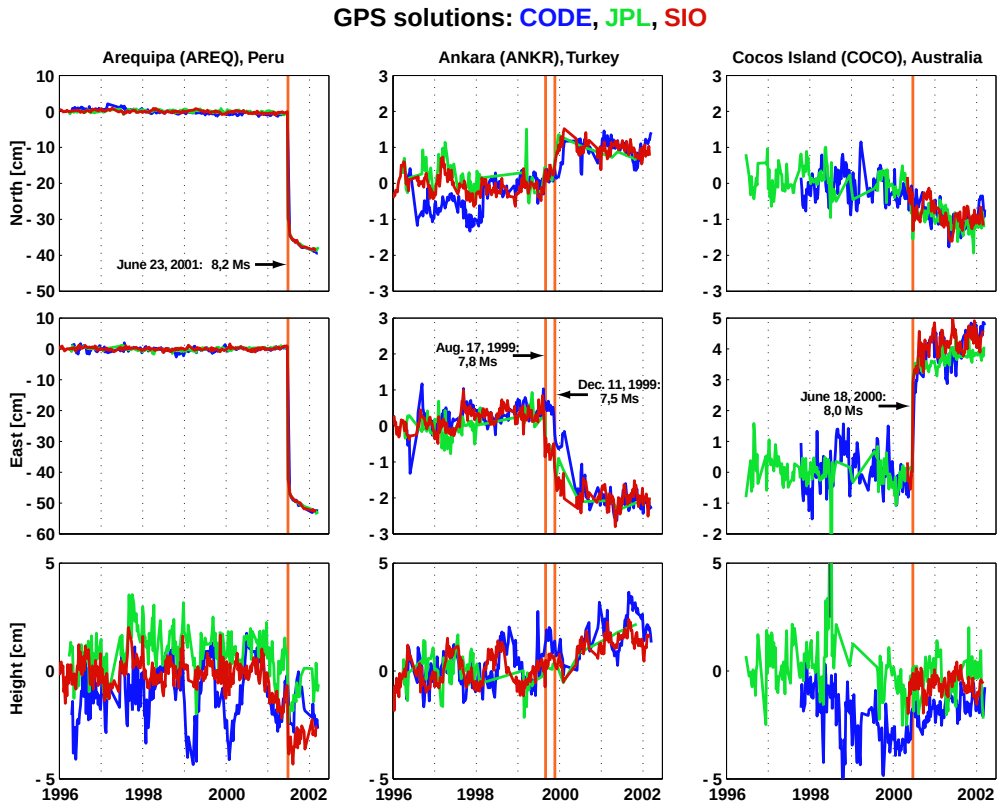

Fig. 8.3: *Effect of large earthquakes on the position time series.*

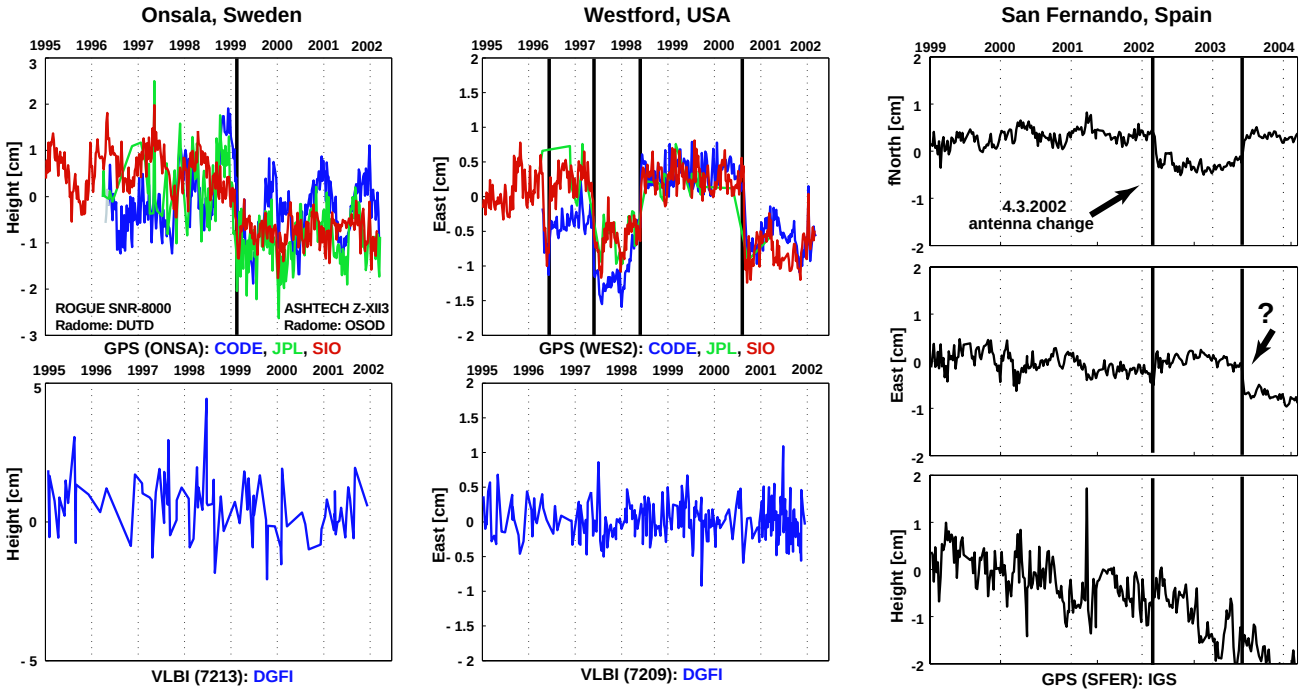

Fig. 8.4: *Effect of equipment changes on the position time series for two co-location sites (height), and for GPS station San Fernando.*

to be identical, which may bias the terrestrial reference frame results.

Figure 8.4 shows examples for the effect of equipment changes. At the GPS station Onsala a change of the radome in early 1999 caused a jump of about 2 cm in the height component (Kaniuth and Huber, 2003). Several receiver and antenna changes at the GPS station Westford are accompanied by significant jumps in the longitude component. Both co-location sites do not show similar effects in the VLBI position series, indicating that the observed jumps are a technique-related problem, and not a "real" site motion caused by geophysical phenomena. The position time series of the GPS station San Fernando shows discontinuities in particular for the horizontal components. The first jump in March 2002 corresponds to an antenna change, the reason for the second jump needs to be investigated.

During the last few years the software systems, models and processing strategies have improved significantly. To achieve consistent results it is necessary to reprocess all the data with the latest software version, state-of-the-art models and the same strategy. In the case of VLBI and SLR all data were reprocessed in a consistent way. At present, this causes inconvenience with GPS, as it requires a tremendous effort to reprocess all GPS data homogeneously. As a consequence many of the time series are affected by changes due to inconsistent software, models and processing strategies (e.g., Rothacher, 2002). An example is the jump in the time series of the SIO scale, caused by a change of the elevation cut-off angle (see figure 8.1). Within a joint project of Technical University Munich and Technical University Dresden, the GPS data of the global IGS network have been reprocessed (back to 1994) with the latest version of the Bernese GPS software and state-of-the-art models to achieve consistent GPS results (e.g., Steigenberger et al., 2004).

Many stations show significant annual signals in the position time series caused among others by loading effects, e.g., increased winter loading of soil moisture, snow and atmospheric loading. These annual signals are mainly observed in the height components. Figure 8.5 shows the time series of weekly positions for three GPS stations. The IGS station Irkutsk (IRKT), Russia, located in Siberia shows a significant annual signal with an amplitude of about 1 cm in the station heights. IGS station Hafelekar (HFLK), located in the Alpes (height 2334m) show annual signals in the north and height component, which are probably caused by heating of the rocks in summer. Reykjavik (REYK), Iceland, shows a jump caused by earthquakes in June 2000, and in addition seasonal variations in the height component, which are not consistent over time.

Figure 8.6 shows station height variations for the co-location site Yarragadee, Australia. GPS provides the most stable results for weekly estimated station heights. The significant annual signal with an amplitude of about 5 mm for the GPS station is obviously not observed by DORIS and SLR. Especially the SLR station does not show an annual signal. The comparisons at co-location sites reveal that there are still inconsistencies between different techniques that need further investigation.

Recommendation 8.3.1: The analysis of position time series of the IERS network stations w.r.t. to discontinuities (e.g., equipment changes, earthquakes) and non-linear motions (e.g., seasonal variations, postseismic deformations) must be enhanced.

Recommendation 8.3.2: The results of the time series analysis should be used to compare (and update) the station log-files provided by the services. Finally, a complete and unique documentation with all necessary information concerning equipment changes, earthquakes, etc. should be provided and continuously be updated for all IERS sites.

Recommendation 8.3.3: The comparison of the time series at co-location sites is important to investigate technique-specific problems, and to minimize remaining discrepancies between different space geodetic techniques.

8.4 Combination methodology

In principle, contributions of one or of different techniques may be combined on the level of observation equations, normal equations or solutions. The most appropriate approach is the combination of observation equations. This requires, however, sophisticated software packages and makes

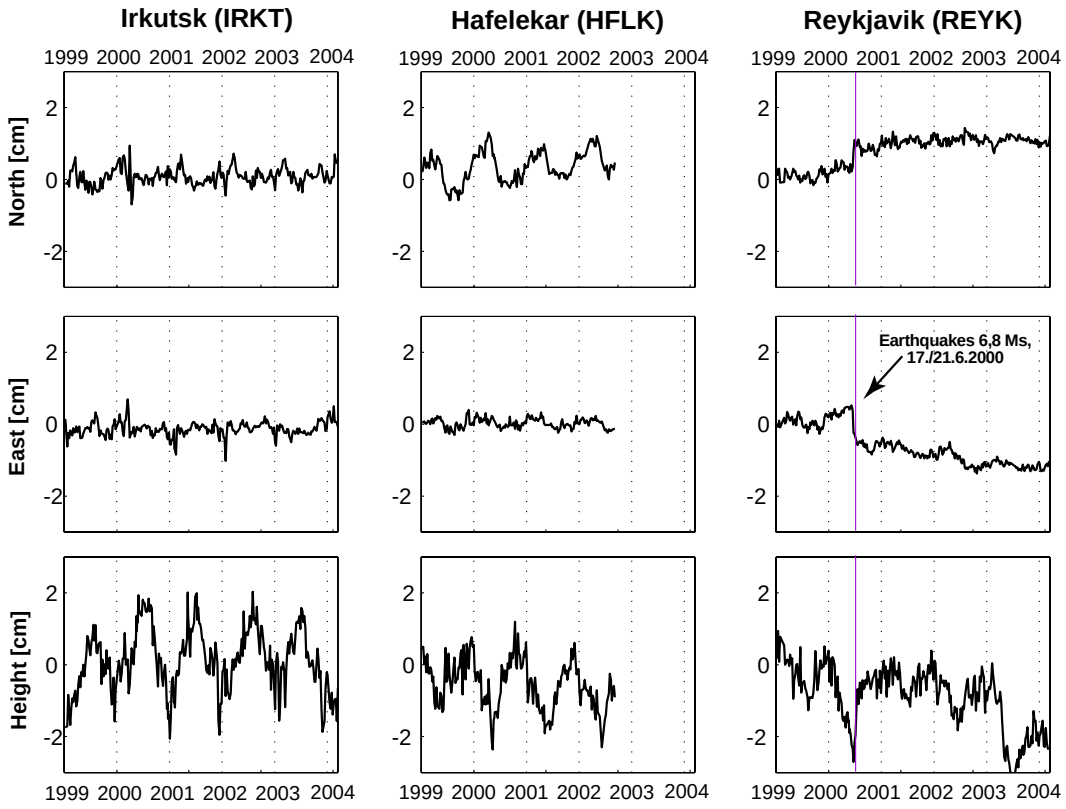

Fig. 8.5 : *Position time series for three GPS stations with significant annual signals.*

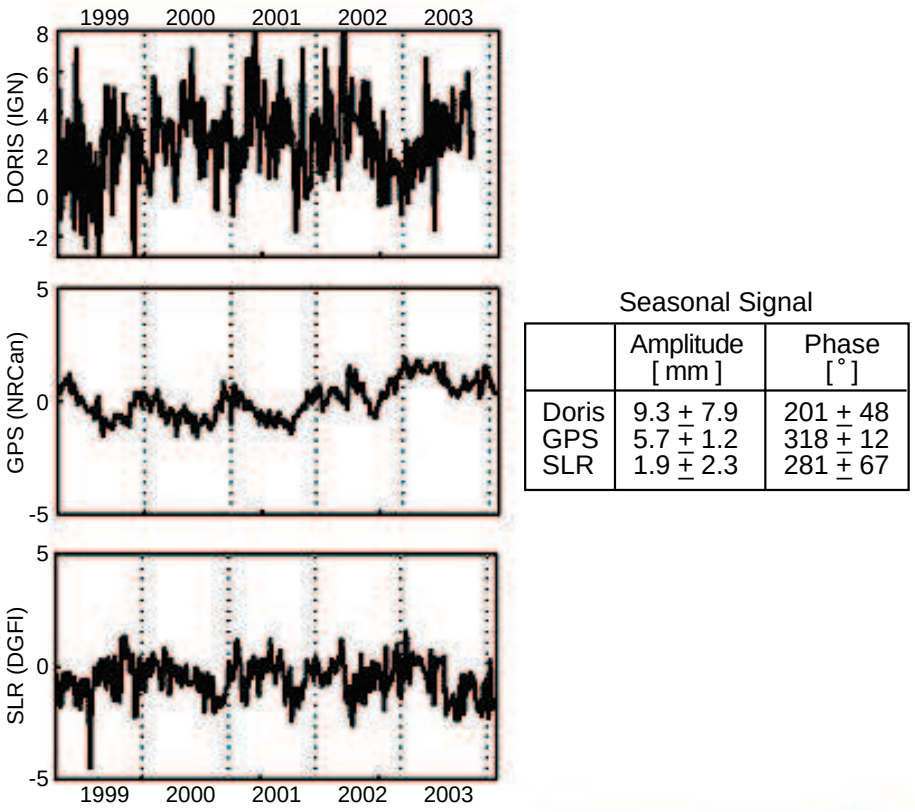

Seasonal Signal

	Amplitude [mm]	Phase [°]
Doris	9.3 ± 7.9	201 ± 48
GPS	5.7 ± 1.2	318 ± 12
SLR	1.9 ± 2.3	281 ± 67

Fig. 8.6 : *Station height variations [cm] for the co-location site Yarragadee, Australia.*

the distributed processing as it is done by the services (e.g., IGS, ILRS, IVS, IDS) very difficult.
The combination of normal equations is equivalent to the observation level if all the used models and required parameters are identically introduced. This approach directly allows the analysis of constraints (which eventually might be introduced in the computations), and, in the case of unconstrained normal equations, the combination can be done directly without inversion.
The combination of solutions with their variance-covariance matrix does not directly allow the analysis of constraints. For this purpose the constraints, which normally are applied to the solutions, have to be removed and unconstrained normal equations must be generated. The necessary inversion may cause loss of precision by numerical effects (Drewes and Angermann, 2003).

Theoretically, the combination on the level of normal equations (as applied at DGFI) and solutions (as for example applied at IGN) should provide identical results. However, this strongly depends on the characteristics of the input data. The solutions submitted for the ITRF2000 realization were classified to include loose, minimum and removable constraints (see section 4.1). We analysed the solutions concerning constraints and found remarkable contradictions with respect to the declarations provided in the SINEX files. In particular the solutions specified as loosely or minimally constrained often included tremendous constraints, which may affect the combination results, if they are not removed.

Present TRF realizations are computed on the basis of multi-year solutions of the different space geodetic techniques with station positions and velocities. Several contributions to a single technique were provided by different analysis centers. By this means, identical observations enter several times into the processing procedure. In the future intra-technique's combined solutions (and normal equations) shall be provided by the services, as they have the expertise for "their" specific space technique.

It is obvious, that the assumption of constant station velocities is in conflict with the observed non-linear effects in positions (see section 8.3). This may evoke errors and systematic effects in the individual solutions, which may degrade the consistency of the ITRF. As a consequence, we analysed the time series of station positions and datums parameters to identify discontinuities and seasonal signals, and computed a first TRF realization based on epoch (weekly/daily) normal equations of the different space techniques using five years (1999–2004) of data (Meisel et al., 2004).

The input data provided by various analysis centers must be consistent concerning modelling and parameterization. This requires the adoption and implementation of common standards and models according to the most recent set of conventions (e.g., IERS Conventions 2003). At present, TRF realizations are based on SINEX files with station positions and velocities, including variance-covariance matrix. Other parameters common to different space techniques (e.g., Earth orientation parameters (EOP)'s, troposphere parameters) were not considered in present TRF computations.

It is well-known from various inter-technique combination efforts, that the integration of different techniques' solutions via local ties (at co-location sites) is problematic, but there are almost no experiences with other integration methods (e.g., by using common parameters as for example EOP's or troposphere parameters). Another critical issue for the combination of different techniques' solutions is the equating of station velocities of co-located instruments. They were forced to be identical in the ITRF2000 computation, thus there is a unique velocity estimate for all stations at a co-location site. However, this strategy may lead to biased TRF results, as for some co-location sites different velocity estimates exist (see chapter 6, table G.1). Thus, it seems more appropriate to decide on the basis of statistical tests whether the station velocities can be equated or not.

Detailed combination studies were performed within the CONT'02 activities of FESG (Forschungseinrichtung Satellitengeodäsie, TU München) and DGFI. The VLBI campaign CONT'02, initiated by the IVS, provides 15 days of continuous VLBI measurements of 8 participating telescopes. This data set is well-suited for the combination of VLBI data with other techniques, and was used at both institutions for detailed combination studies (Krügel et al., 2004; Thaller et al., 2004). For this purpose, free daily normal equations were generated for GPS (at FESG with the Bernese GPS software) and VLBI (at DGFI with the OCCAM software) using

identical models and the same parameterization to avoid any inconsistencies. The combination of these two microwave techniques provides the opportunity to study all common parameters (not only station coordinates and EOPs, but also tropospheric zenith delays and gradients) within this rigorous combination. The results demonstrate the potential of such a rigorous combination, though some details need to be investigated further.

Recommendation 8.4.1: Input data: To overcome the problems concerning the reduction of constraints, we recommend that unconstrained normal equations should be provided. If constrained solutions are provided, all constraints have to be reported in the SINEX files. Furthermore, the adoption of common standards and models according to the most recent set of conventions (e.g., IERS Conventions) for the processing of the different space geodetic data is essential.

Recommendation 8.4.2: Current TRF realizations based on multi-year solutions with station positions and constant velocities are in conflict with non-linear effects in site motions and datum parameters. As a consequence, future TRF computations should be based on epoch input data (e.g., daily in the case of VLBI and weekly for DORIS, GPS and SLR), and non-linear effects must be modelled in the combination besides the linear velocities.

Recommendation 8.4.3: The consistency and accuracy of the major IERS products (ITRF, EOPs and ICRF) has to be improved to the highest possible extent. The final goal is a rigorous combination of ITRF, EOP time series, and ICRF based on "weekly" epoch SINEX files obtained from the different space geodetic techniques. Other parameters common to more than one space technique should be included in the SINEX submission.

9 Conclusions and outlook

In its function as ITRS Combination Center DGFI has computed a terrestrial reference frame realization 2003 based on multi-year VLBI, SLR, GPS and DORIS solutions with station positions and velocities. The performed TRF computations provide valuable results to assess the current accuracy of the terrestrial reference frame, to identify remaining deficiencies and to enhance the combination methodology. Furthermore, the comparison of the DGFI solution to ITRF2000 can be considered as a first "quasi-independent" quality control and external TRF accuracy evaluation. The results of this comparison show, for example, that for about 60% of all 369 common stations the spherical (3-dimensional) differences in positions and velocities are below 1 cm and 2.5 mm/yr, respectively. On the other hand there are too many stations (about 10%) with position and velocity differences larger than 5 cm and 1 cm/yr, which is not tolerable for a precise reference frame.

The scope and accuracy of the space geodetic observation techniques improved continuously and allow today the determination of geodetic parameters such as station positions or Earth orientation parameters with a precision of a few millimeters (or even better). However, this high accuracy is not fully reflected in current TRF realizations. Major deficiencies are still remaining systematic errors (biases) between techniques, and non-linear site motions (e.g., seismic effects, seasonal signals, equipment changes) that were not considered in past TRF realizations with positions and constant velocities. With the high accuracy of the space geodetic techniques time-variable effects of station positions and datum parameters (e.g., TRF origin) become detectable. We analysed the time series for these parameters obtained from daily VLBI and weekly SLR, GPS and DORIS solutions to identify various effects, such as periodic motions (e.g., seasonal variations) and discontinuities (e.g., caused by earthquakes or instrumentation changes), and computed a first TRF realization based on epoch normal equations of the different techniques. This new approach has major advantages compared to past TRF realizations based on multi-year solutions.

At present, the IERS products (ITRF, ICRF and EOPs) are computed (combined) separately by different product centers. Consequently, the results are not consistent, e.g., different ITRF realizations produce offsets and drifts in the EOP series (Rothacher, 2000). The results of the IERS Analysis Campaign to align EOP's to ITRF2000/ICRF reveal that significant biases between EOP series exist (Dill and Rothacher, 2003). The discrepancies are observed not only between different techniques, but also between solutions of the same technique. This means that there are clear deficiencies in the present IERS product generation, and the different strengths of the individual space techniques are not fully exploited. To achieve the hightest accuracy and consistency, it is crucial to proceed towards a rigorous combination of all the parameters common to more than one space geodetic technique.

As a first step towards a rigorous and consistent combination, the IERS SINEX Combination Campaign has been initiated in 2002. Various analysis centers submitted epoch SINEX files (e.g., monthly and weekly solutions for SLR, weekly solutions for GPS and DORIS, 24-hour sessions for VLBI) with station positions and EOPs (Angermann et al., 2003). Major goal of this campaign was to combine the SINEX files of the different techniques, to assess systematic biases, and to develop suitable combination methods for the computation of the IERS products. Results of the IERS SINEX Combination Campaign (e.g., Krügel and Meisel, 2003) prove the potential of such a weekly combination of station positions and EOPs.

At the IERS Retreat in Paris in April 2003 it was decided, that i) an IERS Working Group on Combination (IERS WG3) should be set up, and that ii) the IERS SINEX Combination Campaign should be converted into a pilot project, namely the IERS Combination Pilot Project (CPP). The

working group was set up in the beginning of 2004 and, as a first reaction, the Call for Participation for the the IERS CPP was launched. It aims towards more consistent, routinely generated IERS products. As described in Rothacher (2003), "weekly" SINEX solutions, made available by the various Technique Services and containing site coordinates, EOPs, and possibly quasar coordinates, shall be rigorously and routinely combined into consistent weekly IERS products (SINEX files).

Within this project, DGFI provides individual SLR and VLBI solutions for the intra-technique combination. DGFI has been accepted by the IERS as a combination centre for the inter-technique combination. By combining all the weekly normal equations into one large solution and by setting up velocity parameters, it will be feasible to obtain a new set of ITRF site coordinates and velocities, a series of EOPs fully consistent with this ITRF realization and a new set of corresponding quasar coordinates (ICRF). It is the final goal that such a consistent set of IERS products will eventually replace the present products. More information about the IERS CPP and the present status may be found at <http://www.iers.org/iers/about/wg/wg3>.

At the IERS Directing Board Meeting in September 2004 it was decided that a call for long time series of "weekly" SINEX files for a new ITRF2004 and a supplementation for the IERS Combination Pilot Project shall be prepared and released. ITRF2004 will be based on the combination of time series of station positions and EOPs. This new ITRF solution will include all available data for station positions, such as VLBI and SLR data since eighties. Weekly or (daily VLBI) contributions will allow better monitoring of non-linear motions and other kind of discontinuities in the time series. The ITRS Combination Centers, namely DGFI, IGN, and NRCan, led by the ITRS Product Center (IGN), are in charge of the generation of the ITRF2004 solution. Each Combination Center should generate solutions to be compared and validated among each other. The detailed computation process will be agreed between the Combination Centers in the frame of the ITRF Product Center. The IERS Analysis Coordinator expertise is required for the final product quality assurance.

Acknowledgement

The work of the ITRS CC at DGFI is partly funded by the GEOTECHNOLOGIEN-Projekt of the German BMBF (Bundesministerium für Bildung und Forschung) and DFG (Deutsche Forschungsgemeinschaft), under contract no.

Verbundprojekt: FE : Grant: IERS(03F0336C), and can be referenced as publication no.

GEOTECH-178.

References

ALTAMIMI, Z., P. SILLARD, C. BOUCHER: ITRF2000: A new release of the International Terrestrial Reference Frame for earth science applications, J. Geophys. Res. 107 (B7), 2214, doi:10.1029/2001JB000561, 2002.

ALTAMIMI, Z., P. SILLARD, C. BOUCHER: The impact of a No-Net-Rotation condition on ITRF2000. J. Geophys. Res., 30 (2), 1064, doi: 10.1029/2002GL016279, 2003.

ALTAMIMI, Z., C. BOUCHER, H. DREWES, R. FERLAND, K. LARSON, J. RAY, M. ROTHACHER: Combination of station positions and velocities. Proceedings of the IERS Workshop on Combination Research and Global Geophysical Fluids, B. Richter, W. Schwegmann, W.R. Dick (eds), IERS Technical Note 30, 19–27, Bundesamt für Kartographie und Geodäsie, Frankfurt a. M., 2003.

ANGERMANN, D.: Combination of space geodetic observations. IAG CSTG Bulletin No. 17, 42–50, Munich, 2002.

ANGERMANN, D., H. MÜLLER, M. GERSTL: Geocenter variations derived from SLR data to LAGEOS 1 and 2. In: J. Adam and K.-P. Schwarz (Eds.): Vistas for Geodesy in the New Millennium, International Association of Geodesy Symposia, Vol. 125, pp. 30–35, Springer, 2002a.

ANGERMANN, D., M. GERSTL, R. KELM, W. SEEMÜLLER, M. VEI: Time evolution of an SLR reference frame, Advances in Space Research, Vol. 30/2, pp. 201–206, Elsevier, 2002b.

ANGERMANN, D., D. THALLER, M. ROTHACHER: IERS SINEX Combination Campaign, Proceedings of the IERS Workshop on Combination Research and Global Geophysical Fluids, B. Richter, W. Schwegmann, W.R. Dick (eds), IERS Technical Note 30, 94–101, Bundesamt für Kartographie und Geodäsie, Frankfurt a. M., 2003.

ANGERMANN, D., H. DREWES, M. GERSTL, R. KELM, M. KRÜGEL, B. MEISEL: ITRF combination – Status and recommendations for the future, IAG Proceedings, IUGG2003, Springer, in print, 2004a.

ANGERMANN, D., M. KRÜGEL, B. MEISEL, H. MÜLLER, V. TESMER: Time evolution of the terrestrial reference frame, IAG Proceedings, IUGG2003, Springer, in print, 2004b.

ARGUS, D. F, R. GORDON: No-net-rotation model of current plate velocities incorporation plate motion model Nuvel-1. Geophys. Res. Lett., 18, 2038–2042, 1991.

BLEWITT, G., D. LAVALLEE, P. CLARKE, K. NURUTDINOV: A new global mode of Earth deformation: Seasonal cycle detected. Science, 294 (5550), pp. 2342–2345.

BOUCHER, C., Z. ALTAMIMI, P. SILLARD, M. FEISSEL-VERNIER: The ITRF2000: IERS ITRS Centre, Institut Geographique National (IGN), Laboratoire de Recherche en Geodesie (LAREG), Ecole Nationale de Sciences Geographiques (ENSG), IERS Technical Note 31, Verlag des Bundesamtes für Kartographie und Geodäsie, Frankfurt am Main, 2004.

DEMETS, C., R. G. GORDON, D. F. ARGUS, S. STEIN: Current plate motions. Geophys. J. Int., 101, 425–478, 1990.

DEMETS, C., R. G. GORDON, D. F. ARGUS, S. STEIN: Effect of recent revisions of the geomagnetic reversal timescale on estimates of current plate motions. Geophys. Res. Lett., 21(20), 2191–2194, 1994.

DILL, R., M. ROTHACHER: IERS analysis campaign to align EOP's to ITRF2000/ICRF, GEOTECHNOLOGIEN Science Report No. 3, 36–39, Koordinierungsbüro Geotechnologien, Potsdam, 2003.

DONG, D, T. YUNCK, M. HEFLIN: Origin of the International Terrestrial Reference Frame, J. Geophys. Res., Vol. 108, No. B4, 2200, doi:10/1029/2002JB0022035, 2003.

DREWES, H.: Combination of VLBI, SLR and GPS determined station velocities for actual plate kinematic and crustal deformation models. In: IAG symposia, vol. 119, R. Forsberg, M. Feissel, and R. Dietrich (Eds.), 377–382, Springer-Verlag, 1998.

DREWES, H., D. ANGERMANN: Remarks on some problems in the combination of station coordinate and velocity solutions. Proceedings of the IERS Workshop on Combination Research and Global Geophysical Fluids, IERS Technical Note 30, 30–32, Verlag des Bundesamtes für Kartographie und Geodäsie, Frankfurt a. M., 2003.

DREWES, H., B. MEISEL: An actual plate motion and deformation model as a kinematic terrestrial reference system, GEOTECHNOLOGIEN Science Re-

port No. 3, 40–43, Koordinierungsbüro Geotechnologien, Potsdam, 2003.

DREWES, H. C. REIGBER: The IAG Project "Integrated Global Geodetic Observing System (IGGOS)" - Setup of Initial Phase. IVS General Meeting Proceedings, pp. 32–37, NASA/CP-2004-212255, 2004.

IERS Annual Report 2002: W.R. DICK, B. RICHTER (eds), Verlag des Bundesamtes für Kartographie und Geodäsie, Frankfurt am Main, 2003.

IERS Conventions (2003): D. MCCARTHY, G. PETIT (eds)., IERS Technical Note, 32, Verlag des Bundesamtes für Kartographie und Geodäsie, Frankfurt am Main, 2004.

FERLAND, R., J. KOUBA, D. HUTCHISON: Analysis methodology an recent results of the IGS network combination, Earth Planets and Space, 52, 953–957, 2000.

FERLAND, R.: Activities of the International GPS Service (IGS) Reference Frame Working Group. In: J. Adam and K.-P. Schwarz (Eds.). Vistas for Geodesy in the New Millennium, International Association of Geodesy Symposia, Vol. 125, pp. 3–8, Springer, 2002.

FERLAND, R.: E-mail communication, 2003.

GERSTL, M.: Bezugssysteme der Satellitengeodäsie, In: 3. DFG-Rundgespräch zum Thema Bezugssysteme, 110–119, Bundesamt für Kartographie und Geodäsie, Frankfurt a. M., 1999.

GERSTL, M., B. RICHTER: Referenzsysteme in DOGS-OC. Manual II für DOGS Version 4.04, Internal Report, 3rd ed., DGFI, 1998.

GERSTL, M.: Numerical aspects of combination at the observation equation and normal equation level, Proceedings of the IERS Workshop on Combination Research and Global Geophysical Fluids, B. Richter, W. Schwegmann, W.R. Dick (eds), IERS Technical Note 30, 89–93, Bundesamt für Kartographie und Geodäsie, Frankfurt a. M., 2003.

GORDON, R. G.: Present plate motions and plate boundaries. In: T. J. Ahrens (ed.), Global Physics, A Handbook of Physical Constants. AGU Reference Shelf 1, pp. 66–87, 1995.

KANIUTH, K., H. MÜLLER, W. SEEMÜLLER: Displacement of the space geodetic observatory Arequipa due to recent earthquakes. Zeitschrift für Vermessungswesen, Heft 4, pp. 238–243, 2002.

KANIUTH, K., S. HUBER: An assessment of radome effects on height estimates in the EUREF network. Mitt. des Bundesamtes für Kartographie und Geodäsie 29, 97–102, 2003.

KELM, R.: Rank defect analysis and variance component estimation for inter-technique combination, Proceedings of the IERS Workshop on Combination Research and Global Geophysical Fluids, B. Richter, W. Schwegmann, W.R. Dick (eds), IERS Technical Note 30, 112–114, Bundesamt für Kartographie und Geodäsie, Frankfurt a. M., 2003.

KLOTZ. J., D. ANGERMANN, G. W. MICHEL, R. PORTH, C. REIGBER, J. REINKING, J. VIRAMONTE, R. PERDOMO, V.H. RIOS, S. BARIENTOS, R. BARRIGA, O. CIFUENTES: GPS-derived deformation of the Central Andes including the 1995 Antofagasta Mw=8.0 Earthquake, Pure and Appl. Geophys., 154, pp. 709–730, 1999.

KLOTZ, J., G. KHAZARADZE, D. ANGERMANN, C. REIGBER, R. PERDOMO, O. CIFUENTES: Earthquake cylce dominates contemporary crustal deformation in Central and Southern Andes. Earth and Planetary Science Letters 193, pp. 437–446, Elsevier, 2001.

KOCH, R.: Parameter estimation and hypothesis testing in linear models, Springer-Verlag, Berlin, 1999.

KREEMER, C., W.E. HOLT: A no-net-rotation model of present-day surface motions, Geophys. Res. Lett., 28, 4407–4410, 2001.

KRÜGEL, M., B. MEISEL: DGFI results of the IERS SINEX combination campaign, GEOTECHNOLOGIEN Science Report No. 3, 96–99, Koordinierungsbüro Geotechnologien, Potsdam, 2003.

KRÜGEL, M., V. TESMER, D. ANGERMANN, D. THALLER, M. ROTHACHER, R. SCHMID: CONT'02 campaign – Combination of VLBI and GPS, IVS General Meeting Proceedings, 418–422, NASA/CP-2004-212255, 2004.

MEISEL, B., D. ANGERMANN, M. KRÜGEL, H. DREWES, M. GERSTL, R. KELM, H. MÜLLER, V. TESMER: Refined approaches for terrestrial reference frame computations, submitted to Adv. Space Res., 2004.

NOTHNAGEL, A., R. DILL, M. FEISSEL-VERNIER, R. FERLAND, R. NOOMEN, P. WILLIS: EOP alignment campaign, IDS/IGS/ILRS/IVS combinations, systematic errors. Proceedings of the IERS Workshop on Combination Research and Global Geophysical Fluids, IERS Technical Note 30, 51–56, Bundesamt für Kartographie und Geodäsie, Frankfurt a. M., 2003.

ROTHACHER, M.: Towards an Integrated Global Geodetic Observing System. In: R. Rummel, H. Drewes, W. Bosch, H. Hornik (eds.), Towards an Integrated Global Geodetic Observing System (IGGOS), International Association of Geodesy Symposia, Vol. 120, 41–52, Springer 2000.

ROTHACHER, M.: Estimation of station heights with GPS. In: *Vertical Reference Systems, IAG Symposia*, H. Drewes, A. Dodson, L. Fortes, L. Sanchez, P. Sandoval (eds), Vol. 124, pp. 81–90, Springer, 2002.

ROTHACHER, M.: Towards a Rigorous Combination of Space Geodetic Techniques. Proceedings of the IERS Workshop on Combination Research and Global Geophysical Fluids, IERS Technical Note 30, 7–18, Bundesamt für Kartographie und Geodäsie, Frankfurt a. M., 2003.

RUMMEL, R., H. DREWES, G. BEUTLER: Integrated Global Geodetic Observing System (IGGOS): A Candidate IAG Project. In: Vistas for Geodesy in the New Millinium, Eds. J. Adam and K.-P. Schwarz, International Association of Geodesy Symposia, Vol. 125, 609–614, Springer 2002.

SCHWEGMANN, W., B. RICHTER: Development for an information and database system for the IERS, status and outlook. GEOTECHNOLOGIEN Science Report No. 3, 156–160, Koordinierungsbüro Geotechnologien, Potsdam, 2003.

SMITH, D., R. KOLENKIEWICZ, P. DUNN, M. TORRENCE: Earth scale below a part per billion from Satllite Laser Ranging. In : K.-P. Schwarz (Ed.), Geodesy beyond 2000 – The challenge of the first decade, International Association of Geodesy Symposia, Vol. 121, 3–11, Springer 2000.

STEIGENBERGER, P., M. ROTHACHER, R. DIETRICH, M. FRITSCHE, A. RÜLKE: Reprocessing of a Global GPS Network. European Geosciences Union, 1st General Assembly, 25–30 April 2004, Nice, Geophysical Research Abstracts, Vol. 6, ISSN:1029–7006, European Geophysical Society, 2004.

TESMER, V.: VLBI Solution DGFI01R01 based on least-squares estimation using OCCAM 5.0 and DOGS-CS. In: Vandenberg, N., K. Baver (Eds.): IVS General Meeting Proceedings, NASA/CP-2002-210002, 295–299, 2002.

THALLER, D., R. SCHMID, M. ROTHACHER, V. TESMER, D. ANGERMANN: Towards a rigorous combination of VLBI and GPS using the CONT02 campaign. IAG Proceedings, Springer, in print, 2004.

WILLIS, P., Y. BAR-SEVER, G. TAVERNIER: DORIS as a potential part of a Global Geodetic Observing System, IAG proceedings, IUGG 2003, in press.

A List of Acronyms

BKG Bundesamt für Kartographie und Geodäsie.
BMBF Bundesministerium für Bildung und Forschung.

CRL Communications Research Laboratory, Japan.
CSR Center of Space Research, USA.

DFG Deutsche Forschungsgemeinschaft.
DGFI Deutsches Geodätisches Forschungsinstitut.
DOGS DGFI Orbit and Geodetic Parameter Estimation System.
DORIS Doppler Orbitography and Radio Positioning Integrated by Satellite.

EOP Earth orientation parameter.

FESG Forschungseinrichtung Satellitengeodäsie, TU München.
FGS Forschungsgruppe Satellitengeodäsie.

GFZ GeoForschungsZentrum Potsdam.
GGOS Global Geodetic Observing System.
GIUB Geodätisches Institut, Universität Bonn.
GNSS Global Navigation Satellite Systems.
GPS Global Positioning System.
GRGS Groupe de Researche de Géodésie Spatiale, France.
GSFC Goddard Space Flight Center, USA.

IAG International Association of Geodesy.
ICRF International Celestial Reference Frame.
IDS International DORIS Service.
IERS International Earth Rotation and Reference Systems Service.
IGN Institute Géographique National.
IGS International GPS Service.
ILRS International Laser Ranging Service.
ITRF International Terrestrial Reference Frame.
ITRS International Terrestrial Reference System.
ITRS CC ITRS Combination Center.
IUGG International Union of Geodesy and Geophysics.
IVS International VLBI Service for Geodesy and Astrometry.

JCET Joint Center for Earth System Technology, USA.
JPL Jet Propulsion Laboratory, USA.

NNR No-Net-Rotation.
NNT No-Net-Translation.
NRCan National Resources Canada.

SHA Shanghai Astronomical Observatory, China.
SINEX Solution INdependent EXchange format.
SLR/LLR Satellite and Lunar Laser Ranging.

TRF Terrestrial Reference Frame.

VLBI Very Long Baseline Interferometry.

B Formal comparison with the ITRF 2000 combination model

Concerning the combination model used for ITRF 2000, we refer to a description which is given in

ALTAMIMI, Z., P. SILLARD and C. BOUCHER: ITRF 2000: A new release of the International Terrestrial Reference Frame for earth science applications. J. Geophys. Res. 107(B10), 2214ff, 2002

and is electronically available in the appendix of the IERS Technical Note 31 (2004),

`http://www.iers.org/iers/publications/tn/tn31`.

Throughout this chapter, $\vec{x}(t)$ and $\dot{\vec{x}}(t)$ will refer to the cartesian coordinate vectors of position and velocity in space as a function of time t. Any station movement will be represented by a **linear model relative to a reference epoch**. If t_0 denotes the reference epoch, the linear model reads

$$\vec{x}(t) \;=\; \vec{x}(t_0) \;+\; (t{-}t_0)\,\dot{\vec{x}}(t_0)\,.$$

The six model parameters are

$$p \;=\; p(t_0) \;=\; \begin{bmatrix} \vec{x}(t_0) \\ \dot{\vec{x}}(t_0) \end{bmatrix}.$$

B.1 Recapitulation of parameter transformations

(a) Transformation of epoch in the linear model

The transformation of a linear modell from an epoch t_0 to a new epoch t_1 could be derived from application (c) of (3.14) reduced to the first two parameters,

$$\begin{bmatrix} \vec{x}(t_1) \\ \dot{\vec{x}}(t_1) \end{bmatrix} \;=\; \underbrace{\begin{bmatrix} \mathrm{I} & (t_1{-}t_0)\,\mathrm{I} \\ 0 & \mathrm{I} \end{bmatrix}}_{T_{\mathrm{E}}(\triangle t)} \begin{bmatrix} \vec{x}(t_0) \\ \dot{\vec{x}}(t_0) \end{bmatrix}. \tag{B.1}$$

With $\triangle t := (t_1{-}t_0)$ the transformation matrix follows the rules

$$T_{\mathrm{E}}(\triangle t_2)\cdot T_{\mathrm{E}}(\triangle t_1) \;=\; T_{\mathrm{E}}(\triangle t_2 + \triangle t_1)\,, \qquad T_{\mathrm{E}}(\triangle t)^{-1} \;=\; T_{\mathrm{E}}(-\triangle t)\,.$$

(b) Similarity transformation in the linear model

Let $\mu = \mu(t) \in \mathbb{R}$ be the scale parameter, $\alpha = \alpha(t) \in \mathbb{R}^3$ the rotation angles, and $d = d(t) \in \mathbb{R}^3$ the translation vector of the 7-parameter similarity transformation introduced with (3.18) and denoted by

$$\vec{x} \;\longmapsto\; \tilde{\vec{x}} \;=\; H(\vec{x},\eta) \;=\; (1{+}\mu)R(\alpha)\,\vec{x} \;+\; d\,, \qquad \eta \;=\; \begin{bmatrix} \mu \\ \alpha \\ d \end{bmatrix} \in \mathbb{R}^7\,.$$

If η is according to $\vec{x}$ represented by a linear model $\eta(t) = \eta(t_0) + (t-t_0)\dot{\eta}(t_0)$, the similarity above extends to the 14-parameter similarity transformation

$$\begin{bmatrix} \tilde{\vec{x}}(t_0) \\ \dot{\tilde{\vec{x}}}(t_0) \end{bmatrix} = \begin{bmatrix} \Big[(1+\mu)R(\alpha)\Big](t_0) & 0 \\ \Big[(1+\mu)\dot{R}+\dot{\mu}R(\alpha)\Big](t_0) & \Big[(1+\mu)R(\alpha)\Big](t_0) \end{bmatrix} \begin{bmatrix} \vec{x}(t_0) \\ \dot{\vec{x}}(t_0) \end{bmatrix} + \begin{bmatrix} d(t_0) \\ \dot{d}(t_0) \end{bmatrix},$$

the similarity parameters of which are $\eta(t_0) \in \mathbb{R}^7$ and $\dot{\eta}(t_0) \in \mathbb{R}^7$.

(c) Infinitesimal similarity transformation of the first kind

This transformation was derived in (3.19) and (3.21) as a linearization of $\eta \longmapsto H(\vec{x},\eta)$ about $\eta^o = 0$. For the linear model we had with (3.21)

$$\begin{bmatrix} \tilde{\vec{x}}(t_0) \\ \dot{\tilde{\vec{x}}}(t_0) \end{bmatrix} = \begin{bmatrix} \vec{x}(t_0) \\ \dot{\vec{x}}(t_0) \end{bmatrix} + \begin{bmatrix} H_\eta(\vec{x}(t_0),0) & 0 \\ \dot{H}_\eta(\vec{x}(t_0),0) & H_\eta(\vec{x}(t_0),0) \end{bmatrix} \begin{bmatrix} \delta\eta(t_0) \\ \dot{\delta\eta}(t_0) \end{bmatrix} + \ldots \tag{B.2}$$

where

$$H_\eta(\vec{x},0) = \begin{bmatrix} x_1 & 0 & -x_3 & x_2 & 1 & 0 & 0 \\ x_2 & x_3 & 0 & -x_1 & 0 & 1 & 0 \\ x_3 & -x_2 & x_1 & 0 & 0 & 0 & 1 \end{bmatrix}, \quad \dot{H}_\eta(\vec{x},0) = \begin{bmatrix} \dot{x}_1 & 0 & -\dot{x}_3 & \dot{x}_2 & 0 & 0 & 0 \\ \dot{x}_2 & \dot{x}_3 & 0 & -\dot{x}_1 & 0 & 0 & 0 \\ \dot{x}_3 & -\dot{x}_2 & \dot{x}_1 & 0 & 0 & 0 & 0 \end{bmatrix}.$$

This corresponds to (A1) in the ITRF 2000 description, whereby attention must be paid to the fact that the rotation part in $H_\eta(\vec{x},0)$ and $\dot{H}_\eta(\vec{x},0)$ gets the opposite sign, because there the elementary rotations were used with the opposite sign of angle. The sign used for ITRF 2000 was also adopted into the IERS Conventions 2003.

(d) Infinitesimal similarity transformation of the second kind

This transformation was derived in (3.20) and (3.21) as a linearization of $(\vec{x},\eta) \longmapsto H(\vec{x},\eta)$ about $(\vec{x},\eta) = (\vec{x}^o,0)$. For the linear model (3.21) yields

$$\begin{bmatrix} \tilde{\vec{x}}(t_0) \\ \dot{\tilde{\vec{x}}}(t_0) \end{bmatrix} = \begin{bmatrix} \vec{x}(t_0) \\ \dot{\vec{x}}(t_0) \end{bmatrix} + \begin{bmatrix} H_\eta(\vec{x}^o,0) & 0 \\ \dot{H}_\eta(\vec{x}^o,0) & H_\eta(\vec{x}^o,0) \end{bmatrix} \begin{bmatrix} \delta\eta(t_0) \\ \dot{\delta\eta}(t_0) \end{bmatrix} + \ldots \tag{B.3}$$

This corresponds to (A4) in the ITRF 2000 description; but it cannot be obtained by simply rewriting (A1). As to the epoch transformation, there apply the following rules

$$h_2(\,\cdot\,,\delta\eta_2) \circ h_2(\,\cdot\,,\delta\eta_1) = h_2(\,\cdot\,,\delta\eta_2+\delta\eta_1)\,, \qquad h_2(\,\cdot\,,\delta\eta)^{-1} = h_2(\,\cdot\,,-\delta\eta)\,.$$

B.2 Notation and prerequisites

When combining several given systems of normal equations $\{N_k,\ y_k,\ b_k^T P_k b_k,\ \sigma_0^2,\ p_k^o\}$ or solutions $\{\mathrm{Var}(\hat{x}_k),\ \hat{x}_k,\ e_k^T P_k e_k,\ \hat{\sigma}_0^2,\ p_k^o\}$, $(k = 1,\ldots,K)$, the notation will be as follows

$p_k\,,\ p_k^o \in \mathbb{R}^{n_k}$	the parameter vector of the k-th system and its approximate values,
$x_k := p_k - p_k^o$	the variables of the k-th system of equations,
$\hat{x}_k\,,\ \hat{p}_k = p_k^o + \hat{x}_k$	the estimated corrections and parameters,
$N_k\,x_k = y_k$	the (reconstructed) free normal equations,
$A_k\,x_k = b_k - e_k$	the (unknown) original observation equations.

Since ITRF 2000 is restricted to station positions and velocities only, the parameter vector of the k-th system is composed of the cartesian coordinates of M_k stations,

$$p_k = \begin{bmatrix} p_{1k} \\ \vdots \\ p_{M_k k} \end{bmatrix} \in \mathbb{R}^{6M_k} \qquad \text{with} \quad p_{ik} = \begin{bmatrix} \vec{x}_{ik}(t_{ik};\mathcal{F}_k) \\ \dot{\vec{x}}_{ik}(t_{ik};\mathcal{F}_k) \end{bmatrix} \quad (i = 1,\dots,M_k)\,,$$

where p_{ik} represents a linear model with the epoch t_{ik} depending on station i and solution k. Since each solution gets its own reference frame $\mathcal{F}_k$, the notation of $\vec{x}_{ik}$ was supplemented by an argument for the frame.

The parameter vector p of the combined solution is supposed to comprise M stations, the union of all the stations contained in the p_k. The common epoch of all the linear models and the frame of the combined solution are denoted by $(t_0;\mathcal{F}_0)$. Thus

$$p = \begin{bmatrix} p_1 \\ \vdots \\ p_M \end{bmatrix} \in \mathbb{R}^{6M} \qquad \text{with} \quad p_i = \begin{bmatrix} \vec{x}_i(t_0;\mathcal{F}_0) \\ \dot{\vec{x}}_i(t_0;\mathcal{F}_0) \end{bmatrix} \quad (i = 1,\dots,M)\,.$$

Since generally $M_k < M$, we make use of the embedding and shrinking operators, that were defined in (3.6) as

$$p_k = E_k\,p\,, \quad p = E_k^T p_k \qquad \text{where} \quad E_k E_k^T = \mathrm{I}\,, \quad E_k^+ = E_k^T\,.$$

Prior to combining it is necessary for all the systems or solutions to be at equal variance level. We assume $\sigma_{0k}{=}1$ or $\hat{\sigma}_{0k}{=}1$ for $k = 1,\dots,K$.

Finally we suppose that the approximate values of a station in p_k^o and p^o are conformal in the sense that they coincide after transformation to the same epoch.

B.3 The combination model of ITRF 2000

The following table relates the notation used herein with the symbols of the ITRF 2000 description given on the left (in blue color).

$X^i_{\text{itrf}} = \vec{x}_i(t_0;\mathcal{F}_0)$ $\dot{X}^i_{\text{itrf}} = \dot{\vec{x}}_i(t_0;\mathcal{F}_0)$	the coordinates of the i-th station in the combined system of equations at the common epoch t_0 in frame $\mathcal{F}_0$ (= ITRF). A linear modell with constant velocity is assumed.
$X^i_{\text{s}} = \vec{x}_i(t_{ik};\mathcal{F}_k)$ $\dot{X}^i_{\text{s}} = \dot{\vec{x}}_i(t_{ik};\mathcal{F}_k)$	the coordinates of the i-th station in the k-th partial system of equations at the station epoch $t_{ik} = t^i_{\text{s}}$ in the solution frame $\mathcal{F}_k$. The indices s and k coincide in the ITRF 2000 description!
$\theta = \delta\eta_k(t_k)$ $\dot{\theta} = \dot{\delta\eta}_k(t_k)$	the 7 parameters of the infinitesimal similarity transformation $\mathcal{F}_0 \longmapsto \mathcal{F}_k$ at epoch t_k and the rates of them.
$T_k = \begin{bmatrix} \delta\eta_k \\ \dot{\delta\eta}_k \end{bmatrix} = h_k$	the 14 parameters of the corresponding transformation of the linear model. In the ITRF 2000 description the symbol T_k is overlappingly used for both the vector of the 14 similarity transformation parameters and the translation vector of that transformation.

The station coordinates from the combined solution are transformed to those of the k-th partial solution by a concatenation of the following three mappings

$$\begin{matrix}\text{combined}\\ \text{solution}\end{matrix} \quad (t_0;\mathcal{F}_0) \underset{1.}{\longmapsto} (t_k;\mathcal{F}_0) \underset{2.}{\longmapsto} (t_k;\mathcal{F}_k) \underset{3.}{\longmapsto} (t_{ik};\mathcal{F}_k) \quad \begin{matrix}k\text{-th partial}\\ \text{solution}\end{matrix}$$

1. Transformation of epoch $t_0 \longmapsto t_k$ in frame $\mathcal{F}_0$ (see (B.1)):

$$\begin{bmatrix} \vec{x}_i(t_k;\mathcal{F}_0) \\ \dot{\vec{x}}_i(t_k;\mathcal{F}_0) \end{bmatrix} = \begin{bmatrix} \mathrm{I} & (t_k - t_0)\,\mathrm{I} \\ 0 & \mathrm{I} \end{bmatrix} \begin{bmatrix} \vec{x}_i(t_0;\mathcal{F}_0) \\ \dot{\vec{x}}_i(t_0;\mathcal{F}_0) \end{bmatrix} = T_{\mathrm{E}}(t_k - t_0)\, p_i(t_0)$$

2. Similarity transformation $\mathcal{F}_0 \longmapsto \mathcal{F}_k$ at epoch t_k, using the infinitesimal transformation of the second kind (B.3) and neglecting $\dot{H}_\eta$:

$$\begin{bmatrix} \vec{x}_i(t_k;\mathcal{F}_k) \\ \dot{\vec{x}}_i(t_k;\mathcal{F}_k) \end{bmatrix} = \begin{bmatrix} \vec{x}_i(t_k;\mathcal{F}_0) \\ \dot{\vec{x}}_i(t_k;\mathcal{F}_0) \end{bmatrix} + \begin{bmatrix} H_\eta(\vec{x}_i^{\,o},0) & 0 \\ 0 & H_\eta(\vec{x}_i^{\,o},0) \end{bmatrix} \begin{bmatrix} \delta\eta_{0k} \\ \dot{\delta\eta}_{0k} \end{bmatrix} + \ldots$$

3. Transformation of epoch $t_k \longmapsto t_{ik}$ in frame $\mathcal{F}_k$:

$$\begin{bmatrix} \vec{x}_i(t_{ik};\mathcal{F}_k) \\ \dot{\vec{x}}_i(t_{ik};\mathcal{F}_k) \end{bmatrix} = \begin{bmatrix} \mathrm{I} & (t_{ik} - t_k)\,\mathrm{I} \\ 0 & \mathrm{I} \end{bmatrix} \begin{bmatrix} \vec{x}_i(t_k;\mathcal{F}_k) \\ \dot{\vec{x}}_i(t_k;\mathcal{F}_k) \end{bmatrix} = T_{\mathrm{E}}(t_{ik} - t_k)\, p_{ik}(t_k)$$

The concatenation of the three mappings yields

$$\underbrace{\begin{bmatrix} \vec{x}_i(t_{ik};\mathcal{F}_k) \\ \dot{\vec{x}}_i(t_{ik};\mathcal{F}_k) \end{bmatrix}}_{p_{ik}(t_{ik})} = \underbrace{\begin{bmatrix} \mathrm{I} & (t_{ik} - t_0)\,\mathrm{I} \\ 0 & \mathrm{I} \end{bmatrix}}_{T_{ik}} \underbrace{\begin{bmatrix} \vec{x}_i(t_0;\mathcal{F}_0) \\ \dot{\vec{x}}_i(t_0;\mathcal{F}_0) \end{bmatrix}}_{p_i(t_0)} + \underbrace{\begin{bmatrix} H_\eta(\vec{x}_i^{\,o},0) & (t_{ik} - t_k) H_\eta(\vec{x}_i^{\,o},0) \\ 0 & H_\eta(\vec{x}_i^{\,o},0) \end{bmatrix}}_{S_{ik}} \underbrace{\begin{bmatrix} \delta\eta_{0k} \\ \dot{\delta\eta}_{0k} \end{bmatrix}}_{h_k} \tag{B.4}$$

Written out by element this equals to equation (A9) in the ITRF 2000 description

$$\begin{aligned} \vec{x}_i(t_{ik};\mathcal{F}_k) &= \vec{x}_i(t_0;\mathcal{F}_0) + (t_{ik} - t_0)\,\dot{\vec{x}}_i(t_0;\mathcal{F}_0) + H_\eta(\vec{x}_i^{\,o},0)\big(\,\delta\eta_{0k} + (t_{ik} - t_k)\,\dot{\delta\eta}_{0k}\big) \\ \dot{\vec{x}}_i(t_{ik};\mathcal{F}_k) &= \dot{\vec{x}}_i(t_0;\mathcal{F}_0) + H_\eta(\vec{x}_i^{\,o},0)\,\dot{\delta\eta}_{0k}\,. \end{aligned}$$

Here conformal transformation of the approximate values means that the approximate values join in the two epoch transformations:

$$\vec{x}_i^{\,o}(t_{ik}) = \vec{x}_i^{\,o}(t_0) + (t_{ik} - t_0)\,\dot{\vec{x}}_i^{\,o}(t_0)\,, \qquad \dot{\vec{x}}_i^{\,o}(t_{ik}) = \dot{\vec{x}}_i^{\,o}(t_0)$$

or

$$p_{ik}^o = \begin{bmatrix} \vec{x}_i^{\,o}(t_{ik}) \\ \dot{\vec{x}}_i^{\,o}(t_{ik}) \end{bmatrix} = T_{\mathrm{E}}(t_{ik} - t_0) \begin{bmatrix} \vec{x}_i^{\,o}(t_0) \\ \dot{\vec{x}}_i^{\,o}(t_0) \end{bmatrix} = T_{ik}\, p_i^o$$

Subtracting this equation from (B.4) we get

$$x_{ik} = p_{ik} - p_{ik}^o = T_{ik}(p_i - p_i^o) + S_{ik}\, h_k = T_{ik}\, x_i + S_{ik}\, h_k$$

Thus, the transformation equation (B.4) holds for both the parameters p_{ik} and their corrections x_{ik}

$$\begin{aligned} p_{ik} &= T_{ik}\, p_i + S_{ik}\, h_k \\ x_{ik} &= T_{ik}\, x_i + S_{ik}\, h_k \end{aligned} \qquad i = 1, \ldots, M_k\,. \tag{B.5}$$

If the station parameters $p_{ik} = p_{ik}(t_{ik};\mathcal{F}_k)$, $i = 1, \ldots, M_k$, from the k-th solution are arranged in the parameter vector p_k, and if the station parameters $p_i = p_i(t_0;\mathcal{F}_0)$ are embedded in the parameter

vector p according to (3.6), we get

$$\underbrace{\begin{bmatrix} p_{1k} \\ p_{2k} \\ \vdots \\ p_{M_k k} \end{bmatrix}}_{p_k} = \underbrace{\begin{bmatrix} T_{1k} & & & \\ & T_{2k} & & \\ & & \ddots & \\ & & & T_{Nk} \end{bmatrix}}_{T_k} E_k \cdot \underbrace{\begin{bmatrix} p_1 \\ p_2 \\ \vdots \\ p_M \end{bmatrix}}_{p} + \underbrace{\begin{bmatrix} S_{1k} \\ S_{2k} \\ \vdots \\ S_{Nk} \end{bmatrix}}_{S_k} \cdot h_k \,.$$

Assuming conformal approximate values the same applies to the corrections $x = p - p^o$ and $x_k = p_k - p_k^o$ as well

$$x_k \;=\; T_k\, x \;+\; S_k\, h_k \,.$$

In the ITRF 2000 model this equation is made observation equations (OEQ)

$$\text{OEQ}: \qquad \begin{bmatrix} T_k & S_k \end{bmatrix} \cdot \begin{bmatrix} x \\ h_k \end{bmatrix} \;=\; \hat{x}_k - e_k \,, \qquad \text{Var}(\hat{x}_k) \;=\; \big(N_k + D_k\big)^{-1}. \tag{B.6}$$

The "observations" at the right-hand side of these equations are the available estimated coordinate corrections of the k-th solution.

Since the free normal equations of all the space observation techniques show a rank deficiency, $\mathcal{V}(\hat{x}_k)^{-1}$ contains a part D_k fixing the datum of the k-th solution. These constraints D_k are, as far as known, removed from the inverse variance matrix and replaced by "minimum constraints" $\tilde{D}_k$. That exchange of constraints changes the solution $\hat{x}_k$ too, and may become numerically dangerous, if $\text{rank}(\mathcal{V}(\hat{x}_k)^{-1})$ is changed. For "loose constraints" and constraints to reduced parameters that adaption is omitted.

If $N_k x_k = y_k$ denote the free normal equations for the k-th solution, and $N_k^{\text{c}} := N_k + \tilde{D}_k$ the inverse variance matrix after the exchange of constraints, the following normal equations (NEQ) are built from (B.6)

$$\text{NEQ}: \qquad \begin{bmatrix} T_k^T \\ S_k^T \end{bmatrix} N_k^{\text{c}} \begin{bmatrix} T_k & S_k \end{bmatrix} \cdot \begin{bmatrix} x \\ h_k \end{bmatrix} \;=\; \begin{bmatrix} T_k^T \\ S_k^T \end{bmatrix} N_k^{\text{c}} x_k \,. \tag{B.7}$$

These normal equations are equivalent to (A10) in the ITRF 2000 description if we relate

with here	T_{ik}	S_{ik}	$H_p(\vec{x}_i^o, 0)$	T_k	S_k	N_k^{c}	x	h_k	$\hat{x}_k$
ITRF 2000	$A1_s^i$	$A2_s^i$	A_s^i	$A1_s$	$A2_s$	P_s	X	T_k	B_s

Note that the vector X in (A10) of the ITRF 2000 description does not contain the station coordinates itselves but their corrections $X = x = p - p^o$. The combination of these normal equations for all solutions ($k = 1, \ldots, K$) yields

$$\begin{bmatrix} \sum\limits_k T_k^T N_k^{\text{c}} T_k & T_1^T N_1^{\text{c}} S_1 & T_2^T N_2^{\text{c}} S_2 & \ldots & T_K^T N_K^{\text{c}} S_K \\ S_1^T N_1^{\text{c}} T_1 & S_1^T N_1^{\text{c}} S_1 & 0 & \ldots & 0 \\ S_2^T N_2^{\text{c}} T_2 & 0 & S_2^T N_2^{\text{c}} S_2 & & 0 \\ \vdots & \vdots & & \ddots & \vdots \\ S_K^T N_K^{\text{c}} T_K & 0 & 0 & \ldots & S_K^T N_K^{\text{c}} S_K \end{bmatrix} \cdot \begin{bmatrix} x \\ h_1 \\ h_2 \\ \vdots \\ h_K \end{bmatrix} = \begin{bmatrix} \sum\limits_k T_k^T N_k^{\text{c}} \hat{x}_k \\ S_1^T N_1^{\text{c}} \hat{x}_1 \\ S_2^T N_2^{\text{c}} \hat{x}_2 \\ \vdots \\ S_K^T N_K^{\text{c}} \hat{x}_K \end{bmatrix} .$$

B.4 The combination model for free normal equations

The station coordinates from the k-th partial solution are transformed to those of the combined solution by a concatenation of the following three mappings

$$(t_{ik};\mathcal{F}_k) \underset{1.}{\longmapsto} (t_k;\mathcal{F}_k) \underset{2.}{\longmapsto} (t_k;\mathcal{F}_0) \underset{3.}{\longmapsto} (t_0;\mathcal{F}_0)$$

1. Transformation of epoch $t_{ik} \longmapsto t_k$ in frame $\mathcal{F}_k$:

$$\begin{bmatrix} \vec{x}_i(t_k;\mathcal{F}_k) \\ \dot{\vec{x}}_i(t_k;\mathcal{F}_k) \end{bmatrix} = \begin{bmatrix} \mathrm{I} & (t_k - t_{ik})\,\mathrm{I} \\ 0 & \mathrm{I} \end{bmatrix} \begin{bmatrix} \vec{x}_i(t_{ik};\mathcal{F}_k) \\ \dot{\vec{x}}_i(t_{ik};\mathcal{F}_k) \end{bmatrix} = T_{\mathrm{E}}(t_k - t_{ik})\, p_{ik}$$

2. Infinitesimal similarity transformation $\mathcal{F}_k \longmapsto \mathcal{F}_0$ at epoch t_k:

$$\begin{bmatrix} \vec{x}_i(t_k;\mathcal{F}_0) \\ \dot{\vec{x}}_i(t_k;\mathcal{F}_0) \end{bmatrix} = \begin{bmatrix} \vec{x}_i(t_k;\mathcal{F}_k) \\ \dot{\vec{x}}_i(t_k;\mathcal{F}_k) \end{bmatrix} + \begin{bmatrix} H_\eta(\vec{x}_i^{\,o},0) & 0 \\ 0 & H_\eta(\vec{x}_i^{\,o},0) \end{bmatrix} \begin{bmatrix} \delta\eta_{k0} \\ \dot{\delta\eta}_{k0} \end{bmatrix} + \ldots$$

3. Transformation of epoch $t_k \longmapsto t_0$ in frame $\mathcal{F}_0$:

$$\begin{bmatrix} \vec{x}_i(t_0;\mathcal{F}_0) \\ \dot{\vec{x}}_i(t_0;\mathcal{F}_0) \end{bmatrix} = \begin{bmatrix} \mathrm{I} & (t_0 - t_k)\,\mathrm{I} \\ 0 & \mathrm{I} \end{bmatrix} \begin{bmatrix} \vec{x}_i(t_k;\mathcal{F}_0) \\ \dot{\vec{x}}_i(t_k;\mathcal{F}_0) \end{bmatrix} = T_{\mathrm{E}}(t_0 - t_k)\, p_i(t_k)$$

Note: At the DGFI we use the more accurate infinitesimal similarity transformation of the first kind (B.2) for the transformation $\mathcal{F}_k \longmapsto \mathcal{F}_0$ and do not neglect $\dot{H}_\eta$. If the approximate values are good enough, this difference is of second order and not essential for the comparison. Here it is not taken into account in order to keep the compared equations simple.

The concatenation of the three mappings yields

$$\underbrace{\begin{bmatrix} \vec{x}_i(t_0;\mathcal{F}_0) \\ \dot{\vec{x}}_i(t_0;\mathcal{F}_0) \end{bmatrix}}_{p_i} = \underbrace{\begin{bmatrix} \mathrm{I} & (t_0 - t_{ik})\,\mathrm{I} \\ 0 & \mathrm{I} \end{bmatrix}}_{T_{ik}^{-1}} \underbrace{\begin{bmatrix} \vec{x}_i(t_{ik};\mathcal{F}_k) \\ \dot{\vec{x}}_i(t_{ik};\mathcal{F}_k) \end{bmatrix}}_{p_{ik}} + \underbrace{\begin{bmatrix} H_\eta(\vec{x}_i^{\,o},0) & (t_0 - t_k) H_\eta(\vec{x}_i^{\,o},0) \\ 0 & H_\eta(\vec{x}_i^{\,o},0) \end{bmatrix}}_{T_{ik}^{-1} S_{ik}} \underbrace{\begin{bmatrix} \delta\eta_{k0} \\ \dot{\delta\eta}_{k0} \end{bmatrix}}_{-\,h_k}$$

Inversion of this equation leads to

$$\begin{aligned} p_{ik} &= T_{ik}\, p_i + S_{ik}\, h_k \\ x_{ik} &= T_{ik}\, x_i + S_{ik}\, h_k \end{aligned} \qquad i = 1, \ldots, M_k\,. \tag{B.8}$$

As before all M_k stations contained in the k-th solution will be combined to give

$$\begin{aligned} p_k &= T_k\, p + S_k\, h_k \\ x_k &= T_k\, x + S_k\, h_k \end{aligned} \tag{B.9}$$

The combination model used at the DGFI comes from the original system of observation equations which is generally not given and needs not be available,

$$\mathrm{OEQ}: \qquad A_k\, x_k = b_k - e_k\,, \qquad \mathrm{Var}(b_k) = P_k^{-1}\,. \tag{B.10}$$

Substituting (B.9) for x_k extends the observation equations by the similarity transformation parameters

$$\text{OEQ:} \qquad \left[\, A_k T_k \,,\; A_k S_k \,\right] \cdot \begin{bmatrix} x \\ h_k \end{bmatrix} \;=\; b_k - e_k \,, \qquad \mathrm{Var}(b_k) \;=\; P_k^{-1} \,. \tag{B.11}$$

The right-hand side of both observation equations are the real observations (observed − computed). Therefrom it follows the extended system of normal equations

$$\text{NEQ:} \qquad \begin{bmatrix} T_k^T \\ S_k^T \end{bmatrix} \underbrace{A_k^T P_k A_k}_{N_k} \left[\, T_k \; S_k \,\right] \cdot \begin{bmatrix} x \\ h_k \end{bmatrix} \;=\; \begin{bmatrix} T_k^T \\ S_k^T \end{bmatrix} \underbrace{A_k^T P_k b_k}_{y_k} \,. \tag{B.12}$$

The extended normal equations can be directly set up from the given normal equations.
The combination of these normal equations for all solutions ($k{=}1, \ldots, K$) yields

$$\begin{bmatrix} \sum\limits_k T_k^T N_k T_k & T_1^T N_1 S_1 & T_2^T N_2 S_2 & \ldots & T_K^T N_K S_K \\ S_1^T N_1 T_1 & S_1^T N_1 S_1 & 0 & \ldots & 0 \\ S_2^T N_2 T_2 & 0 & S_2^T N_2 S_2 & & 0 \\ \vdots & \vdots & & \ddots & \vdots \\ S_K^T N_K T_K & 0 & 0 & \ldots & S_K^T N_K S_K \end{bmatrix} \cdot \begin{bmatrix} x \\ h_1 \\ h_2 \\ \vdots \\ h_K \end{bmatrix} = \begin{bmatrix} \sum\limits_k T_k^T y_k \\ S_1^T y_1 \\ S_2^T y_2 \\ \vdots \\ S_K^T y_K \end{bmatrix}$$

Only to these generally singular normal equations the regularizing datum is added.

B.5 Comparison

In the following table the equations of both methods are opposed to each other. The equations coincide to the first order exept for the constraints. The crucial point is that in case of combining solutions the constraints have to be applied **before** the combination at epoch t_{ik} in frame $\mathcal{F}_k$, and in case of combining normal or observation equations the constraints are applied once **after** the combination at epoch t_0 and in the solution frame $\mathcal{F}_0$. That the constraints applied before and after combination have to be set up at different epochs and in possibly different frames, does not matter; but quite the fact that the partial normal equations $N_k x_k{=}y_k$ generally have a larger rank deficiency than the combined normal equations. So the partial systems of equations need "more" constraints, $D_k = D + \Delta_k$.

Further comments to the solution method:

- The sum of "loose" constraints may no longer be "loose"
  (note the factor K in the last equation of the table).
- Constraints, which are minimum for some N_k, may overconstrain $N = \sum N_k$. That holds especially for constraints fixing a rank deficiency not of type translation, rotation, or scaling.
- Constraints on already reduced parameters cannot be removed.
- The SINEX-format does not allow to specify every kind of constraints.

Normal equation model used at DGFI

Observation equations for the k-th partial system:

$$A_k\, x_k \;=\; b_k - e_k\,, \qquad \mathrm{Var}(b_k) \;=\; P_k^{-1}\,.$$

Extended observation equations:

$$\Big[\; A_k T_k \;\; A_k S_k \;\Big] \cdot \begin{bmatrix} x \\ h_k \end{bmatrix} \;=\; b_k - e_k\,, \qquad \mathrm{Var}(b_k) \;=\; P_k^{-1}\,.$$

Extended normal equations:

$$\begin{bmatrix} T_k^T \\ S_k^T \end{bmatrix} N_k \Big[\; T_k \;\; S_k \;\Big] \cdot \begin{bmatrix} x \\ h_k \end{bmatrix} \;=\; \begin{bmatrix} T_k^T \\ S_k^T \end{bmatrix} y_k\,.$$

Effect of the datum in case of identical epochs $t_{ik}{=}t_0$, i.e. $T_k{=}\mathrm{I}$:
Common datum D applied **after combination**

$$\Big(\sum_{k=1}^{K} N_k\Big) \;+\; D\,.$$

Solution model used for ITRF 2000

Observation equations for the k-th partial solution:

$$\mathrm{I}\, x_k \;=\; \hat{x}_k - e_k\,, \qquad \mathrm{Var}(\hat{x}_k) \;=\; (N_k{+}\tilde{D}_k)^{-1}\,.$$

Extended observation equations:

$$\Big[\; T_k \;\; S_k \;\Big] \cdot \begin{bmatrix} x \\ h_k \end{bmatrix} \;=\; \hat{x}_k - e_k\,, \qquad \mathrm{Var}(\hat{x}_k) \;=\; \big(N_k{+}\tilde{D}_k\big)^{-1}.$$

Extended normal equations:

$$\begin{bmatrix} T_k^T \\ S_k^T \end{bmatrix} \Big(N_k{+}\tilde{D}_k\Big) \Big[\; T_k \;\; S_k \;\Big] \cdot \begin{bmatrix} x \\ h_k \end{bmatrix} \;=\; \begin{bmatrix} T_k^T \\ S_k^T \end{bmatrix} \Big(N_k{+}\tilde{D}_k\Big) \hat{x}_k\,.$$

Effect of the datums in case of identical epochs $t_{ik}{=}t_0$, i.e. $T_k{=}\mathrm{I}$:
Datum $\tilde{D}_k = D + \Delta_k$ applied **before combination**

$$\sum_{k=1}^{K} (N_k + \tilde{D}_k) \;=\; \Big(\sum_{k=1}^{K} (N_k + \Delta_k)\Big) \;+\; K \cdot D\,.$$

Tab. B.1: *Comparison of the methods for combination.*

C VLBI, SLR, GPS and DORIS stations

Tab. C.1: *Observation periods for VLBI stations are mainly taken from the GSFC solution SINEX file (GSFC00R01), the number of sessions available per station are extracted from the DGFI VLBI session data base.*

[1] "T" denotes the space technique, i.e. R=VLBI.

[2] The stations used for the intra-technique combination are identified by a "$*$". About 50 "poorly" observed stations with a short data time span ($<$ 1 yr) and/or few daily sessions were excluded ($-^1$).

[3] The column "RF" denotes the selected VLBI reference frame stations used to realize the VLBI datum.

[4] The number of daily sessions is the sum for A1 and A2.

VLBI Observation Statistic

Domes No.	CDP No.	Sol. No.	T[1]	Site Name	Data Time Span	$\triangle$t [yrs]	# daily sessions	used[2]	RF[3]
10002M003	7605	A1	R	Grasse, France	1989 - 1989	0.0	4	$-^1$	
10003M003	7608	A1	R	Toulouse, France	1992 - 1992	0.0	3	$-^1$	
10004M002	7604	A1	R	Brest, France	1989 - 1989	0.0	4	$-^1$	
10204M001	7635	A1	R	Hofn, Iceland	1992 - 1992	0.0	4	$-^1$	
10302M002	7602	A1	R	Tromso, Norway	1989 - 1992	3.1	8	$*$	
10317 S 003	7331	A1	R	Ny Alesund	1994 - 2000	6.0	242	$*$	$*$
10329M001	7607	A1	R	Trysil, Norway	1991 - 1993	1.4	15	$*$	
10402M006	7211	A1	R	Onsala, Sweden	1992 - 1992	0.0	1	$-^1$	
10402 S 002	7213	A1	R	Onsala, Sweden	1980 - 2000	20.0	372	$*$	$*$
10503M002	7601	A1	R	Metsahovi, Finland	1989 - 1989	0.0	5	$-^1$	
12337 S 008	7332	A1	R	Simeis Crimea Ukraine	1994 - 2000	5.9	40	$*$	
12342 S 001	7247	A1	R	Ussuriisk, Russia	2000 - 2000	0.0	1	$-^1$	
12711 S 001	7230	A1	R	Bologna, Italy	1987 - 1996	8.2	121[4]	$*$	
12711 S 001	7230	A2	R	Bologna, Italy	1996 - 2000	3.5	-	$*$	
12717 S 001	7547	A1	R	Noto, Sicily, Italy	1989 - 2000	11.0	83	$*$	$*$
12734 S 005	7243	A1	R	Matera, Italy	1990 - 2000	9.9	249	$*$	$*$
13201 S 002	7215	A1	R	Chilbolton, England	1980 - 1980	0.0	7	$-^1$	
13296M002	7603	A1	R	Carnoustie, Scotland	1989 - 1989	0.0	4	$-^1$	
13407 S 003	1561	A1	R	Madrid, Spain	1983 - 1983	0.0	2	$-^1$	
13407 S 010	1565	A1	R	Madrid, Spain (34-M)	1988 - 1996	8.3	111[4]	$*$	$*$
13407 S 010	1565	A2	R	Madrid, Spain (34-M)	1997 - 1999	2.0	-	$*$	
13420 S 001	7333	A1	R	Yebes, Spain	1995 - 2000	4.9	21	$*$	
14201 S 004	7224	A1	R	Wettzell, FRG	1983 - 2000	16.9	1531	$*$	$*$
14201 S 100	7593	A1	R	TIGO at Wettzell, FRG	1997 - 2000	2.4	23	$-^1$	
14202M002	7600	A1	R	Hohenbunstorf, FRG	1989 - 1989	0.0	5	$-^1$	

continued

VLBI Stations continued

Domes No.	CDP No.	Sol. No.	T[1]	Site Name	Data Time Span	△t [yrs]	# avail. sessions	used[2]	RF[3]
14209 S 001	7203	A1	R	Effelsberg, FRG	1980 - 1995	15.4	22[4]	*	
14209 S 001	7203	A2	R	Effelsberg, FRG	1996 - 1999	3.1	-	*	
14213M002	7630	A1	R	Hohenpeissenberg FRG	1992 - 1992	0.0	3	–[1]	
14260M001	7632	A1	R	Karlsburg, FRG	1992 - 1992	0.0	2	–[1]	
14261M001	7631	A1	R	Kirschberg, FRG	1992 - 1992	0.0	3	–[1]	
21605 S 008	7226	A1	R	Shanghai, China	2000 - 2000	0.0	1	–[1]	
21605 S 009	7227	A1	R	Shanghai, China	1988 - 2000	11.8	83	*	*
21612 S 001	7330	A1	R	Urumqi, China	1997 - 2000	2.4	29	*	
21701 S 001	1856	A1	R	Kashima, Japan	1984 - 2000	16.6	258	*	*
21701 S 004	1857	A1	R	Kashima, Japan	1990 - 2000	10.5	73	*	*
21701 S 006	7334	A1	R	Kashima, Japan	2000 - 2000	0.5	2	–[1]	
21702 S 009	7314	A1	R	Mizusawa, Japan	1991 - 1991	0.2	6	–[1]	
21702 S 010	7324	A1	R	Mizusawa, Japan	1993 - 1999	6.2	13	*	
21704 S 004	7327	A1	R	Koganei, Japan	2000 - 2000	0.5	2	–[1]	
21718 S 001	7312	A1	R	Miyazaki, Japan	1986 - 1988	2.0	4	–[1]	
21725 S 001	7244	A1	R	Nobeyama, Japan	1990 - 1991	1.5	7	–[1]	
21729 S 001	7246	A1	R	Usuda, Japan	1990 - 1990	0.0	1	–[1]	
21730 S 001	7311	A1	R	Tsukuba, Japan	1984 - 1991	7.0	10	*	
21730 S 007	7345	A1	R	Tsukuba, Japan (32 m)	1998 - 2000	1.9	30	*	
21731 S 001	7315	A1	R	Shintotsugawa, Japan	1990 - 1990	0.0	4	–[1]	
21731 S 003	7346	A1	R	Shintotsukawa, Japan	1999 - 1999	0.4	3	–[1]	
21732 S 001	7316	A1	R	Chichi Jima, Japan	1987 - 1989	2.0	4	–[1]	
21732 S 004	7347	A1	R	Chichijima, Japan	1999 - 1999	0.7	6	–[1]	
21733 S 002	7310	A1	R	Marcus, Japan	1989 - 1993	3.9	16	*	
21737 S 001	7325	A1	R	Sagara, Japan	1992 - 1993	0.3	2	–[1]	
21738 S 001	7326	A1	R	Daito Islands, Japan	2000 - 2000	0.0	4	–[1]	
21739 S 001	7336	A1	R	Miura, Japan	2000 - 2000	0.5	2	–[1]	
21740 S 001	7338	A1	R	Tateyama, Japan	2000 - 2000	0.5	2	–[1]	
21742 S 002	7348	A1	R	Aira, Japan	1999 - 1999	0.7	5	–[1]	
23903 S 001	7353	A1	R	Suwon, Korea	1995 - 1995	0.0	3	–[1]	
30302 S 001	7232	A1	R	Hartebeesthoek S Afr.	1986 - 2000	14.5	413	*	*
31906M001	7609	A1	R	Sao Miguel, Azores	1992 - 1992	0.0	5	–[1]	
40104 S 001	7282	A1	R	Algonquin Park Canada	1984 - 2000	16.1	304	*	*
40105M001	7283	A1	R	Penticton, Canada	1984 - 1990	5.9	7	*	
40118M001	7284	A1	R	Whitehorse, Canada	1984 - 1986	2.0	9[4]	–[1]	
40118M001	7284	A2	R	Whitehorse, Canada	1988 - 1989	1.0	-	–[1]	
40127M001	7285	A1	R	Yellowknife, Canada	1984 - 1985	1.0	2	–[1]	
40127M004	7296	A1	R	Yellowknife, Canada	1991 - 2000	9.2	54	*	
40129M001	7289	A1	R	Victoria, Canada	1990 - 1990	0.0	3	–[1]	
40400M003	7263	A1	R	Pasadena, CA	1982 - 1988	6.1	24	*	
40403M001	7268	A1	R	Palos Verdes, CA	1983 - 1990	6.2	9	*	
40404M001	7254	A1	R	Pearblossom, CA	1983 - 1988	5.0	10	*	
40405M013	7288	A1	R	Goldstone, CA	1987 - 1987	0.0	1	–[1]	
40405 S 009	7222	A1	R	Goldstone, CA	1983 - 1992	9.0	731[4]	*	
40405 S 009	7222	A2	R	Goldstone, CA	1992 - 1992	0.2	-	*	
40405 S 014	1513	A1	R	Goldstone, CA	1981 - 1991	9.7	24	*	

continued

VLBI Stations continued

Domes No.	CDP No.	Sol. No.	T[1]	Site Name	Data Time Span	△t [yrs]	# avail. sessions	used[2]	RF[3]
40405 S 019	1515	A1	R	Goldstone, CA	1987 - 1989	1.7	97[4]	*	
40405 S 019	1515	A2	R	Goldstone, CA	1993 - 1999	6.6	-	*	
40406M001	7252	A1	R	San Francisco, CA	1983 - 1989	5.5	22[4]	*	
40406M001	7252	A2	R	San Francisco, CA	1989 - 1991	1.7	-	*	
40407M001	7256	A1	R	Pinyon Flats, CA	1983 - 1990	6.3	21	*	
40408 S 002	7225	A1	R	Fairbanks, AK	1984 - 2000	16.3	1511	*	*
40410M001	7251	A1	R	Point Reyes, CA	1983 - 1991	7.9	20	*	
40412M003	7271	A1	R	Austin, TX	1987 - 1987	0.0	1	–[1]	
40416M001	7277	A1	R	Cape Yakataga, AK	1984 - 1987	3.0	16[4]	*	
40416M001	7277	A2	R	Cape Yakataga, AK	1988 - 1990	1.9	-	*	
40419M001	7278	A1	R	Kodiak, AK	1984 - 1990	5.9	15	*	
40420M002	7223	A1	R	Vandenberg AFB, CA	1983 - 1991	7.9	181	*	
40421M001	7279	A1	R	Nome, AK	1984 - 1990	5.9	10	*	
40423M001	7280	A1	R	Sand Point, AK	1984 - 1990	6.0	13	*	
40424 S 001	1311	A1	R	Kokee Park Kauai, HI	1984 - 1994	9.7	522	*	*
40424 S 007	7298	A1	R	Kokee Park Kauai, HI	1993 - 2000	7.4	607	*	*
40425M001	7281	A1	R	Sourdough, AK	1984 - 1987	3.1	16[4]	*	
40425M001	7281	A2	R	Sourdough, AK	1988 - 1989	1.0	-	*	
40427M001	7266	A1	R	Fort Ord, CA	1983 - 1988	4.5	11	*	
40427M002	7241	A1	R	Fort Ord, CA	1988 - 1989	0.5	19[4]	*	
40427M002	7241	A2	R	Fort Ord, CA	1989 - 1991	1.7	-	*	
40428M001	7255	A1	R	Santa Paula, CA	1983 - 1990	6.4	10	*	
40430M001	7269	A1	R	Black Butte, CA	1983 - 1988	5.0	12	*	
40431M001	7267	A1	R	Deadman Lake, CA	1984 - 1988	3.9	5	–[1]	
40432M001	7286	A1	R	Ely, NV	1984 - 1990	6.5	12	*	
40433M004	7221	A1	R	Quincy, CA	1982 - 1990	8.0	22	*	
40437M001	7259	A1	R	Mammoth Lakes, CA	1983 - 1986	3.3	4	*	
40439M004	7853	A1	R	Owens Valley, CA	1987 - 1987	0.0	1	–[1]	
40439 S 002	7207	A1	R	Owens Valley, CA	1979 - 1988	9.3	131	*	
40439 S 006	7616	A1	R	Owens Valley, CA VLBA	1992 - 2000	7.7	30	*	
40440 S 002	7205	A1	R	Westford, MA	1979 - 1992	12.9	89	*	
40440 S 003	7209	A1	R	Westford, MA	1981 - 2000	19.2	1386	*	*
40441 S 001	7204	A1	R	Green Bank, WV	1979 - 1996	16.8	17	*	
40441 S 004	7214	A1	R	Green Bank, WV	1989 - 1990	1.6	617[4]	*	
40441 S 004	7214	A2	R	Green Bank, WV	1990 - 1996	5.7	-	*	
40441 S 005	7248	A1	R	Green Bank, WV	1992 - 1992	0.0	2	–[1]	
40441 S 007	7208	A1	R	Green Bank, WV	1995 - 2000	5.4	307	*	*
40442M008	7850	A1	R	Fort Davis, TX	1988 - 1988	0.0	1	–[1]	
40442M009	7900	A1	R	Fort Davis, TX	1988 - 1988	0.0	1	–[1]	
40442 S 003	7216	A1	R	Fort Davis, TX	1980 - 1991	11.1	743	*	
40442 S 017	7613	A1	R	Ft. Davis, TX VLBA	1991 - 2000	9.1	80	*	*
40445M002	7120	A1	R	LURE Obs., Maui, HI	1988 - 1988	0.0	3	–[1]	
40449M001	7270	A1	R	Ocotillo, CA	1984 - 1985	1.0	3	–[1]	
40451M102	7102	A1	R	Washington, D.C.	1989 - 1992	3.0	9	*	
40451M125	7108	A1	R	Washington, D.C.	1993 - 2000	7.1	26	*	
40452M001	7291	A1	R	Bloomington, IN	1987 - 1987	0.0	1	–[1]	

continued

VLBI Stations continued

Domes No.	CDP No.	Sol. No.	T[1]	Site Name	Data Time Span	$\triangle$t [yrs]	# avail. sessions	used[2]	RF[3]
40453M001	7228	A1	R	Carrolton, GA	1987 - 1987	0.0	1	$-^1$	
40454M001	7292	A1	R	Leonard, OK	1987 - 1987	0.0	1	$-^1$	
40455M001	7038	A1	R	Miles City, MT	1988 - 1988	0.0	1	$-^1$	
40456 S 001	7234	A1	R	Pie Town, NM VLBA	1988 - 2000	11.7	69	*	*
40457M001	7229	A1	R	Seattle, WA	1986 - 1990	4.0	3	*	
40463 S 001	7611	A1	R	Los Alamos, NM VLBA	1991 - 2000	9.0	84	*	*
40465 S 001	7612	A1	R	North Liberty IA VLBA	1992 - 2000	7.7	42	*	
40466 S 001	7610	A1	R	Kitt Peak, AZ VLBA	1992 - 2000	7.7	19	*	
40471 S 001	7618	A1	R	Hancock, NH VLBA	1992 - 2000	7.7	27	*	
40473 S 001	7614	A1	R	Brewster, WA VLBA	1993 - 2000	7.1	38	*	
40477 S 001	7617	A1	R	Mauna Kea, HI VLBA	1993 - 2000	6.8	37	*	*
40489 S 001	7218	A1	R	Hat Creek, CA	1983 - 1990	7.4	181	*	
40490 S 001	7217	A1	R	Maryland Point, MD	1982 - 1989	7.2	78	*	
40491M003	7261	A1	R	Flagstaff, AZ	1984 - 1990	6.6	8	*	
40492M002	7290	A1	R	Vernal, UT	1986 - 1990	4.6	8	*	
40493M001	7894	A1	R	Yuma, AZ	1983 - 1988	5.0	21	*	
40496M002	7258	A1	R	Platteville, CO	1983 - 1990	7.4	23	*	
40497M003	7274	A1	R	Monument Peak, CA	1982 - 1990	8.1	38	*	
40498 S 001	7619	A1	R	VLA, Magdalena, NM	1983 - 1983	0.0	1	$-^1$	
40499 S 001	7219	A1	R	Richmond, FL	1984 - 1992	8.6	784	*	*
40499 S 019	7201	A1	R	Miami, FL	1995 - 1996	1.0	20	*	
41602 S 001	7297	A1	R	Fortaleza, Brazil	1993 - 2000	7.5	516	*	*
41705 S 006	1404	A1	R	Santiago, Chile	1991 - 1996	5.0	125	*	*
41709 S 001	7239	A1	R	SEST, Chile	1990 - 1990	0.1	3	$-^1$	
42501M002	7294	A1	R	Bermuda	1987 - 1987	0.0	4	$-^1$	
43201 S 001	7615	A1	R	St. Croix, VI VLBA	1993 - 2000	6.9	40	*	*
50103 S 001	1543	A1	R	Tidbinbilla Australia	1991 - 1991	0.0	31	$-^1$	
50103 S 010	1545	A1	R	Tidbinbilla Australia	1988 - 1999	11.6	133	*	*
50108 S 001	7202	A1	R	Parkes, Australia	1992 - 1995	3.1	6	*	
50116 S 002	7242	A1	R	Hobart, Tasmania	1989 - 2000	10.8	294	*	*
50505 S 003	4968	A1	R	Kwajalein Marshall Is	1984 - 1988	4.1	20	*	
66006 S 002	7342	A1	R	Syowa, Antarctic	1999 - 2000	0.3	3	$-^1$	
66008 S 001	7245	A1	R	O'Higgins, Antarctica	1993 - 2000	7.1	40	*	

Tab. C.2: *Observation periods for SLR stations obtained from the SLR data analysis at DGFI.*

[1] "T" denotes the space technique, i.e. L=SLR.

[2] The stations used for the intra-technique combination are identified by a "∗". About 40 "poorly" observed stations with a short data time span (< 1 yr) and/or few weeks of observations were excluded ($-^1$).

[3] The column "RF" denotes the selected SLR reference frame stations used to realise the SLR datum.

SLR Stations

Domes No.	CDP No.	Sol. No.	T[1]	Site Name	Data Time Span	△t [yrs]	# obs. Weeks	used[2]	RF[3]
10002 S 001	7835	A1	L	Grasse, France	1984.0 – 2002.7	18.7	788	∗	∗
10002 S 002	7845	A1	L	Grasse (LLR), France	1998.0 – 2002.7	4.7	186	∗	
10302M002	7602	A1	L	Tromso, Norway	1990.6 – 1990.7	0.1	7	$-^1$	
10503 S 001	7805	A1	L	Metsahovi, Finland	1982.9 – 1997.1	14.2	43	∗	
10503 S 014	7806	A1	L	Metsahovi, Finland	1998.2 – 2002.5	4.3	87	∗	
11001 S 002	7839	A1	L	Graz, Austria	1983.7 – 2002.7	18.9	790	∗	∗
11101M001	7505	A1	L	Sofia, Bulgaria	1995.8 – 1995.9	0.1	4	$-^1$	
12205 S 001	7811	A1	L	Borowiec, Poland	1988.5 – 2002.6	14.2	388	∗	∗
12302M001	7560	A1	L	Riga, Latvia	1991.7 – 1991.8	0.1	4	$-^1$	
12302 S 002	1884	A1	L	Riga, Latvia	1987.7 – 2002.7	14.9	418	∗	∗
12337M001	7561	A1	L	Simeiz, Ukraine	1991.8 – 1991.9	0.1	6	$-^1$	
12337 S 003	1873	A1	L	Simeiz, Ukraine	1989.2 – 2002.6	13.4	156	∗	
12337 S 006	1893	A1	L	Katsively, Ukraine	1988.8 – 2002.6	13.9	152	∗	
12340 S 001	1863	A1	L	Maidanak, Uzbekistan	1992.8 – 1993.9	1.1	16	$-^1$	
12340 S 002	1864	A1	L	Maidanak, Uzbekistan	1993.8 – 2002.6	8.7	248	∗	
12341 S 001	1868	A1	L	Komsomolsk, Russia	1992.8 – 2002.6	9.8	153	∗	
12343 S 001	1869	A1	L	Balkhash, Russia	1993.4 – 1993.8	0.5	12	$-^1$	
12344 S 001	1867	A1	L	Evpatoria, Ukraine	1992.8 – 1994.3	1.5	8	$-^1$	
12602M002	7515	A1	L	Dionysos, Greece	1986.6 – 1992.5	5.9	25	∗	
12612M001	7510	A1	L	Askites, Greece	1986.4 – 1992.6	6.2	40	∗	
12613M001	7517	A1	L	Roumellli, Greece	1986.4 – 1992.6	6.2	40	∗	
12614M001	7520	A1	L	Karitsa, Greece	1986.3 – 1995.7	9.5	18	∗	
12615M001	7512	A1	L	Katavia, Greece	1986.7 – 1992.4	5.6	20	∗	
12616M001	7525	A1	L	Xrisokalaria, Greece	1986.7 – 1994.8	8.1	38	∗	
12706M001	7544	A1	L	Lampedusa, Italy	1987.7 – 1992.8	5.1	24	∗	
12711M002	7546	A1	L	Medicina, Italy	1988.3 – 1988.4	0.1	6	$-^1$	
12717M001	7543	A1	L	Noto, Italy	1990.9 – 1993.8	2.9	17	∗	
12718M002	7550	A1	L	Trieste, Italy	1986.3 – 1989.6	3.3	13	∗	
12725M002	7545	A1	L	Cagliari, Italy	1985.9 – 1994.2	8.4	33	∗	
12725 S 013	7548	A1	L	Cagliari, Italy	1994.7 – 2001.9	7.2	100	∗	
12734M004	7541	A1	L	Matera, Italy	1986.0 – 1994.5	8.4	17	∗	
12734M005	7540	A1	L	Matera, Italy	1986.1 – 1986.2	0.2	7	$-^1$	
12734 S 001	7939	A1	L	Matera, Italy	1983.7 – 2001.0	17.3	725	∗	∗
12749M001	7542	A1	L	Mte. Venda, Italy	1991.6 – 1991.7	0.1	7	$-^1$	
13212 S 001	7840	A1	L	Herstmonceux, UK	1983.8 – 2002.7	18.9	957	∗	∗
13402 S 004	7824	A1	L	San Fernando, Spain	1995.4 – 1999.0	3.6	60	∗	
13402 S 007	7824	B1	L	San Fernando, Spain	1999.2 – 2002.7	3.5	147	∗	

continued

SLR Stations continued

Domes No.	CDP No.	Sol. No.	T[1]	Site Name	Data Time Span	△t [yrs]	# obs. Weeks	used[2]	RF[3]
13504M002	8833	A1	L	Kootwijk, Netherlands	1984.3 – 1995.7	11.3	39	*	
13504S001	7833	A1	L	Kootwijk, Netherlands	1981.1 – 1984.8	3.7	59	*	
14001S001	7810	A1	L	Zimmerwald, Switzerl.	1984.4 – 1995.3	10.9	354	*	*
14001S007	7810	B1	L	Zimmerwald, Switzerl.	1995.7 – 2002.7	7.0	214	*	*
14005M002	7590	A1	L	Mt. Genero, Switzerl.	1985.7 – 1985.8	0.1	4	–[1]	
14106S001	1181	A1	L	Potsdam, Germany	1983.7 – 1992.2	8.5	238	*	
14106S009	7836	A1	L	Potsdam, Germany	1993.0 – 2002.7	9.6	414	*	*
14201M004	7596	A1	L	Wettzell, Germany	1985.2 – 1985.7	0.5	8	–[1]	
14201M005	7597	A1	L	Wettzell, Germany	1995.5 – 1997.0	1.5	8	*	
14201M200	7594	A1	L	Wettzell, Germany	1998.3 – 1998.7	0.4	13	–[1]	
14201S002	7834	A1	L	Wettzell, Germany	1981.2 – 1991.1	10.0	322	*	
14201S018	8834	A1	L	Wettzell, Germany	1991.1 – 2002.7	11.6	499	*	*
20101S001	7832	A1	L	Riyad, Saudi Arabia	1996.1 – 2002.7	6.5	124	*	
20702M001	7530	A1	L	Bar Giyyora, Israel	1986.5 – 1994.7	8.2	64	*	
20801M001	7575	A1	L	Diyarbakir, Turkey	1987.3 – 1989.8	2.4	7	*	
20802M001	7585	A1	L	Yozgat, Turkey	1987.4 – 1992.7	5.2	13	*	
20803M001	7580	A1	L	Melengiclick, Turkey	1987.3 – 1993.0	5.7	16	*	
20804M001	7587	A1	L	Yigilca, Turkey	1987.4 – 1992.9	5.4	23	*	
20805M001	7589	A1	L	Ankara, Turkey	1993.2 – 1993.5	0.3	7	–[1]	
21601M002	7343	A1	L	Beijing, China	2000.7 – 2000.9	0.1	8	–[1]	
21601S004	7249	A1	L	Beijing, China	1995.2 – 2002.7	7.5	169	*	
21602S003	7236	A1	L	Wuhan, China	1993.2 – 1999.5	6.3	71	*	
21602S004	7231	A1	L	Wuhan, China	2000.5 – 2001.6	1.1	19	–[1]	
21605S001	7837	A1	L	Shanghai, China	1983.9 – 2002.7	18.8	425	*	*
21609S002	7820	A1	L	Kunming, China	1999.1 – 2002.4	3.3	92	*	
21611S001	7237	A1	L	Changchun, China	1991.7 – 2002.7	11.0	286	*	*
21701M002	7335	A1	L	Kashima, Japan	1998.9 – 2001.1	2.2	53	*	
21704M001	7328	A1	L	Koganei, Japan	1998.9 – 2000.7	1.7	61	*	
21704S002	7308	A1	L	Tokyo, Japan	1995.9 – 1997.9	2.0	28	*	
21726S001	7838	A1	L	Simosato, Japan	1983.0 – 2002.7	19.7	606	*	*
21733S001	7300	A1	L	Minami, Japan	1989.1 – 1989.2	0.2	5	–[1]	
21739M001	7337	A1	L	Muira, Japan	1998.9 – 2000.4	1.5	40	*	
21740M001	7339	A1	L	Tateyama, Japan	1998.7 – 2001.8	3.1	85	*	
30101S001	7831	A1	L	Helwan, Egypt	1983.8 – 2000.9	17.1	165	*	*
30302M003	7501	A1	L	Hartebeesth, S Afr.	1993.5 – 2002.7	9.1	102	*	
30314M001	7502	A1	L	Sutherland, S. Afr.	1993.7 – 1993.8	0.2	9	–[1]	
40104M003	7410	A1	L	Algonquin, Canada	1993.5 – 1993.7	0.2	12	–[1]	
40132M001	7411	A1	L	La Grande, Canada	1994.6 – 1994.7	0.2	7	–[1]	
40405M002	7115	A1	L	Goldstone, USA	1981.0 – 1981.3	0.2	8	–[1]	
40405M006	7265	A1	L	Goldstone, USA	1984.1 – 1984.2	0.1	7	–[1]	
40405M013	7288	A1	L	Goldstone, USA	1988.2 – 1991.2	3.0	47	*	
40429S001	7884	A1	L	Albuquerque, USA	1995.4 – 1997.2	1.8	18	*	
40433M001	7051	A1	L	Quincy, USA	1981.2 – 1981.4	0.2	11	–[1]	
40433M002	7109	A1	L	Quincy, USA	1981.7 – 1997.4	15.7	645	*	*
40433M005	7886	A1	L	Quincy, USA	1983.6 – 1984.8	1.2	17	*	
40434M002	7888	A1	L	Mt. Hopkins, USA	1982.1 – 1982.3	0.2	11	–[1]	
40434S001	7921	A1	L	Mt. Hopkins, USA	1982.0 – 1982.2	0.2	7	–[1]	
40436M002	7062	A1	L	San Diego, USA	1981.8 – 1984.0	2.2	23	*	

continued

SLR Stations continued

Domes No.	CDP No.	Sol. No.	T[1]	Site Name	Data Time Span	△t [yrs]	# obs. Weeks	used[2]	RF[3]
40436M003	7035	A1	L	San Diego, USA	1988.6 – 1988.7	0.1	7	$-^1$	
40438M001	7082	A1	L	Bear Lake, USA	1981.3 – 1984.0	2.8	11	*	
40438M002	7046	A1	L	Bear Lake, USA	1990.6 – 1991.8	1.2	12	*	
40439M001	7114	A1	L	Owens Valley, USA	1981.6 – 1983.1	1.4	16	*	
40439M004	7853	A1	L	Owens Valley, USA	1988.8 – 1990.6	1.8	9	*	
40440M001	7091	A1	L	Westford, USA	1988.7 – 1991.0	2.3	16	*	
40442M001	7086	A1	L	Fort Davis, USA	1982.6 – 1988.1	5.5	200	*	
40442M005	7885	A1	L	Fort Davis, USA	1982.6 – 1982.7	0.2	8	$-^1$	
40442M006	7080	A1	L	Fort Davis, USA	1988.2 – 2002.7	14.5	698	*	*
40442M008	7850	A1	L	Fort Davis, USA	1993.2 – 1993.4	0.2	11	$-^1$	
40445M001	7210	A1	L	Maui, USA	1981.7 – 2002.7	20.9	895	*	*
40445M002	7120	A1	L	Maui, USA	1981.0 – 1982.0	1.0	46	$-^1$	
40451M102	7102	A1	L	Washington, USA	1981.1 – 1983.5	2.4	41	*	
40451M103	7103	A1	L	Washington, USA	1982.6 – 1982.8	0.2	8	$-^1$	
40451M105	7105	A1	L	Washington, USA	1981.2 – 2002.7	21.5	938	*	*
40451M112	7063	A1	L	Washington, USA	1981.0 – 1981.7	0.6	19	$-^1$	
40451M114	7125	A1	L	Washington, USA	1985.4 – 1985.5	0.1	8	$-^1$	
40451M117	7920	A1	L	Washington, USA	1988.9 – 1990.8	1.9	15	*	
40451M120	7918	A1	L	Washington, USA	1990.3 – 1997.6	7.3	76	*	
40491M002	7891	A1	L	Flagstaff, USA	1981.5 – 1981.6	0.1	5	$-^1$	
40492M001	7892	A1	L	Vernal, USA	1981.3 – 1982.5	1.2	11	$-^1$	
40493M001	7894	A1	L	Yuma, USA	1983.2 – 1983.5	0.3	10	$-^1$	
40496M001	7112	A1	L	Platteville, USA	1981.1 – 1992.0	10.9	150	*	
40497M001	7110	A1	L	Monument Peak, USA	1981.5 – 2002.7	21.1	990	*	*
40497M002	7220	A1	L	Monument Peak, USA	1983.7 – 1983.8	0.2	10	$-^1$	
40499M002	7295	A1	L	Richmond, USA	1988.3 – 1995.3	7.1	41	*	
40504M001	7122	A1	L	Mazatlan, Mexico	1983.4 – 1993.1	9.7	344	*	
40505M001	7882	A1	L	Cabo San Lucas, Mex.	1984.1 – 1994.4	10.3	30	*	
40506M001	7883	A1	L	Ensenada, Mexico	1989.4 – 1994.1	4.8	38	*	
40701 S 001	1953	A1	L	Santiago, Cuba	1988.2 – 1996.5	8.3	90	*	
41604 S 001	7929	A1	L	Natal, Brazil	1981.0 – 1981.7	0.7	15	$-^1$	
41703M001	7061	A1	L	Easter Island, Chile	1983.2 – 1984.7	1.5	23	$-^1$	
41703M002	7097	A1	L	Easter Island, Chile	1987.9 – 1995.3	7.4	121	*	*
41705M001	7400	A1	L	Santiago, Chile	1984.2 – 1984.4	0.2	9	$-^1$	
41705M004	7404	A1	L	Santiago, Chile	1995.6 – 1996.5	0.9	13	$-^1$	
41706M001	7401	A1	L	Cerro Tololo, Chile	1984.4 – 1991.2	6.8	32	*	
42202M003	7403	A1	L	Arequipa, Peru	1990.5 – 2002.7	12.1	414	*	*
42202 S 001	7907	A1	L	Arequipa, Peru	1981.0 – 1992.6	11.6	466	*	
50103 S 003	7943	A1	L	Canberra, Australia	1981.0 – 1982.1	1.1	39	$-^1$	
50103 S 007	7843	A1	L	Orroral, Australia	1986.6 – 1998.9	12.3	359	*	
50107M001	7090	A1	L	Yarragadee, Australia	1981.0 – 2002.7	21.7	1044	*	*
50107 S 009	7847	A1	L	Yarragadee, Australia	1996.2 – 1996.3	0.1	7	$-^1$	
50119 S 001	7849	A1	L	Mt Stromlo, Australia	1998.6 – 2002.6	4.0	202	*	*
92201M007	7124	A1	L	Papeete, Societe Isl.	1998.0 – 2002.7	4.7	111	*	*
92202M002	7121	A1	L	Huahine, Societe Isl.	1983.7 – 1986.3	2.6	87	*	
92202M004	7123	A1	L	Huahine, Societe Isl.	1987.6 – 1993.9	6.3	89	*	

Tab. C.3: *Observation periods for GPS stations, which are included in the cumulative combined IGS solution (IGS03P01.snx) provided by National Resources Canada (NRCan, see Ferland, 2002).*

[1] "T" denotes the space technique, i.e. P=GPS.

[2] The GPS stations used for the TRF computation are identified by a "$*$". Stations with a data time span less than one year or too few observations ($-^1$), and two additional stations with large Helmert transformation residuals w.r.t. ITRF2000 station positions ($-^2$) were excluded.

[3] The column "RF" denotes the GPS reference frame stations as defined by the IGS.

GPS Stations

Domes No.	4-Char ID	Sol. No.	T[1]	Site Name	Data Time Span	$\triangle$t [yrs]	used[2]	RF[3]
10002M006	GRAS	A1	P	Caussols, France	1996 - 2003	7.0	*	
10003M004	TOUL	A1	P	Toulouse, France	1997 - 2001	3.6	*	
10003M009	TLSE	A1	P	Toulouse, France	2001 - 2003	1.8	*	
10090M001	SJDV	A1	P	Saint Jean des Vignes, France	1998 - 2002	2.8	*	
10202M001	REYK	A1	P	Reykjavik, Iceland	1996 - 2003	7.0	*	
10204M002	HOFN	A1	P	Hoefn, Iceland	1996 - 2002	5.9	*	
10204M002	HOFN	A2	P	Hoefn, Iceland	2002 - 2003	1.0	$-^1$	
10302M003	TROM	A1	P	Tromsoe, Norway	1996 - 2003	7.0	*	*
10302M006	TRO1	A1	P	Tromsoe, Norway	1996 - 2003	7.0	*	
10317M001	NYAL	A1	P	Ny-Alesund, Norway	1996 - 2003	7.0	*	*
10317M003	NYA1	A1	P	Ny-Alesund, Norway	1996 - 2003	7.0	*	
10402M004	ONSA	A1	P	Onsala, Sweden	1996 - 2003	7.0	*	*
10403M002	KIRU	A1	P	Kiruna, Sweden	1996 - 2003	7.0	*	
10503 S 011	METS	A1	P	Kirkkonummi, Finland	1996 - 2003	7.0	*	
11001M002	GRAZ	A1	P	Graz, Austria	1996 - 2003	7.0	*	*
11006 S 003	HFLK	A1	P	Innsbruck, Austria	1998 - 2002	4.7	*	
11101M002	SOFI	A1	P	Sofia, Bulgaria	1997 - 2002	5.4	*	
11206M006	PENC	A1	P	Penc, Hungary	1998 - 2003	4.7	*	
11401M001	BUCU	A1	P	Bucuresti, Romania	1999 - 2002	4.0	*	
11502M002	GOPE	A1	P	Ondrejov, Czech Republic	1996 - 2003	7.0	*	
12204M001	JOZE	A1	P	Jozefoslaw, Poland	1996 - 2003	7.0	*	
12205M002	BOR1	A1	P	Borowiec, Poland	1996 - 2003	7.0	*	
12207M002	BOGO	A1	P	Borowa Gora, Poland	1998 - 2000	2.1	*	
12209M001	LAMA	A1	P	Olsztyn, Poland	1996 - 2003	7.0	*	
12309M002	MDVO	A1	P	Mendeleevo, Russia	1996 - 2003	7.0	*	
12312M001	NSSP	A1	P	Yerevan, Armenia	1998 - 2002	3.8	*	
12313M001	IRKT	A1	P	Irutzk, Russia	1996 - 2003	7.0	*	*
12329M003	YSSK	A1	P	Yuzhno-Sakhalinsk, Russia	1996 - 2003	7.0	*	
12330M001	ZWEN	A1	P	Zweningorod, Russia	1996 - 2003	7.0	*	*
12334M001	KIT3	A1	P	Kitab, Uzbekistan	1996 - 2003	7.0	*	*
12348M001	POL2	A1	P	Bishkek, Kyrghyzstan	1996 - 2003	7.0	*	
12349M002	KSTU	A1	P	Krasnoyarsk, Russia	1996 - 2003	7.0	*	
12351M001	ZECK	A1	P	Zelenchukskaya, Russia	1996 - 2003	7.0	*	
12352M001	SELE	A1	P	Almany, Kazakstan	1996 - 2003	7.0	*	
12353M001	YAKA	A1	P	Yakutzk, Russia	1998 - 1999	1.3	*	
12353M001	YAKA	A2	P	Yakutzk, Russia	1999 - 2001	2.0	$-^1$	

continued

GPS Stations continued

Domes No.	4-Char ID	Sol. No.	T[1]	Site Name	Data Time Span	△t [yrs]	used[2]	RF[3]
12353M002	YAKT	A1	P	Yakutzk, Russia	1996 - 2003	7.0	*	
12354M001	MAG0	A1	P	Magadan, Russia	1996 - 2003	7.0	*	
12355M001	PETR	A1	P	Petropavlovsk, Russia	1996 - 1999	3.5	*	
12355M002	PETP	A1	P	Petropavlovsk, Russia	1996 - 2003	7.0	*	
12356M001	GLSV	A1	P	Kiev, Ukraine	1996 - 2003	7.0	*	
12360M001	TIXI	A1	P	Tixi, Russia	1996 - 2003	7.0	*	
12362M001	ARTU	A1	P	Arti, Russia	1996 - 2003	7.0	*	
12363M001	BILI	A1	P	Bilibino, Russia	1996 - 2002	6.2	*	
12363M001	BILI	A2	P	Bilibino, Russia	2002 - 2003	0.8	$-^{1}$	
12364M001	NRIL	A1	P	Norilsk, Russia	1996 - 2003	7.0	*	
12711M003	MEDI	A1	P	Medicina, Italy	1996 - 2003	7.0	*	
12717M003	NOTO	A1	P	Noto, Italy	1996 - 2000	4.7	*	
12717M004	NOT1	A1	P	Noto, Italy	2000 - 2003	2.3	*	
12725M003	CAGL	A1	P	Cagliary, Italy	1996 - 2003	7.0	*	
12734M008	MATE	A1	P	Matera, Italy	1996 - 2003	7.0	*	*
12750M002	UPAD	A1	P	Padova, Italy	1996 - 2001	5.0	*	
13101M004	BRUS	A1	P	Brussels, Belgium	1996 - 2003	7.0	*	
13212M007	HERS	A1	P	Hailsham, UK	1996 - 2003	7.0	*	
13234M003	NPLD	A1	P	Teddington, UK	2001 - 2002	1.7	*	
13299S001	MORP	A1	P	Morpeth, UK	2002 - 2003	0.1	$-^{1}$	
13402M004	SFER	A1	P	San Fernando, Spain	1996 - 2003	7.0	*	
13406M001	VILL	A1	P	Villafrance, Spain	1996 - 2003	7.0	*	*
13407S012	MADR	A1	P	Robeledo, Spain	1996 - 2003	7.0	*	
13410M001	EBRE	A1	P	Roquetes, Spain	1998 - 2002	5.5	*	
13504M003	KOSG	A1	P	Kootwijk, Netherlands	1996 - 2003	7.0	*	
13506M005	WSRT	A1	P	Westerbork, Netherlands	1996 - 2003	7.0	*	*
13909S001	CASC	A1	P	Cascais, Portugal	1998 - 1999	0.9	$-^{1}$	
14001M004	ZIMM	A1	P	Zimmerwald, Switzerland	1996 - 2003	7.0	*	
14106M003	POTS	A1	P	Potsdam, Germany	1996 - 2003	7.0	*	*
14201M009	WETT	A1	P	Wettzell, Germany	1996 - 1997	1.1	*	
14201M010	WTZR	A1	P	Wettzell, Germany	1996 - 2003	7.0	*	*
14208M001	OBER	A1	P	Oberpfaffenhofen, Germany	1996 - 2001	5.4	*	
14302M001	NICO	A1	P	Nicosia, Cyprus	1997 - 2003	5.3	*	
20703S001	RAMO	A1	P	Mitzpe Ramon, Israel	1996 - 2003	7.0	*	
20705M001	BSHM	A1	P	Haifa, Israel	1999 - 2002	4.2	*	
20706M001	ELAT	A1	P	Eilat, Israel	1996 - 2002	6.3	*	
20710S001	DRAG	A1	P	Metzoki Dragot, Israel	1996 - 2002	6.5	*	
20711S001	ELRO	A1	P	Kibutz El-Rom, Israel	1996 - 2002	6.5	*	
20805M002	ANKR	A1	P	Ankara, Turkey	1996 - 2003	7.0	*	
20806M001	TUBI	A1	P	Gebze, Turkey	1999 - 2002	1.4	*	
20808M001	TRAB	A1	P	Trabzon, Turkey	2000 - 2000	2.8	*	
21602M001	WUHN	A1	P	Wuhan City, P.R.China	1996 - 2002	6.4	*	
21602M001	WUHN	A2	P	Wuhan City, P.R.China	2002 - 2003	0.6	$-^{1}$	
21605M002	SHAO	A1	P	Sheshan, China	1996 - 2002	6.7	*	*
21609M001	KUNM	A1	P	Kunming, China	1996 - 2003	7.0	*	
21612M001	URUM	A1	P	Urumqi, China	1996 - 2003	7.0	*	
21613M001	LHAS	A1	P	Lhasa, China	1996 - 2003	6.3	*	*
21614M001	XIAN	A1	P	Lintong, P.R.China	1996 - 2001	4.6	*	

continued

GPS Stations continued

Domes No.	4-Char ID	Sol. No.	T[1]	Site Name	Data Time Span	$\triangle$t [yrs]	used[2]	RF[3]
21729S007	USUD	A1	P	Usuda, Japan	1996 - 2003	7.0	*	
21730S005	TSKB	A1	P	Tsukuba, Japan	1996 - 2003	7.0	*	*
22003M001	PIMO	A1	P	Quezon City, Phillipines	1996 - 2003	7.0	*	
22201M001	AMMN	A1	P	Amman, Jordan	2000 - 2001	1.8	*	
22306M002	IISC	A1	P	Bangalore, India	1996 - 2003	7.0	*	
22601M001	NTUS	A1	P	Singapore, Singapore	1996 - 2003	7.0	*	
23101M002	BAKO	A1	P	Cibinong, Indonesia	1996 - 2003	7.0	*	
23601M001	TAIW	A1	P	Taipei, Taiwan	1996 - 1997	2.0	*	
23902M001	TAEJ	A1	P	Taejon, South Korea	1996 - 1999	3.1	*	
23902M002	DAEJ	A1	P	Taejon, Korea	1996 - 2003	7.0	*	
23903M001	SUWN	A1	P	Suwon-Shi, Korea	1996 - 2003	7.0	*	
24901M002	BAHR	A1	P	Manama, Bahrain	1996 - 2003	7.0	*	*
30302M004	HRAO	A1	P	Krugersdorp, South Afrika	1996 - 2003	7.0	*	*
30302M007	HARK	A1	P	Pretoria, South Africa	1996 - 2000	4.5	*	
30302M009	HARB	A1	P	Pretoria, South Africa	1996 - 2003	7.0	*	
30314M002	SUTH	A1	P	Sutherland, South Africa	1996 - 2003	7.0	*	
30315M001	RBAY	A1	P	Richardsbay, South Africa	2000 - 2003	2.3	*	
30602M001	ASC1	A1	P	Ascension Island, UK	1996 - 2003	7.0	*	*
30608M001	GOUG	A1	P	Gough Island, UK	1998 - 2003	4.3	*	
30802M001	DGAR	A1	P	Diego Garcia Island, UK	1996 - 2002	6.9	*	*
31303M002	MAS1	A1	P	Masplaomas, Spain	1996 - 2003	7.0	*	
32809M002	NKLG	A1	P	Libreville, Gabon	1996 - 2003	7.0	*	
32810M001	MSKU	A1	P	Franceville, Gabon	1996 - 2002	6.7	*	
33201M001	MALI	A1	P	Malindi, Kenya	1996 - 2003	7.0	*	*
35001M001	IAVH	A1	P	Rabat, Marocco	1998 - 1998	0.2		
35001M002	RABT	A1	P	Rabat, Marocco	1996 - 2003	7.0	*	
39801M001	SEY1	A1	P	La Misere, Seychelles	1996 - 2002	6.5	*	
40101M001	STJO	A1	P	St. John's, Canada	1996 - 2003	7.0	*	
40104M002	ALGO	A1	P	Algonquin Park, Canada	1996 - 2003	7.0	*	*
40105M002	DRAO	A1	P	Penticton, Canada	1996 - 2003	7.0	*	*
40114M001	NRC1	A1	P	Ottawa, Canada	1996 - 2003	7.0	*	
40124M001	PRDS	A1	P	Calgary, Canada	1996 - 2003	7.0	*	
40127M003	YELL	A1	P	Yellowknife, Canada	1996 - 2003	7.0	*	*
40128M002	CHUR	A1	P	Churchill, Canada	1996 - 2003	7.0	*	
40129M003	ALBH	A1	P	Victoria, Canada	1996 - 2003	7.0	*	
40130M001	HOLB	A1	P	Holberg, Canada	1998 - 2003	4.9	*	
40133M001	SCHE	A1	P	Schefferville, Canada	1996 - 1996	0.5	$-^1$	
40133M002	SCH2	A1	P	Schefferville, Canada	1996 - 2003	7.0	*	
40134M001	WILL	A1	P	Williams Lake, Canada	1996 - 2003	7.0	*	
40135M001	FLIN	A1	P	CFS Flin Flon, Canada	1996 - 2003	7.0	*	
40136M001	WHIT	A1	P	Whitehorse, Canada	1996 - 2003	7.0	*	
40137M001	DUBO	A1	P	Lac du Bonnet, Canada	1996 - 2003	7.0	*	
40138M001	NANO	A1	P	Nanoose Bay, Canada	1998 - 2002	4.8	*	
40140M001	UCLU	A1	P	Ucluelet, Canada	1998 - 2003	3.7	*	
40141M001	WSLR	A1	P	Whistler, Canada	1998 - 2000	3.4	*	
40400M007	JPLM	A1	P	Pasadena, USA	1996 - 2003	7.0	*	
40400S201	CIT1	A1	P	Pasadena, USA	1998 - 1999	0.6	$-^1$	
40405S031	GOLD	A1	P	Goldstone, USA	1996 - 2003	7.0	*	

continued

GPS Stations continued

Domes No.	4-Char ID	Sol. No.	T[1]	Site Name	Data Time Span	△t [yrs]	used[2]	RF[3]
40408M001	FAIR	A1	P	Fairbanks, USA	1996 - 2002	6.8	*	*
40408M001	FAIR	A2	P	Fairbanks, USA	2002 - 2003	0.2	−[1]	
40419 S 003	KODK	A1	P	Kodiak, USA	2000 - 2003	2.7	*	
40420M101	HARV	A1	P	Vandenberg, USA	1996 - 2002	6.5	*	
40424M004	KOKB	A1	P	Kokee Park, USA	1996 - 2002	6.8	*	*
40424M004	KOKB	A2	P	Kokee Park, USA	2002 - 2003	0.2	−[1]	
40433M004	QUIN	A1	P	Quincy, USA	1996 - 2003	7.0	*	
40437M002	CASA	A1	P	Mammoth Lakes, USA	1996 - 2002	6.3	*	
40440 S 020	WES2	A1	P	Westford, USA	1996 - 2003	7.0	*	*
40442M012	MDO1	A1	P	Fort Davis, USA	1996 - 2003	7.0	*	*
40451M123	GODE	A1	P	Greenbelt, USA	1996 - 2003	7.0	*	*
40451 S 003	USNO	A1	P	Washington, USA	1996 - 2003	7.0	*	
40456M001	PIE1	A1	P	Pie Town, USA	1996 - 2003	7.0	*	*
40460M004	SIO3	A1	P	La Jolla, USA	1999 - 2000	1.0	*	
40460M004	SIO3	A2	P	La Jolla, USA	2000 - 2003	2.7	−[1]	
40465M001	NLIB	A1	P	North Liberty, USA	1996 - 2003	7.0	*	*
40472 S 003	AMCT	A1	P	Falcone Air Force Base, USA	1996 - 1999	3.5	−[2]	
40472 S 004	AMC2	A1	P	Colorado Springs, USA	1996 - 2003	7.0	*	
40477M001	MKEA	A1	P	Mauna, Kea, USA	1996 - 2003	7.0	*	
40483 S 001	AOA1	A1	P	Westlake, USA	1999 - 2002	3.0	−[2]	
40488M001	CAT1	A1	P	Catalina, USA	1999 - 2000	2.0	*	
40497M004	MONP	A1	P	Laguna, Mountains, USA	1996 - 2003	6.4	*	
40499 S 018	RCM5	A1	P	Perrine, USA	1996 - 1996	1.0	−[1]	
40499 S 020	RCM6	A1	P	PERRINE, USA	1996 - 1998	1.7	*	
40507M001	INEG	A1	P	Aguascalientes, Mexico	1996 - 2002	6.2	*	
40508M001	CICE	A1	P	Ensenada, Mexico	1996 - 1999	3.0	*	
40508M002	CIC1	A1	P	Ensenada, Mexico	1999 - 2003	3.7	*	
40601M001	MOIN	A1	P	Moin, Costa Rica	1996 - 1998	1.3	*	
40901 S 001	GUAT	A1	P	Guatemala City, Guatemala	1996 - 2003	7.0	*	
41102 S 001	SLOR	A1	P	San Lorenzo, Honduras	2001 - 2001	1.5	*	
41202 S 001	ESTI	A1	P	Esteli, Nicaragua	2000 - 2002	2.3	*	
41401 S 001	SSIA	A1	P	San Salvador, El Salvador	1996 - 2002	6.5	*	
41401 S 001	SSIA	A2	P	San Salvador, El Salvador	2002 - 2003	0.5	−[1]	
41507M004	RIOG	A1	P	Rio Grande, Argentina	1996 - 2003	7.0	*	*
41510M001	LPGS	A1	P	La Plata, Argentina	1996 - 2003	7.0	*	*
41511M001	CORD	A1	P	Cordoba, Argentina	1999 - 2002	2.2	*	
41514M001	UNSA	A1	P	Salta, Argentina	1996 - 2003	7.0	*	
41602M001	FORT	A1	P	Fortaleza, Brazil	1996 - 2003	7.0	*	*
41606M001	BRAZ	A1	P	Brasilia, Brazil	1996 - 2003	6.5	*	
41703M003	EISL	A1	P	Easter Island, Chile	1996 - 2003	7.0	*	
41705M003	SANT	A1	P	Santiago, Chile	1996 - 2003	7.0	*	*
41901M001	BOGT	A1	P	Bogota, Colombia	1996 - 2003	7.0	*	
42005M001	GALA	A1	P	Galapagos Island, Ecuador	1996 - 2003	6.8	*	
42006M001	RIOP	A1	P	Riobamba, Equador	1999 - 2001	3.0	*	
42202M005	AREQ	A1	P	Arequipa, Peru	1996 - 2001	5.5	*	
42202M005	AREQ	A2	P	Arequipa, Peru	2001 - 2002	1.1	−[1]	
42202M005	AREQ	A3	P	Arequipa, Peru	2002 - 2003	0.4	−[1]	
42501 S 004	BRMU	A1	P	Bermuda, UK	1996 - 2003	7.0	*	*

continued

GPS Stations continued

Domes No.	4-Char ID	Sol. No.	T[1]	Site Name	Data Time Span	△t [yrs]	used[2]	RF[3]
42601S001	JAMA	A1	P	Kingston, Jamaica	1996 - 2003	7.0	*	
43001M001	THU1	A1	P	Thule, Greenland	1996 - 2003	7.0	*	*
43005M001	KELY	A1	P	Kangerlussuaq, Greenland	1996 - 2003	7.0	*	
43201M001	CRO1	A1	P	Christiansted, USA	1996 - 2003	7.0	*	
43401S001	BARB	A1	P	Bridgetown, Barbados	1998 - 2001	3.0	*	
49907S001	SOL1	A1	P	Solomons Island, USA	1998 - 2003	5.9	*	
49908S001	USNA	A1	P	Annapolis, USA	1998 - 2003	4.8	*	
49909S001	SNI1	A1	P	San Nicolas Island, USA	1999 - 2002	3.6	*	
49913S001	HNPT	A1	P	Cambridge, USA	2000 - 2003	2.7	*	
49914S001	AOML	A1	P	Key Biscayne, Miami, USA	1996 - 2003	7.0	*	
49915M001	SCIP	A1	P	San Clmentine Island, USA	1996 - 2002	6.9	*	
49927S001	BARH	A1	P	Bar Habour, USA	2001 - 2003	1.8	*	
49928S001	EPRT	A1	P	Eastport, USA	1999 - 2003	3.8	*	
49934M001	ATWC	A1	P	Alaska Tsunami Warning, USA	2000 - 2001	1.2	–[1]	
49970S001	HNLC	A1	P	Honolulu, USA	2001 - 2003	1.7	*	
50103M108	TIDB	A1	P	Tidbinbilla, Australia	1996 - 2003	7.0	*	*
50107M004	YAR1	A1	P	Mingenewa, Australia	1996 - 2003	7.0	*	*
50116M004	HOB2	A1	P	Hobart, Australia	1996 - 2003	7.0	*	*
50119M002	STR1	A1	P	Canberra, Australia	1999 - 2003	3.0	*	
50127M001	COCO	A1	P	Cocos Island, Australia	1996 - 2002	6.1	*	
50127M001	COCO	A2	P	Cocos Island, Australia	2002 - 2003	0.9	–[1]	
50133M001	PERT	A1	P	Perth, Australia	1996 - 2003	7.0	*	*
50134M001	DARW	A1	P	Darwin, Australia	1996 - 2003	7.0	*	
50135M001	MAC1	A1	P	MacQuarie Island, Australia	1996 - 2003	7.0	*	*
50136M001	JAB1	A1	P	Jabiru, Australia	1998 - 2003	4.2	*	
50137M001	ALIC	A1	P	Alice Sorings, Australia	1996 - 2003	7.0	*	
50138M001	CEDU	A1	P	Ceduna, Australia	1996 - 2003	7.0	*	*
50139M001	KARR	A1	P	Karratha, Australia	1996 - 2003	7.0	*	
50140M001	TOW2	A1	P	Cape Ferguson, Australia	1996 - 2003	7.0	*	
50207M001	CHAT	A1	P	Waitangi, New Zealand	1996 - 2003	7.0	*	*
50209M001	AUCK	A1	P	Whangaparaoa Pen., New Zealand	1996 - 2003	7.0	*	*
50501M002	GUAM	A1	P	Guam, USA	1996 - 2002	6.7	*	*
50501M002	GUAM	A2	P	Guam, USA	2002 - 2003	0.3	–[1]	
50506M001	KWJ1	A1	P	Kwajalein Atoll, USA	1996 - 2003	7.0	*	*
66001M003	MCM4	A1	P	Ross Island, Antarctica	1996 - 2003	7.0	*	
66004M001	MAW1	A1	P	Mawson, Antarctica	1996 - 2003	7.0	*	
66006S002	SYOG	A1	P	East Ongle Island, Antarctica	1996 - 2003	7.0	*	
66008M001	OHIG	A1	P	O'Higgins, Antarctica	1996 - 2002	6.1	*	*
66009M001	VESL	A1	P	Sanae IV, Antarctica	1998 - 2003	4.3	*	
66010M001	DAV1	A1	P	Davis, Antarctica	1996 - 2003	7.0	*	*
66011M001	CAS1	A1	P	Casey, Antarctica	1996 - 2003	7.0	*	*
91201M002	KERG	A1	P	Port Aux Francais, Kerguelen	1996 - 2003	7.0	*	*
92201M003	PAMA	A1	P	Pamatai, Tahiti	1996 - 1997	1.2	*	
92201M006	TAHI	A1	P	Papeete, Tahiti, Societe Isl.	1996 - 1999	3.6	*	
92201M009	THTI	A1	P	Papeete, Tahiti, Societe Isl.	1996 - 2003	7.0	*	
92701M003	NOUM	A1	P	Noumea, France	1996 - 2003	7.0	*	
97301M210	KOUR	A1	P	Kourou, French Guyana	1996 - 2003	7.0	*	*

Tab. C.4: *Observation periods for DORIS stations; the information is obtained from weekly DORIS solutions provided by IGN.*

[1] "T" denotes the space technique, i.e. D=DORIS.

[2] The stations used for the intra-technique combination are identified by a "$*$". About 10 "poorly" observed stations with a short data time span ($<$ 1 yr) excluded ($-^1$). Furthermore stations were not used for the intra-technique combination; these stations are included in only one DORIS solution ($-^2$).

[3] The column "RF" denotes the selected DORIS reference frame stations used to realise the DORIS datum.

DORIS Stations

Domes No.	4-Char ID	Sol. No.	T[1]	Site Name	Data Time Span	$\triangle$t [yrs]	weeks	used[2]	RF[3]
10003S001	TLSA	A1	D	Toulouse, France	1993.0 - 1997.6	4.6	241	*	*
10003S003	TLHA	A1	D	Toulouse, France	1997.6 - 2003.0	5.4	281	*	*
10202S001	REYA	A1	D	Reykjavik, Iceland	1993.0 - 1998.7	5.6	265	*	*
10202S002	REYB	A1	D	Reykjavik, Iceland	1998.7 - 2003.0	4.2	211	*	*
10317S002	SPIA	A1	D	Ny-Alesund, Norway	1993.0 - 1999.2	6.2	314	*	*
10317S004	SPIB	A1	D	Ny-Alesund, Norway	1999.6 - 2002.9	3.3	151	$-^2$	
10503S013	META	A1	D	Metsahovi, Finland	1993.0 - 2000.8	7.8	402	*	*
10503S015	METB	A1	D	Metsahovi, Finland	2000.9 - 2003.0	2.1	63	$-^2$	
12329S001	SAKA	A1	D	Sakhalinsk, Russia	1993.0 - 1994.7	1.7	90	$-^2$	
12329S001	SAKA	A2	D	Sakhalinsk, Russia	1994.9 - 1999.0	4.1	175	$-^2$	
12329S001	SAKA	A3	D	Sakhalinsk, Russia	2002.1 - 2003.0	0.9	47	$-^1$	
12334S004	KITA	A1	D	Kitab, Uzbekistan	1993.0 - 1996.4	3.4	160	*	*
12334S005	KITB	A1	D	Kitab, Uzbekistan	1996.4 - 2001.3	4.9	180	*	
12334S006	KIUB	A1	D	Kitab, Uzbekistan	2001.4 - 2003.0	1.6	69	$-^2$	
12338S001	BADA	A1	D	Badary, Russia	1993.0 - 2002.5	9.5	423	*	*
12339S001	PASB	A1	D	Kouriles, Russia	1997.8 - 1998.1	0.3	16	$-^1$	
12349S001	KRAB	A1	D	Krasnoyarsk, Russia	1997.7 - 1998.6	0.9	44	$-^1$	
12349S001	KRAB	A2	D	Krasnoyarsk, Russia	1999.4 - 2003.0	3.6	166	$-^2$	
12602S011	DIOA	A1	D	Dionysos, Greece	1993.4 - 1995.2	1.8	85	*	
12602S011	DIOA	A2	D	Dionysos, Greece	1995.3 - 2003.0	7.7	329	$-^2$	
21501S001	EVEB	A1	D	Everest. Nepal	1993.4 - 2002.2	8.8	419	*	
21604S003	PURA	A1	D	Purple Mountain, China	1993.0 - 2003.0	10.0	430	*	
22006S001	MANA	A1	D	Manila, The Philippines	1993.1 - 2003.0	9.9	455	*	*
23101S001	CIBB	A1	D	Cibinong, Indonesia	1993.0 - 2000.7	7.7	347	*	
23101S002	CICB	A1	D	Cibinong, Indonesia	2001.1 - 2003.0	1.9	98	$-^2$	
23501S001	COLA	A1	D	Colombo, Sri Lanka	1993.0 - 1994.9	1.9	61	$-^2$	
23501S001	COLA	A2	D	Colombo, Sri Lanka	1994.9 - 2003.0	8.1	308	$-^2$	
30302S005	HBLA	A1	D	Hartebeesthoek, S. Afr.	1997.4 - 2000.6	3.2	165	*	
30302S006	HBKB	A1	D	Hartebeesthoek, S. Afr.	2000.6 - 2003.0	2.4	125	$-^2$	
30302S202	HBKA	A1	D	Hartebeesthoek, S. Afr.	1993.0 - 1997.4	4.4	230	*	
30313S001	MARA	A1	D	Marion Isl., S. Africa	1993.0 - 1998.5	5.5	266	*	*
30313S002	MARB	A1	D	Marion Isl., S. Africa	1999.5 - 2002.4	2.9	122	$-^2$	
30602S004	ASDB	A1	D	Ascension Isl., UK	1999.3 - 2003.0	3.7	183	$-^2$	
30604S001	TRIA	A1	D	Tristan da Cunha, UK	1993.0 - 2001.4	8.4	434	*	*

continued

DORIS Stations continued

Domes No.	4-Char ID	Sol. No.	T[1]	Site Name	Data Time Span	$\triangle$t [yrs]	weeks	used[2]	RF[3]
30604S002	TRIB	A1	D	Tristan da Cunha, UK	2002.1 - 2003.0	0.9	47	$-^1$	
30606S002	HELA	A1	D	Sainte-Helene, UK	1993.0 - 1997.3	4.3	205	*	
30606S003	HELB	A1	D	Sainte-Helene, UK	1998.3 - 2003.0	4.7	219	*	
31901S001	FLOA	A1	D	Flores, Portugal	1993.0 - 1993.5	0.5	25	$-^1$	
31903S001	SAMB	A1	D	Santa Maria, Portugal	1994.0 - 1997.9	3.9	200	*	*
31906S001	PDLB	A1	D	Ponta del Gada, Port.	1998.9 - 2001.6	2.8	145	$-^2$	
31906S002	PDMB	A1	D	Ponta del Gada, Port.	2001.8 - 2003.0	1.2	65	$-^2$	
32809S002	LIBA	A1	D	Libreville, Gabun	1993.0 - 1999.1	6.1	303	*	*
32809S003	LIBB	A1	D	Libreville, Gabun	1999.2 - 2003.0	3.8	197	$-^2$	
33710S002	ARMA	A1	D	Arlit, Niger	1993.0 - 1999.4	6.3	228	*	*
34101S004	DAKA	A1	D	Dakar, Senegal	1993.1 - 2001.0	7.9	386	*	*
39801S005	MAHB	A1	D	Mahe Isl. Seychelles	2001.5 - 2003.0	1.5	78	$-^2$	
39901S002	DJIA	A1	D	Djibouti, Djibouti	1993.0 - 2000.5	7.5	383	*	
39901S003	DJIB	A1	D	Djibouti, Djibouti	2000.6 - 2003.0	2.5	118	$-^2$	
40101S002	STJB	A1	D	St John's, Canada	1999.8 - 2003.0	3.2	164	$-^2$	
40102S009	OTTA	A1	D	Ottawa, Canada	1994.1 - 1998.0	3.9	199	*	*
40102S011	OTTB	A1	D	Ottawa, Canada	1998.1 - 2000.6	2.5	129	*	*
40127S007	YELA	A1	D	Yellowknife, Canada	1993.0 - 2001.8	8.8	458	*	*
40127S008	YELB	A1	D	Yellowknife, Canada	2001.8 - 2003.0	1.2	61	$-^2$	
40405S005	GOMA	A1	D	Goldstone, USA	1994.6 - 1996.7	2.1	107	*	
40405S035	GOLA	A1	D	Goldstone, USA	1993.0 - 1994.6	1.6	80	*	
40405S037	GOMB	A1	D	Goldstone, USA	1996.8 - 2003.0	6.2	326	*	
40408S004	FAIA	A1	D	Fairbanks, USA	1993.0 - 1999.4	6.4	332	*	*
40408S005	FAIB	A1	D	Fairbanks, USA	2000.1 - 2003.0	3.0	155	$-^2$	
40424S008	KOKA	A1	D	Kauai (Hawaii), USA	1993.0 - 2002.9	9.9	506	*	*
40451S176	GREB	A1	D	Washington, USA	2000.5 - 2003.0	2.5	131	$-^2$	
40475S001	WAIA	A1	D	Waimea (Hawaii), USA	1993.0 - 1993.5	0.5	3	$-^1$	
40476S001	HVOA	A1	D	Hawaiiam Vol. Obs. USA	1993.0 - 1993.5	0.4	12	$-^1$	
40499S016	RIDA	A1	D	Richmond, USA	1993.1 - 2003.0	9.9	459	*	
40503S003	SODA	A1	D	Socorro Isl., Mexico	1996.0 - 1997.8	1.8	96	$-^2$	
40503S004	SODB	A1	D	Socorro Isl., Mexico	1998.4 - 2002.8	4.4	136	$-^2$	
40503S004	SODB	A2	D	Socorro Isl., Mexico	2002.8 - 2003.0	0.2	13	$-^1$	
41507S003	RIOA	A1	D	Rio Grande, Argentina	1993.0 - 1995.0	2.0	107	*	*
41507S004	RIOB	A1	D	Rio Grande, Argentina	1995.1 - 2001.0	6.0	308	*	*
41507S005	RIPB	A1	D	Rio Grande, Argentina	2001.2 - 2003.0	1.8	94	$-^2$	
41609S001	CACB	A1	D	Cachoeira, Brazil	1993.0 - 2003.0	10.0	482	*	
41703S008	EASA	A1	D	Easter Island, Chile	1993.0 - 2001.0	8.0	400	*	*
41703S009	EASB	A1	D	Easter Island, Chile	2001.9 - 2003.0	1.0	43	$-^2$	
41705S007	SANA	A1	D	Santiago, Chile	1993.0 - 1996.9	3.9	195	*	
41705S008	SAOB	A1	D	Santiago, Chile	1997.1 - 2000.9	3.9	159	*	*
41705S009	SANB	A1	D	Santiago, Chile	2001.5 - 2003.0	1.5	78	$-^2$	
41708S001	IQUB	A1	D	Iquique, Chile	1993.9 - 1998.5	4.5	46	*	
41710S001	CARB	A1	D	Cariquima, Chile	1993.3 - 1993.9	0.6	3	$-^1$	
42004S001	GALA	A1	D	San Cristobal, Ecuador	1993.0 - 2003.0	10.0	345	*	
42202S005	AREA	A1	D	Arequipa, Peru	1993.5 - 2001.5	8.0	415	*	
42202S005	AREA	A2	D	Arequipa, Peru	2001.5 - 2001.9	0.4	21	$-^1$	

continued

DORIS Stations continued

Domes No.	4-Char ID	Sol. No.	T[1]	Site Name	Data Time Span	△t [yrs]	weeks	used[2]	RF[3]
42202S006	AREB	A1	D	Arequipa, Peru	2002.0 - 2003.0	1.0	55	−[2]	
50103S201	ORRA	A1	D	Canberra, Australia	1993.0 - 1996.2	3.2	154	*	
50103S202	ORRB	A1	D	Canberra, Australia	1997.0 - 1998.8	1.7	91	*	
50107S006	YARA	A1	D	Yarragadee, Australia	1993.0 - 1999.8	6.7	330	*	*
50107S010	YARB	A1	D	Yarragadee, Australia	1999.8 - 2003.0	3.2	165	−[2]	
50119S002	MSOB	A1	D	Mount Stromlo, Austr.	1998.9 - 2003.0	4.1	214	−[2]	
50207S001	CHAB	A1	D	Chatham Isl., New Zeal.	1999.2 - 2003.0	3.8	153	−[2]	
50501S001	GUAB	A1	D	Guam, USA	1994.0 - 2000.6	6.6	325	*	*
51001S001	MORA	A1	D	Port Moresby, Papua	1993.0 - 2002.2	9.2	276	*	
51001S002	MORB	A1	D	Port Moresby, Papua	2002.3 - 2003.0	0.7	37	−[1]	
66006S001	SYOB	A1	D	Syowa, Antartica	1993.3 - 1998.3	5.0	263	*	*
66006S003	SYPB	A1	D	Syowa, Antartica	1999.3 - 2003.0	3.7	192	−[2]	
66007S001	ROTA	A1	D	Rothera, Antartica	1993.0 - 2003.0	10.0	511	*	*
91201S002	KERA	A1	D	Kerguelen Islands	1993.0 - 1994.9	1.9	98	*	
91201S003	KERB	A1	D	Kerguelen Islands	1994.9 - 2001.2	6.3	320	*	*
91201S004	KESB	A1	D	Kerguelen Islands	2001.3 - 2003.0	1.7	89	−[2]	
91401S001	AMSA	A1	D	Amsterdam Islands	1993.0 - 1996.0	3.0	153	*	
91401S003	AMTB	A1	D	Amsterdam Islands	2001.3 - 2003.0	1.7	88	−[2]	
91501S001	ADEA	A1	D	Ile des Petrels, Adelie	1993.0 - 2002.2	9.1	473	*	*
91501S002	ADEB	A1	D	Ile des Petrels, Adelie	2002.2 - 2003.0	0.7	14	−[1]	
92201S007	PAPB	A1	D	Papeete, Tahiti	1995.6 - 1998.3	2.7	139	*	*
92201S008	PAQB	A1	D	Papeete, Tahiti	1998.7 - 2003.0	4.3	220	*	
92202S009	HUAA	A1	D	Huahine, Societe Isl.	1993.0 - 1994.6	1.6	78	−[2]	
92403S001	RAQB	A1	D	Rapa, Tubai Islands	1996.3 - 2003.0	6.7	305	*	
92701S001	NOUA	A1	D	Noumea, New Caledonia	1993.0 - 2000.6	7.6	367	*	*
92701S002	NOUB	A1	D	Noumea, New Caledonia	2002.2 - 2002.8	0.6	30	−[1]	
92722S001	LIFB	A1	D	Ile Lifou, New Caledonia	1993.9 - 1998.5	4.6	50	*	
92802S001	TANB	A1	D	Tanna, New Hebrida	1997.5 - 1998.5	1.0	48	−[1]	
92901S001	WALA	A1	D	Wallis	1993.0 - 2000.9	7.9	378	*	*
92902S001	FUTB	A1	D	Futuna	2001.1 - 2003.0	1.9	101	−[2]	
97301S004	KRUB	A1	D	Kourou, French Guiana	1993.0 - 2003.0	10.0	450	*	*
97401S001	REUA	A1	D	La Reunion, Reunion	1993.0 - 1998.9	5.9	299	*	*
97401S002	REUB	A1	D	La Reunion, Reunion	1999.0 - 2003.0	4.0	210	*	

D VLBI intra-technique combination

Tab. D.1 : *This table shows the VLBI stations used for the intra-technique combinations. Some outliers were rejected in the individual solutions (see $-^1$ and $-^2$). The last column denotes the VLBI reference frame stations.*
$-^1$: The estimated station position of a particular solution differs by more than 3 cm (absolute value) from the mean of the other solutions (see chapter 5.1).
$-^2$: The normalised position or velocity differences exceed the boundary value of 10.

VLBI stations used for intra-technique combination

Domes No.	CDP No.	Sol. No.	Site Name	DGFI	GIUB	GSFC	SHA	used	RF
10302M002	7602	A1	Tromso, Norway			*	*	*	
10317S003	7331	A1	Ny Alesund	*	$-^2$	*	*	*	*
10329M001	7607	A1	Trysil, Norway			*	*	*	
10402S002	7213	A1	Onsala, Sweden	*	*	*	*	*	*
12337S008	7332	A1	Simeis Crimea Ukraine	*	*	*	*	*	
12711S001	7230	A1	Bologna, Italy	*	*	*	*	*	
12711S001	7230	A2	Bologna, Italy	*	*	*	*	*	
12717S001	7547	A1	Noto, Sicily, Italy	*	*	*	*	*	*
12734S005	7243	A1	Matera, Italy	*	*	*	*	*	*
13407S010	1565	A1	Madrid, Spain (34-M)	*	*	*	*	*	*
13407S010	1565	A2	Madrid, Spain (34-M)	*	*	*	*	*	
13420S001	7333	A1	Yebes, Spain	*	*	*	*	*	
14201S004	7224	A1	Wettzell, FRG	*	*	*	*	*	*
14209S001	7203	A1	Effelsberg, FRG	*	*	*	*	*	
14209S001	7203	A2	Effelsberg, FRG	*	*	*	*	*	
21605S009	7227	A1	Shanghai, China	*	*	*	*	*	*
21612S001	7330	A1	Urumqi, China	*	*	*	*	*	
21701S001	1856	A1	Kashima, Japan	*	*	*	*	*	*
21701S004	1857	A1	Kashima, Japan	*	*	*	*	*	*
21702S010	7324	A1	Mizusawa, Japan		$-^1$	*	$-^1$	*	
21730S001	7311	A1	Tsukuba, Japan			*	*	*	
21730S007	7345	A1	Tsukuba, Japan (32 m)	$-^1$	$-^1$	$-^1$	$-^1$	–	
21733S002	7310	A1	Marcus, Japan		*	*	*	*	
30302S001	7232	A1	Hartebeesthoek S Afr.	*	*	*	*	*	*
40104S001	7282	A1	Algonquin Park Canada	*	*	*	*	*	*
40105M001	7283	A1	Penticton, Canada			*	*	*	
40127M004	7296	A1	Yellowknife, Canada			*	*	*	
40400M003	7263	A1	Pasadena, CA			*	*	*	
40403M001	7268	A1	Palos Verdes, CA			$-^1$	$-^1$	–	

continued

VLBI intra-technique combination continued

Domes No.	CDP No.	Sol. No.	Site Name	DGFI	GIUB	GSFC	SHA	used	RF
40404M001	7254	A1	Pearblossom, CA			$-^1$	$-^1$	–	
40405S009	7222	A1	Goldstone, CA	*	*	*	*	*	
40405S009	7222	A2	Goldstone, CA	*	*	*	*	*	
40405S014	1513	A1	Goldstone, CA		$-^1$	*	*	*	
40405S019	1515	A1	Goldstone, CA	*	*	*	*	*	
40405S019	1515	A2	Goldstone, CA	*	*	*	*	*	
40406M001	7252	A1	San Francisco, CA			*	*	*	
40406M001	7252	A2	San Francisco, CA			*	*	*	
40407M001	7256	A1	Pinyon Flats, CA			$-^1$	$-^1$	–	
40408S002	7225	A1	Fairbanks, AK	*	*	*	*	*	*
40410M001	7251	A1	Point Reyes, CA			*	*	*	
40416M001	7277	A1	Cape Yakataga, AK			*	*	*	
40416M001	7277	A2	Cape Yakataga, AK			*	*	*	
40419M001	7278	A1	Kodiak, AK			*	*	*	
40420M002	7223	A1	Vandenberg AFB, CA			*	*	*	
40421M001	7279	A1	Nome, AK			*	*	*	
40423M001	7280	A1	Sand Point, AK			*	*	*	
40424S001	1311	A1	Kokee Park Kauai, HI	*	*	*	*	*	*
40424S007	7298	A1	Kokee Park Kauai, HI	*	*	*	*	*	*
40425M001	7281	A1	Sourdough, AK			*	*	*	
40425M001	7281	A2	Sourdough, AK			*	*	*	
40427M001	7266	A1	Fort Ord, CA			*	*	*	
40427M002	7241	A1	Fort Ord, CA			*	*	*	
40427M002	7241	A2	Fort Ord, CA			*	*	*	
40428M001	7255	A1	Santa Paula, CA			*	*	*	
40430M001	7269	A1	Black Butte, CA			$-^1$	$-^1$	–	
40432M001	7286	A1	Ely, NV			$-^1$	$-^1$	–	
40433M004	7221	A1	Quincy, CA			*	*	*	
40437M001	7259	A1	Mammoth Lakes, CA			$-^1$	$-^1$	–	
40439S002	7207	A1	Owens Valley, CA	$-^1$	$-^1$	*	*	*	
40439S006	7616	A1	Owens Valley, CA VLBA	*	*	*	*	*	
40440S002	7205	A1	Westford, MA	*	*	*	*	*	
40440S003	7209	A1	Westford, MA	*	*	*	*	*	*
40441S001	7204	A1	Green Bank, WV	*	$-^1$	*	*	*	
40441S004	7214	A1	Green Bank, WV	*	*	*	*	*	
40441S004	7214	A2	Green Bank, WV	*	*	*	*	*	
40441S007	7208	A1	Green Bank, WV	*	*	*	*	*	*
40442S003	7216	A1	Fort Davis, TX	$-^1$	$-^1$	*	*	*	
40442S017	7613	A1	Ft. Davis, TX VLBA	*	*	*	*	*	*
40451M102	7102	A1	Washington, D.C.			*	*	*	
40451M125	7108	A1	Washington, D.C.			*	*	*	
40456S001	7234	A1	Pie Town, NM VLBA	*	*	*	*	*	*
40457M001	7229	A1	Seattle, WA			$-^1$	$-^1$	–	
40463S001	7611	A1	Los Alamos, NM VLBA	*	*	*	*	*	*
40465S001	7612	A1	North Liberty IA VLBA	*	*	*	*	*	

continued

VLBI intra-technique combination continued

Domes No.	CDP No.	Sol. No.	Site Name	DGFI	GIUB	GSFC	SHA	used	RF
40466S001	7610	A1	Kitt Peak, AZ VLBA	*	*	*	*	*	
40471S001	7618	A1	Hancock, NH VLBA	*	*	*	*	*	
40473S001	7614	A1	Brewster, WA VLBA	*	*	*	*	*	
40477S001	7617	A1	Mauna Kea, HI VLBA	*	*	*	*	*	*
40489S001	7218	A1	Hat Creek, CA	*	*	*	*	*	
40490S001	7217	A1	Maryland Point, MD		$-^1$	*	*	*	
40491M003	7261	A1	Flagstaff, AZ			*	*	*	
40492M002	7290	A1	Vernal, UT			*	*	*	
40493M001	7894	A1	Yuma, AZ			*	*	*	
40496M002	7258	A1	Platteville, CO			*	*	*	
40497M003	7274	A1	Monument Peak, CA			*	*	*	
40499S001	7219	A1	Richmond, FL	*	*	*	*	*	*
40499S019	7201	A1	Miami, FL		*	*	*	*	
41602S001	7297	A1	Fortaleza, Brazil	*	*	*	*	*	*
41705S006	1404	A1	Santiago, Chile	*	*	*	*	*	*
43201S001	7615	A1	St. Croix, VI VLBA	*	*	*	*	*	*
50103S001	1543	A1	Tidbinbilla Australia	*	*	*	*	*	*
50108S001	7202	A1	Parkes, Australia			$-^1$	$-^1$	–	
50116S002	7242	A1	Hobart, Tasmania	$-^2$	*	*	*	*	*
50505S003	4968	A1	Kwajalein Marshall Is	$-^1$		*	*	*	
66008S001	7245	A1	O'Higgins, Antarctica	*	*	*	*	*	

Tab. D.2: *This table shows the VLBI station position and velocity residuals (north, east, up) of the individual solutions w.r.t. the combined intra-technique solution. Units are [mm] for positions and [mm/yr] for velocities. For some VLBI stations a second position was estimated (identified by "A2") due to various reasons (e.g. station displacements caused by earthquakes). Note that in these cases the station velocities of solution "A2" are identical with "A1", and thus are not displayed in this table.*

VLBI intra-technique combination results

Domes No.	CDP No.	Sol. No.	AC	△N	△E	△H	△vel$_N$	△vel$_E$	△vel$_H$
Tromsoe, Norway									
10302M002	7602	A1	GSFC	2.3	1.4	−9.0	0.3	0.3	−1.5
10302M002	7602	A1	SHA	−1.4	0.8	3.0	−0.3	0.0	−0.3
Ny Alesund									
10317S003	7331	A1	DGFI	0.4	−0.6	3.0	0.1	0.3	0.2
10317S003	7331	A1	GSFC	0.1	0.6	−7.9	0.3	0.0	−1.8
10317S003	7331	A1	SHA	0.3	0.3	−7.1	0.2	−0.2	−0.5
Trysil, Norway									
10329M001	7607	A1	GSFC	−0.3	−0.1	−2.4	−0.2	−0.1	−0.6
10329M001	7607	A1	SHA	−0.2	0.5	−2.6	−0.2	−0.2	−0.6
Onsala, Sweden									
10402S002	7213	A1	DGFI	0.0	−0.5	−2.9	0.2	0.1	0.3
10402S002	7213	A1	GIUB	−0.8	0.4	0.8	−0.5	0.2	−0.6
10402S002	7213	A1	GSFC	1.2	0.7	10.5	0.3	0.1	−0.2
10402S002	7213	A1	SHA	−1.2	0.1	9.8	−0.5	−0.2	−0.1
Simeis Crimea Ukraine									
12337S008	7332	A1	DGFI	−0.1	−1.1	−6.9	−0.1	0.3	0.1
12337S008	7332	A1	GIUB	−0.4	2.1	2.5	0.0	−0.5	−1.9
12337S008	7332	A1	GSFC	−0.1	−0.2	0.2	−0.2	0.0	−0.3
12337S008	7332	A1	SHA	0.1	0.2	1.0	0.1	0.7	0.8
Bologna, Italy									
12711S001	7230	A1	DGFI	0.1	1.2	−2.7	0.3	0.4	−0.2
12711S001	7230	A1	GIUB	0.2	0.2	1.5	−0.3	0.1	−0.7
12711S001	7230	A1	GSFC	0.5	−0.6	8.7	0.1	−0.2	0.8
12711S001	7230	A1	SHA	−0.7	−0.2	8.1	−0.4	−0.3	−0.2
12711S001	7230	A2	DGFI	−0.7	−0.8	−3.7	—	—	—
12711S001	7230	A2	GIUB	0.3	0.6	−1.6	—	—	—
12711S001	7230	A2	GSFC	−0.2	0.3	6.2	—	—	—
12711S001	7230	A2	SHA	0.6	0.5	10.7	—	—	—
Noto, Sicily, Italy									
12717S001	7547	A1	DGFI	−0.1	0.5	−1.5	0.1	0.0	−0.4
12717S001	7547	A1	GIUB	−0.6	0.6	1.5	−0.2	0.2	0.2
12717S001	7547	A1	GSFC	0.2	−0.5	2.2	0.0	−0.1	0.1
12717S001	7547	A1	SHA	−0.1	0.1	−2.8	−0.3	−0.2	−0.3
Matera, Italy									
12734S005	7243	A1	DGFI	−0.1	0.1	−3.6	0.2	0.0	−0.1
12734S005	7243	A1	GIUB	0.2	0.3	0.4	−0.2	0.2	−0.6
12734S005	7243	A1	GSFC	−0.1	0.0	7.4	−0.1	0.0	0.3
12734S005	7243	A1	SHA	−0.2	0.0	6.9	−0.3	−0.2	−0.1

continued

VLBI intra-technique combination continued

Domes No.	CDP No.	Sol. No.	AC	△N	△E	△H	△vel$_N$	△vel$_E$	△vel$_H$
Madrid, Spain									
13407S010	1565	A1	DGFI	−0.5	0.8	−2.0	0.1	0.2	0.1
13407S010	1565	A1	GIUB	1.0	−0.5	0.0	−0.1	0.0	−0.1
13407S010	1565	A1	GSFC	0.2	0.0	4.6	0.1	−0.1	0.1
13407S010	1565	A1	SHA	−0.4	0.4	6.3	−0.4	−0.2	−0.4
13407S010	1565	A2	DGFI	0.7	0.0	−2.7	—	—	—
13407S010	1565	A2	GIUB	−0.4	1.7	1.9	—	—	—
13407S010	1565	A2	GSFC	0.4	−0.3	3.7	—	—	—
13407S010	1565	A2	SHA	−0.5	−0.1	5.9	—	—	—
Yebes, Spain									
13420S001	7333	A1	DGFI	0.8	−1.1	2.3	0.0	0.4	−1.7
13420S001	7333	A1	GIUB	−2.1	1.6	0.1	0.7	−0.1	6.5
13420S001	7333	A1	GSFC	0.4	0.1	−3.2	−0.3	−0.3	0.1
13420S001	7333	A1	SHA	0.2	0.6	−2.5	0.1	−0.4	2.1
Wettzell, FRG									
14201S004	7224	A1	DGFI	−0.2	−0.1	−2.5	0.2	0.1	0.1
14201S004	7224	A1	GIUB	0.1	0.5	1.8	−0.3	0.2	−0.8
14201S004	7224	A1	GSFC	0.1	0.3	0.5	0.0	0.0	0.0
14201S004	7224	A1	SHA	0.0	0.1	1.6	−0.3	−0.3	−0.1
Effelsberg, FRG									
14209S001	7203	A1	DGFI	0.9	0.5	3.5	0.6	0.4	−0.5
14209S001	7203	A1	GIUB	−0.1	3.4	16.1	−0.2	1.2	3.2
14209S001	7203	A1	GSFC	1.0	0.4	−12.8	0.2	0.0	−0.4
14209S001	7203	A1	SHA	−1.2	−0.1	−18.2	−0.8	−0.3	−0.9
14209S001	7203	A2	DGFI	−1.5	−0.5	4.7	—	—	—
14209S001	7203	A2	GIUB	3.5	−2.4	−11.3	—	—	—
14209S001	7203	A2	GSFC	0.7	0.0	−13.5	—	—	—
14209S001	7203	A2	SHA	−2.8	1.4	−7.7	—	—	—
Shanghai, China									
21605S009	7227	A1	DGFI	−4.3	−0.3	−1.7	−0.2	0.2	0.4
21605S009	7227	A1	GIUB	2.0	1.9	−0.5	0.2	0.4	−0.7
21605S009	7227	A1	GSFC	1.1	−0.4	0.1	0.3	−0.1	0.5
21605S009	7227	A1	SHA	0.3	1.3	−2.3	0.3	−0.3	−1.0
Urumqi, China									
21612S001	7330	A1	DGFI	−5.3	5.0	−12.7	1.1	−1.7	0.5
21612S001	7330	A1	GIUB	1.5	1.6	−1.3	0.1	−0.2	2.4
21612S001	7330	A1	GSFC	1.3	−1.9	3.0	−0.1	0.9	−0.9
21612S001	7330	A1	SHA	1.2	−2.2	−7.7	−1.1	1.8	6.1
Kashima, Japan									
21701S001	1856	A1	DGFI	−3.0	−1.2	−5.0	−0.2	0.2	0.0
21701S001	1856	A1	GIUB	−0.2	0.7	0.6	−0.1	0.3	−0.6
21701S001	1856	A1	GSFC	0.4	1.6	2.7	0.1	0.1	0.2
21701S001	1856	A1	SHA	−1.0	1.0	0.1	−0.1	−0.2	−0.5
21701S004	1857	A1	DGFI	7.9	−3.3	−3.1	2.0	−0.4	1.6
21701S004	1857	A1	GIUB	4.9	−5.4	8.2	0.8	−0.9	1.8
21701S004	1857	A1	GSFC	−1.9	2.5	5.8	−0.2	0.3	−1.0
21701S004	1857	A1	SHA	4.9	−2.2	23.7	1.1	−0.8	1.4
Mizusawa, Japan									
21702S010	7324	A1	GSFC	0.0	1.5	−1.1	0.2	0.0	0.2

continued

VLBI intra-technique combination continued

Domes No.	CDP No.	Sol. No.	AC	△N	△E	△H	△vel$_N$	△vel$_E$	△vel$_H$
Tsukuba, Japan									
21730S001	7311	A1	GSFC	−6.8	−1.2	0.1	−1.1	−0.3	0.6
21730S001	7311	A1	SHA	7.6	4.3	2.7	1.3	0.3	0.0
21730S007	7345	A2	DGFI	0.4	−3.4	0.3	−0.3	0.2	0.0
Marcus, Japan									
21733S002	7310	A1	GIUB	7.6	−7.2	0.2	1.2	−0.8	−1.6
21733S002	7310	A1	GSFC	−3.0	2.6	−8.1	−0.2	0.1	−0.2
21733S002	7310	A1	SHA	1.4	−1.3	8.6	0.0	−0.6	0.6
Hartebeesthoek, S Afr.									
30302S001	7232	A1	DGFI	−1.6	3.8	1.7	−0.5	−0.2	−0.3
30302S001	7232	A1	GIUB	−1.8	−3.4	−2.4	−0.2	−1.1	−1.0
30302S001	7232	A1	GSFC	−1.4	−1.1	−3.2	0.6	0.2	0.5
30302S001	7232	A1	SHA	0.6	−4.0	0.3	0.1	−1.5	0.7
Algonquin Park, Canada									
40104S001	7282	A1	DGFI	−0.3	−0.7	3.4	0.2	−0.3	0.4
40104S001	7282	A1	GIUB	0.1	0.0	−1.2	−0.1	0.1	−1.1
40104S001	7282	A1	GSFC	0.5	0.2	−4.3	−0.1	0.1	−0.5
40104S001	7282	A1	SHA	0.3	0.3	−2.3	−0.3	0.1	−0.3
Penticton, Canada									
40105M001	7283	A1	GSFC	0.7	−1.4	4.7	0.1	−0.2	0.6
40105M001	7283	A1	SHA	0.7	1.4	−5.1	−0.1	0.2	−0.8
Yellowknife, Canada									
40127M004	7296	A1	GSFC	0.8	−0.1	0.0	0.1	−0.1	0.1
40127M004	7296	A1	SHA	−0.3	0.1	−0.2	−0.2	0.2	−0.4
Pasadena, CA									
40400M003	7263	A1	GSFC	0.7	−0.8	8.3	0.2	−0.1	1.2
40400M003	7263	A1	SHA	−0.5	−0.1	−7.5	−0.4	−0.1	−1.1
Goldstone, CA									
40405S009	7222	A1	DGFI	−2.9	0.1	−2.0	−0.4	−0.1	−0.5
40405S009	7222	A1	GIUB	−2.2	−0.7	−0.6	−0.7	−0.4	−1.2
40405S009	7222	A1	GSFC	0.9	0.0	−2.0	0.2	0.0	0.0
40405S009	7222	A1	SHA	−0.2	−1.1	−1.9	−0.3	−0.2	−0.4
40405S009	7222	A2	DGFI	−3.4	−1.2	3.7	—	—	—
40405S009	7222	A2	GIUB	−2.7	−2.2	−6.0	—	—	—
40405S009	7222	A2	GSFC	1.4	0.6	−1.4	—	—	—
40405S009	7222	A2	SHA	−0.5	−0.6	−2.5	—	—	—
40405S014	1513	A1	GSFC	1.0	−0.4	−1.4	0.2	0.0	−0.1
40405S014	1513	A1	SHA	0.2	−1.0	1.9	−0.3	−0.2	−0.1
40405S019	1515	A1	DGFI	11.9	4.1	29.5	0.2	0.8	−2.0
40405S019	1515	A1	GIUB	1.7	2.2	0.4	−0.6	−0.7	−0.9
40405S019	1515	A1	GSFC	−0.8	−5.9	3.5	0.1	−0.6	0.4
40405S019	1515	A1	SHA	−1.1	−0.1	14.7	−0.4	0.0	1.5
40405S019	1515	A2	DGFI	0.2	0.0	3.6	—	—	—
40405S019	1515	A2	GIUB	0.1	−0.5	−0.8	—	—	—
40405S019	1515	A2	GSFC	0.3	0.3	−0.6	—	—	—
40405S019	1515	A2	SHA	−0.5	0.2	0.0	—	—	—
San Francisco, CA									
40406M001	7252	A1	GSFC	1.0	1.9	2.7	0.1	0.2	0.4
40406M001	7252	A1	SHA	−1.0	−2.5	1.3	−0.4	−0.3	−0.2

continued

VLBI intra-technique combination continued

Domes No.	CDP No.	Sol. No.	AC	△N	△E	△H	△vel$_N$	△vel$_E$	△vel$_H$
40406M001	7252	A2	GSFC	0.4	1.2	−0.8	—	—	—
40406M001	7252	A2	SHA	−0.6	−2.0	2.1	—	—	—
Fairbanks, AK									
40408S002	7225	A1	DGFI	−0.9	−0.1	−3.1	−0.2	−0.1	0.5
40408S002	7225	A1	GIUB	−0.3	0.1	−0.9	−0.3	0.0	−0.9
40408S002	7225	A1	GSFC	0.9	−0.4	1.3	0.2	−0.1	0.1
40408S002	7225	A1	SHA	−0.3	0.2	2.1	−0.2	0.2	−0.2
Point Reyes, CA									
40410M001	7251	A1	GSFC	−1.1	0.6	−2.8	−0.1	0.1	0.0
40410M001	7251	A1	SHA	0.5	−1.8	1.2	−0.2	−0.3	−0.3
Cape Yakataga, AK									
40416M001	7277	A1	GSFC	0.5	−0.8	14.1	0.1	−0.1	1.4
40416M001	7277	A2	GSFC	0.6	−0.8	10.6	−8.6	31.1	−24.8
40416M001	7277	A2	SHA	0.1	0.2	−9.4	−1.8	0.9	0.2
Kodiak, AK									
40419M001	7278	A1	GSFC	0.4	−1.6	0.9	0.1	−0.3	0.1
40419M001	7278	A1	SHA	0.0	−0.2	−5.3	−0.1	0.1	−1.0
Vandenberg AFB, CA									
40420M002	7223	A1	GSFC	0.8	0.1	−2.4	0.2	0.0	−0.2
40420M002	7223	A1	SHA	0.1	−1.4	−0.6	−0.3	−0.2	−0.3
Nome, AK									
40421M001	7279	A1	GSFC	1.1	−1.6	−5.1	0.2	−0.3	−0.7
40421M001	7279	A1	SHA	0.6	0.8	4.7	0.1	0.3	0.2
Sand Point, AK									
40423M001	7280	A1	GSFC	1.5	0.0	1.7	0.2	−0.1	0.1
40423M001	7280	A1	SHA	−0.2	−1.4	−4.8	0.0	0.0	−0.8
Kokee Park Kauai, HI									
40424S001	1311	A1	DGFI	1.8	−4.4	−2.3	0.4	−0.1	0.9
40424S001	1311	A1	GIUB	1.2	−4.3	4.0	0.1	−0.9	0.4
40424S001	1311	A1	GSFC	−1.2	1.4	0.0	0.1	−0.1	−0.3
40424S001	1311	A1	SHA	−2.3	0.3	−2.3	−0.4	−0.2	−0.7
40424S007	7298	A1	DGFI	−1.3	−2.5	−0.2	−0.4	0.5	0.4
40424S007	7298	A1	GIUB	0.2	1.1	2.6	−0.2	0.8	0.1
40424S007	7298	A1	GSFC	0.0	1.2	−9.9	0.3	−0.3	0.2
40424S007	7298	A1	SHA	−0.2	2.2	−8.8	0.1	0.7	0.1
Sourdough, AK									
40425M001	7281	A1	GSFC	6.7	2.4	−9.7	0.7	0.2	−0.8
40425M001	7281	A1	SHA	−4.4	−1.8	7.4	−0.6	0.0	0.2
40425M001	7281	A2	GSFC	5.0	1.7	−6.6	—	—	—
40425M001	7281	A2	SHA	−3.3	−1.5	5.1	—	—	—
Fort Ord, CA									
40427M001	7266	A1	GSFC	−0.5	2.3	−9.4	0.0	0.2	−1.0
40427M001	7266	A1	SHA	0.5	−2.8	10.1	−0.3	−0.4	0.9
40427M002	7241	A1	GSFC	0.4	−1.5	−4.7	0.1	−0.2	−0.4
40427M002	7241	A1	SHA	−1.6	0.9	1.1	−0.5	0.0	−0.2
40427M002	7241	A2	GSFC	0.4	−1.3	−3.8	—	—	—
40427M002	7241	A2	SHA	−1.6	0.5	−0.1	—	—	—
Quincy, CA									
40433M004	7221	A1	GSFC	2.2	−0.3	−2.1	0.3	0.0	−0.2

continued

VLBI intra-technique combination continued

Domes No.	CDP No.	Sol. No.	AC	△N	△E	△H	△vel$_N$	△vel$_E$	△vel$_H$
40433M004	7221	A1	SHA	−1.8	−1.5	−2.0	−0.5	−0.2	−0.6
Owens Valley, CA									
40439S002	7207	A1	GSFC	0.2	0.7	1.3	0.1	0.1	0.2
40439S002	7207	A1	SHA	−0.6	−1.9	−2.1	−0.4	−0.3	−0.5
40439S006	7616	A1	DGFI	0.1	−0.2	0.5	−0.1	0.0	−1.1
40439S006	7616	A1	GIUB	1.6	−0.1	3.3	0.5	0.1	2.9
40439S006	7616	A1	GSFC	0.0	0.0	3.2	0.0	−0.1	−0.1
40439S006	7616	A1	SHA	−0.6	−0.2	7.8	−0.2	0.2	4.2
Westford, MA									
40440S002	7205	A1	DGFI	−4.8	8.3	−14.6	−0.3	1.0	−1.0
40440S002	7205	A1	GIUB	−3.6	2.5	18.3	−0.7	0.3	1.1
40440S002	7205	A1	GSFC	0.3	0.0	−5.3	−0.1	0.0	−0.6
40440S002	7205	A1	SHA	1.5	−1.1	1.2	−0.1	−0.2	−0.3
40440S003	7209	A1	DGFI	0.1	−0.6	2.3	0.3	−0.2	0.4
40440S003	7209	A1	GIUB	0.3	−0.4	−0.4	−0.1	−0.1	−0.9
40440S003	7209	A1	GSFC	0.0	0.5	−1.3	−0.1	0.0	−0.3
40440S003	7209	A1	SHA	0.5	−0.1	0.1	−0.2	−0.1	−0.3
Green Bank, WV									
40441S001	7204	A1	DGFI	3.5	0.4	16.7	−0.6	0.2	0.0
40441S001	7204	A1	GSFC	−5.5	−0.6	−0.3	−0.2	−0.1	0.0
40441S001	7204	A1	SHA	−4.3	0.5	−10.7	−0.4	−0.1	−1.3
40441S004	7214	A1	DGFI	0.8	0.1	6.2	0.3	−0.1	0.4
40441S004	7214	A1	GIUB	0.0	−1.7	1.3	−0.3	−0.3	−0.4
40441S004	7214	A1	GSFC	−1.2	−0.2	0.4	0.0	0.0	0.4
40441S004	7214	A1	SHA	−2.8	1.4	−3.9	−0.4	0.1	−0.8
40441S004	7214	A2	DGFI	1.9	0.1	6.2	—	—	—
40441S004	7214	A2	GIUB	0.3	−0.8	−1.1	—	—	—
40441S004	7214	A2	GSFC	−2.1	0.2	0.5	—	—	—
40441S004	7214	A2	SHA	−3.5	0.1	−2.7	—	—	—
40441S007	7208	A1	DGFI	0.0	−0.3	2.3	0.4	−0.1	0.9
40441S007	7208	A1	GIUB	−0.4	0.3	0.3	0.0	0.0	−0.8
40441S007	7208	A1	GSFC	0.5	−0.1	−6.4	−0.2	−0.1	−0.1
40441S007	7208	A1	SHA	0.2	0.0	−6.2	−0.1	0.2	0.4
Fort Davis, TX									
40442S003	7216	A1	GSFC	0.0	0.1	−0.8	0.0	0.0	0.0
40442S017	7613	A1	DGFI	0.0	−0.6	0.5	0.0	−0.1	−0.2
40442S017	7613	A1	GIUB	0.1	0.4	−1.7	−0.1	0.2	−0.4
40442S017	7613	A1	GSFC	0.2	0.1	1.4	0.0	−0.1	0.0
40442S017	7613	A1	SHA	−1.8	0.1	−1.5	−0.7	0.1	−1.1
Washington, D.C.									
40451M102	7102	A1	GSFC	−1.3	0.6	0.8	−0.4	0.0	0.4
40451M102	7102	A1	SHA	0.1	−0.6	−3.0	−0.1	−0.1	−0.8
40451M125	7108	A1	GSFC	0.3	−0.4	−3.4	−0.3	−0.3	−1.2
40451M125	7108	A1	SHA	−0.8	0.7	1.2	0.0	0.4	1.3
Pie Town, NM VLBA									
40456S001	7234	A1	DGFI	0.3	0.4	4.4	0.1	0.0	0.5
40456S001	7234	A1	GIUB	−0.9	−2.2	−5.2	−0.6	−0.7	−2.1
40456S001	7234	A1	GSFC	0.0	0.0	−4.6	0.1	0.1	0.1
40456S001	7234	A1	SHA	−1.8	−1.5	−9.1	−0.7	−0.4	−1.1

continued

VLBI intra-technique combination continued

Domes No.	CDP No.	Sol. No.	AC	△N	△E	△H	△vel$_N$	△vel$_E$	△vel$_H$
Los Alamos, NM VLBA									
40463S001	7611	A1	DGFI	0.1	−0.3	1.1	0.1	0.0	−0.2
40463S001	7611	A1	GIUB	0.2	−0.4	1.1	−0.1	−0.1	0.1
40463S001	7611	A1	GSFC	0.1	0.1	−2.1	0.0	−0.1	0.0
40463S001	7611	A1	SHA	0.0	0.3	−1.5	−0.2	0.2	−0.4
North Liberty IA VLBA									
40465S001	7612	A1	DGFI	−0.1	−0.5	−0.4	0.1	−0.1	0.1
40465S001	7612	A1	GIUB	−0.2	0.1	−2.4	−0.6	−0.1	0.0
40465S001	7612	A1	GSFC	0.1	0.1	5.6	0.1	0.0	0.0
40465S001	7612	A1	SHA	−1.7	−1.6	−4.9	−0.8	−0.4	−2.1
Kitt Peak, AZ VLBA									
40466S001	7610	A1	DGFI	−0.1	−0.3	2.1	0.0	0.0	−0.3
40466S001	7610	A1	GIUB	1.1	−0.2	1.2	0.3	0.1	1.2
40466S001	7610	A1	GSFC	−0.1	0.0	−3.6	0.1	0.0	0.1
40466S001	7610	A1	SHA	0.8	1.2	−0.3	0.5	0.7	0.4
Hancock, NH VLBA									
40471S001	7618	A1	DGFI	0.4	−0.7	0.2	0.2	0.0	0.1
40471S001	7618	A1	GIUB	0.3	0.0	0.5	0.0	0.1	0.8
40471S001	7618	A1	GSFC	−0.1	0.4	4.4	0.0	−0.1	0.3
40471S001	7618	A1	SHA	2.1	−0.7	2.7	0.9	−0.2	0.6
Brewster, WA VLBA									
40473S001	7614	A1	DGFI	−0.1	−0.3	−0.4	0.1	−0.2	−1.6
40473S001	7614	A1	GIUB	1.6	−0.8	−0.3	0.3	−0.2	0.2
40473S001	7614	A1	GSFC	0.1	0.1	1.6	0.0	0.0	0.6
40473S001	7614	A1	SHA	−0.3	0.6	4.3	−0.2	0.6	2.1
Mauna Kea, HI VLBA									
40477S001	7617	A1	DGFI	−1.6	−1.8	−2.4	−0.2	0.3	−0.2
40477S001	7617	A1	GIUB	1.3	1.1	2.1	0.2	1.0	1.5
40477S001	7617	A1	GSFC	0.0	1.4	5.3	0.3	−0.2	0.0
40477S001	7617	A1	SHA	1.6	1.4	5.5	1.0	0.8	2.4
Hat Creek, CA									
40489S001	7218	A1	DGFI	−2.3	0.2	−12.3	−0.1	−0.2	−0.3
40489S001	7218	A1	GIUB	−10.3	0.9	−15.8	−1.1	−0.1	−2.2
40489S001	7218	A1	GSFC	2.3	−0.1	−7.0	0.2	0.0	−0.8
40489S001	7218	A1	SHA	−0.3	−2.0	−1.8	−0.4	−0.3	−0.6
Maryland Point, MD									
40490S001	7217	A1	GSFC	2.1	−2.1	−7.7	0.0	−0.1	−0.6
40490S001	7217	A1	SHA	−1.6	0.4	1.2	−0.3	−0.1	−0.2
Flagstaff, AZ									
40491M003	7261	A1	GSFC	2.7	1.9	−14.6	0.3	0.2	−1.3
40491M003	7261	A1	SHA	−0.8	−2.0	3.5	−0.4	−0.3	−0.1
Vernal, UT									
40492M002	7290	A1	GSFC	0.9	0.3	−8.2	0.1	0.0	−1.1
40492M002	7290	A1	SHA	0.3	−1.3	−3.4	−0.2	−0.2	−0.8
Yuma, AZ									
40493M001	7894	A1	GSFC	−1.2	0.1	−2.3	0.0	0.0	0.0
40493M001	7894	A1	SHA	1.6	−1.3	−2.0	−0.2	−0.2	−0.5
Platteville, CO									
40496M002	7258	A1	GSFC	1.7	1.2	−16.3	0.2	0.1	−2.0

continued

VLBI intra-technique combination continued

Domes No.	CDP No.	Sol. No.	AC	△N	△E	△H	△vel$_N$	△vel$_E$	△vel$_H$
40496M002	7258	A1	SHA	−0.7	−1.8	4.6	−0.4	−0.3	0.2
Monument Peak, CA									
40497M003	7274	A1	GSFC	1.2	−0.3	−3.5	0.2	0.0	−0.2
40497M003	7274	A1	SHA	−0.5	−1.0	1.7	−0.3	−0.2	0.0
Richmond, FL									
40499S001	7219	A1	DGFI	2.4	1.9	0.4	0.4	0.2	0.3
40499S001	7219	A1	GIUB	−0.5	−0.2	−2.8	−0.4	−0.1	−1.3
40499S001	7219	A1	GSFC	−2.3	−0.1	−0.1	−0.2	−0.1	0.1
40499S001	7219	A1	SHA	−1.8	−0.5	0.1	−0.4	−0.1	−0.1
40499S019	7201	A1	GIUB	−4.7	−0.4	−5.1	−4.5	−0.5	−3.5
40499S019	7201	A1	GSFC	2.2	0.3	2.0	2.3	0.3	1.1
40499S019	7201	A1	SHA	3.5	0.3	2.2	3.7	0.4	2.9
Fortaleza, Brazil									
41602S001	7297	A1	DGFI	0.1	2.0	−1.8	0.2	−0.6	0.8
41602S001	7297	A1	GIUB	−1.6	−1.2	0.2	0.1	−0.5	−0.7
41602S001	7297	A1	GSFC	−1.5	−1.2	−2.1	−0.4	0.1	−0.1
41602S001	7297	A1	SHA	1.0	−1.2	−1.7	0.4	−0.4	0.4
Santiago, Chile									
41705S006	1404	A1	DGFI	−6.7	4.9	−5.2	−0.8	−0.1	3.0
41705S006	1404	A1	GIUB	0.0	−1.7	3.6	1.0	0.4	1.0
41705S006	1404	A1	GSFC	1.5	−2.6	−1.4	0.5	−0.1	−0.7
41705S006	1404	A1	SHA	5.0	−0.5	2.8	1.0	−0.1	0.6
St. Croix, VI VLBA									
43201S001	7615	A1	DGFI	1.7	0.6	2.9	0.1	−0.4	0.4
43201S001	7615	A1	GIUB	−1.2	−0.8	−11.0	0.0	−0.7	−3.1
43201S001	7615	A1	GSFC	−1.0	−0.9	2.6	0.0	0.3	−0.1
43201S001	7615	A1	SHA	−0.4	0.9	−5.9	0.0	0.4	−7.2
Tidbinbilla Australia									
50103S010	1545	A1	DGFI	−1.4	−7.5	1.7	−0.5	−0.2	−0.5
50103S010	1545	A1	GIUB	−2.4	4.2	−2.5	0.4	1.1	0.2
50103S010	1545	A1	GSFC	−2.4	3.2	−0.2	0.2	0.1	−0.3
50103S010	1545	A1	SHA	−0.6	3.9	−0.7	−0.9	0.7	−1.2
Parkes, Australia									
50116S002	7242	A1	DGFI	0.3	−6.4	7.2	−0.5	0.2	0.4
50116S002	7242	A1	GIUB	−4.0	4.4	−7.2	0.1	1.0	−1.1
50116S002	7242	A1	GSFC	−2.2	2.6	−2.3	0.3	0.0	−0.3
50116S002	7242	A1	SHA	−1.2	3.8	−2.6	−1.2	0.7	−1.3
Kwajalein Marshall Isl.									
50505S003	4968	A1	GSFC	−1.2	1.1	−3.3	0.2	−0.1	−0.2
50505S003	4968	A1	SHA	−0.9	−3.9	−2.4	−0.2	−0.7	−0.4
O'Higgins, Antarctica									
66008S001	7245	A1	DGFI	−4.5	4.3	−11.4	0.1	−0.3	−1.4
66008S001	7245	A1	GIUB	−0.6	−0.9	2.5	0.9	0.1	0.3
66008S001	7245	A1	GSFC	1.0	−2.4	2.0	0.0	0.1	1.8
66008S001	7245	A1	SHA	6.4	−1.5	−1.3	1.3	−0.1	−0.6

E SLR intra-technique combination

Tab. E.1: *This table shows the SLR stations used for the intra-technique combinations. Some outliers were rejected in the individual solutions (see $-^1$, $-^2$ and $-^3$). The last column denotes the SLR reference frame stations.*
$-^1$: The estimated station position of a particular solution differs by more than 5 cm (absolute value) from the mean of the other solutions (see chapter 5.2).
$-^2$: The normalised position or velocity differences exceed the boundary value of 10.
$-^3$: Both criteria $-^1$ and $-^2$ were fulfilled.

SLR stations used for intra-technique combination

Domes No.	CDP No.	Sol. No.	Site Name	CRL	CSR	DGFI	JCET	used	RF
10002S001	7835	A1	Grasse, France	*	*	*	*	*	*
10002S002	7845	A1	Grasse (LLR), France	*	*	*		*	
10503S001	7805	A1	Metsahovi, Finland	$-^1$	$-^1$	$-^1$		–	
10503S014	7806	A1	Metsahovi, Finland	$-^1$	*	*	*	*	
11001S002	7839	A1	Graz, Austria	*	*	*	*	*	*
12205S001	7811	A1	Borowiec, Poland	*	*	*	*	*	*
12302S002	1884	A1	Riga, Latvia	*	*	*	*	*	*
12337S003	1873	A1	Simeiz, Ukraine	$-^1$	*	*	*	*	
12337S006	1893	A1	Katsively, Ukraine	*	$-^1$	*	*	*	
12340S002	1864	A1	Maidanak, Uzbekistan	$-^3$	*	*	*	*	
12341S001	1868	A1	Komsomolsk, Russia	$-^1$	$-^1$	$-^1$	$-^1$	–	
12602M002	7515	A1	Dionysos, Greece		*	*		*	
12612M001	7510	A1	Askites, Greece		*	*		*	
12613M001	7517	A1	Roumelli, Greece		*	*		*	
12614M001	7520	A1	Karitsa, Greece		*	*		*	
12615M001	7512	A1	Katavia, Greece		*	*		*	
12616M001	7525	A1	Xrisokalaria, Greece	$-^1$	$-^1$	$-^1$		–	
12706M001	7544	A1	Lampedusa, Italy		*	*		*	
12717M001	7543	A1	Noto, Italy		*	*		*	
12718M002	7550	A1	Trieste, Italy		$-^1$	$-^1$		–	
12725M002	7545	A1	Cagliari, Italy	*	$-^1$	*	*	*	
12725S013	7548	A1	Cagliari, Italy	*	$-^1$	*	*	*	
12734M004	7541	A1	Matera, Italy		*	*		*	
12734S001	7939	A1	Matera, Italy	*	*	*	*	*	*
13212S001	7840	A1	Herstmonceux, UK	*	*	*	*	*	*
13402S004	7824	A1	San Fernando, Spain	*	$-^3$	*	*	*	
13402S007	7824	B1	San Fernando, Spain	*		*	*	*	
13504M002	8833	A1	Kootwijk, Netherlands		*	*		*	

continued

SLR intra-technique combination continued

Domes No.	CDP No.	Sol. No.	Site Name	CRL	CSR	DGFI	JCET	used	RF
13504S001	7833	A1	Kootwijk, Netherlands		$-^{1}$	$-^{1}$		–	
14001S001	7810	A1	Zimmerwald, Switzerl.	*	*	*	*	*	*
14001S007	7810	B1	Zimmerwald, Switzerl.	*		*	*	*	*
14106S001	1181	A1	Potsdam, Germany	*	$-^{1}$	*		*	
14106S009	7836	A1	Potsdam, Germany	*	*	*	*	*	*
14201M005	7597	A1	Wettzell, Germany	$-^{1}$	*	*	$-^{1}$	*	
14201S002	7834	A1	Wettzell, Germany	*	$-^{1}$	*		*	
14201S018	8834	A1	Wettzell, Germany	*	*	*	*	*	*
20101S001	7832	A1	Riyad, Saudi Arabia	$-^{1}$	*	*	$-^{1}$	*	
20702M001	7530	A1	Bar Giyyora, Israel	*	*	$-^{1}$		*	
20801M001	7575	A1	Diyarbakir, Turkey		$-^{1}$	$-^{1}$		–	
20802M001	7585	A1	Yozgat, Turkey		$-^{1}$	$-^{1}$		–	
20803M001	7580	A1	Melengiclick, Turkey		$-^{1}$	$-^{1}$		–	
20804M001	7587	A1	Yigilca, Turkey		$-^{1}$	$-^{1}$		–	
21601S004	7249	A1	Beijing, China	$-^{1}$	$-^{1}$	$-^{1}$	$-^{3}$	–	
21602S003	7236	A1	Wuhan, China	*	*	$-^{1}$	*	*	
21605S001	7837	A1	Shanghai, China	*	*	*	*	*	
21609S002	7820	A1	Kunming, China		$-^{1}$	$-^{3}$	$-^{1}$	–	
21611S001	7237	A1	Changchun, China	*	*	*	*	*	
21701M002	7335	A1	Kashima, Japan	$-^{1}$	$-^{1}$	$-^{1}$	$-^{1}$	–	
21704M001	7328	A1	Koganei, Japan	*	*	*	*	*	
21704S002	7308	A1	Tokyo, Japan	$-^{1}$	*	*	*	*	
21726S001	7838	A1	Simosato, Japan	*	*	*	$-^{1}$	*	
21739M001	7337	A1	Muira, Japan	*	*	*	$-^{1}$	*	
21740M001	7339	A1	Tateyama, Japan	*	*	*	$-^{3}$	*	
30101S001	7831	A1	Helwan, Egypt	*	*	*	*	*	*
30302M003	7501	A1	Hartebeesth, S Afr.		*	*		*	
40405M013	7288	A1	Goldstone, USA	$-^{1}$	$-^{1}$	$-^{1}$		–	
40429S001	7884	A1	Albuquerque, USA		$-^{1}$	*	*	*	
40433M002	7109	A1	Quincy, USA	*	*	*	*	*	*
40433M005	7886	A1	Quincy, USA		$-^{1}$	$-^{1}$		–	
40436M002	7062	A1	San Diego, USA		$-^{1}$	$-^{1}$		–	
40438M001	7082	A1	Bear Lake, USA		$-^{1}$	$-^{1}$		–	
40438M002	7046	A1	Bear Lake, USA		$-^{1}$	$-^{1}$		–	
40439M001	7114	A1	Owens Valley, USA		$-^{1}$	$-^{1}$		–	
40439M004	7853	A1	Owens Valley, USA		$-^{1}$	$-^{1}$		–	
40440M001	7091	A1	Westford, USA		$-^{1}$	$-^{1}$		–	
40442M001	7086	A1	Fort Davis, USA		*	*		*	
40442M006	7080	A1	Fort Davis, USA	*	*	*	*	*	*
40445M001	7210	A1	Maui, USA	*	*	$-^{2}$	*	*	*
40451M102	7102	A1	Washington, USA		^{1}	$-^{1}$		–	
40451M105	7105	A1	Washington, USA	*	*	*	*	*	*
40451M117	7920	A1	Washington, USA		*	*	*	*	
40451M120	7918	A1	Washington, USA	*	*	*	*	*	
40496M001	7112	A1	Platteville, USA	$-^{1}$	$-^{1}$	$-^{1}$		–	

continued

SLR intra-technique combination continued

Domes No.	CDP No.	Sol. No.	Site Name	CRL	CSR	DGFI	JCET	used	RF
40497M001	7110	A1	Monument Peak, USA	*	*	*	*	*	*
40499M002	7295	A1	Richmond, USA	*	*	*	$-^{1}$	*	
40504M001	7122	A1	Mazatlan, Mexico	*	*	*	$-^{1}$	*	
40505M001	7882	A1	Cabo San Lucas, Mex.	*	*	*	$-^{1}$	*	
40506M001	7883	A1	Ensenada, Mexico	*	*	*		*	
40701S001	1953	A1	Santiago, Cuba	$-^{1}$	$-^{1}$	$-^{1}$	$-^{1}$	–	
41703M002	7097	A1	Easter Island, Chile	*	$-^{1}$	*		*	*
41706M001	7401	A1	Cerro Tololo, Chile	$-^{1}$	$-^{1}$	$-^{1}$		–	
42202M003	7403	A1	Arequipa, Peru	*	*	*	*	*	*
42202S001	7907	A1	Arequipa, Peru	*	$-^{1}$	*		*	
50103S007	7843	A1	Orroral, Australia	*	$-^{3}$	*	*	*	
50107M001	7090	A1	Yarragadee, Australia	*	*	*	*	*	
50119S001	7849	A1	Mt Stromlo, Australia	*	*	*	*	*	*
92201M007	7124	A1	Papeete, Societe Isl.	*	*	*	$-^{1}$	*	*
92202M002	7121	A1	Huahine, Societe Isl.		$-^{1}$	$-^{1}$		–	
92202M004	7123	A1	Huahine, Societe Isl.	*	*	*	*	*	

Tab. E.2: *This table shows the SLR station position and velocity residuals (north, east, up) of the individual solutions w.r.t. the combined intra-technique solution. Units are [mm] and [mm/yr].*

SLR intra-technique combination results

Domes No.	CDP No.	Sol. No.	AC	△N	△E	△H	△vel$_N$	△vel$_E$	△vel$_H$
Grasse, France									
10002S001	7835	A1	CRL	2.3	−1.8	9.4	0.9	0.4	−2.2
10002S001	7835	A1	DGFI	−0.2	1.5	−5.2	−0.7	0.0	−0.2
10002S001	7835	A1	JCET	−1.7	1.4	1.6	1.4	−0.3	2.6
10002S002	7845	A1	CRL	−6.1	−6.3	19.1	2.6	0.8	−5.3
10002S002	7845	A1	CSR	−0.8	−0.4	−5.1	1.8	0.6	0.1
10002S002	7845	A1	DGFI	−3.9	1.2	4.9	1.1	0.8	−1.9
Metsahovi, Finland									
10503S014	7805	A1	CSR	−6.5	10.3	−43.2	1.7	−0.7	13.4
10503S014	7806	A1	DGFI	10.9	−19.2	5.9	−1.9	4.1	−2.2
10503S014	7806	A1	JCET	48.1	−52.0	44.6	−13.0	6.8	−10.3
Graz, Austria									
11001S002	7839	A1	CRL	1.0	−0.2	−4.8	0.4	0.1	2.8
11001S002	7839	A1	CSR	1.0	0.2	−0.5	0.8	0.0	1.1
11001S002	7839	A1	DGFI	0.6	0.6	−2.7	0.2	0.1	−1.3
11001S002	7839	A1	JCET	−0.5	1.1	4.2	0.5	−0.4	2.0
Borowiec, Poland									
12205S001	7811	A1	CRL	−2.8	6.0	−36.2	1.5	0.8	6.6
12205S001	7811	A1	CSR	−2.6	3.2	−39.5	0.3	−1.4	7.5
12205S001	7811	A1	DGFI	−1.3	−0.3	5.7	−0.2	0.5	−0.2
12205S001	7811	A1	JCET	−2.9	3.0	−10.9	2.0	−0.9	−4.0
Riga, Latvia									
12302S002	1884	A1	CRL	3.4	2.1	16.7	1.9	0.4	1.1
12302S002	1884	A1	CSR	−2.9	−2.5	−24.6	2.4	1.6	−3.1
12302S002	1884	A1	DGFI	3.3	−1.3	−2.3	−1.0	−0.3	0.5
12302S002	1884	A1	JCET	0.9	−4.5	13.1	−0.5	−0.1	−2.2
Simeiz/Katsively, Ukraine									
12337S003	1873	A1	CSR	13.5	30.6	24.8	−0.6	5.4	1.8
12337S003	1873	A1	DGFI	−7.7	20.7	−4.7	−0.3	5.3	−3.0
12337S003	1873	A1	JCET	9.5	37.6	26.9	−10.4	18.3	2.1
12337S006	1893	A1	CRL	14.5	−4.9	−17.5	6.9	−2.3	3.6
12337S006	1893	A1	DGFI	−4.4	0.5	15.3	2.2	−4.0	−2.6
12337S006	1893	A1	JCET	−8.8	−16.2	−5.6	−7.6	8.5	3.2
Maidanak, Uzbekistan									
12340S002	1864	A1	CSR	−10.9	1.5	4.9	7.1	1.2	20.2
12340S002	1864	A1	DGFI	−1.8	1.0	0.5	2.0	−0.2	1.4
12340S002	1864	A1	JCET	−6.7	−4.3	−35.8	−2.2	−1.9	−16.9
Dionysos, Greece									
12602M002	7515	A1	CSR	0.7	−1.7	−10.7	0.7	−0.1	0.0
12602M002	7515	A1	DGFI	−0.7	7.2	1.1	0.5	1.0	0.0
Askites, Greece									
12612M001	7510	A1	CSR	−2.5	0.3	−35.3	0.3	0.0	−1.6
12612M001	7510	A1	DGFI	21.5	−8.4	0.8	2.8	0.0	0.0

continued

SLR intra-technique combination continued

Domes No.	CDP No.	Sol. No.	AC	△N	△E	△H	△vel$_N$	△vel$_E$	△vel$_H$
Roumelli, Greece									
12613M001	7517	A1	CSR	1.2	0.2	−25.9	0.8	0.1	−0.3
12613M001	7517	A1	DGFI	−0.6	−5.2	7.2	0.1	−0.3	0.7
Karitsa, Greece									
12614M001	7520	A1	CSR	0.2	−0.6	−27.3	0.5	−0.1	−6.3
12614M001	7520	A1	DGFI	3.0	3.9	−0.4	1.0	0.8	−0.1
Katavia, Greece									
12615M001	7512	A1	CSR	3.3	−5.9	−19.9	1.0	−0.5	−0.1
12615M001	7512	A1	DGFI	−16.5	35.5	5.2	−1.6	3.2	0.5
Lampedusa, Italy									
12706M001	7544	A1	CSR	0.0	−1.0	−7.8	0.5	−0.1	−1.5
12706M001	7544	A1	DGFI	40.3	19.6	−0.8	5.7	2.7	−0.3
Noto, Italy									
12717M001	7543	A1	CSR	0.9	−2.5	30.6	0.9	−0.3	6.3
12717M001	7543	A1	DGFI	1.1	12.8	−4.7	−1.3	1.6	−0.6
Cagliari, Italy									
12725M002	7545	A1	CRL	−5.0	−0.1	−1.6	−1.0	0.3	0.9
12725M002	7545	A1	DGFI	22.4	−9.6	5.3	3.3	−0.4	0.9
12725S013	7548	A1	CRL	−13.0	−29.9	25.5	−3.5	10.2	3.6
12725S013	7548	A1	DGFI	3.9	−13.1	−2.2	0.9	9.4	3.9
12725S013	7548	A1	JCET	−21.8	9.7	−17.3	−13.9	−0.7	−13.3
Matera, Italy									
12734M004	7541	A1	CSR	19.3	5.2	−24.2	3.1	0.6	−2.3
12734M004	7541	A1	DGFI	12.4	10.2	−12.0	1.6	0.7	−1.7
12734S001	7939	A1	CRL	−4.3	1.8	−11.0	−0.8	1.0	3.1
12734S001	7939	A1	CSR	2.2	−0.7	−15.0	0.9	−0.1	−0.1
12734S001	7939	A1	DGFI	−4.1	0.3	10.2	−0.4	0.0	0.1
12734S001	7939	A1	JCET	−4.1	3.6	10.6	−1.5	−0.4	−1.9
Herstmonceux, UK									
13212S001	7840	A1	CRL	1.2	1.5	−1.3	−0.3	0.0	0.3
13212S001	7840	A1	CSR	1.0	0.3	6.4	0.6	−0.1	0.2
13212S001	7840	A1	DGFI	0.0	0.5	0.4	0.4	0.1	−0.1
13212S001	7840	A1	JCET	−0.1	−0.3	−3.3	0.0	−0.3	0.9
San Fernando, Spain									
13402S004	7824	A1	CRL	−17.4	−25.5	−24.0	23.8	15.1	7.9
13402S004	7824	A1	DGFI	−0.5	2.1	4.7	−1.2	7.6	−1.1
13402S004	7824	A1	JCET	0.7	−18.8	−2.6	−12.9	11.2	6.9
13402S007	7824	B1	CRL	−28.1	−9.3	−44.1	10.6	3.7	20.9
13402S007	7824	B1	DGFI	48.5	13.7	−42.8	−14.4	−3.8	11.9
Kootwijk, Netherlands									
13504M002	8833	A1	CSR	1.0	0.4	−21.7	0.7	−0.3	−3.4
13504M002	8833	A1	DGFI	−3.1	−5.7	1.9	−0.5	0.6	0.3
Zimmerwald, Switzerl.									
14001S001	7810	A1	CRL	0.4	−5.9	16.9	−1.1	−0.9	0.8
14001S001	7810	A1	CSR	1.1	0.2	11.5	0.7	0.0	−1.9
14001S001	7810	A1	DGFI	5.4	6.6	−7.0	0.1	0.4	−0.2
14001S001	7810	A1	JCET	0.5	−0.1	10.1	1.0	−0.1	1.2
14001S007	7810	B1	CRL	5.4	4.4	−5.6	−1.4	−1.4	−2.5
14001S007	7810	B1	DGFI	0.4	2.3	10.1	−0.2	−0.1	−1.7

continued

SLR intra-technique combination continued

Domes No.	CDP No.	Sol. No.	AC	△N	△E	△H	△vel$_N$	△vel$_E$	△vel$_H$
14001S007	7810	B1	JCET	−0.9	2.6	3.7	0.7	−0.4	−2.2
Potsdam, Germany									
14106S001	1181	A1	CRL	−2.2	2.0	55.5	−1.7	0.4	4.9
14106S001	1181	A1	DGFI	−24.1	−1.2	23.6	−2.8	−0.2	2.7
14106S009	7836	A1	CRL	2.9	1.6	0.7	1.1	0.3	1.9
14106S009	7836	A1	CSR	0.7	0.8	4.4	0.7	0.0	−0.2
14106S009	7836	A1	DGFI	0.7	0.4	−0.3	0.0	−0.4	−0.2
14106S009	7836	A1	JCET	−0.4	−0.7	−1.4	0.2	−0.2	0.6
Wettzell, Germany									
14201M005	7597	A1	CSR	−5.3	−2.0	9.5	−2.2	−0.3	6.5
14201M005	7597	A1	DGFI	−4.5	8.6	9.1	−3.6	−0.1	8.2
14201S002	7834	A1	CRL	−10.7	−2.3	−20.7	−1.0	−0.2	0.1
14201S002	7834	A1	DGFI	−14.5	8.8	8.5	−1.6	0.4	0.7
14201S018	8834	A1	CRL	1.9	1.4	4.1	0.2	0.1	0.3
14201S018	8834	A1	CSR	0.9	0.0	7.7	0.7	0.4	−0.8
14201S018	8834	A1	DGFI	0.8	1.7	−3.3	−0.7	0.6	0.8
14201S018	8834	A1	JCET	−0.1	0.5	2.4	0.4	−0.8	−0.5
Riyad, Saudi Arabia									
20101S001	7832	A1	CSR	2.1	−2.9	37.3	2.1	−5.6	−7.3
20101S001	7832	A1	DGFI	−2.9	5.6	1.0	−0.6	−0.5	0.4
Bar Giyyora, Israel									
20702M001	7530	A1	CRL	45.7	26.2	0.0	17.2	7.4	1.9
20702M001	7530	A1	CSR	7.9	−4.3	−2.0	1.4	−0.2	−2.2
Wuhan, China									
21602S003	7236	A1	CRL	−11.6	5.7	−0.4	−16.6	5.4	5.4
21602S003	7236	A1	CSR	14.7	−22.0	13.1	4.2	−3.6	−1.8
21602S003	7236	A1	JCET	18.6	10.6	−15.7	6.8	19.9	−12.9
Shanghai, China									
21605S001	7837	A1	CRL	0.6	2.1	−18.8	1.3	0.4	−3.1
21605S001	7837	A1	CSR	4.6	−3.7	0.7	1.7	−0.1	−3.1
21605S001	7837	A1	DGFI	−2.5	5.0	5.2	−1.3	0.5	1.3
21605S001	7837	A1	JCET	−7.2	3.2	6.8	2.1	0.4	−1.7
Changchun, China									
21611S001	7237	A1	CRL	−1.1	−6.7	1.7	2.3	0.6	−8.1
21611S001	7237	A1	CSR	−0.8	9.7	−12.5	1.1	−4.4	−7.0
21611S001	7237	A1	DGFI	1.7	−3.8	0.4	−0.2	1.1	2.0
21611S001	7237	A1	JCET	12.1	6.2	−7.4	−4.0	0.5	0.4
Koganei/Tokyo, Japan									
21704M001	7328	A1	CRL	3.3	−12.9	−4.9	−0.5	8.4	9.0
21704M001	7328	A1	CSR	0.5	14.4	−25.8	0.4	−4.6	7.0
21704M001	7328	A1	DGFI	33.3	−42.5	6.9	−1.0	0.6	−10.4
21704M001	7328	A1	JCET	−1.1	−44.3	−32.6	1.6	13.9	9.6
21704S002	7308	A1	CSR	−6.6	1.7	27.6	−0.4	0.9	8.4
21704S002	7308	A1	DGFI	1.1	−2.7	−7.8	−9.5	−14.9	11.5
21704S002	7308	A1	JCET	5.2	1.8	35.8	10.5	0.3	−4.7
Simosato, Japan									
21726S001	7838	A1	CRL	1.7	4.4	40.7	3.3	−0.2	2.9
21726S001	7838	A1	CSR	0.5	−0.6	15.5	0.5	0.4	−2.8
21726S001	7838	A1	DGFI	1.9	−2.6	−19.3	0.1	−0.5	−0.9

continued

SLR intra-technique combination continued

Domes No.	CDP No.	Sol. No.	AC	△N	△E	△H	△vel$_N$	△vel$_E$	△vel$_H$
Muira, Japan									
21739M001	7337	A1	CRL	−19.1	4.5	−15.8	8.3	1.5	17.1
21739M001	7337	A1	CSR	11.5	7.8	−19.6	−2.8	−2.5	11.9
21739M001	7337	A1	DGFI	−26.0	−9.1	−22.2	9.7	4.7	4.1
Tateyama, Japan									
21740M001	7339	A1	CRL	−1.4	−17.3	−3.1	1.8	7.5	3.5
21740M001	7339	A1	CSR	3.3	10.2	−1.9	−0.1	−3.1	0.4
Helwan, Egypt									
30101S001	7831	A1	CRL	−3.3	−3.5	0.5	−3.1	0.8	−4.2
30101S001	7831	A1	CSR	1.8	−1.6	22.0	0.9	0.4	3.6
30101S001	7831	A1	DGFI	4.4	−8.4	−6.6	1.9	−2.4	−0.3
30101S001	7831	A1	JCET	−2.6	2.9	−10.8	1.1	−3.2	−4.1
Hartebeesth, S Afr.									
30302M003	7501	A1	DGFI	−1.6	3.7	2.1	−0.2	−0.4	0.7
Albuquerque, USA									
40429S001	7884	A1	DGFI	−1.3	13.0	−1.7	0.7	7.5	0.7
40429S001	7884	A1	JCET	−2.2	−4.2	−3.1	−2.0	−0.4	−5.0
Quincy, USA									
40433M002	7109	A1	CRL	−0.8	−1.1	−2.3	1.2	−0.4	−0.8
40433M002	7109	A1	CSR	2.4	0.3	5.4	0.2	0.0	0.1
40433M002	7109	A1	DGFI	2.9	2.2	−2.9	0.1	0.2	−0.3
40433M002	7109	A1	JCET	0.2	−4.0	−5.2	1.1	0.4	−2.4
Fort Davis, USA									
40442M001	7086	A1	CSR	1.4	−16.5	−32.1	0.2	−1.4	1.1
40442M001	7086	A1	DGFI	5.3	−8.2	16.2	−0.4	−0.7	0.9
40442M006	7080	A1	CRL	−0.7	0.3	−4.7	0.4	−0.2	0.3
40442M006	7080	A1	CSR	2.6	0.1	−11.7	0.3	0.0	0.6
40442M006	7080	A1	DGFI	0.6	1.2	4.3	−0.2	0.6	−0.5
40442M006	7080	A1	JCET	−2.4	−2.4	−1.8	0.5	0.9	0.1
Maui, USA									
40445M001	7210	A1	CRL	−1.9	0.6	1.3	1.6	−1.1	3.0
40445M001	7210	A1	CSR	2.2	0.6	4.7	0.4	0.2	−0.2
40445M001	7210	A1	JCET	−1.3	−4.8	−0.1	0.3	0.2	−0.9
Washington, USA									
40451M105	7105	A1	CRL	0.1	−0.7	0.7	0.3	−0.6	0.7
40451M105	7105	A1	CSR	2.5	0.7	−2.4	0.3	−0.1	1.6
40451M105	7105	A1	DGFI	0.3	0.5	−1.9	0.1	0.2	−0.6
40451M105	7105	A1	JCET	−2.7	−2.9	−0.9	1.0	0.7	1.2
40451M117	7920	A1	CSR	19.3	2.8	27.5	2.7	0.3	5.4
40451M117	7920	A1	DGFI	13.3	6.1	24.5	2.5	0.6	3.2
40451M117	7920	A1	JCET	4.6	−0.1	12.1	3.4	1.1	5.1
40451M120	7918	A1	CRL	1.6	−2.4	0.0	0.5	−0.2	−0.1
40451M120	7918	A1	CSR	6.6	2.8	−7.5	2.2	0.4	2.4
40451M120	7918	A1	DGFI	5.8	7.1	−0.7	1.9	0.8	0.2
40451M120	7918	A1	JCET	1.6	−1.4	2.9	3.0	1.2	2.1
Monument Peak, USA									
40497M001	7110	A1	CRL	−1.0	−0.1	−1.7	0.6	0.0	0.5
40497M001	7110	A1	CSR	2.4	0.0	−1.6	0.3	0.0	−0.8
40497M001	7110	A1	DGFI	1.1	2.3	−1.9	−0.3	−0.2	0.0
40497M001	7110	A1	JCET	−0.9	−1.9	4.1	−0.3	1.2	0.6

continued

SLR intra-technique combination continued

Domes No.	CDP No.	Sol. No.	AC	△N	△E	△H	△vel$_N$	△vel$_E$	△vel$_H$
Richmond, USA									
40499M002	7295	A1	CRL	12.5	−0.9	1.8	5.0	−0.9	0.4
40499M002	7295	A1	CSR	−2.8	−1.2	−10.8	−1.0	0.2	−3.3
40499M002	7295	A1	DGFI	14.4	1.2	−4.4	2.2	0.3	−0.7
Mazatlan, Mexico									
40504M001	7122	A1	CRL	27.1	5.7	−6.2	4.5	0.8	1.7
40504M001	7122	A1	CSR	−0.6	0.9	−43.6	0.0	0.0	−4.3
40504M001	7122	A1	DGFI	6.7	4.9	20.2	0.8	0.7	2.1
Cabo San Lucas, Mex.									
40505M001	7882	A1	CRL	13.6	20.2	−2.6	4.1	5.9	0.4
40505M001	7882	A1	CSR	−7.0	4.3	−3.0	−1.3	0.0	−4.4
40505M001	7882	A1	DGFI	20.0	−15.0	18.1	3.6	−2.2	2.4
Ensenada, Mexico									
40506M001	7883	A1	CRL	−36.1	13.3	3.3	−7.1	2.3	2.0
40506M001	7883	A1	CSR	23.7	−3.6	−11.5	4.2	−0.5	−4.0
40506M001	7883	A1	DGFI	0.5	2.7	17.7	0.1	0.5	2.2
Easter Island, Chile									
41703M002	7097	A1	CRL	5.9	0.4	−6.4	1.1	−1.9	1.0
41703M002	7097	A1	DGFI	−5.9	−3.1	4.6	−0.8	0.5	−0.1
Arequipa, Peru									
42202M003	7403	A1	CRL	2.2	2.7	1.5	−1.2	−0.3	−0.9
42202M003	7403	A1	CSR	2.1	0.9	8.6	0.1	−0.1	−1.9
42202M003	7403	A1	DGFI	−2.0	1.8	0.5	−0.2	−0.4	0.9
42202M003	7403	A1	JCET	−1.6	−4.3	−2.4	1.4	1.7	−1.5
42202S001	7907	A1	CRL	15.4	−36.8	−5.3	1.6	−7.1	0.2
42202S001	7907	A1	DGFI	−15.2	13.3	22.6	−1.2	1.3	2.4
Orroral, Australia									
50103S007	7843	A1	CRL	−5.7	2.7	13.5	3.2	−1.3	0.3
50103S007	7843	A1	DGFI	1.0	−2.9	−0.3	−0.8	−1.1	−3.0
50103S007	7843	A1	JCET	1.1	0.0	2.8	0.1	0.5	0.3
Yarragadee, Australia									
50107M001	7090	A1	CRL	−5.0	−0.2	−3.0	3.5	0.4	1.6
50107M001	7090	A1	CSR	0.5	−1.1	−4.1	0.9	0.2	−0.1
50107M001	7090	A1	DGFI	0.2	1.2	0.4	−0.8	−0.1	−0.1
50107M001	7090	A1	JCET	−0.5	1.2	7.1	−0.1	0.2	−0.3
Mt Stromlo, Australia									
50119S001	7849	A1	CRL	19.1	−2.9	−1.2	−7.1	−0.2	2.8
50119S001	7849	A1	CSR	0.2	−6.1	−15.1	0.8	2.4	6.7
50119S001	7849	A1	DGFI	−6.9	−5.0	1.0	1.8	0.8	0.0
50119S001	7849	A1	JCET	−5.2	7.3	−18.0	1.6	−1.8	6.1
Papeete, Societe Isl.									
92201M007	7124	A1	CRL	0.5	0.0	2.3	−2.1	−1.6	−2.2
92201M007	7124	A1	CSR	4.6	5.5	21.4	0.6	−1.8	−8.6
92201M007	7124	A1	DGFI	−8.4	−4.3	1.9	1.8	2.0	0.6
Huahine, Societe Isl.									
92202M004	7123	A1	CRL	−3.8	−3.9	31.9	2.1	−3.3	7.3
92202M004	7123	A1	CSR	3.8	1.1	22.6	0.8	−0.1	0.5
92202M004	7123	A1	DGFI	8.5	−13.1	9.8	0.6	−1.5	0.9

F DORIS intra-technique combination

Tab. F.1 : *This table shows the DORIS stations used for the intra-technique combinations. Some outliers were rejected in the individual solutions (see $-^1$). The last column denotes the DORIS reference frame stations.*
$-^1$: The estimated station position of a particular solution differs by more than 7 cm (absolute value) from the mean of the other solutions (see chapter 5.4).

DORIS stations used for intra-technique combination

Domes No.	4-CHID	Sol. No.	Site Name	GRGS	IGN	used	RF
10003S001	TLSA	A1	Toulouse, France	*	*	*	*
10003S003	TLHA	A1	Toulouse, France	*	*	*	*
10202S001	REYA	A1	Reykjavik, Iceland	*	*	*	*
10202S002	REYB	A1	Reykjavik, Iceland	*	*	*	*
10317S002	SPIA	A1	Ny-Alesund, Norway	*	*	*	*
10503S013	META	A1	Metsahovi, Finland	*	*	*	*
12334S004	KITA	A1	Kitab, Uzbekistan	*	*	*	*
12334S005	KITB	A1	Kitab, Uzbekistan	$-^1$	$-^1$	–	
12338S001	BADA	A1	Badary, Russia	*	*	*	*
12602S011	DIOA	A1	Dionysos, Greece	*	*	*	
21501S001	EVEB	A1	Everest, Nepal	*	*	*	
21604S003	PURA	A1	Purple Mountain, China	$-^1$	$-^1$	–	
22006S001	MANA	A1	Manila, The Philippines	*	*	*	*
23101S001	CIBB	A1	Cibinong, Indonesia	$-^1$	$-^1$	–	
30302S005	HBLA	A1	Hartebeesthoek, S. Afr.	*	*	*	
30302S202	HBKA	A1	Hartebeesthoek, S. Afr.	*	*	*	
30313S001	MARA	A1	Marion Isl., S. Africa	*	*	*	*
30604S001	TRIA	A1	Tristan da Cunha, UK	*	*	*	*
30606S002	HELA	A1	Sainte-Helene, UK	*	*	*	
30606S003	HELB	A1	Sainte-Helene, UK	*	*	*	
31903S001	SAMB	A1	Santa Maria, Portugal	*	*	*	*
32809S002	LIBA	A1	Libreville, Gabun	*	*	*	*
33710S002	ARMA	A1	Arlit, Niger	*	*	*	*
34101S004	DAKA	A1	Dakar, Senegal	*	*	*	*
39901S002	DJIA	A1	Djibouti, Djibouti	*	*	*	
40102S009	OTTA	A1	Ottawa, Canada	*	*	*	*
40102S011	OTTB	A1	Ottawa, Canada	*	*	*	*
40127S007	YELA	A1	Yellowknife, Canada	*	*	*	*
40405S005	GOMA	A1	Goldstone, USA	*	*	*	

continued

DORIS intra-technique combination continued

Domes No.	4-CHAR	Sol. No.	Site Name	GRGS	IGN	used	RF
40405S035	GOLA	A1	Goldstone, USA	*	*	*	
40405S037	GOMB	A1	Goldstone, USA	*	*	*	
40408S004	FAIA	A1	Fairbanks, USA	*	*	*	*
40424S008	KOKA	A1	Kauai (Hawaii), USA	*	*	*	*
40499S016	RIDA	A1	Richmond, USA	*	*	*	
41507S003	RIOA	A1	Rio Grande, Argentina	*	*	*	*
41507S004	RIOB	A1	Rio Grande, Argentina	*	*	*	*
41609S001	CACB	A1	Cachoeira, Brazil	–[1]	–[1]	–	
41703S008	EASA	A1	Easter Island, Chile	*	*	*	*
41705S007	SANA	A1	Santiago, Chile	–[1]	–[1]	–	
41705S008	SAOB	A1	Santiago, Chile	*	*	*	*
41708S001	IQUB	A1	Iquique, Chile	–[1]	–[1]	–	
42004S001	GALA	A1	San Cristobal, Ecuador	*	*	*	
42202S005	AREA	A1	Arequipa, Peru	*	*	*	
50103S201	ORRA	A1	Canberra, Australia	*	*	*	
50103S202	ORRB	A1	Canberra, Australia	*	*	*	
50107S006	YARA	A1	Yarragadee, Australia	*	*	*	*
50501S001	GUAB	A1	Guam, USA	*	*	*	*
51001S001	MORA	A1	Port Moresby, Papua	–[1]	–[1]	–	
66006S001	SYOB	A1	Syowa, Antartica	*	*	*	*
66007S001	ROTA	A1	Rothera, Antartica	*	*	*	*
91201S002	KERA	A1	Kerguelen Islands	*	*	*	
91201S003	KERB	A1	Kerguelen Islands	*	*	*	*
91401S001	AMSA	A1	Amsterdam Islands	*	*	*	
91501S001	ADEA	A1	Ile des Petrels, Adelie	*	*	*	*
92201S007	PAPB	A1	Papeete, Tahiti	*	*	*	*
92201S008	PAQB	A1	Papeete, Tahiti	–[1]	–[1]	–	
92403S001	RAQB	A1	Rapa, Tubai Islands	*	*	*	
92701S001	NOUA	A1	Noumea, New Caledonia	*	*	*	*
92722S001	LIFB	A1	Ile Lifou, New Caledonia	–[1]	–[1]	–	
92901S001	WALA	A1	Wallis	*	*	*	*
97301S004	KRUB	A1	Kourou, French Guiana	*	*	*	*
97401S001	REUA	A1	La Reunion, Reunion	*	*	*	*
97401S002	REUB	A1	La Reunion, Reunion	*	*	*	

Tab. F.2 : *This table shows the DORIS station position and velocity residuals (north, east, up) of the individual solutions w.r.t. the combined intra-technique solution. Units are [mm] and [mm/yr].*

DORIS intra-technique combination results

Domes No.	4-CHID	Sol. No.	AC	△N	△E	△H	△vel$_N$	△vel$_E$	△vel$_H$
Toulouse, France									
10003S001	TLSA	A1	IGN	−4.9	−8.7	−1.6	2.4	2.2	0.3
10003S001	TLSA	A1	GRGS	7.1	15.4	4.7	2.3	2.1	1.3
10003S003	TLHA	A1	IGN	−13.3	−4.7	−3.3	2.5	2.2	0.4
10003S003	TLHA	A1	GRGS	8.5	10.2	5.3	2.5	2.1	1.3
Reykjavik, Iceland									
10202S001	REYA	A1	IGN	−0.5	11.1	0.0	−2.8	2.8	0.3
10202S001	REYA	A1	GRGS	−0.9	0.1	1.2	−1.7	2.1	1.1
10202S002	REYB	A1	IGN	−21.4	44.2	6.8	5.8	−3.5	−2.4
10202S002	REYB	A1	GRGS	−9.6	23.8	18.1	−2.0	2.3	1.2
Ny-Alesund, Norway									
10317S002	SPIA	A1	IGN	1.8	−1.7	−2.5	2.3	−1.5	−0.8
10317S002	SPIA	A1	GRGS	0.0	1.4	−0.7	−0.4	−0.2	−0.4
Metsahovi, Finland									
10503S013	META	A1	IGN	6.6	3.5	8.9	0.6	0.3	−0.4
10503S013	META	A1	GRGS	−8.5	−3.7	−13.7	−2.1	1.1	−4.4
Kitab, Uzbekistan									
12334S004	KITA	A1	IGN	40.4	−11.6	0.4	−1.1	−1.6	−2.0
12334S004	KITA	A1	GRGS	−10.1	8.6	−1.9	1.1	1.6	1.2
Badary, Russia									
12338S001	BADA	A1	IGN	−3.0	−13.9	−0.1	−1.0	2.2	0.0
12338S001	BADA	A1	GRGS	3.7	10.8	1.9	2.7	−1.0	2.1
Dionysos, Greece									
12602S011	DIOA	A1	IGN	4.3	−1.3	−10.5	−0.9	2.0	2.7
12602S011	DIOA	A1	GRGS	−5.6	−4.8	3.2	−0.8	−0.2	−4.4
Everest, Nepal									
21501S001	EVEB	A1	IGN	−7.4	−10.3	14.9	0.7	3.1	−2.7
21501S001	EVEB	A1	GRGS	4.4	12.2	−14.8	0.7	−1.4	−0.6
Manila, The Philippines									
22006S001	MANA	A1	IGN	26.3	−3.3	7.6	−4.2	1.4	−0.5
22006S001	MANA	A1	GRGS	−26.8	6.5	−11.5	−6.4	−2.0	−3.1
Hartebeesthoek, S. Afr.									
30302S005	HBLA	A1	IGN	−5.3	−0.7	−3.4	1.9	−1.4	7.6
30302S005	HBLA	A1	GRGS	−2.9	23.6	−22.8	−0.3	2.2	−5.0
30302S202	HBKA	A1	IGN	15.2	24.2	0.6	−0.8	2.6	−3.6
30302S202	HBKA	A1	GRGS	−9.0	−13.5	−14.7	−0.3	2.1	−4.9
Marion Isl., S. Africa									
30313S001	MARA	A1	IGN	0.4	5.5	3.8	−1.1	0.7	−0.8
30313S001	MARA	A1	GRGS	−2.9	−7.2	−3.7	−0.3	−0.2	0.8
Tristan da Cunha, UK									
30604S001	TRIA	A1	IGN	−7.2	−14.5	9.5	0.3	2.7	−1.1
30604S001	TRIA	A1	GRGS	6.5	22.4	−14.8	1.5	1.4	−3.0
Sainte-Helene, UK									
30606S002	HELA	A1	IGN	4.3	−12.6	0.9	7.9	−4.6	2.1
30606S002	HELA	A1	GRGS	13.2	−2.0	6.2	4.3	−1.2	1.6
30606S003	HELB	A1	IGN	−16.1	−32.4	15.3	1.9	8.6	−3.6

continued

DORIS intra-technique combination continued

Domes No.	4-Ch ID	Sol. No.	AC	△N	△E	△H	△vel$_N$	△vel$_E$	△vel$_H$
30606S003	HELB	A1	GRGS	17.0	14.3	−2.6	4.5	−1.2	1.6
Santa Maria, Portugal									
31903S001	SAMB	A1	IGN	17.6	4.9	−17.4	−4.1	−7.9	−1.3
31903S001	SAMB	A1	GRGS	−11.5	−11.5	16.2	0.4	6.0	−1.1
Libreville, Gabun									
32809S002	LIBA	A1	IGN	−15.4	−8.8	0.4	−0.8	0.6	−1.8
32809S002	LIBA	A1	GRGS	6.2	8.9	0.6	0.2	2.6	1.7
Arlit, Niger									
33710S002	ARMA	A1	IGN	−11.1	−1.2	8.3	0.5	2.4	0.3
33710S002	ARMA	A1	GRGS	4.1	4.1	−8.5	−0.1	−1.0	0.2
Dakar, Senegal									
34101S004	DAKA	A1	IGN	−2.7	−4.5	−2.5	1.4	2.3	−0.6
34101S004	DAKA	A1	GRGS	2.4	6.6	5.2	−0.6	0.3	2.1
Djibouti, Djibouti									
39901S002	DJIA	A1	IGN	15.0	14.0	6.9	−0.1	−1.7	−0.2
39901S002	DJIA	A1	GRGS	−11.9	−21.5	−9.8	−3.0	−0.4	−1.8
Ottawa, Canada									
40102S009	OTTA	A1	IGN	31.7	17.3	14.6	−3.3	−0.2	5.5
40102S009	OTTA	A1	GRGS	−14.4	−21.6	−16.3	−3.0	−1.0	−5.6
40102S011	OTTB	A1	IGN	28.3	9.0	−18.4	−3.4	−0.2	5.5
40102S011	OTTB	A1	GRGS	−13.2	−18.0	9.5	−3.1	−1.0	−5.6
Yellowknife, Canada									
40127S007	YELA	A1	IGN	0.1	−14.0	−0.7	0.7	0.6	−1.1
40127S007	YELA	A1	GRGS	−0.4	12.9	1.7	−0.2	2.3	1.6
Goldstone, USA									
40405S005	GOMA	A1	IGN	−5.4	−4.7	12.3	1.0	1.8	−0.9
40405S005	GOMA	A1	GRGS	4.0	10.3	−10.8	1.7	0.3	0.1
40405S035	GOLA	A1	IGN	−0.5	23.7	3.2	1.0	1.8	−0.9
40405S035	GOLA	A1	GRGS	6.1	−16.4	−3.4	1.7	0.3	0.1
40405S037	GOMB	A1	IGN	−2.3	−6.7	1.3	1.0	1.8	−0.9
40405S037	GOMB	A1	GRGS	−2.5	8.1	−4.9	1.7	0.4	0.1
Fairbanks, USA									
40408S004	FAIA	A1	IGN	−30.4	23.3	−3.0	1.2	−2.2	−1.7
40408S004	FAIA	A1	GRGS	10.3	−27.3	1.2	0.5	0.4	1.1
Kauai (Hawaii), USA									
40424S008	KOKA	A1	IGN	−11.2	−2.8	2.6	2.1	0.7	−0.7
40424S008	KOKA	A1	GRGS	5.6	6.5	−7.4	0.9	1.0	−2.4
Richmond, USA									
40499S016	RIDA	A1	IGN	26.8	15.1	−8.0	−3.1	−1.4	−0.2
40499S016	RIDA	A1	GRGS	−16.2	−23.5	15.3	−4.4	−1.4	3.6
Rio Grande, Argentina									
41507S003	RIOA	A1	IGN	−11.2	16.7	4.2	0.0	−1.1	1.3
41507S003	RIOA	A1	GRGS	4.5	−8.7	2.3	0.3	0.6	0.5
41507S004	RIOA	A1	IGN	−6.7	10.6	−6.9	−0.1	−1.1	1.4
41507S004	RIOA	A1	GRGS	0.8	−2.5	3.6	0.3	0.6	0.5
Easter Island, Chile									
41703S008	EASA	A1	IGN	−1.6	14.2	−2.4	−0.4	−3.2	−2.5
41703S008	EASA	A1	GRGS	−0.8	−13.0	10.1	−0.8	1.7	6.3
Santiago, Chile									
41705S008	SAOB	A1	IGN	19.5	4.4	5.8	−9.4	1.6	−2.1
41705S008	SAOB	A1	GRGS	−5.9	−13.3	−6.8	7.1	−7.7	−0.9

continued

DORIS intra-technique combination continued

Domes No.	4-Ch ID	Sol. No.	AC	△N	△E	△H	△vel$_N$	△vel$_E$	△vel$_H$
Arequipa, Peru									
42202S005	AREA	A1	IGN	−8.3	12.9	18.0	1.4	−0.9	−5.4
42202S005	AREA	A1	GRGS	3.2	−24.8	−23.5	−1.4	−8.0	−0.3
Canberra, Australia									
50103S201	ORRA	A1	IGN	15.0	17.2	23.4	6.6	4.6	13.7
50103S201	ORRA	A1	GRGS	−11.0	−12.2	−35.1	−4.0	−2.6	−18.7
50103S202	ORRB	A1	IGN	20.4	14.4	−34.9	−6.5	−28.1	44.6
50103S202	ORRB	A1	GRGS	−8.6	4.6	18.0	−4.0	−2.6	−18.7
Yarragadee, Australia									
50107S006	YARA	A1	IGN	1.5	10.2	−8.3	−0.3	1.5	−1.9
50107S006	YARA	A1	GRGS	−1.8	−15.6	11.4	0.0	−3.5	4.3
Guam, USA									
50501S001	GUAB	A1	IGN	6.6	13.6	3.8	−1.4	−2.9	−0.3
50501S001	GUAB	A1	GRGS	−8.0	−23.2	−4.8	−0.8	−2.3	−0.6
Syowa, Antartica									
66006S001	SYOB	A1	IGN	−16.6	−12.2	−14.1	−4.9	0.3	1.1
66006S001	SYOB	A1	GRGS	4.7	3.9	12.8	2.0	0.5	−0.6
Rothera, Antartica									
66007S001	ROTA	A1	IGN	−12.2	12.6	−1.5	1.8	−0.6	−0.4
66007S001	ROTA	A1	GRGS	4.5	1.9	5.5	0.0	0.7	3.0
Kerguelen Islands									
91201S002	KERA	A1	IGN	6.5	−14.2	3.3	1.2	2.1	1.2
91201S002	KERA	A1	GRGS	−2.2	24.1	−22.1	0.6	1.8	−7.3
91201S003	KERB	A1	IGN	−3.0	−10.7	3.7	1.2	2.1	1.2
91201S003	KERB	A1	GRGS	0.8	9.8	−7.8	0.6	1.8	−7.3
Amsterdam Islands									
91401S001	AMSA	A1	IGN	−2.1	1.4	18.1	0.7	9.1	10.5
91401S001	AMSA	A1	GRGS	−1.8	−8.5	−3.6	−0.8	−9.9	−4.4
Ile des Petrels, Adelie									
91501S001	ADEA	A1	IGN	3.7	−8.4	3.0	1.1	1.9	−0.7
91501S001	ADEA	A1	GRGS	−6.3	−8.6	−2.1	−1.5	−4.4	1.1
Papeete, Tahiti									
92201S007	PAPB	A1	IGN	1.9	−14.6	−1.2	2.6	0.8	−2.8
92201S007	PAPB	A1	GRGS	−0.8	18.2	0.5	−1.5	1.0	1.6
Rapa, Tubai Islands									
92403S001	PAQB	A1	IGN	9.2	4.1	4.0	−1.8	−0.1	−1.0
92403S001	PAQB	A1	GRGS	−5.2	−7.6	−1.5	2.2	−0.4	−6.4
Noumea, New Caledonia									
92701S001	NOUA	A1	IGN	14.4	−11.8	1.9	−0.6	2.9	0.0
92701S001	NOUA	A1	GRGS	−16.8	16.4	−2.6	−3.8	−3.3	−0.7
Wallis									
92901S001	WALA	A1	IGN	−7.3	−1.4	−2.2	0.4	0.8	−1.3
92901S001	WALA	A1	GRGS	6.9	0.3	8.7	2.3	−2.0	5.1
Kourou, French Guiana									
97301S004	KRUB	A1	IGN	−5.4	9.9	−5.8	2.5	−0.1	−0.5
97301S004	KRUB	A1	GRGS	−1.9	−18.4	12.8	−4.2	−4.0	5.0
La Reunion, Reunion									
97401S001	REUA	A1	IGN	4.7	−0.2	15.4	−2.2	−1.8	1.3
97401S001	REUA	A1	GRGS	−5.2	−5.0	−16.1	0.3	−0.4	−2.4
97401S002	REUB	A1	IGN	−4.9	−27.6	−6.4	1.3	7.7	2.4
97401S002	REUB	A1	GRGS	−3.5	−40.2	−29.0	0.2	−0.5	−2.5

G Inter-technique combination

Tab. G.1: *This table shows the station velocities for different techniques at co-location sites in north, east, up [mm], along with their standard deviations in [mm/yr]. Note that the standard deviations are referred to the variance level of the inter-technique combination by applying the scale factors displayed in table 6.1.*
[1]: R = *VLBI*, P = *GPS*, L = *SLR*, D = *DORIS*.

Station velocities at co-location sites

Domes No.	ID	Sol. No.	T[1]	Data time span	$\triangle t$	vel_N	vel_E	vel_H	$\sigma_{\mathrm{vel}N}$	$\sigma_{\mathrm{vel}E}$	$\sigma_{\mathrm{vel}H}$
Grasse, France											
10002M006	GRAS	A1	P	1996.0 - 2003.0	7.0	15.0	20.0	−0.8	0.9	0.8	0.9
10002S001	7835	A1	L	1984.0 - 2002.7	18.7	15.0	19.7	−2.2	1.1	1.0	1.1
10002S002	7845	A1	L	1998.0 - 2002.7	4.7	13.2	19.2	0.8	8.2	6.7	8.3
Toulouse, France											
10003M004	TOUL	A1	P	1997 - 2001	3.6	15.6	18.8	1.2	1.4	0.9	1.4
10003M009	TLSE	A1	P	2001 - 2003	1.8	13.4	19.5	−0.2	4.2	1.3	4.2
10003S001	TLSA	A1	D	1993.0 - 1997.6	4.6	13.3	16.5	−1.4	1.4	2.1	1.4
10003S003	TLHA	A1	D	1997.6 - 2003.0	5.4	13.1	16.5	−1.5	1.4	2.1	1.4
Reykjavik, Iceland											
10202M001	REYK	A1	P	1996.0 - 2003.0	7.0	21.2	−11.2	−2.9	0.8	0.8	0.7
10202S001	REYA	A1	D	1993.0 - 1998.7	5.6	21.4	−12.6	−3.3	1.4	1.5	1.2
10202S002	REYB	A1	D	1998.7 - 2003.0	4.2	21.7	−12.7	−3.4	1.4	1.5	1.3
Tromsoe, Norway											
10302M002	7602	A1	R	1989 - 1992	3.1	13.3	26.1	6.0	13.2	8.1	23.7
10302M003	TROM	A1	P	1996.0 - 2003.0	7.0	14.8	15.3	1.1	0.9	0.8	0.7
10302M006	TRO1	A1	P	1996.0 - 2003.0	7.0	15.8	16.8	2.2	0.9	0.8	0.8
Ny-Alesund, Norway											
10317M001	NYAL	A1	P	1996.0 - 2003.0	7.0	14.5	10.9	7.1	0.9	0.8	0.8
10317M003	NYA1	A1	P	1996.0 - 2003.0	7.0	14.5	10.2	5.9	0.9	0.8	0.9
10317S002	SPIA	A1	D	1993.0 - 1999.2	6.2	16.0	6.8	3.9	1.2	1.1	0.8
10317S003	7331	A1	R	1994 - 2000	6.0	14.1	10.4	5.2	0.5	0.4	0.8
Onsala, Sweden											
10402M004	ONSA	A1	P	1996.0 - 2003.0	7.0	14.1	17.2	0.0	0.8	0.8	0.8
10402S002	7213	A1	R	1980 - 2000	20.0	13.5	17.3	3.0	0.4	0.4	0.5
Metsahovi, Finland											
10503S011	METS	A1	P	1996.0 - 2003.0	7.0	12.0	20.2	3.2	0.8	0.8	0.8
10503S013	META	A1	D	1993.0 - 2000.8	7.8	14.7	19.2	4.9	1.3	1.4	1.2
10503S014	7806	A1	L	1998.2 - 2002.5	4.3	12.7	18.1	8.6	22.9	21.9	21.5

continued

Station velocities at co-location sites continued

Domes No.	ID	Sol. No.	T[1]	Data time span	$\triangle t$	vel_N	vel_E	vel_H	$\sigma_{\mathrm{vel}N}$	$\sigma_{\mathrm{vel}E}$	$\sigma_{\mathrm{vel}H}$
Graz, Austria											
11001M002	GRAZ	A1	P	1996.0 - 2003.0	7.0	14.3	21.4	−0.5	0.8	0.8	0.8
11001S002	7839	A1	L	1983.7 - 2002.7	18.9	14.2	21.4	−1.0	0.9	0.7	0.9
Borowiec, Poland											
12205M002	BOR1	A1	P	1996.0 - 2003.0	7.0	13.9	20.7	−1.3	0.8	0.8	0.8
12205S001	7811	A1	L	1988.5 - 2002.6	14.2	12.2	19.4	−0.4	4.0	3.6	3.9
Kitab, Uzbekistan											
12334M001	KIT3	A1	P	1996.0 - 2003.0	7.0	3.7	27.8	−3.2	0.8	0.9	0.8
12334S004	KITA	A1	D	1993.0 - 1996.4	3.4	2.9	30.6	3.8	2.5	3.4	2.6
Simeiz, Ukraine											
12337S003	1873	A1	L	1989.2 - 2002.6	13.4	9.5	16.5	0.1	18.7	20.0	18.8
12337S006	1893	A1	L	1988.8 - 2002.6	13.9	6.7	26.3	−1.1	8.0	7.6	8.0
12337S008	7332	A1	R	1994 - 2000	5.9	11.6	24.9	1.7	2.3	1.7	2.3
Yakutzk, Russia											
12353M001	YAKA	A1	P	1998.2 - 1999.5	1.3	−11.8	21.0	−3.2	1.0	0.9	1.1
12353M002	YAKT	A1	P	1996.0 - 2003.0	7.0	−12.9	18.8	2.5	1.7	1.5	2.1
Petropavlovsk, Russia											
12355M001	PETR	A1	P	1996 - 1999	3.5	−4.3	9.7	39.1	11.1	6.4	11.8
12355M002	PETP	A1	P	1996.0 - 2003.0	7.0	−9.3	−5.3	−0.4	0.9	0.8	0.9
Dionysos, Greece											
12602M002	7515	A1	L	1986.6 - 1992.5	5.9	−12.9	6.2	−5.4	15.6	12.5	15.5
12602S011	DIOA	A1	D	1993.4 - 1995.2	1.8	−7.5	3.8	−1.7	1.3	1.7	1.3
Medicina, Italy											
12711M003	MEDI	A1	P	1996.0 - 2003.0	7.0	16.9	22.3	−3.6	0.9	0.9	0.9
12711S001	7230	A1	R	1987 - 1996	8.2	16.1	22.7	−3.5	0.9	0.5	0.9
12711S001	7230	A2	R	1996 - 2000	3.5	16.1	22.7	−3.5	0.9	0.5	0.9
Noto, Italy											
12717M001	7543	A1	L	1990.9 - 1993.8	2.9	13.9	26.2	−10.5	19.9	15.7	21.0
12717M003	NOTO	A1	P	1996 - 2000	4.7	17.3	20.0	−6.7	1.0	0.9	1.0
12717M004	NOT1	A1	P	2000 - 2003	2.3	18.3	21.8	−1.1	2.3	1.4	2.4
12717S001	7547	A1	R	1989 - 2000	11.0	18.3	21.9	−1.2	0.9	0.6	0.9
Cagliari, Italy											
12725M002	7545	A1	L	1985.9 - 1994.2	8.4	12.7	22.9	−2.6	7.0	5.1	7.1
12725M003	CAGL	A1	P	1996.0 - 2003.0	7.0	14.6	22.5	−5.2	0.9	0.9	0.9
12725S013	7548	A1	L	1994.7 - 2001.9	7.2	15.2	13.0	−5.2	19.6	18.0	20.1
Matera, Italy											
12734M004	7541	A1	L	1986.0 - 1994.5	8.4	15.7	22.8	1.2	8.7	6.6	8.9
12734M008	MATE	A1	P	1996.0 - 2003.0	7.0	17.8	24.4	0.4	0.8	0.8	0.9
12734S001	7939	A1	L	1983.7 - 2001.0	17.3	17.9	23.4	−1.0	1.5	1.0	1.5
12734S005	7243	A1	R	1990 - 2000	9.9	17.9	23.7	−0.6	0.7	0.5	0.6
Herstmonceux, UK											
12312M007	HERS	A1	P	1996.0 - 2003.0	7.0	16.1	18.9	−0.4	0.9	0.8	0.8
12312S001	7840	A1	L	1983.8 - 2002.7	18.9	15.0	17.2	0.0	0.9	0.6	0.9
San Fernando, Spain											
13402M004	SFER	A1	P	1996.0 - 2003.0	7.0	14.1	17.7	1.3	1.0	0.9	1.1

continued

Station velocities at co-location sites continued

Domes No.	ID	Sol. No.	T[1]	Data time span	$\triangle t$	vel_N	vel_E	vel_H	$\sigma_{\mathrm{vel}N}$	$\sigma_{\mathrm{vel}E}$	$\sigma_{\mathrm{vel}H}$
13402S004	7824	A1	L	1995.4 - 1999.0	3.6	11.9	10.5	16.1	80.4	75.0	78.2
13402S007	7824	B1	L	1999.2 - 2002.7	3.5	25.1	21.9	3.1	45.2	39.2	47.5
Madrid, Spain											
13407S010	1565	A1	R	1988 - 1996	8.3	15.7	18.8	2.3	1.3	0.6	1.3
13407S010	1565	A2	R	1997 - 1999	2.0	15.7	18.8	2.3	1.3	0.6	1.3
13407S012	MADR	A1	P	1996.0 - 2003.0	7.0	15.4	18.3	−2.5	0.8	0.8	0.8
Kootwijk, Netherlands											
13504M002	8833	A1	L	1984.3 - 1995.7	11.3	11.5	19.6	−5.4	11.5	11.4	11.3
13504M003	KOSG	A1	P	1996.0 - 2003.0	7.0	15.6	17.8	−0.1	0.8	0.8	0.8
Zimmerwald, Switzerlan											
14001M004	ZIMM	A1	P	1996.0 - 2003.0	7.0	14.7	20.9	−3.9	0.8	0.8	0.8
14001S001	7810	A1	L	1984.4 - 1995.3	10.9	14.3	19.4	−0.6	2.0	1.0	2.0
14001S007	7810	B1	L	1995.7 - 2002.7	7.0	14.6	19.9	2.7	5.4	4.2	5.4
Potsdam, Germany											
14106M003	POTS	A1	P	1996.0 - 2003.0	7.0	14.3	19.1	−1.4	0.8	0.8	0.8
14106S001	1181	A1	L	1983.7 - 1992.2	8.5	16.6	19.1	−4.4	45.4	44.0	41.2
14106S009	7836	A1	L	1993.0 - 2002.7	9.6	13.7	19.3	−1.3	2.0	1.4	2.0
Wettzell, Germany											
14201M005	7597	A1	L	1995.5 - 1997.0	1.5	16.9	20.6	−5.4	51.9	23.0	53.2
14201M010	WTZR	A1	P	1996.0 - 2003.0	7.0	14.5	20.3	0.0	0.8	0.8	0.8
14201S002	7834	A1	L	1981.2 - 1991.1	10.0	15.3	20.1	2.2	6.6	6.5	6.4
14201S004	7224	A1	R	1983 - 2000	16.9	14.2	20.3	−0.9	0.4	0.4	0.4
14201S018	8834	A1	L	1991.1 - 2002.7	11.6	14.0	19.9	2.0	1.4	1.0	1.4
Wuhan City, P.R.China											
21602M001	WUHN	A1	P	1996.0 - 2002.4	6.4	−13.0	32.4	−1.2	0.8	1.0	0.8
21602S003	7236	A1	L	1993.2 - 1999.5	6.3	−14.6	34.2	13.4	21.2	17.8	24.4
Shanghai, China											
21605M002	SHAO	A1	P	1996 - 2002	6.7	−14.6	31.1	−1.0	0.8	0.9	0.8
21605S001	7837	A1	L	1983.9 - 2002.7	18.8	−13.2	30.2	−3.6	2.7	2.7	2.9
21605S009	7227	A1	R	1988 - 2000	11.8	−13.7	32.1	−0.8	1.1	1.1	1.1
Urumqi, China											
21612M001	URUM	A1	P	1996.0 - 2003.0	7.0	5.9	29.4	1.0	0.9	1.0	1.0
21612S001	7330	A1	R	1997 - 2000	2.4	6.1	31.4	−1.7	6.4	2.9	6.4
Kashima, Japan											
21701S001	1856	A1	R	1984 - 2000	16.6	−11.2	−3.8	−2.8	0.6	0.5	0.5
21701S004	1857	A1	R	1990 - 2000	10.5	−9.4	−3.9	−5.0	1.1	1.0	1.1
Koganei/Tokyo, Japan											
21704M001	7328	A1	L	1998.9 – 2000.7	1.7	−6.2	−12.8	6.4	12.2	12.0	12.1
21704S002	7308	A1	L	1995.9 – 1997.9	2.0	−5.7	−4.7	−6.7	27.3	25.9	26.7
Tsukuba, Japan											
21730S001	7311	A1	R	1984 - 1991	7.0	−10.3	−3.2	−1.5	12.4	12.5	12.5
21730S005	TSKB	A1	P	1996.0 - 2003.0	7.0	−8.7	−4.0	−0.9	0.8	0.9	0.8
Taejon, South Korea											
23902M001	TAEJ	A1	P	1996 - 1999	3.1	−16.7	29.1	−15.0	1.1	1.0	1.1
23902M002	DAEJ	A1	P	1996.0 - 2003.0	7.0	−14.3	25.8	0.4	1.1	0.9	1.0

continued

Station velocities at co-location sites continued

Domes No.	ID	Sol. No.	T[1]	Data time span	$\triangle t$	vel_N	vel_E	vel_H	$\sigma_{\mathrm{vel}N}$	$\sigma_{\mathrm{vel}E}$	$\sigma_{\mathrm{vel}H}$
Hartebeesth, S Africa											
30302M003	7501	A1	L	1993.5 - 2002.7	9.1	17.9	16.5	−2.7	9.3	9.3	8.7
30302M004	HRAO	A1	P	1996.0 - 2003.0	7.0	17.3	18.0	−0.5	0.9	1.1	1.1
30302M007	HARK	A1	P	1996 - 2000	4.5	20.6	20.0	4.0	1.0	1.1	1.2
30302M009	HARB	A1	P	1996.0 - 2003.0	7.0	16.2	19.1	−0.9	1.4	1.5	1.7
30302S001	7232	A1	R	1986 - 2000	14.5	17.8	18.0	−0.2	0.8	0.9	1.0
30302S005	HBLA	A1	D	1997.4 - 2000.6	3.2	18.7	16.5	−0.4	1.8	2.6	2.1
30302S202	HBKA	A1	D	1993.0 - 1997.4	4.4	18.7	16.5	−0.5	1.8	2.6	2.1
Sainte-Helene, UK											
30606S002	HELA	A1	D	1993.0 - 1997.3	4.3	16.0	25.4	2.5	1.9	3.0	1.8
30606S003	HELB	A1	D	1998.3 - 2003.0	4.7	15.7	25.5	2.4	1.9	3.0	1.8
Libreville, Gabun											
32809M002	NKLG	A1	P	1996.0 - 2003.0	7.0	18.2	21.3	−6.1	0.9	1.1	1.7
32809S002	LIBA	A1	D	1993.0 - 1999.1	6.1	21.3	17.1	1.3	1.6	2.7	1.7
Ottawa, Canada											
40102S009	OTTA	A1	D	1994.1 - 1998.0	3.9	10.5	−17.5	−0.5	1.8	2.5	1.8
40102S011	OTTB	A1	D	1998.1 - 2000.6	2.5	10.6	−17.5	−0.5	1.8	2.5	1.8
Algonquin Park, Canada											
40104M002	ALGO	A1	P	1996.0 - 2003.0	7.0	1.6	−16.6	4.2	0.7	0.9	0.7
40104S001	7282	A1	R	1984 - 2000	16.1	1.0	−16.5	1.4	0.5	0.4	0.5
Penticton, Canada											
40105M001	7283	A1	R	1984 - 1990	5.9	−12.1	−12.5	21.8	26.1	17.3	27.3
40105M002	DRAO	A1	P	1996.0 - 2003.0	7.0	−11.4	−13.6	1.4	0.7	0.9	0.7
Yellowknife, Canada											
40127M003	YELL	A1	P	1996.0 - 2003.0	7.0	−11.8	−17.3	5.2	0.7	0.8	0.6
40127M004	7296	A1	R	1991 - 2000	9.2	−11.8	−17.2	5.3	1.4	0.9	2.0
40127S007	YELA	A1	D	1993.0 - 2001.8	8.8	−12.2	−19.1	5.1	1.0	1.3	0.9
Pasadena, CA, USA											
40400M003	7263	A1	R	1982 - 1988	6.1	7.2	−37.3	5.6	16.1	13.4	17.3
40400M007	JPLM	A1	P	1996.0 - 2003.0	7.0	12.2	−38.1	0.4	0.7	0.9	0.8
Goldstone, USA											
40405S005	GOMA	A1	D	1994.6 - 1996.7	2.1	−7.5	−24.3	−2.6	1.5	2.1	1.6
40405S009	7222	A1	R	1983 - 1992	9.0	−5.2	−16.8	−3.3	1.0	0.6	0.9
40405S009	7222	A2	R	1992 - 1992	0.2	−5.2	−16.8	−3.3	1.0	0.6	0.9
40405S014	1513	A1	R	1981 - 1991	9.7	−5.7	−16.8	−6.1	4.4	3.2	4.4
40405S019	1515	A1	R	1987 - 1989	1.7	−5.8	−18.4	0.1	1.7	1.2	1.6
40405S019	1515	A2	R	1993 - 1999	6.6	−5.8	−18.4	0.1	1.7	1.2	1.6
40405S031	GOLD	A1	P	1996.0 - 2003.0	7.0	−5.9	−20.1	0.8	0.7	0.9	0.8
40405S035	GOLA	A1	D	1993.0 - 1994.6	1.6	−7.5	−24.3	−2.6	1.5	2.1	1.6
40405S037	GOMB	A1	D	1996.8 - 2003.0	6.2	−7.4	−24.3	−2.6	1.5	2.0	1.6
Fairbanks, USA											
40408M001	FAIR	A1	P	1996.0 - 2002.8	6.8	−22.1	−8.4	−3.1	0.8	0.8	0.7
40408S002	7225	A1	R	1984 - 2000	16.3	−22.5	−8.9	0.4	0.4	0.4	0.4
40408S004	FAIA	A1	D	1993.0 - 1999.4	6.4	−21.5	−8.7	2.2	1.2	1.2	1.0
Kodiak, AK, USA											

continued

Station velocities at co-location sites continued

Domes No.	ID	Sol. No.	T[1]	Data time span	$\triangle t$	vel_N	vel_E	vel_H	$\sigma_{\mathrm{vel}N}$	$\sigma_{\mathrm{vel}E}$	$\sigma_{\mathrm{vel}H}$
40419M001	7278	A1	R	1984 - 1990	5.9	−15.3	−12.5	10.9	18.1	11.1	22.9
40419S003	KODK	A1	P	2000 - 2003	2.7	−11.7	−16.7	8.4	1.3	1.1	1.5
Vandenberg AFB, USA											
40420M002	7223	A1	R	1983 - 1991	7.9	21.7	−42.0	2.8	2.7	2.2	2.7
40420M101	HARV	A1	P	1996 - 2002	6.5	22.1	−43.1	−1.3	1.9	1.8	2.0
Kokee Park Hawaii, USA											
40424M004	KOKB	A1	P	1996.0 - 2002.8	6.8	32.3	−62.8	2.7	0.7	0.9	0.9
40424S001	1311	A1	R	1984 - 1994	9.7	33.6	−64.0	−0.7	1.1	0.8	1.1
40424S007	7298	A1	R	1993 - 2000	7.4	32.8	−62.3	−0.0	0.6	0.5	0.6
40424S008	KOKA	A1	D	1993.0 - 2002.9	9.9	32.5	−64.6	0.6	1.1	1.6	1.1
Ford Ord, CA											
40427M001	7266	A1	R	1983 - 1988	4.5	21.8	−40.9	6.7	17.5	15.1	17.8
40427M002	7241	A1	R	1988 - 1989	0.5	25.6	−42.0	11.5	26.1	22.4	26.5
40427M002	7241	A2	R	1989 - 1991	1.7	25.6	−42.0	11.5	26.1	22.4	26.5
Quincy, USA											
40433M002	7109	A1	L	1981.7 - 1997.4	15.7	−5.0	−21.1	0.1	1.0	0.8	1.0
40433M004	7221	A1	R	1982 - 1990	8.0	−7.8	−22.2	−4.1	10.2	8.0	10.1
40433M004	QUIN	A1	P	1996.0 - 2003.0	7.0	−5.2	−22.4	−1.4	0.9	1.0	0.9
Owens Valley, CA											
40439S002	7207	A1	R	1979 - 1988	9.3	−5.7	−19.0	−4.3	2.2	1.5	2.3
40439S004	7616	A1	R	1992 - 2000	7.7	−6.2	−19.2	−3.3	0.6	0.5	0.5
Westford, MA, USA											
40440S002	7205	A1	R	1979 - 1992	12.9	4.4	−14.4	−1.0	1.3	0.7	1.2
40440S003	7209	A1	R	1981 - 2000	19.2	4.1	−15.2	−1.8	0.4	0.4	0.4
40440S020	WES2	A1	P	1996.0 - 2003.0	7.0	4.2	−16.0	0.9	0.7	0.9	0.7
Green Bank, WV											
40441S001	7204	A1	R	1979 - 1996	16.8	1.0	−14.6	−2.6	1.3	0.5	1.4
40441S004	7214	A1	R	1989 - 1990	1.6	1.0	−14.2	−3.0	0.8	0.5	0.8
40441S004	7214	A2	R	1990 - 1996	5.7	1.0	−14.2	−3.0	0.8	0.5	0.8
40441S007	7208	A1	R	1995 - 2000	5.4	2.1	−14.5	1.0	0.7	0.5	0.7
Fort Davis, USA											
40442M006	7080	A1	L	1988.2 - 2002.7	14.5	−5.6	−13.6	−0.8	1.0	0.8	1.0
40442M012	MDO1	A1	P	1996.0 - 2003.0	7.0	−7.5	−12.6	−1.0	0.7	0.9	0.8
40442S003	7216	A1	R	1980 - 1991	11.1	−7.4	−12.3	−5.2	2.0	1.0	2.2
40442S017	7613	A1	R	1991 - 2000	9.1	−7.3	−12.3	−1.0	0.6	0.5	0.6
Washington, D.C.											
40451M102	7102	A1	R	1989 - 1992	3.0	4.1	−14.3	−1.8	16.9	7.1	17.5
40451M105	7105	A1	L	1981.2 - 2002.7	21.5	3.6	−15.2	−1.6	0.8	0.7	0.7
40451M117	7920	A1	L	1988.9 - 1990.8	1.9	1.2	−15.6	−5.4	11.4	11.1	11.7
40451M120	7918	A1	L	1990.3 - 1997.6	7.3	1.6	−15.7	−2.4	3.8	2.8	3.8
40451M123	GODE	A1	P	1996.0 - 2003.0	7.0	3.2	−14.5	−2.0	0.7	0.9	0.8
40451M125	7108	A1	R	1993 - 2000	7.1	0.9	−14.4	−4.5	3.8	1.7	3.9
40451S003	USNO	A1	P	1996.0 - 2003.0	7.0	2.5	−15.2	−1.3	0.7	0.9	0.8
Pie Town, USA											
40456M001	PIE1	A1	P	1996.0 - 2003.0	7.0	−9.7	−13.0	1.2	0.7	0.9	0.8

continued

Station velocities at co-location sites continued

Domes No.	ID	Sol. No.	T[1]	Data time span	$\triangle t$	vel_N	vel_E	vel_H	$\sigma_{\text{vel}N}$	$\sigma_{\text{vel}E}$	$\sigma_{\text{vel}H}$
40456S001	7234	A1	R	1988 - 2000	11.7	−10.1	−14.2	−1.5	0.6	0.5	0.5
North Liberty, USA											
40465M001	NLIB	A1	P	1996.0 - 2003.0	7.0	−2.8	−15.7	−1.2	0.7	0.9	0.7
40465S001	7612	A1	R	1992 - 2000	7.7	−2.3	−15.2	−3.8	0.6	0.4	0.6
Mauna, Kea, USA											
40477M001	MKEA	A1	P	1996.0 - 2003.0	7.0	32.5	−63.7	−0.9	0.8	0.9	0.9
40477S001	7617	A1	R	1993 - 2000	6.8	32.7	−63.1	−2.3	0.8	0.8	0.9
Monument Peak, USA											
40497M001	7110	A1	L	1981.5 - 2002.7	21.1	18.8	−39.7	0.2	0.8	0.7	0.8
40497M003	7274	A1	R	1982 - 1990	8.1	13.4	−43.1	−7.0	8.4	6.7	9.3
40497M004	MONP	A1	P	1996.0 - 2003.0	6.4	17.4	−38.3	2.1	0.8	0.9	0.8
Richmond, USA											
40499M002	7295	A1	L	1988.3 - 1995.3	7.1	1.7	−12.0	−1.1	5.3	4.6	6.4
40499S001	7219	A1	R	1984 - 1992	8.6	0.6	−9.8	−1.2	0.9	0.6	0.9
40499S016	RIDA	A1	D	1993.1 - 2003.0	9.9	6.7	−9.7	−1.3	1.2	2.0	1.0
40499S019	7201	A1	R	1995 - 1996	1.0	−2.3	−4.5	16.4	25.7	14.2	35.1
40499S020	RCM6	A1	P	1996 - 1998	1.7	1.8	−9.7	0.5	1.4	1.1	2.0
Ensenada, Mexico											
40508M001	CICE	A1	P	1996 - 1999	3.0	16.5	−40.2	−1.9	5.2	5.0	6.0
40508M002	CIC1	A1	P	1999 - 2003	3.7	18.7	−40.8	1.9	1.7	1.6	1.9
Rio Grande, Argentina											
41507M004	RIOG	A1	P	1996.0 - 2003.0	7.0	3.5	10.7	1.5	0.8	1.1	0.9
41507S003	RIOA	A1	D	1993.0 - 1995.0	2.0	12.5	8.3	0.6	1.5	1.7	1.4
41507S004	RIOB	A1	D	1995.1 - 2001.0	6.0	12.5	8.3	0.6	1.4	1.7	1.4
Fortaleza, Brazil											
41602M001	FORT	A1	P	1996.0 - 2003.0	7.0	11.0	−4.2	0.2	0.7	1.0	1.0
41602S001	7297	A1	R	1993 - 2000	7.5	11.4	−4.2	0.4	0.6	0.8	0.8
Easter Island, Chile											
41703M002	7097	A1	L	1987.9 - 1995.3	7.4	−7.2	64.5	−3.1	8.1	8.1	8.3
41703M003	EISL	A1	P	1996.0 - 2003.0	7.0	−8.6	67.4	−1.8	0.8	1.1	1.0
41703S008	EASA	A1	D	1993.0 - 2001.0	8.0	−2.2	68.9	0.0	1.2	1.7	1.2
Santiago, Chile											
41705M003	SANT	A1	P	1996.0 - 2003.0	7.0	14.9	20.5	2.4	0.8	1.2	0.9
41705S006	1404	A1	R	1991 - 1996	5.0	15.8	19.9	5.4	3.2	2.5	3.5
41705S008	SAOB	A1	D	1997.1 - 2000.9	3.9	14.3	13.8	−0.5	3.2	4.6	3.4
Arequipa, Peru											
42202M003	7403	A1	L	1990.5 - 2002.7	12.1	14.8	9.3	−1.4	1.3	1.4	1.7
42202M005	AREQ	A1	P	1996.0 - 2001.5	5.5	13.0	12.4	0.6	0.7	1.1	1.0
42202S001	7907	A1	L	1981.0 - 1992.6	11.6	14.7	12.6	−10.1	5.0	5.5	5.4
42202S005	AREA	A1	D	1993.5 - 2001.5	8.0	16.8	13.0	−3.4	1.6	2.5	1.6
St. Croix, USA											
43201M001	CRO1	A1	P	1996.0 - 2003.0	7.0	11.8	9.9	−6.0	0.7	1.0	0.9
43201S001	7615	A1	R	1993 - 2000	6.9	11.5	11.1	−0.8	0.9	0.8	1.1
Tidbinbilla, Australia											
50103M108	TIDB	A1	P	1996.0 - 2003.0	7.0	54.8	18.2	3.2	0.9	1.1	1.0

continued

Station velocities at co-location sites continued

Domes No.	ID	Sol. No.	T[1]	Data time span	$\triangle t$	vel_N	vel_E	vel_H	$\sigma_{\mathrm{vel}N}$	$\sigma_{\mathrm{vel}E}$	$\sigma_{\mathrm{vel}H}$
50103S007	7843	A1	L	1986.6 - 1998.9	12.3	55.6	18.0	−0.5	1.9	1.8	1.9
50103S010	1545	A1	R	1988 - 1999	11.6	53.9	18.0	0.5	1.0	1.0	1.1
50103S201	ORRA	A1	D	1993.0 - 1996.2	3.2	59.9	22.9	−16.0	4.2	5.1	4.6
50103S202	ORRB	A1	D	1997.0 - 1998.8	1.7	59.8	22.9	−15.9	4.2	5.1	4.6
Yarragadee, Australia											
50107M001	7090	A1	L	1981.0 - 2002.7	21.7	56.8	38.0	−0.7	0.7	0.7	0.7
50107M004	YAR1	A1	P	1996.0 - 2003.0	7.0	55.4	39.1	−1.1	0.8	1.1	1.0
50107S006	YARA	A1	D	1993.0 - 1999.8	6.7	56.1	38.1	3.5	1.3	2.1	1.6
Hobart, Australia											
50116M004	HOB2	A1	P	1996.0 - 2003.0	7.0	55.2	13.7	4.3	0.9	1.1	1.0
50116S002	7242	A1	R	1989 - 2000	10.8	54.7	14.1	0.7	1.0	0.9	1.0
Canberra, Australia											
50119M002	STR1	A1	P	1999 - 2003	3.0	55.4	17.9	4.8	4.8	4.7	5.1
50119S001	7849	A1	L	1998.6 - 2002.6	4.0	53.3	16.2	1.7	6.0	5.5	6.0
Guam, USA											
50501M002	GUAM	A1	P	1996.0 - 2002.7	6.7	2.2	−11.4	1.5	0.7	0.9	1.0
50501S001	GUAB	A1	D	1994.0 - 2000.6	6.6	3.1	−7.6	0.9	1.4	2.0	1.8
Syowa, Antartica											
66006S001	SYOB	A1	D	1993.3 - 1998.3	5.0	2.1	−9.2	2.0	1.4	1.4	1.2
66006S002	SYOG	A1	P	1996.0 - 2003.0	7.0	1.6	−3.1	5.8	1.4	1.3	1.8
O'Higgins, Antarctica											
66008M001	OHIG	A1	P	1996 - 2002	6.1	10.0	14.8	6.5	1.1	1.2	0.8
66008S001	7245	A1	R	1993 - 2000	7.1	8.0	14.9	8.1	4.5	3.3	6.4
Kerguelen Island											
91201M002	KERG	A1	P	1996.0 - 2003.0	7.0	−3.6	5.5	4.3	0.9	1.2	0.9
91201S002	KERA	A1	D	1993.0 - 1994.9	1.9	−3.8	−1.3	0.8	1.4	2.0	1.3
91201S003	KERB	A1	D	1994.9 - 2001.2	6.3	−3.8	−1.4	0.8	1.3	1.9	1.3
Pamatai, Tahiti											
92201M003	PAMA	A1	P	1996 - 1997	1.2	29.7	−74.7	4.9	3.1	5.5	5.8
92201M006	TAHI	A1	P	1996 - 1999	3.6	35.5	−62.3	−15.9	3.7	6.1	6.7
92201M007	7124	A1	L	1998.0 - 2002.7	4.7	33.2	−64.2	1.7	10.7	11.8	12.1
92201M009	THTI	A1	P	1996.0 - 2003.0	7.0	31.6	−66.5	−0.3	0.9	1.2	1.3
92201S007	PAPB	A1	D	1995.6 - 1998.3	2.7	36.7	−60.6	10.3	3.8	6.0	5.3
Noumea, France											
92701M003	NOUM	A1	P	1996.0 - 2003.0	7.0	45.6	19.5	0.8	0.8	1.0	1.1
92701S001	NOUA	A1	D	1993.0 - 2000.6	7.6	46.7	17.9	−2.2	1.5	2.6	1.6
Kourou, French Guyana											
97301M210	KOUR	A1	P	1996.0 - 2003.0	7.0	11.0	−4.7	3.8	0.7	1.0	1.0
97301S004	KRUB	A1	D	1993.0 - 2003.0	10.0	13.1	−2.5	−1.8	1.4	1.6	1.5
La Reunion, Reunion											
97401S001	REUA	A1	D	1993.0 - 1998.9	5.9	15.5	16.0	0.4	1.3	1.9	1.6
97401S002	REUB	A1	D	1999.0 - 2003.0	4.0	15.5	16.1	0.5	1.3	1.9	1.6

Tab. G.2: *Comparison of space geodetic results and local ties at co-location sites. This table shows the discrepancies between the space geodetic estimated intra-site vectos and the local ties (and the station velocity differences of co-located instruments. Note that in both cases the absolute (3-dimensional) differences are displayed.*
[1]*: Local tie information available in IERS data base. The local tie in Potsdam (14106S001-S009) is obtained from the ILRS.*
[2]*: Discrepancies (△tie) and station velocities differences (△vel) obtained from intra-technique solutions (without applying local tie information and without equating station velocities).*
[3]*: Discrepancies (△tie) and station velocities differences (△vel) obtained from combined TRF solution (selected local ties were applied and station velocities were equated).*
[4]*: Selected local ties in iteration "i", see chapter 6).*
[5]*: Equating of station velocities: (T=together with local tie selection, V=afterwards in a separate step).*

Comparison at co-location sites

DOMES No. A	DOMES No. B	Techn. A – B	Ties[1] avail.	△tie[2] [mm]	△vel.[2] [mm/yr]	△tie[3] [mm]	△vel.[3] [mm/yr]	Selected Ties[4]	Equated Vel.[5]
Grasse, France									
10002S001	10002M006	L – P	*	8.6	1.6	3.2	1.2	2	T
10002M006	10002S002	P – L	*	16.0	2.6	1.6	0.4	3	T
Toulouse, France									
10003M004	10003M009	P – P	–	–	2.7	–	2.6	–	V
10003S001	10003M004	D – P	*	39.6	3.7	27.1	3.8	–	V
10003S001	10003S003	D – D	*	9.5	0.2	4.5	0.2	4	T
Reykjavik, Iceland									
10202M001	10202S002	P – D	*	15.1	1.8	11.4	0.6	4	T
10202S001	10202S002	D – D	*	20.3	0.3	27.6	0.5	4	T
Tromsoe, Norway									
10302M002	10302M003	R – P	*	118.2	15.1	105.1	11.9	–	V
10302M002	10302M006	P – P	–	–	10.3	–	9.4	–	V
Ny-Alesund, Norway									
10317M001	10317M003	P – P	*	33.5	1.4	32.6	1.4	–	V
10317M003	10317S002	P – D	*	29.7	4.1	24.5	2.6	4	T
10317M003	10317S003	P – R	–	–	0.9	–	0.9	–	V
Onsala, Sweden									
10402M004	10402S002	P – R	*	7.0	3.3	2.9	2.6	2	T
Metsahovi, Finland									
10503S011	10503S013	P – D	*	32.8	3.6	26.5	1.5	4	T
10503S011	10503S014	P – L	–	–	5.9	–	6.1	–	V
Graz, Austria									
11001M002	11001S002	P – L	*	4.0	0.9	0.9	1.1	1	T
Borowiec, Poland									
12205M002	12205S001	P – L	*	12.1	1.7	1.2	0.1	2	T
Kitab, Uzbekistan									
12334M001	12334S004	P – D	*	45.0	9.4	42.6	9.0	–	–
Simeiz, Ukraine									
12337S003	12337S006	L – L	–	–	10.4	–	9.9	–	V
12337S003	12337S008	L – R	–	–	9.7	–	9.0	–	V

continued

Comparison at co-location sites continued

DOMES No. A	DOMES No. B	Techn. A – B	Ties[1] avail.	△tie[2] [mm]	△vel.[2] [mm/yr]	△tie[3] [mm]	△vel.[3] [mm/yr]	Selected Ties[4]	Equated Vel.[5]
Yakutzk, Russia									
12353M001	12353M002	P – P	–	–	6.6	–	6.1	–	–
Petropavlovsk, Russia									
12355M001	12355M002	P – P	–	–	42.5	–	42.7	–	–
Dionysos, Greece									
12602M002	12602S011	L – D	*	91.9	7.9	89.2	5.4	–	V
Medicina, Italy									
12711M003	12711S001	P – R	*	14.9	0.8	20.0	2.1	–	–
Noto, Italy									
12717M001	12717S001	L – R	*	45.6	11.5	37.5	9.4	–	V
12717M003	12717S001	P – R	*	30.0	6.0	32.0	4.5	–	–
12717M003	12717M004	P – P	–	–	6.0	–	5.9	–	–
Cagliari, Italy									
12725M002	12725M003	L – P	*	50.0	3.0	49.1	3.2	–	V
12725M002	12725S013	L – L	–	–	10.6	–	10.7	–	V
Matera, Italy									
12734M008	12734S001	P – L	*	13.3	2.2	14.1	0.8	3	T
12734M008	12734M004	P – R	*	10.4	1.6	5.8	0.6	3	T
12734S005	12734M004	R – L	*	6.0	2.1	5.9	0.7	2	T
Herstmonceux, UK									
13212M007	13212S001	P – L	*	8.5	1.2	3.9	0.6	2	T
San Fernando, Spain									
13402M004	13402S004	P – L	*	51.8	16.4	50.0	15.5	–	V
13402S004	13402S007	L – L	*	41.2	20.0	41.4	21.2	–	V
Madrid, Spain									
13407S010	13407S012	R – P	*	11.1	8.5	4.8	1.4	2	T
Kootwijk, Netherlands									
13504M002	13504M003	L – P	*	38.4	6.4	41.1	6.9	–	V
Zimmerwald, Switzerlan									
14001M004	14001S007	P – L	*	13.5	6.8	8.0	4.8	–	–
14001S001	14001S007	L – L	*	10.8	3.7	1.4	0.4	2	T
Potsdam, Germany									
14106M003	14106S009	P – L	*	4.4	0.3	0.4	1.3	1	T
14106S001	14106S009	L – L	ILRS	92.1	4.3	???	4.2	–	V
Wettzell, Germany									
14201M010	14201M005	P – L	*	15.0	6.8	13.7	4.9	–	V
14201M010	14201S002	P – L	*	55.1	2.6	51.9	3.6	–	V
14201M010	14201S004	P – R	*	3.8	0.8	2.0	1.2	1	T
14201M010	14201S018	P – L	*	14.5	1.7	7.6	1.5	3	T
Wuhan City, P.R.China									
21602M001	21602S003	P – L	–	–	15.2	–	15.4	–	V
Shanghai, China									
21605S001	21605S009	L – R	*	45.8	2.9	49.4	3.7	–	V
21605S001	21605M002	L – P	–	–	3.1	–	2.5	–	V
Urumqi, China									
21612M001	21612S001	P – R	–	–	3.4	–	3.5	–	V
Kashima, Japan									
21701S001	21701S004	R – R	–	–	2.8	–	2.8	–	V

continued

Comparison at co-location sites continued

DOMES No. A	DOMES No. B	Techn. A – B	Ties[1] avail.	△tie[2] [mm]	△vel.[2] [mm/yr]	△tie[3] [mm]	△vel.[3] [mm/yr]	Selected Ties[4]	Equated Vel.[5]
Koganei/Tokyo, Japan									
21704M001	21704S002	L – L	–	–	15.4	–	15.2	–	V
Tsukuba, Japan									
21730S001	21730S005	R – P	*	33.4	7.1	1.5	1.4	2	T
Taejon, South Korea									
23902M001	23902M002	P – P	–	–	15.8	–	15.6	–	–
Hartebeesth, S Africa									
30302M004	30302M003	P – L	–	–	2.7	–	2.5	–	V
30302M004	30302M007	P – P	*	10.6	5.9	9.3	8.0	–	–
30302M004	30302M009	P – P	–	–	1,6	–	1.4	–	V
30302M004	30302S001	P – R	*	25.8	0.6	25.7	1.0	–	V
30302M004	30302S005	P – D	*	54.9	2.7	73.9	2.8	–	V
30302S005	30302S202	D – D	*	31.7	0.2	10.3	0.3	4	T
Sainte-Helene, UK									
30606S002	30606S003	D – D	–	–	0.3	–	0.2	–	V
Libreville, Gabun									
32809M002	32809S002	P – D	–	–	9.1	–	8.0	–	–
Ottawa, Canada									
40102S009	40102S011	D – D	–	–	0.1	–	0.1	–	V
Algonquin Park, Canada									
40104M002	40104S001	P – R	*	17.6	2.3	11.1	1.9	3	T
Penticton, Canada									
40105M001	40105M002	R – P	*	148.2	20.8	142.0	20.7	–	V
Yellowknife, Canada									
40127M003	40127M004	P – R	*	21.4	0.2	5.2	0.8	2	T
40127M003	40127S007	P – D	*	26.6	2.9	10.0	0.4	4	T
Pasadena, CA, USA									
40400M003	40400M007	R – P	*	99.6	6.4	97.2	8.0	–	V
Goldstone, USA									
40405S009	40405S014	R – R	*	19.5	3.3	17.1	2.0	3	T
40405S009	40405S019	R – R	*	18.5	4.1	10.1	0.8	3	T
40405S009	40405S037	R – D	*	75.2	6.9	74.5	2.7	–	–
40405S037	40405S005	D – D	*	31.9	0.1	11.9	0.1	4	T
40405S037	40405S035	D – D	*	83.7	0.1	72.6	0.1	–	V
40405S009	40405S031	R – P	–	–	5.3	–	3.8	–	–
Fairbanks, USA									
40408M001	40408S002	P – R	*	27.8	3.6	25.8	4.6	–	–
40408M001	40408S004	P – D	*	37.7	5.4	35.3	5.3	–	–
Kodiak, AK, USA									
40419M001	40419S003	R – P	–	–	6.6	–	6.7	–	V
Vandenberg AFB, USA									
40420M002	40420M101	R – P	–	–	4.3	–	5.1	–	–
Kokee Park Hawaii, USA									
40424M004	40424S001	P – R	*	19.3	3.7	15.0	2.7	–	–
40424M004	40424S007	P – R	*	8.6	3.2	6.6	1.3	3	T
40424S001	40424S008	R – D	*	34.3	3.3	11.9	0.4	4	T
Ford Ord, CA									
40427M001	40427M002	R – R	–	–	6.2	–	6.1	–	V

continued

Comparison at co-location sites continued

DOMES No. A	DOMES No. B	Techn. A – B	Ties[1] avail.	△tie[2] [mm]	△vel.[2] [mm/yr]	△tie[3] [mm]	△vel.[3] [mm/yr]	Selected Ties[4]	Equated Vel.[5]
Quincy, USA									
40433M002	40433M004	L – R	*	39.3	7.1	34.8	4.2	–	V
40433M002	40433M004	L – P	*	5.4	1.5	1.9	1.8	2	T
Owens Valley, CA									
40439S002	40439S004	R – R	–	–	1.1	–	1.2	–	V
Westford, MA, USA									
40440S002	40440S003	R – R	*	15.6	1.1	8.0	0.6	3	T
40440S003	40440S020	R – P	*	18.1	2.5	15.4	2.0	3	T
Green Bank, WV									
40441S001	40441S004	R – R	–	–	0.6	–	0.7	–	V
40441S001	40441S007	R – R	–	–	3.8	–	3.8	–	–
Fort Davis, USA									
40442M006	40442S017	L – R	*	10.6	0.9	5.9	1.3	2	T
40442S017	40442M012	R – P	*	11.0	1.2	3.8	0.5	2	T
40442S003	40442S017	R – R	*	38.2	3.9	51.5	5.2	–	–
Washington, D.C.									
40451M105	40451M102	L – R	*	23.5	5.9	0.5	0.3	2	T
40451M105	40451M117	L – L	*	20.3	4.2	23.6	4.6	–	V
40451M105	40451M120	L – L	*	7.6	1.9	5.7	0.3	2	T
40451M120	40451M123	L – P	*	6.9	2.0	6.8	0.5	3	T
40451M105	40451M125	L – P	*	24.7	3.8	26.8	3.1	–	V
40451M105	40451S003	L – P	–	–	1.2	–	1.1	–	V
Pie Town, USA									
40456M001	40456S001	P – R	*	18.7	2.7	14.5	2.0	3	T
North Liberty, USA									
40465M001	40465S001	P – R	*	3.9	2.4	1.2	1.5	1	T
Mauna, Kea, USA									
40477M001	40477S001	P – R	*	5.0	2.0	0.7	2.0	1	T
Monument Peak, USA									
40497M001	40497M003	L – R	*	51.6	10.1	70.8	10.1	–	–
40497M001	40497M004	L – P	*	11.2	2.5	8.1	1.8	3	T
Richmond, USA									
40499M002	40499S001	L – R	*	11.9	2.1	23.8	0.7	–	V
40499M002	40499S016	L – R	*	63.0	7.2	64.2	6.3	–	–
40499M002	40499S019	L – R	–	–	19.5	–	19.2	–	V
40499M002	40499S020	L – P	–	–	2.8	–	3.2	–	V
Rio Grande, Argentina									
41507M004	41507S003	P – D	*	36.2	9.0	32.5	6.5	–	–
41507S004	41507S003	D – D	*	32.2	0.1	8.1	0.2	4	T
Ensenada, Mexico									
40508M001	40508M002	P – P	–	–	4.4	–	4.6	–	V
Fortaleza, Brazil									
41602M001	41602S001	P – R	*	13.4	1.4	6.6	0.9	2	T
Easter Island, Chile									
41703M002	41703M003	L – P	*	41.3	2.9	40.3	2.3	–	V
41703M002	41703S008	L – D	*	34.1	8.6	34.2	7.9	–	V
Santiago, Chile									
41705M003	41705S006	P – R	*	11.5	6.1	19.5	4.4	–	V

continued

Comparison at co-location sites continued

DOMES No. A	DOMES No. B	Techn. A – B	Ties[1] avail.	△tie[2] [mm]	△vel.[2] [mm/yr]	△tie[3] [mm]	△vel.[3] [mm/yr]	Selected Ties[4]	Equated Vel.[5]
41705M003	41705S008	P – D	*	33.7	4.1	11.1	0.4	4	T
Arequipa, Peru									
42202M003	42202M005	L – P	*	16.1	3.2	5.6	1.4	2	T
42202M003	42202S001	L – L	*	55.7	9.8	64.8	11.1	–	–
42202M003	42202S005	L – D	*	56.0	5.6	56.7	5.4	–	–
St. Croix, USA									
43201M001	43201S001	P – R	*	21.3	6.0	20.4	5.2	–	–
Tidbinbilla, Australia									
50103M108	50103S007	P – L	*	35.0	3.5	38.9	3.3	–	V
50103M108	50103S010	P – R	*	6.9	1.6	7.1	0.8	3	T
50103M108	50103S202	P – D	*	75.6	18.7	???	14.3	–	–
50103S201	50103S202	D – D	*	21.6	0.0	3.6	0.0	4	T
Yarragadee, Australia									
50107M001	50107M004	L – P	*	2.8	1.3	0.6	3.6	1	T
50107M004	50107S006	P – D	*	43.1	5.5	40.8	6.0	–	–
Hobart, Australia									
50116M004	50116S002	P – R	*	6.1	2.7	15.1	2.5	–	V
Canberra, Australia									
50119M002	50119S001	P – L	*	7.2	2.1	2.4	0.9	2	T
Guam, USA									
50501M002	50501S001	P – D	*	52.5	4.0	49.3	2.9	–	–
Syowa, Antartica									
66006S001	66006S002	D – P	*	52.4	7.0	53.4	6.4	–	–
O'Higgins, Antarctica									
66008M001	66008S001	P – R	*	38.0	2.1	42.5	3.8	–	V
Kerguelen Island									
91201M002	91201S003	P – D	*	30.9	9.5	36.9	8.4	–	–
91201S002	91201S003	D – D	*	23.2	0.0	11.4	0.1	4	T
Pamatai, Tahiti									
92201M006	92201M003	P – P	–	–	24.9	–	24.8	–	–
92201M006	92201M009	P – P	*	8.1	16.6	8.1	16.5	–	–
92201M009	92201M007	P – L	*	21.1	3.8	23.5	4.5	–	V
92201M006	92201S007	P – D	*	18.9	26.5	20.1	26.3	–	–
Noumea, France									
92701M003	92701S001	P – D	*	41.4	3.2	40.8	3.1	–	–
Kourou, French Guyana									
97301M210	97301S004	P – D	*	80.4	7.0	60.3	6.4	–	–
La Reunion, Reunion									
97401S001	97401S002	D – D	–	–	0.1	–	0.1	–	V